Field Theory in Cosmology

Statistics, non-Linearity and the CMB

Tobias Baldauf*

March 9, 2021

*t.baldauf@damtp.cam.ac.uk

In the Michaelmas course you focused on the history and composition of the homogeneous Universe, described linear fluctuations to the metric, their evolution and their creation in vanilla slow-roll inflation. This term, we will be focusing on making contact with observables in our Universe. Due to the stochastic origin of the fluctuations we will be requiring a statistical approach to compare theory and observations, and the relevant tools will be the topic of the first part of these lectures. You will then learn about Gaussian fluctuations in the Cosmic Microwave Background (CMB) temperature and polarization signals. Afterwards we will be considering modifications of inflation and their statistical signatures. In the last part of the lectures we will be concerned with non-linear structure formation in the late time Universe.

So far, the observed state of the Universe is compatible with the concordance ΛCDM model, where around 70% of the energy content of the Universe are in the form of dark energy, 25 % in the form of dark matter and only 5% in the form of baryonic matter. The fluctuations follow a spectrum resembling the one predicted by inflation and are very Gaussian. However, there are still many open questions, which we would like to answer using all possible observables available to us:

- What is causing the current accelerated expansion of the Universe? Is it simply a cosmological constant, is it a scalar field or do we need to modify Einstein's gravity?
- What is the nature of Dark Matter?
- What are the dynamics and field content of inflation?
- What is the mass of the neutrinos, which of the two hierarchies applies?
- How did the rich structures in our Universe arise from the small initial perturbations and how can we understand the process analytically?

In contrast to particle physics, where a particle collision can be repeated many times, we have only one Universe at our disposal and need to extract as much information as possible from the observables that are available to us:

- CMB (in particular lensing, polarization, small scales, also spectral distortions)
- Large-Scale Structure (LSS) - galaxy positions and weak gravitational lensing of the photons emitted by background galaxies or the CMB
- higher order statistics of LSS or the CMB
- 21 cm
- Ly-alpha forest

Unfortunately there is no textbook covering all aspects of this course, but here are some overview texts that should provide insightful additional reading for the first two parts of the course:

- R. Durrer *The Cosmic Microwave Background* [Durrer, 2008]
- S. Dodelson *Modern Cosmology* [Dodelson, 2003]
- P. Peebles *The Large-Scale Structure of the Universe* [Peebles, 1980]
- F. Bernardeau, S. Colombi, E. Gaztanaga, R. Scoccimarro *Large-Scale Structure of the Universe and Cosmological Perturbation Theory* [arXiv:astro-ph/0112551] [Bernardeau et al., 2002]

This list will be updated and extended as we go along.

These lecture notes are evolving and I would be grateful if you could report mistakes or typos to t.baldauf@damtp.cam.ac.uk. Thanks to Barry Chiang for pointing out typos in these notes.

Contents

1. Statistics

The currently favoured model for creating the fluctuations in the Universe is cosmological inflation, a quantum mechanical process. Due due it's quantum nature, it is impossible to predict the realization of fluctuations in the Universe, but only it's statistical properties. There are many different realisations of the Universe that are statistically equivalent. To compare theory and observation, we will need to measure statistical properties of the Universe and compare the result to the same statistics evaluated in the model of the Universe under consideration.

1.1. Random Fields in 3D Space

The cosmological principle asserts that on large enough scales the Universe is isotropic and homogeneous. We will demand that the statistics are:

- invariant under rotations ⇒ **statistical isotropy**,
- invariant translations ⇒ **statistical homogeneity**.

We will start to consider random fields in three dimensional space. As these fields describe deviations from or fluctuations around the background Universe, we will only consider mean zero fields $\langle f \rangle = 0$. For instance we can consider the temperature fluctuations in the CMB

$$\theta = \frac{T}{\bar{T}} - 1 = \frac{\Delta T}{T} \tag{1.1}$$

or the the **overdensity**

$$\delta(\boldsymbol{x}) = \frac{\rho(\boldsymbol{x})}{\bar{\rho}} - 1 = \frac{n(\boldsymbol{x})}{\bar{n}} - 1\,, \tag{1.2}$$

where ρ is a density and $n(\boldsymbol{x}) = \delta N(\boldsymbol{x})/\delta V$ is a number density as appropriate for discrete objects.

1.1.1. Power Spectrum

Correlators are expectation values of products of field values at different spatial locations (or different Fourier modes). In the first part of the cosmology course you were exposed to the **power spectrum**[1]

$$\langle \delta(\boldsymbol{k})\delta(\boldsymbol{k}')\rangle = (2\pi)^3\delta^{(\mathrm{D})}(\boldsymbol{k}+\boldsymbol{k}')P(|\boldsymbol{k}|) \tag{1.3}$$

By statistical isotropy the power spectrum may depend only on the magnitude of $\boldsymbol{k}$. The Dirac delta function ensures that the power spectrum is invariant under spatial translations. We will show this in more detail below. Distinct Fourier modes are uncorrelated and thus statistically independent. The above definition gives the power per unit Fourier space volume $\mathrm{d}^3k/(2\pi)^3$, sometimes one defines the power in a shell or **dimensionless power spectrum**

$$\Delta^2(k) = \frac{k^3P(k)}{2\pi^2} \tag{1.4}$$

[1] The prefactor of $(2\pi)^3$ is due to the Fourier convention used here, for other conventions it might be absent or arise with an exponten of 3/2 instead of 3.

such that $\Delta^2(k)\mathrm{d}\ln k = P(k)\mathrm{d}^3k/(2\pi)^3$ after integrating out the azimuthal angle. For real valued configuration space fields we have $\langle\delta(\boldsymbol{k})\delta^*(\boldsymbol{k}')\rangle = \langle\delta(\boldsymbol{k})\delta(-\boldsymbol{k}')\rangle$, which is why you might sometimes encounter a different definition of the power spectrum

$$\langle\delta(\boldsymbol{k})\delta^*(\boldsymbol{k}')\rangle = (2\pi)^3\delta^{(\mathrm{D})}(\boldsymbol{k}-\boldsymbol{k}')P(|\boldsymbol{k}|)\,. \tag{1.5}$$

1.1.2. Correlation Function

The real space equivalent of the power spectrum is the **correlation function**

$$\langle\delta(\boldsymbol{x})\delta(\boldsymbol{x}+\boldsymbol{r})\rangle = \xi(|\boldsymbol{r}|) \tag{1.6}$$

By statistical homogeneity the correlation function can only depend on the difference of the positions $\boldsymbol{x}+\boldsymbol{r}$ and $\boldsymbol{x}$ and statistical isotropy enforces dependence on the magnitude only. Correlation function and power spectrum are related by a simple Fourier transformation and thus contain the same information. They do however have their respective advantages and disadvantages, both from a theoretical point of view regarding how apparent certain features are but also in terms of estimating the statistic.

An alternative interpretation of the correlation function defined above can be found in terms of the multi-point probability distribution functions. We will consider the background density field to be traced by a certain species with number density $\bar{n}$ and consider infinitesimally small volumes δV, which either host or don't host one tracer particle. This setup is sketched in Fig. 1.1. The one point probability for finding a particle in the small volume δV_1 is $\mathbb{P}_{1\mathrm{pt}}(1) = \bar{n}\delta V_1$. If we had a purely random field the joint or two point probability of finding particles both in volumes δV_1 and δV_2 separated by $r_{12} = |\boldsymbol{x}_1 - \boldsymbol{x}_2|$ would be given by the product of the independent probabilities

$$\mathbb{P}_{2\mathrm{pt}}(1,2) = \mathbb{P}_{1\mathrm{pt}}(1)\mathbb{P}_{1\mathrm{pt}}(2) = \bar{n}^2\delta V_1\delta V_2. \tag{1.7}$$

For a correlated sample the probabilities will no longer be independent and the correlation function can now be defined as the excess over random probability of finding two particles in volumes δV_1 and δV_2 separated by r_{12}

$$\mathbb{P}_{2\mathrm{pt}}(1,2) = \bar{n}^2\left[1+\xi(r_{12})\right]\delta V_1\delta V_2. \tag{1.8}$$

Since the probability of having a particle in δV_1 is given by $\bar{n}\delta V_1$, we can write the conditional probability to find a particle in δV_2 given there is one in δV_1

$$\mathbb{P}_{1\mathrm{pt}}(2|1) = \frac{\mathbb{P}_{2\mathrm{pt}}(1,2)}{\mathbb{P}_{1\mathrm{pt}}(1)} = \bar{n}\left[1+\xi(r_{12})\right]\delta V_2, \tag{1.9}$$

where we used Bayes theorem for the conditional probability. So we see that for correlated samples ($\xi(r_{12}) > 0$) the probability of finding a second particle is enhanced over random, whereas it is suppressed over random for the anti-correlated case ($\xi(r_{12}) < 0$). One can straightforwardly deduce a correlation function estimator from the above equation: count the number of neighbours in a shell of volume V around a given particle and compare to the expected number of pairs in a random field $\bar{n}V$.

We can also consider moments of the fields, which are products of the field at the same spatial location, for instance the **variance** of the field

$$\sigma_R^2 = \left\langle\delta_R^2\right\rangle = \xi_R(r=0). \tag{1.10}$$

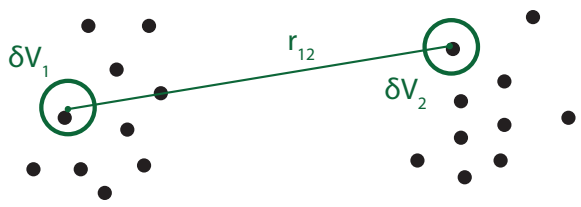

Figure 1.1.: Clustering in a point distribution with a preferred distance, i.e., correlation length.

Here the subscript R symbolizes a smoothing on a spatial scale R. We will relate the variance to the power spectrum shortly but note here that it is an important cosmological parameter describing the typical amplitude of fluctuations, which by convention is quantified in spheres of radius $R = 8\,h^{-1}$Mpc and amounts to about $\sigma_8 \approx 0.8$.

Ergodicity

We understand the Universe to be a realization of an ensemble of universes and thus expectation values are understood as averages over many realizations. As we have only one Universe at our disposal to perform measurements we need to make use of **ergodic theorem** to replace ensemble averages by spatial averages. That the two agree is non-trivial and only the case if the correlation of field values vanishes in the large distance limit, and far apart regions of the Universe can effectively be considered as separate realizations.

1.1.3. Higher order Correlators

In the simple case of linearly evolved fluctuations from single field inflation, the power spectrum or two-point function is sufficient to describe the statistics. However, deviations from the simple inflationary models, non-linear evolution or the consideration of tracers of the cosmic density distribution will require higher order correlators. The simplest of those is the **bispectrum**

$$\langle\delta(\boldsymbol{k}_1)\delta(\boldsymbol{k}_2)\delta(\boldsymbol{k}_3)\rangle = (2\pi)^3\delta^{(\mathrm{D})}(\boldsymbol{k}_1+\boldsymbol{k}_2+\boldsymbol{k}_3)B(k_1,k_2,k_3),\,. \tag{1.11}$$

Statistical homogeneity leads to the delta function that forces the three wavevectors to form a triangle and due to statistical isotropy the triangle can be fully described by three lengths or two lengths and one enclosed angle. The Fourier transform of the bispectrum is the three point correlation function $\zeta = \mathrm{FT}(B)$, which in the above probabilistic interpretation can be defined as

$$\mathbb{P}_{3\mathrm{pt}}(1,2,3) = \bar{n}^3\left[1+\xi(r_{12})+\xi(r_{23})+\xi(r_{31})+\zeta(r_{12},r_{23},r_{31})\right]\delta V_1\delta V_2\delta V_3\,. \tag{1.12}$$

Adding yet another field we obtain the **trispectrum**

$$\langle\delta(\boldsymbol{k}_1)\delta(\boldsymbol{k}_2)\delta(\boldsymbol{k}_3)\delta(\boldsymbol{k}_4)\rangle = (2\pi)^3\delta^{(\mathrm{D})}(\boldsymbol{k}_1+\boldsymbol{k}_2+\boldsymbol{k}_3+\boldsymbol{k}_4)T(k_1,k_2,k_3,k_4,|\boldsymbol{k}_1+\boldsymbol{k}_2|,|\boldsymbol{k}_2+\boldsymbol{k}_3|)\,, \tag{1.13}$$

which we will encounter again when discussing cosmic variance below.

1.2. Fourier Space

It will prove convenient to build up the actual density field from a superposition of modes that describe the behaviour on a certain scale.
We introduce the following Fourier convention:

$$\delta(\boldsymbol{k}) = \int \mathrm{d}^3r\exp\left[-\mathrm{i}\boldsymbol{k}\cdot\boldsymbol{r}\right]\delta(\boldsymbol{r}), \tag{1.14}$$

$$\delta(\boldsymbol{r}) = \int \frac{\mathrm{d}^3k}{(2\pi)^3}\exp\left[\mathrm{i}\boldsymbol{k}\cdot\boldsymbol{r}\right]\delta(\boldsymbol{k}). \tag{1.15}$$

The k-space representation of the nabla operator is given by $\boldsymbol{\nabla}\to\mathrm{i}\boldsymbol{k}$. More often than not, the configuration space fields will be real, leading to $\delta^*(\boldsymbol{k}) = \delta(-\boldsymbol{k})$. Under a spatial shift $\boldsymbol{x}\to\boldsymbol{x}+\boldsymbol{\Delta x}$ the Fourier modes transform as

$$\delta(\boldsymbol{k})\to\exp\left[\mathrm{i}\boldsymbol{k}\cdot\boldsymbol{\Delta x}\right]\delta(\boldsymbol{k}) \tag{1.16}$$

and the power spectrum thus transforms as

$$\delta(\boldsymbol{k})\delta(\boldsymbol{k}')\to\delta(\boldsymbol{k})\delta(\boldsymbol{k}')\exp\left[\mathrm{i}(\boldsymbol{k}+\boldsymbol{k}')\cdot\boldsymbol{\Delta x}\right], \tag{1.17}$$

thus invariance under translations obviously requires $\boldsymbol{k}' = -\boldsymbol{k}$ and thus $\delta^{(\mathrm{D})}(\boldsymbol{k}+\boldsymbol{k}')$. An equivalent argument can be made for higher n-point functions.

The Dirac delta function is thus given by

$$\delta^{(\mathrm{D})}(\boldsymbol{x}+\boldsymbol{x}') = \int \frac{\mathrm{d}^3 q}{(2\pi)^3} \exp\left[\mathrm{i}(\boldsymbol{x}+\boldsymbol{x}')\boldsymbol{q}\right]. \tag{1.18}$$

In particular, for finite volumes this leads to

$$\delta^{(\mathrm{D})}(\boldsymbol{k}-\boldsymbol{k}') = \frac{V}{(2\pi)^3}\delta^{(\mathrm{K})}_{\boldsymbol{k},\boldsymbol{k}'}\,. \tag{1.19}$$

An important advantage of working in Fourier space is that convolutions in real space become simple multiplications in k-space as per the **convolution theorem**

$$f(\boldsymbol{x}) = [g \star h](\boldsymbol{x}) = \int \mathrm{d}^3 y\; g(\boldsymbol{y})h(\boldsymbol{x}-\boldsymbol{y}) \Rightarrow f(\boldsymbol{k}) = g(\boldsymbol{k})h(\boldsymbol{k}). \tag{1.20}$$

This is of particular advantage, when **smoothing** operations are considered.

$$f_R(\boldsymbol{x}) = \int \mathrm{d}^3 y\; W_R(\boldsymbol{y})f(\boldsymbol{x}-\boldsymbol{y}) \Rightarrow f_R(\boldsymbol{k}) = f(\boldsymbol{k})W_R(\boldsymbol{k}). \tag{1.21}$$

For the variance of spheres in real space we consider a spatial **top-hat filter** $W_{\mathrm{TH},R}(r) = 3\theta(R-r)/4\pi R^3$ leading to

$$W_{\mathrm{TH},R}(k) = 3\frac{\sin(kR) - (kR)\cos(kR)}{(kR)^3} \tag{1.22}$$

In case of spherical symmetry we can perform the angular integration in the definition of the Fourier transform

$$f(r) = \frac{1}{2\pi^2}\int \mathrm{d}k\; k^2 \frac{\sin kr}{kr} f(k) = \frac{1}{2\pi^2}\int \mathrm{d}k\; k^2 j_0(kr) f(k) \tag{1.23}$$

where j_0 is the spherical Bessel function. For the inverse transform this yields

$$f(k) = 4\pi \int \mathrm{d}r\; r^2 j_0(kr) f(r). \tag{1.24}$$

$$\begin{aligned}\xi(r) &= \int \frac{\mathrm{d}^3 k}{(2\pi)^3}\int \frac{\mathrm{d}^3 k'}{(2\pi)^3}\left\langle\delta(\boldsymbol{k})\delta(\boldsymbol{k}')\right\rangle \exp\left[\mathrm{i}\boldsymbol{k}\cdot\boldsymbol{x}\right]\exp\left[\mathrm{i}\boldsymbol{k}'\cdot(\boldsymbol{x}+\boldsymbol{r})\right],\\ &= \int \frac{\mathrm{d}^3 k}{(2\pi)^3} P(k)\exp\left[\mathrm{i}\boldsymbol{k}\cdot\boldsymbol{r}\right] = \frac{1}{2\pi^2}\int \mathrm{d}k k^2 P(k) j_0(kr)\,.\end{aligned} \tag{1.25}$$

In the other direction we have

$$\begin{aligned}\left\langle\delta(\boldsymbol{k})\delta(\boldsymbol{k}')\right\rangle &= \int \mathrm{d}^3 x \int \mathrm{d}^3 x' \exp\left[-\mathrm{i}\boldsymbol{k}\cdot\boldsymbol{x}\right]\exp\left[-\mathrm{i}\boldsymbol{k}'\cdot\boldsymbol{x}\right]\left\langle\delta(\boldsymbol{x})\delta(\boldsymbol{x}')\right\rangle\\ &= (2\pi)^3\delta^{(\mathrm{D})}(\boldsymbol{k}+\boldsymbol{k}')\int \mathrm{d}^3 r \exp\left[-\mathrm{i}\boldsymbol{k}'\cdot\boldsymbol{r}\right]\xi(r)\,.\end{aligned} \tag{1.26}$$

Since the last line has the same form as the definition of the power spectrum, the power spectrum is in turn related to the correlation function by

$$P(k) = \int \mathrm{d}^3 r \xi(r)\exp\left[-\mathrm{i}\boldsymbol{k}\cdot\boldsymbol{r}\right] = 4\pi\int \mathrm{d}r r^2 \xi(r) j_0(kr)\,. \tag{1.27}$$

Let us finally consider the **variance** of the smoothed density field

$$\sigma_R^2 = \left\langle\delta^2_{\mathrm{TH},R}\right\rangle = \frac{1}{2\pi^2}\int \mathrm{d}k k^2 P(k) W^2_{\mathrm{TH},R}(k)\,. \tag{1.28}$$

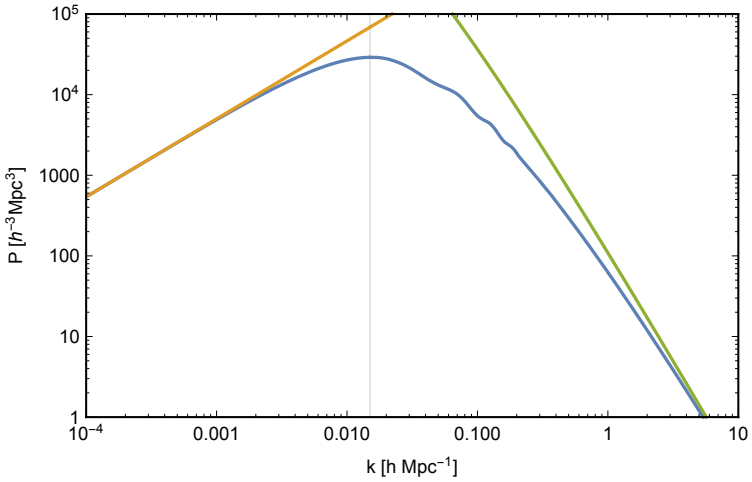

Figure 1.2.: Linear matter power spectrum $P_{\delta\delta}$ of the ΛCDM model (blue) and its low- and high-k approximations.

1.3. Recap: Shape of the Power Spectrum

The shape of the matter power spectrum is given by linear transformations of the power spectrum generated by inflation. In the cosmology course it was shown that the power spectrum of the metric perturbations scales as

$$P_{\mathcal{RR}}(k) \propto k^{n_\mathrm{s}-4} \tag{1.29}$$

where n_s is proportional to the slow-roll parameters and observed to be close to unity $n_\mathrm{s} \approx 0.967$. The modes seeded during inflation are subject to different total growth rates depending on whether they reentered the horizon before or after matter-radiation equality. To account for this fact it is convenient to introduce the **transfer function** $T(k)$, which can be implicitly defined as a relation between the late matter power spectrum after recombination and the seed fluctuations produced by inflation

$$P_{\delta\delta}(k) \propto T^2(k) k^4 P_{\mathcal{RR}}(k) \propto T^2(k) k^{n_\mathrm{s}} \tag{1.30}$$

where we used that inside the horizon $k^2\mathcal{R} \propto k^2\phi \propto \delta$

- outside the horizon potential fluctuations are constant ⇒ transfer function constant on large scales
- modes that enter during radiation domination have a supressed growth ⇒ transfer function is supressed on small scales

As you have discussed in the cosmology course last term, the transfer function can be parametrized as

$$T^2(k) \propto \begin{cases} 1 & k < k_\mathrm{eq}\,, \\ \frac{k_\mathrm{eq}^4}{k^4}\left(1+\ln\left(\frac{k}{k_\mathrm{eq}}\right)\right)^2 & k > k_\mathrm{eq}\,. \end{cases} \tag{1.31}$$

The expansion factor at equality is given by

$$a_\mathrm{eq} = \frac{\Omega_{\mathrm{r},0}}{\Omega_{\mathrm{m},0}} \tag{1.32}$$

and we can use $\rho_\mathrm{r} = \frac{\pi^2}{15} T_\mathrm{CMB}^4$ to calculate the radiation density parameter $\Omega_{\mathrm{r},0} \approx 8 \times 10^{-5}$ yielding $a_\mathrm{eq} \approx 3 \times 10^{-4}$. The horizon wavenumber at equality is then given by $k_\mathrm{eq}/\mathcal{H}_\mathrm{eq} = 1$, giving $k_\mathrm{eq} \approx 0.015 h^{-1}\mathrm{Mpc}$. An example of the power spectrum as well as its low- and high-k limits is given in Fig. 1.2. The power spectrum thus contains information about the initial conditions, which are unperturbed on large scales as well as information on the various components affecting the suppression of growth on small scales. The mass of neutrinos for instances directly affects the matter transfer function and allows us to put constraints on neutrino mass that are close to the minimal mass required from neutrino oscillation experiments. The

full shape of the transfer function can be obtained using Boltzmann solvers such as CMBfast, CAMB or CLASS.

Let us focus on the impact and relevance of the **Baryon Acoustic Oscillation** (BAO) feature in the correlation function and power spectrum. In the correlation function the BAO shows up as a distinct feature at $r_{\rm BAO} \approx 100\ h^{-1}$Mpc. Let us for simplicity consider the BAO to be a Dirac delta function in one spatial dimension and calculate the corresponding power spectrum

$$P_{\rm 1D}(k) = \int \mathrm{d}x\ \left[\delta^{(\rm D)}(x - r_{\rm BAO}) + \delta^{(\rm D)}(x + r_{\rm BAO})\right] \exp\left[-\mathrm{i}kx\right] = 2\cos(kr_{\rm BAO})\,. \tag{1.33}$$

We thus see that the wiggles in the power spectrum correspond to a spatially localized feature in the correlation function. In reality the BAO gets broadended at a scale w in the correlation function and the corresponding wiggles in the power spectrum are suppressed at high wavenumbers

$$\begin{aligned} P(k) &= \int \mathrm{d}x\ \frac{1}{\sqrt{2\pi}w}\left\{\exp\left[-\frac{(x - r_{\rm BAO})^2}{2w^2}\right] + \exp\left[-\frac{(x + r_{\rm BAO})^2}{2w^2}\right]\right\}\exp\left[-\mathrm{i}kx\right] \\ &= 2\cos(kr_{\rm BAO})\exp\left[-\frac{1}{2}k^2w^2\right]. \end{aligned} \tag{1.34}$$

The BAO scale is very well known from CMB observations and thus forms a standard ruler in LSS. When observing this scale in transverse galaxy clustering we are probing the angular diameter distance and when observing it along the line of sight, we are probing the Hubble rate. Both of these quantities depend on the expansion history of the Universe and thus on the dark energy equation of state $w = p/\rho$. Constraining the dark energy equation of state at the 10% level requires 1% precision in the measurement of distances or $H(z)$.

1.4. Gaussian Random Fields

1.4.1. Probability and Characteristic Function

Gaussian Random Field

A vector $\boldsymbol{f} = [f_1, \ldots, f_N]$ of random variables is called Gaussian, if the joint probability density function (PDF) is a multivariate Gaussian

$$\mathbb{P}(\boldsymbol{f}) = \frac{1}{\sqrt{(2\pi)^N |C|}} \exp\left[-\frac{1}{2} f_i C^{-1}_{ij} f_j\right], \tag{1.35}$$

where the positive definite, symmetric $N \times N$-matrix $C_{ij} = \langle f_i f_j \rangle$ is called the **covariance matrix**. A random field $f : \mathbb{R}^3 \to \mathbb{R}$ is a **Gaussian random field** (GRF) if for arbitrary collections of field points $(\boldsymbol{x}_1, \ldots, \boldsymbol{x}_N)$ the variables $[f(\boldsymbol{x}_1), \ldots, f(\boldsymbol{x}_N)]$ are joint Gaussian variables.

For the GRF, the PDF can be expressed as a Gaussian functional of f, for practical purposes we will often work with a finite set of tracer points or pixels and denote $f_i = f(\boldsymbol{x}_i)$.

For a GRF, by statistical homogeneity the covariance matrix C can only depend on the separation $\boldsymbol{x}_i - \boldsymbol{x}_j$ and by statistical isotropy only on the magnitude $|\boldsymbol{x}_i - \boldsymbol{x}_j|$. As $f(\boldsymbol{k})$ is linear in $f(\boldsymbol{x})$, the PDF of the Fourier modes $f(\boldsymbol{k})$ is Gaussian as well. In particular, the canonical commutation relations and the resulting momentum conserving delta function ensure a diagonal covariance matrix for the Fourier modes. As you can show yourself, irrelevant degrees of freedom can be integrated out from the PDF

$$\mathbb{P}(f_1, \ldots, f_{N-M}) = \left\{\prod_{i=N-M+1}^{N} \int \mathrm{d}f_i\right\} \mathbb{P}(\boldsymbol{f})\,. \tag{1.36}$$

The simplest inflationary models predict Gaussian primordial fluctuations, but there are distinct models that can predict non-Gaussian features. Those were studied in the first part of this course and for now we will work under the assumption of Gaussian seeds. The Gaussian property is conserved by linear evolution. As the (primary) CMB is very nearly linear in the initial fluctuations the fluctuations look very Gaussian, there are however small non-Gaussian deviations imprinted by gravitational lensing of CMB photons by the large-scale structure of the Universe. Non-linear structure formation at late times leads to strong deviations from Gaussianity that will be discussed in the last part of this course.

Let us first note that the multivariate Gaussian is appropriately normalized, i.e., that the probability integrates to unity $\int \mathrm{d}^N f \mathbb{P}(\boldsymbol{f}) = 1$

$$\int \mathrm{d}^N f \ \mathbb{P}(\boldsymbol{f}) = \prod_i \Big\{ \int_{-\infty}^{\infty} \mathrm{d}f_i \Big\} \frac{1}{\sqrt{(2\pi)^N |C|}} \exp\left[-\frac{1}{2} f_i C_{ij}^{-1} f_j \right] . \tag{1.37}$$

Let us orthogonalize $C^{-1} = O^{-1} D O$ (where $O^{-1} = O^{\mathrm{T}}$) and $y = O^{-1} f$, i.e., we are performing a rotation in the Euclidean space we are integrating over. With $D = \mathrm{diag}\left\{1/\sigma_i^2\right\}$ we have

$$\prod_i \Big\{ \int_{-\infty}^{\infty} \mathrm{d}y_i \frac{1}{\sqrt{2\pi\sigma_i^2}} \exp\left[-\frac{1}{2} \frac{y_i^2}{\sigma_i^2} \right] \Big\} = 1 . \tag{1.38}$$

For the density field at one point we have thus

$$\mathbb{P}(\delta) = \frac{1}{\sqrt{2\pi}\sigma} \exp\left[-\frac{1}{2} \frac{\delta^2}{\sigma^2} \right] . \tag{1.39}$$

This can be used to calculate the probability of a point in a density field smoothed on scale R to exceed a certain density threshold δ_{c}

$$\mathbb{P}(\delta_R > \delta_{\mathrm{c}}) = \frac{1}{\sqrt{2\pi}\sigma} \int_{\delta_{\mathrm{c}}}^{\infty} \mathrm{d}\delta \ \exp\left[-\frac{1}{2} \frac{\delta^2}{\sigma^2} \right] = \frac{1}{2} \mathrm{erfc}\left(\frac{\delta_{\mathrm{c}}}{\sqrt{2}\sigma_R} \right) \tag{1.40}$$

We will return to this towards the end of this course, when we calculate the abundance of collapsed objects (dark matter haloes), which can be identified with regions of mass $M \propto R^3$ whose linear overdensity is exceeding the threshold $\delta_{\mathrm{c}} = 1.686$.

We can now calculate the **characteristic function** of the Gaussian PDF

$$\mathcal{M}(\mathrm{i}\boldsymbol{J}) = \langle \exp\left[\mathrm{i}\boldsymbol{J} \cdot \boldsymbol{f} \right] \rangle = \int \mathrm{d}^N f \frac{1}{\sqrt{(2\pi)^N |C|}} \exp\left[-\frac{1}{2} f_i C_{ij}^{-1} f_j + \mathrm{i} J_i f_i \right] = \exp\left[-\frac{1}{2} J_i C_{ij} J_j \right] \tag{1.41}$$

This Gaussian integral can be easily evaluated by completing the squares. Generic moments of the field f can now be generated from derivatives of the characteristic function at $J = 0$

$$\langle f_{i_1} \dots f_{i_N} \rangle = (-\mathrm{i})^N \frac{\partial}{\partial J_{i_1}} \dots \frac{\partial}{\partial J_{i_N}} \langle \exp\left[\mathrm{i}\boldsymbol{J} \cdot \boldsymbol{f} \right] \rangle \Big|_{J=0} \tag{1.42}$$

Let us first show that the correlation function is indeed $\langle f_i f_j \rangle = C_{ij}$. For $N = 2$ we obtain

$$\begin{aligned} \langle f_m f_n \rangle =& (-\mathrm{i})^2 \frac{\partial}{\partial J_m} \frac{\partial}{\partial J_n} \langle \exp\left[\mathrm{i}\boldsymbol{J} \cdot \boldsymbol{f} \right] \rangle \Big|_{J=0} \\ =& \frac{\partial}{\partial J_m} \left(J_j C_{jm} \exp\left[-\frac{1}{2} J_i C_{ij} J_j \right] \right) \Big|_{J=0} = C_{mn} , \end{aligned} \tag{1.43}$$

which proves that the components of the covariance matrix are indeed given by the correlation function.

1.4.2. Gaussian Random Fields in Fourier Space*

Note that the real and imaginary part of the complex density $\delta(\boldsymbol{k}) = a(\boldsymbol{k}) + \mathrm{i}b(\boldsymbol{k})$ field are independent Gaussian random fields with variance $P/2$

$$\langle a(\boldsymbol{k})a(\boldsymbol{k}')\rangle = \frac{1}{4}\langle(\delta+\delta^*)(\delta+\delta^*)\rangle = (2\pi)^3\delta^{(\mathrm{D})}(\boldsymbol{k}-\boldsymbol{k}')\frac{P}{2} + (\boldsymbol{k}'\to-\boldsymbol{k}') \tag{1.44}$$

$$\langle b(\boldsymbol{k})b(\boldsymbol{k}')\rangle = -\frac{1}{4}\langle(\delta-\delta^*)(\delta-\delta^*)\rangle = (2\pi)^3\delta^{(\mathrm{D})}(\boldsymbol{k}-\boldsymbol{k}')\frac{P}{2} - (\boldsymbol{k}'\to-\boldsymbol{k}') \tag{1.45}$$

$$\langle a(\boldsymbol{k})b(\boldsymbol{k}')\rangle = \frac{1}{4\mathrm{i}}\langle(\delta+\delta^*)(\delta-\delta^*)\rangle = 0 \tag{1.46}$$

Thus realisations can be generated by drawing real and imaginary parts from independent Gaussian distributions with mean zero and variance $P/2$. While the real and imaginary parts are independent Gaussian distributed, the magnitude of δ follows a Rayleigh distribution. This can be seen as follows: Both real and imaginary parts are Gaussian distributed with variance $P/2$

$$\mathbb{P}_a(x) = \mathbb{P}_b(x) = \frac{1}{\sqrt{\pi P}}\exp\left[-\frac{x^2}{P}\right] \tag{1.47}$$

The probability has to be invariant under a reparametrization and thus going to polar coordinates $\delta(\boldsymbol{k}) = a(\boldsymbol{k}) + \mathrm{i}b(\boldsymbol{k}) = r\exp[\mathrm{i}\phi]$ yields

$$\mathbb{P}_{|\delta|}(r)\mathbb{P}_\varphi(\varphi)\mathrm{d}r\mathrm{d}\varphi = \mathbb{P}_a(a)\mathbb{P}_a(b)\mathrm{d}a\mathrm{d}b = \frac{r}{\pi P}\exp\left[-\frac{r^2}{P}\right]\mathrm{d}r\mathrm{d}\varphi\,. \tag{1.48}$$

Thus, the probability is uniform for the phase of the mode and Rayleigh for the magnitude.

$$\mathbb{P}_{|\delta|}(r) = \frac{2r}{P}\exp\left[-\frac{r^2}{P}\right], \qquad \mathbb{P}_\varphi(\varphi) = \frac{1}{2\pi}\,. \tag{1.49}$$

1.4.3. Wick's Theorem

Let us state an important result for Gaussian random fields[2]

Wick's Theorem

For a mean zero Gaussian random field the reduced correlation functions of order higher than two either vanish (odd number of fields) or are expressible in terms of products of two-point functions summed over all possible pairings (even number of fields).

$$\begin{aligned}\left\langle f_{i_1},\ldots,f_{i_{2N+1}}\right\rangle &= 0,\\ \left\langle f_{i_1},\ldots,f_{i_{2N}}\right\rangle &= \sum_{\text{ordered pairings }\mathcal{P}_a}\ \prod_{\text{pairs }(i,j)\text{ in the pairing }\mathcal{P}_a} C_{ij}.\end{aligned} \tag{1.50}$$

The odd case obviously vanishes, for the even case it follows from Eq. (1.42).

Alternatively one can also consider all $(2N)!$ possible permutations of $(i_1,\ldots,i_{2N})$, cut each of them up in subsequent pairs and remove the redundancies by dividing by appropriate factors

$$\langle f_{i_1},\ldots,f_{i_{2N}}\rangle = \frac{1}{2^N N!}\underbrace{\left(C_{i_1i_2}C_{i_3i_4}\ldots C_{i_{2N-1}i_{2N}} + \text{perm}\right)}_{(2N)!\text{ permutations}}. \tag{1.51}$$

The factor 2^N counts the redundant terms arising from exchanges of indices $C_{ij} \leftrightarrow C_{ji}$ which leaves the correlator unaffected due to the symmetry of the covariance matrix. The factor $N!$ counts possible

[2] In cosmology this theorem was introduced by Isserlis, but is often associated with the QFT version introduced by Wick.

reorderings of whole pairs $C_{ij}C_{mn} \leftrightarrow C_{mn}C_{ij}$ which leave the correlator unaffected as well. The number of products of correlation functions in the correlator of $2N$ fields is thus $(2N)!/(2^N N!) = (2N-1)!!$. You can convince yourself that this is the case by calculating the four point function explicitly and by induction going from $2N$ to $2N+2$.

In summary, the procedure for calculating correlators of GRF is thus:

1. We first generate all $(2N-1)!!$ possible ordered pairings of indices from $(i_1, \ldots, i_{2N})$, i.e., we generate $\mathcal{P} = \{[(i_1, i_2), \ldots, (i_{2N-1}, i_{2N})], \ldots, [(i_1, i_{2N}), \ldots, (i_2, i_{2N-1})]\}$. For the sake of definiteness we choose $i < j$ for the pairings (i, j).
2. For each of these pairings in $\mathcal{P}$ calculate the product of N correlators, e.g. for $\mathcal{P}_1$ evaluate $C_{i_1 i_2} \ldots C_{i_{2N-1} i_{2N}}$
3. Sum over all of these products of correlators.

Let us consider the example of the four point function. We expect that there will be $3!! = 3$ contributing terms. Indeed, there are three different fields that f_1 can be correlated with. Once this partner for f_1 has been chosen, the remaining fixed pair is correlated as well.

$$\begin{aligned}\langle f_1 f_2 f_3 f_4\rangle =& \langle \overbrace{f_1 f_2} \overbrace{f_3 f_4}\rangle + \langle \overbrace{f_1 \overbrace{f_2 f_3} f_4}\rangle + \langle \overbrace{f_1 \overbrace{f_2 f_3 f_4}}\rangle \\ =& C_{12}C_{34} + C_{13}C_{24} + C_{14}C_{23}\end{aligned} \tag{1.52}$$

In Fourier space this leads to

$$\begin{aligned}\left\langle \delta(\boldsymbol{k}_{i_1}), \ldots, \delta(\boldsymbol{k}_{i_{2N+1}})\right\rangle =& \quad 0, \\ \langle \delta(\boldsymbol{k}_{i_1}), \ldots, \delta(\boldsymbol{k}_{i_{2N}})\rangle =& \sum_{\text{ordered pairings } \mathcal{P}_a} \prod_{\text{pairs } (i,j) \text{ in the pairing } \mathcal{P}_a} \langle \delta(\boldsymbol{k}_i), \delta(\boldsymbol{k}_j)\rangle \,.\end{aligned} \tag{1.53}$$

1.4.4. Weakly non-Gaussian Fields

Let us consider the **moment generating function** which is closely related to the characteristic function discussed in Eq. (1.41) above

$$\mathcal{M}(J) = \sum_{p=0}^{\infty} \frac{\langle \delta^p \rangle}{p!} J^p = \langle \exp[J\delta]\rangle = \int \mathrm{d}\delta\, \mathbb{P}(\delta) \exp[J\delta]\,. \tag{1.54}$$

For a Gaussian field we obviously have

$$\mathcal{M}(J) = \exp\left[\frac{1}{2} J^2 \sigma^2\right] = 1 + \frac{\sigma^2}{2!} J^2 + \frac{3\sigma^4}{4!} J^4 + \ldots \tag{1.55}$$

The moment generating function is the Laplace transform of the PDF and thus the PDF can be written as the inverse Laplace transform of the moment generating function

$$\mathbb{P}(\delta) = \int_{-\mathrm{i}\infty}^{\mathrm{i}\infty} \frac{\mathrm{d}J}{2\pi\mathrm{i}} \exp[-\delta J] \mathcal{M}(J) \tag{1.56}$$

For a Gaussian PDF we can replace $y = -\mathrm{i}J$ and perform the Gaussian integral

$$\mathbb{P}(\delta) = \int_{-\infty}^{\infty} \frac{\mathrm{d}y}{2\pi} \exp\left[-\frac{1}{2}\sigma^2 y^2 - \mathrm{i}y\delta\right] = \frac{1}{\sqrt{2\pi}\sigma} \exp\left[-\frac{1}{2}\frac{\delta^2}{\sigma^2}\right] \tag{1.57}$$

Let us now consider a field that has a non-vanishing cubic moment $\langle \delta^3 \rangle = S_3 \sigma^4$ with $S_3 \ll 1$. Writing the moment generating function as

$$\mathcal{M}(J) = \exp\left[\frac{1}{2} J^2 \sigma^2\right] \left(1 + \frac{\sigma^4 S_3}{3!} J^3\right)\,, \tag{1.58}$$

we obtain for the PDF

$$\mathbb{P}(\delta) = \frac{1}{\sqrt{2\pi}\sigma} \exp\left[-\frac{1}{2}\frac{\delta^2}{\sigma^2}\right]\left(1 + \frac{S_3(\delta^3 - 3\delta\sigma^2)}{3!\sigma^2}\right). \tag{1.59}$$

This is the leading correction to the Gaussian PDF, a more general form is known as the **Edgeworth** or **Gram-Charlier expansion** of the PDF

$$\mathbb{P}(\delta) = \frac{1}{\sqrt{2\pi}\sigma^2} \exp\left[-\frac{1}{2}\nu^2\right]\left[1 + \sigma\frac{S_3 H_3(\nu)}{6} + \sigma^2\left(\frac{S_4 H_4(\nu)}{24} + \frac{S_3^2 H_6(\nu)}{72}\right) + \dots\right], \tag{1.60}$$

where $\nu = \delta/\sigma$ and $H_n(\nu)$ are the Hermite polynomials. Note that the Edgeworth expansion can also be written as a derivative operator acting on the Gaussian PDF

$$\mathbb{P}(\delta) = \left(1 - \frac{S_3\sigma^4}{3!}\frac{\partial^3}{\partial\delta^3}\right)\mathbb{P}_{\rm G}(\delta). \tag{1.61}$$

1.4.5. The simplest form of non-Gaussianity

Non-Gaussian fields can be straightforwardly generated from Gaussian fields by non-linear transformations. Let us consider a very simple model for relating the fluctuations in the galaxy distribution $\delta_{\rm g}$ to the underlying Gaussian matter distribution δ, the so called local bias model, which we will discuss in much more detail at the end of this course

$$\delta_{\rm g}(\boldsymbol{x}) = b_1\delta(\boldsymbol{x}) + \frac{b_2}{2}(\delta^2(\boldsymbol{x}) - \sigma^2) + \mathcal{O}(\delta^3). \tag{1.62}$$

Here the subtraction of the variance in the squared term ensures that the galaxy overdensity averages to zero. Let us now consider the above model in Fourier space, as we have seen before, squaring in real space corresponds to convolutions in Fourier space

$$\delta_{\rm g}(\boldsymbol{k}) = b_1\delta(\boldsymbol{k}) + \frac{b_2}{2}\int\frac{{\rm d}^3q}{(2\pi)^2}\delta(\boldsymbol{q})\delta(\boldsymbol{k}-\boldsymbol{q}) = \delta_{\rm g}^{(1)}(\boldsymbol{k}) + \delta_{\rm g}^{(2)}(\boldsymbol{k}) \tag{1.63}$$

We can now write down the definition of the galaxy bispectrum and write down the contributions, which will start at fourth order through a correlator of a second order contribution (quadratic in the fields in the above equation) with two linear contributions.

$$\begin{aligned}(2\pi)^3\delta^{(\rm D)}(\boldsymbol{k}_1+\boldsymbol{k}_2+\boldsymbol{k}_3)B_{\rm g}(k_1,k_2,k_3) &= \langle\delta_{\rm g}(\boldsymbol{k}_1)\delta_{\rm g}(\boldsymbol{k}_2)\delta_{\rm g}(\boldsymbol{k}_3)\rangle \\ &= \left\langle\delta_{\rm g}^{(2)}(\boldsymbol{k}_1)\delta_{\rm g}^{(1)}(\boldsymbol{k}_2)\delta_{\rm g}^{(1)}(\boldsymbol{k}_3)\right\rangle + 2\text{ cyc.}\end{aligned} \tag{1.64}$$

Using the implicit definition of the linear and quadratic bias contributions in Eq. (1.63) we obtain

$$\left\langle\delta_{\rm g}^{(2)}(\boldsymbol{k}_1)\delta_{\rm g}^{(1)}(\boldsymbol{k}_2)\delta_{\rm g}^{(1)}(\boldsymbol{k}_3)\right\rangle = \frac{1}{2}b_1^2b_2\left\langle\int\frac{{\rm d}^3q}{(2\pi)^3}\delta(\boldsymbol{q})\delta(\boldsymbol{k}_1-\boldsymbol{q})\delta(\boldsymbol{k}_2)\delta(\boldsymbol{k}_3)\right\rangle \tag{1.65}$$

Wick theorem would allow for three different pairings, however the $\langle\delta(\boldsymbol{q})\delta(\boldsymbol{k}_1-\boldsymbol{q})\rangle$ correlator only contributes to the homogenous $\boldsymbol{k}_1 = 0$ mode that is irrelevant for our purposes. The remaining two correlators link the $\boldsymbol{q}$-mode with either $\boldsymbol{k}_2$ or $\boldsymbol{k}_3$. Both of these give the same result as we can exchange $\boldsymbol{q}\leftrightarrow\boldsymbol{k}-\boldsymbol{q}$ in the momentum integral. We obtain

$$\begin{aligned}\left\langle\delta_{\rm g}^{(2)}(\boldsymbol{k}_1)\delta_{\rm g}^{(1)}(\boldsymbol{k}_2)\delta_{\rm g}^{(1)}(\boldsymbol{k}_3)\right\rangle =& b_1^2b_2\int\frac{{\rm d}^3q}{(2\pi)^3}(2\pi)^3\delta^{(\rm D)}(\boldsymbol{q}+\boldsymbol{k}_2)P(k_2)(2\pi)^3\delta^{(\rm D)}(\boldsymbol{k}_1-\boldsymbol{q}+\boldsymbol{k}_3)P(k_3) \\ =& b_1^2b_2(2\pi)^3\delta^{(\rm D)}(\boldsymbol{k}_1+\boldsymbol{k}_2+\boldsymbol{k}_3)P(k_2)P(k_3)\end{aligned} \tag{1.66}$$

One of the delta functions collapsed the momentum integral and the remaining momentum conserving delta function just reproduces the one required in the definition of the bispectrum in Eq. (1.64). Thus, we finally obtain for the bispectrum in the simple quadratic bias model

$$B_{\rm g}(k_1,k_2,k_3) = b_1^2b_2\left[P(k_1)P(k_2) + 2\text{ cyc.}\right]. \tag{1.67}$$

We will discuss a prescription to derive this result from Feynman diagrams later this term.

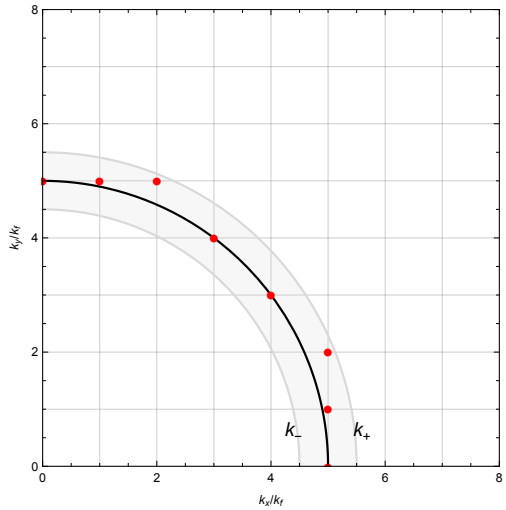

Figure 1.3.: Discrete Fourier grid and discrete modes (red points) contributing to a wavenumber bin (gray shaded region) centered around k.

1.5. Estimators and Cosmic Variance

Given a dataset, i.e., a realization of the underlying statistical ensemble, we need to estimate the relevant statistics and the uncertainty of that estimate.

In observations and numerical simulations the volume is limited, which leaves us with finite Fourier modes, the smallest of them given by the **fundamental mode** $k_\mathrm{f} = 2\pi/L$ and the corresponding volume of the **fundamental cell** is $V_\mathrm{f} = (2\pi)^3/V$. The Dirac Delta function rewritten for discrete k as

$$\delta^{(\mathrm{D})}(\boldsymbol{k_i} - \boldsymbol{k_j}) = \delta^{(\mathrm{D})}\left((\boldsymbol{i} - \boldsymbol{j})k_\mathrm{f}\right) = \frac{1}{k_\mathrm{f}^3}\delta^{(\mathrm{D})}(\boldsymbol{i} - \boldsymbol{j}) = \frac{V}{(2\pi)^3}\delta^{(\mathrm{K})}_{\boldsymbol{i},\boldsymbol{j}} \tag{1.68}$$

All the Fourier modes can now be expressed as $\boldsymbol{k_i} = \boldsymbol{i}k_\mathrm{f}$, where $\boldsymbol{i} = (i_x, i_y, i_z)$ is an integer vector.

1.5.1. Power Spectrum Estimator and Variance

The power spectrum for discrete cells is thus given by

$$V\delta^{(\mathrm{K})}_{\boldsymbol{k},\boldsymbol{k'}} P\left(|\boldsymbol{k}|\right) = \langle \delta(\boldsymbol{k})\delta^*(\boldsymbol{k'})\rangle \tag{1.69}$$

We estimate the power spectrum in bins, i.e. spherical shells of width $\mathrm{d}k$ corresponding to an intervall in wavevector magnitude $[k\pm] = [k_-, k_+) = [k - \mathrm{d}k/2, k + \mathrm{d}k/2)$ centered at k as depicted in Fig. 1.3 averaging all possible directions for the wavevector (making use of statistical isotropy)

$$\hat{P}(k) = \frac{1}{N_k V}\sum_{\boldsymbol{k_i}\in[k_-,k_+)} \delta(\boldsymbol{k_i})\delta^*(\boldsymbol{k_i}), \tag{1.70}$$

where N_k is the number of cells in the k-bin. Effectively, we are estimating the variance of δ in a shell using N_k observations. Note that the estimator is unbiased since $\langle\hat{P}\rangle = P$. Obviously there is some freedom in choosing the configuration of the bins. Basically, the above estimator gives the mean power in the shell $[k_\pm]$, and thus it is advisable to average the theory calculations over the same bins for a fair comparison. The number of grid cells in the bin is given by the shell volume

$$V_\mathrm{shell} = \int_{[k_\pm]} \mathrm{d}^3 q \int \mathrm{d}^3 q' \delta^{(\mathrm{D})}(\boldsymbol{q} + \boldsymbol{q'}) \tag{1.71}$$

divided by the volume of the fundamental cell

$$N_k = \frac{V_{\rm shell}}{V_{\rm f}} = \frac{4\pi k^2 {\rm d}k}{V_{\rm f}} = \frac{4\pi k^3 {\rm d}\ln k}{V_{\rm f}}. \tag{1.72}$$

Let us now calculate the variance of the power spectrum estimator

$$\begin{aligned}\left\langle \hat{P}^2(k)\right\rangle - \left\langle \hat{P}(k)\right\rangle^2 =& \frac{1}{N_k^2 V^2}\sum_{\boldsymbol{k_i},\boldsymbol{k}_j\in[k\pm]} \langle\delta(\boldsymbol{k_i})\delta(-\boldsymbol{k_i})\delta(\boldsymbol{k_j})\delta(-\boldsymbol{k_j})\rangle - P^2(k)\\ =& \frac{1}{N_k^2}\sum_{\boldsymbol{k_i},\boldsymbol{k}_j\in[k\pm]} P(\boldsymbol{k_i})P(\boldsymbol{k_j}) + \frac{2}{N_k^2}\sum_{\boldsymbol{k_i}\in[k\pm]} P^2(|\boldsymbol{k_i}|) - P^2(k)\\ =& \frac{2}{N_k}P^2(k) = \frac{2V_f}{4\pi k^3 {\rm d}\ln k}P^2(k)\end{aligned} \tag{1.73}$$

Thus the relative error on the power spectrum is given by

$$\boxed{\frac{\Delta P}{P} = \sqrt{\frac{2}{N_k}}\,.} \tag{1.74}$$

The number of modes scales as k^3 for logarithmic bins and with $V_f \propto V^{-1}$ we have that the error scales as $V^{-1/2}$. Thus reducing the error bars on a power spectrum measurement requires to observe four times the volume. In the above estimate we assumed Gaussianity of the underlying field, in which case the covariance matrix is diagonal, i.e., power spectrum estimates for distinct wavenumbers are independent. In the more general case of non-Gaussian fields, the connected trispectrum contributes as well.

1.5.2. Bispectrum*

The bispectrum estimator for a fixed configuration $\{k_1, k_2, \mu = \boldsymbol{k}_1\cdot\boldsymbol{k}_2\}$ can be estimated as

$$\hat{B}(k_1,k_2,\mu) = \frac{1}{N_{\rm tr}V}\sum_{\boldsymbol{k_i}\in[k\pm]}\sum_{\boldsymbol{j}k_{\rm f}\in[k\pm,\mu\pm]}\delta(\boldsymbol{k_i})\delta(\boldsymbol{k_j})\delta(-\boldsymbol{k_i}-\boldsymbol{k_i}) \tag{1.75}$$

the estimator is unbiased since $\left\langle\hat{B}\right\rangle = B$. The number of triangles in the bin is given by the shell volume divided by the volume of the fundamental cell squared

$$N_{\rm tr} = \frac{V_{123}}{V_{\rm f}^2} = \frac{8\pi^2 k_1 k_2 k_3 ({\rm d}k)^3}{V_{\rm f}^2} \tag{1.76}$$

For the variance of the bispectrum estimator we have

$$\begin{aligned}\left\langle \hat{B}^2(k_1,k_2,\mu)\right\rangle - \left\langle \hat{B}(k_1,k_2,\mu)\right\rangle^2 =& \frac{1}{N_{\rm tr}^2V^2}\sum_{\boldsymbol{i},\boldsymbol{j},\boldsymbol{l},\boldsymbol{m}}\langle\delta(\boldsymbol{k_i})\delta(\boldsymbol{k_j})\delta(-\boldsymbol{k_i}-\boldsymbol{k_j})\delta(\boldsymbol{k_l})\delta(\boldsymbol{k_m})\delta(-\boldsymbol{k_l}-\boldsymbol{k_m})\rangle\\ & - B^2(k_1,k_2,\mu)\\ =& s_{123}\frac{V}{N_{\rm tr}^2}\sum_{\boldsymbol{i},\boldsymbol{j}}P(\boldsymbol{k_i})P(\boldsymbol{k_j})P(-\boldsymbol{k_i}-\boldsymbol{k_j})\\ =& s_{123}\frac{V}{N_{\rm tr}}P(k_1)P(k_2)P(k_3)\\ =& s_{123}\frac{(2\pi)^3 V_{\rm f}}{8\pi^2 k_1 k_2 k_3 ({\rm d}k)^3 {\rm d}\mu}P(k_1)P(k_2)P(k_3)\end{aligned} \tag{1.77}$$

The factor s_{123} takes on values of $6, 2, 1$ for general, isosceles and equilateral triangles. This is a simple consequence of the fact, that for equilateral triangles the k-modes are indistinguishable. We again assumed Gaussianity, for which $B = 0$.

1.6. Random Fields on the Sphere

We have discussed inhomogeneities in 3D space in some detail. Let us now consider the statistics required to describe anisotropies on S^2. These statistics are natural for our observations of the Universe. For instance the CMB photons are released from a spherical shell surrounding us and we naturally observe the temperature distribution on the sky as a function of azimuth and polar angle. More generally, all observations naturally live on shells of varying distance from the observer and a 3D or flat 2D description is only appropriate in small volumes. *Angular Momentum* [Brink and Satchler, 1993] is a good reference for the spherical harmonics and so is *The Cosmic Microwave Background* [Durrer, 2008], in particular its appendices.

1.6.1. Spherical Harmonics Expansion

Anisotropies on a sphere, for instance CMB fluctuations, can be expanded in **spherical harmonics** $Y_{lm}(\hat{\boldsymbol{n}})$, which are a basis for square integrable functions on S^2

$$f(\hat{\boldsymbol{n}}) = \sum_{l,m} f_{lm} Y_{lm}(\hat{\boldsymbol{n}})\,. \tag{1.78}$$

Here $\hat{\boldsymbol{n}}$ is a unit vector on the sphere $\hat{\boldsymbol{n}}\cdot\hat{\boldsymbol{n}} = 1$. The spherical harmonics are the position space representation of the eigenstates of total angular momentum $\hat{L}^2 = -\nabla^2$ and azimuthal angular momentum $\hat{L}_z = -i\partial_\phi$

$$\hat{L}^2 Y_{lm} = l(l+1) Y_{lm}\,, \tag{1.79}$$

$$\hat{L}_z Y_{lm} = m Y_{lm}\,. \tag{1.80}$$

Note in particular, that the two operators commute $[\hat{L}^2, \hat{L}_z] = 0$. Under parity, the spherical harmonics transform as $Y_{lm}(-\hat{\boldsymbol{n}}) = (-1)^l Y_{lm}(\hat{\boldsymbol{n}})$ and in our convention $Y^*_{l,m} = (-1)^m Y_{l,-m}$.
The spherical harmonics are products of associated Legendre polynomials[3] and an azimuthal phase factor

$$Y_{lm}(\theta,\phi) = \sqrt{\frac{2l+1}{4\pi}\frac{(l-m)!}{(l+m)!}}\,\mathcal{P}_l^m(\cos\theta)\;\exp\left[im\phi\right] \tag{1.83}$$

The spherical harmonics are orthonormal on the sphere

$$\int \mathrm{d}^2\Omega\; Y_{lm}(\hat{\boldsymbol{n}}) Y^*_{l'm'}(\hat{\boldsymbol{n}}) = \delta^{(\mathrm{K})}_{ll'}\delta^{(\mathrm{K})}_{mm'}\,, \tag{1.84}$$

such that the **spherical multipole coefficients** of the expansion can be calculated as

$$f_{lm} = \int \mathrm{d}^2\Omega\; f(\hat{\boldsymbol{n}}) Y^*_{lm}(\hat{\boldsymbol{n}})\;. \tag{1.85}$$

For real valued fields we thus have $f^*_{l,m} = (-1)^m f_{l,-m}$. For a practial implementation the HEALPIX[4] formalism is commonly used. An easy to use Python implementation for dealing with CMB maps, calculation

[3] Legendre polynomials can be derived from Rodrigues' formula

$$\mathcal{P}_l(x) = \frac{1}{2^l l!}\frac{\mathrm{d}^l}{\mathrm{d}x^l}(x^2-1)^l \tag{1.81}$$

whereas the associated Legendre polynomials satisfy

$$\mathcal{P}_l^m(x) = (-1)^m(1-x^2)^{m/2}\frac{\mathrm{d}^m}{\mathrm{d}x^m}\mathcal{P}_l(x) = \frac{(-1)^m}{2^l l!}(1-x^2)^{m/2}\;\frac{\mathrm{d}^{l+m}}{\mathrm{d}x^{l+m}}(x^2-1)^l \tag{1.82}$$

thus $\mathcal{P}_l^0(x) = \mathcal{P}_l(x)$.

[4] HEALPIX: Hierarchical Equal Area isoLatitude Pixelization https://healpix.jpl.nasa.gov

of f_{lm} and CMB power spectra is the HEALPY package.
Let us now calculate the angular correlation function between two points $\hat{\boldsymbol{n}}$ and $\hat{\boldsymbol{n}}'$ on the sphere. By statistical isotropy this quantity can only depend on the (cosine of) the enclosed angle $\mu = \cos\theta = \hat{\boldsymbol{n}} \cdot \hat{\boldsymbol{n}}'$ and thus allows for an expansion in Legendre polynomials

$$C(\theta) = \langle f(\hat{\boldsymbol{n}}), f(\hat{\boldsymbol{n}}')\rangle = \sum_l \frac{2l+1}{4\pi} C_l \mathcal{P}_l(\mu) = \sum_{lm} C_l Y_{lm}(\hat{\boldsymbol{n}}) Y^*_{lm}(\hat{\boldsymbol{n}}') \tag{1.86}$$

here we used the addition theorem for spherical harmonics.[5] At the same time we could have written the angular correlation function naively in terms of the expansion in spherical harmonics Eq. (1.78)

$$C(\theta) = \langle f(\hat{\boldsymbol{n}}), f(\hat{\boldsymbol{n}}')\rangle = \sum_{lm} \sum_{l'm'} \langle f_{lm} f^*_{l'm'}\rangle \, Y_{lm}(\hat{\boldsymbol{n}}) Y^*_{l'm'}(\hat{\boldsymbol{n}}') \tag{1.90}$$

From this we can directly deduce that the correlator of the spherical multipole coefficients yields two Kronecker deltas and the **angular power spectrum** C_l

$$\langle f_{lm} f^*_{l'm'}\rangle = C_l \delta^{(\mathrm{K})}_{ll'} \delta^{(\mathrm{K})}_{mm'}. \tag{1.91}$$

For a more direct proof, we can multiply with $Y^*_{l_1 m_1}(\hat{\boldsymbol{n}}) Y_{l_2 m_2}(\hat{\boldsymbol{n}}')$ and integrate over Ω and Ω'.

Explicit Expressions for the Spherical Harmonics

$$Y_{00}(\hat{\boldsymbol{n}}) = \sqrt{\frac{1}{4\pi}} \tag{1.92}$$

$$Y_{10}(\hat{\boldsymbol{n}}) = \sqrt{\frac{3}{4\pi}} \cos\theta \tag{1.93}$$

$$Y_{1\pm1}(\hat{\boldsymbol{n}}) = \sqrt{\frac{3}{8\pi}} \sin\theta e^{\pm \mathrm{i}\varphi} \tag{1.94}$$

$$Y_{20}(\hat{\boldsymbol{n}}) = \sqrt{\frac{5}{16\pi}} (3\cos^2\theta - 1) \tag{1.95}$$

$$Y_{2,\pm1}(\hat{\boldsymbol{n}}) = -\sqrt{\frac{15}{8\pi}} \sin\theta\cos\theta e^{\pm \mathrm{i}\varphi} \tag{1.96}$$

$$Y_{2,\pm2}(\hat{\boldsymbol{n}}) = \sqrt{\frac{15}{32\pi}} \sin^2\theta e^{\pm 2\mathrm{i}\varphi} \tag{1.97}$$

[5] The addition theorem for spherical harmonics states

$$\mathcal{P}_l(\hat{\boldsymbol{n}} \cdot \hat{\boldsymbol{n}}') = \frac{4\pi}{2l+1} \sum_m Y_{lm}(\hat{\boldsymbol{n}}) Y^*_{lm}(\hat{\boldsymbol{n}}') \tag{1.87}$$

$$\begin{aligned} \sum_n Y_{ln}(D^{-1}\hat{\boldsymbol{n}}) Y^*_{ln}(D^{-1}\hat{\boldsymbol{n}}') &= \sum_{m,m',n} D^l_{mn} Y_{lm}(\hat{\boldsymbol{n}}) D^{l*}_{m'n} Y_{lm'}(\hat{\boldsymbol{n}}') \\ &= \sum_m Y_{lm}(\hat{\boldsymbol{n}}) Y^*_{lm}(\hat{\boldsymbol{n}}') \end{aligned} \tag{1.88}$$

Let us now move to the special case $D^{-1}\hat{\boldsymbol{n}}' = \hat{\boldsymbol{z}}$. Using that $Y_{lm}(\hat{\boldsymbol{z}}) = \sqrt{2l+1/4\pi}\,\delta^{(\mathrm{K})}_{m0}$ we have

$$\sum_m Y_{lm}(\hat{\boldsymbol{n}}) Y_{lm}(\hat{\boldsymbol{n}}') = \sqrt{2l+1/4\pi} Y_{l0}(D^{-1}\hat{\boldsymbol{n}}) = \frac{2l+1}{4\pi} \mathcal{P}_l(\hat{\boldsymbol{n}} \cdot \hat{\boldsymbol{n}}') \tag{1.89}$$

Here we used that the polar angle of $D^{-1}\hat{\boldsymbol{n}}$ is the enclosed angle of $\hat{\boldsymbol{n}}$ and $\hat{\boldsymbol{n}}'$ and that $Y_{l0} \propto \mathcal{P}_l$.

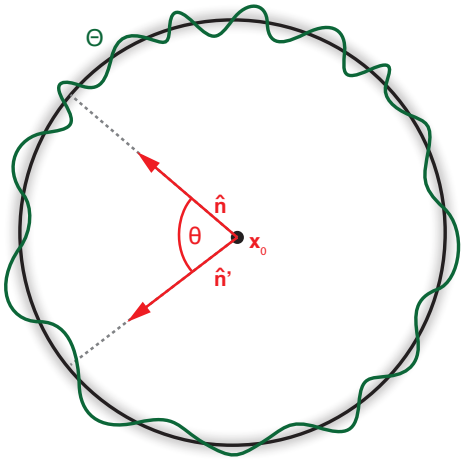

Figure 1.4.: Temperature fluctuations around the mean temperature on the sphere. By statistical isotropy the correlation function can only depend on the relative angle $\mu = \cos\theta = \hat{\boldsymbol{n}} \cdot \hat{\boldsymbol{n}}'$.

1.6.2. Rotations

For statistics on the sphere, statistical isotropy is the relevant symmetry. To understand what independence under spatial rotations entails for the statistics, let us formalize their impact on the f_{lm}. A generic spatial rotation can be described by three Euler angles (α, β, γ) and the rotation $\hat{D}(\alpha, \beta, \gamma)$ is given by *i*) a rotation around the original z-axis by γ, *ii*) a rotation around the original y-axis by β and finally *iii*) another rotation around the original z-axis by α. Obviously the inverse rotation is undoing the above in reverse order, i.e., $\hat{D}^{-1}(\alpha, \beta, \gamma) = \hat{D}(-\gamma, -\beta, -\alpha)$ and $\hat{D} f(\hat{\boldsymbol{n}}) = f(\hat{D}^{-1}\hat{\boldsymbol{n}})$

Under a rotation γ around the z-axis, the spherical harmonics transform as

$$[\hat{D}(0, 0, \gamma) Y_{lm}](\theta, \phi) = Y_{lm}(\theta, \phi - \gamma) = \exp\left[-\mathrm{i}m\gamma\right] Y_{lm}(\theta, \phi)\,. \tag{1.98}$$

Thus the $\hat{L}_i$ are the generators of rotations about the coordinate axes.

$$\hat{D}(\alpha, \beta, \gamma) = \exp\left[-\mathrm{i}\alpha \hat{L}_z\right] \exp\left[-\mathrm{i}\beta \hat{L}_y\right] \exp\left[-\mathrm{i}\gamma \hat{L}_z\right] \tag{1.99}$$

The total and azimuthal angular momentum operators commute. Thus, the total angular momentum is the same in the original and rotated frame and the rotated Y_{lm} can be expressed as a linear combination of the original $(2l + 1)$ Y_{lm}

$$\hat{D} Y_{lm} = \sum_{m'} D^{l}_{m'm} Y_{lm'} \tag{1.100}$$

The transformation matrices are the **Wigner D** matrices.

Acting with the rotation operator on a test function f we have

$$\hat{D} f(\hat{\boldsymbol{n}}) = \sum_{l,m} f_{lm} \hat{D} Y_{lm} = \sum_{l,m'} \sum_{m} f_{lm} D^{l}_{m'm} Y_{lm'}(\hat{\boldsymbol{n}}) = \sum_{l,m'} f_{lm'} Y_{lm'}(\hat{\boldsymbol{n}}) \tag{1.101}$$

Thus the multipole coefficients transform as

$$\tilde{f}_{lm'} = \sum_{m} D_{m'm} f_{lm}\,, \tag{1.102}$$

where the index of $D_{m'm}$ that is summed over is exchanged wrt Eq. (1.100). The rotation operator is unitary

$$\hat{D}^{-1} = \hat{D}^{\dagger}\,. \tag{1.103}$$

This property is inherited by the Wigner D matrices

$$\begin{aligned}\delta^{(\mathrm{K})}_{mm'} &= \int \mathrm{d}\Omega_n \; Y_{lm}(\hat{\boldsymbol{n}})Y^*_{lm'}(\hat{\boldsymbol{n}}) = \int \mathrm{d}\Omega_s \; Y_{lm}(D^{-1}\hat{\boldsymbol{s}})Y^*_{lm'}(D^{-1}\hat{\boldsymbol{s}}) \\ &= \sum_{n,n'} \int \mathrm{d}\Omega_s \; D^l_{nm} Y_{ln}(\hat{\boldsymbol{s}}) D^{l*}_{n'm'} Y^*_{ln'}(\hat{\boldsymbol{s}}) = \sum_n D^l_{nm} D^{l*}_{nm'}\end{aligned} \tag{1.104}$$

$$\begin{aligned}\delta^{(\mathrm{K})}_{mm'} &= \int \mathrm{d}\Omega_n \; Y_{lm}(\hat{\boldsymbol{n}})Y^*_{lm'}(\hat{\boldsymbol{n}}) = \int \mathrm{d}\Omega_s \; Y_{lm}(D\hat{\boldsymbol{s}})Y^*_{lm'}(D\hat{\boldsymbol{s}}) \\ &= \sum_{n,n'} \int \mathrm{d}\Omega_s \; D^{*l}_{mn} Y_{ln}(\hat{\boldsymbol{s}}) D^l_{m'n'} Y^*_{ln'}(\hat{\boldsymbol{s}}) = \sum_n D^{l*}_{mn} D^l_{m'n}\end{aligned} \tag{1.105}$$

The $m = 0$ components of the Wigner matrices are related to the spherical harmonics themselves. To see that, let's consider a unit vector $\hat{\boldsymbol{n}}$ with components (θ, ϕ). This unit vector can obviously be created by rotating a unit vector in z-direction by $D(\phi, \theta, 0)$

$$Y_{lm}(\hat{\boldsymbol{n}}) = Y_{lm}(\hat{D}(\phi,\theta,0)\hat{\boldsymbol{z}}) = D^{l*}_{mm'} Y_{lm'}(\hat{\boldsymbol{z}}) = \sqrt{\frac{2l+1}{4\pi}} D^{l*}_{m0}(\phi,\theta,0) \tag{1.106}$$

Here we used that $\mathcal{P}^m_l(1) = \delta^{(\mathrm{K})}_{m0}$ and $Y_{lm}(\hat{\boldsymbol{z}}) = \sqrt{2l+1/4\pi}\delta^{(\mathrm{K})}_{m0}$ and finally see

$$D^l_{m0}(\phi,\theta,0) = \sqrt{\frac{4\pi}{2l+1}} Y^*_{lm}(\hat{\boldsymbol{n}})\,. \tag{1.107}$$

Let us finish up this section by studying the implications of statistical isotropy on the power spectrum of f_{lm}

$$\left\langle \tilde{f}_{lm} \tilde{f}^*_{l'm'} \right\rangle = \sum_{n,n'} D^l_{mn} D^{l'*}_{m'n'} \left\langle f_{ln} f^*_{l'n'} \right\rangle \tag{1.108}$$

This clearly requires $\langle f_{ln} f^*_{l'n'} \rangle = C_l \delta^{(\mathrm{K})}_{ll'} \delta^{(\mathrm{K})}_{nn'}$

$$C_l \delta^{(\mathrm{K})}_{ll'} \delta^{(\mathrm{K})}_{mm'} = \sum_n D^l_{mn} D^{l*}_{m'n} C_l \delta^{(\mathrm{K})}_{ll'} = C_l \delta^{(\mathrm{K})}_{ll'} \delta^{(\mathrm{K})}_{mm'} \tag{1.109}$$

Finally the structure of the angular power spectrum can be directly deduced from the statistical isotropy of the angular correlation function by using the definition of the f_{lm}

$$\left\langle \tilde{f}_{lm} \tilde{f}^*_{l'm'} \right\rangle = \int \mathrm{d}\Omega \int \mathrm{d}\Omega' C(\hat{\boldsymbol{n}} \cdot \hat{\boldsymbol{n}}') Y^*_{lm}(\hat{\boldsymbol{n}}) Y_{l'm'}(\hat{\boldsymbol{n}}') \tag{1.110}$$

Let's split the angular integration into an reference angle $\hat{\boldsymbol{n}}$ and a relative angle defined wrt $\hat{\boldsymbol{n}}$. Clearly, the correlation function can only depend on the relative angle θ_{r}. Defining a rotation by $\hat{\boldsymbol{n}} = \hat{D}\hat{\boldsymbol{z}}$ we have $\hat{\boldsymbol{n}}^{\mathrm{T}}\hat{\boldsymbol{n}}' = (D^{-1}\hat{\boldsymbol{n}})^{\mathrm{T}} D^{-1}\hat{\boldsymbol{n}}' = \hat{\boldsymbol{z}}^{\mathrm{T}} D^{-1}\hat{\boldsymbol{n}}'$

$$\begin{aligned}\left\langle \tilde{f}_{lm} \tilde{f}^*_{l'm'} \right\rangle =& \int \mathrm{d}\Omega \int \mathrm{d}\Omega_{\mathrm{r}} C(\theta_{\mathrm{r}}) Y^*_{lm}(D\hat{\boldsymbol{z}}) Y_{l'm'}(DD^{-1}\hat{\boldsymbol{n}}') \\ =& \sum_{\tilde{m},\tilde{m}'} \int \mathrm{d}\Omega \int \mathrm{d}\Omega_{\mathrm{r}} C(\theta_{\mathrm{r}}) D^l_{m\tilde{m}} Y^*_{l\tilde{m}}(\hat{\boldsymbol{z}}) D^{l'*}_{m'\tilde{m}'} Y_{l'\tilde{m}'}(D^{-1}\hat{\boldsymbol{n}}') \\ =& \sqrt{\frac{2l+1}{4\pi}\frac{2l'+1}{4\pi}} \int \mathrm{d}\Omega \; D^{l*}_{m0} D^{l'}_{m'0} \int \mathrm{d}\Omega_{\mathrm{r}} C(\theta_{\mathrm{r}}) \mathcal{P}_{l'}(\cos\theta_{\mathrm{r}}) \\ =& \delta^{(\mathrm{K})}_{ll'} \delta^{(\mathrm{K})}_{mm'} \int \mathrm{d}\Omega_{\mathrm{r}} C(\theta_{\mathrm{r}}) \mathcal{P}_{l'}(\cos\theta_{\mathrm{r}})\end{aligned} \tag{1.111}$$

Thus

$$C_l = \int \mathrm{d}\Omega_{\mathrm{r}} C(\theta_{\mathrm{r}}) P_{l'}(\cos\theta_{\mathrm{r}}) = 2\pi \int \mathrm{d}\mu C(\mu) \mathcal{P}_l(\mu) \tag{1.112}$$

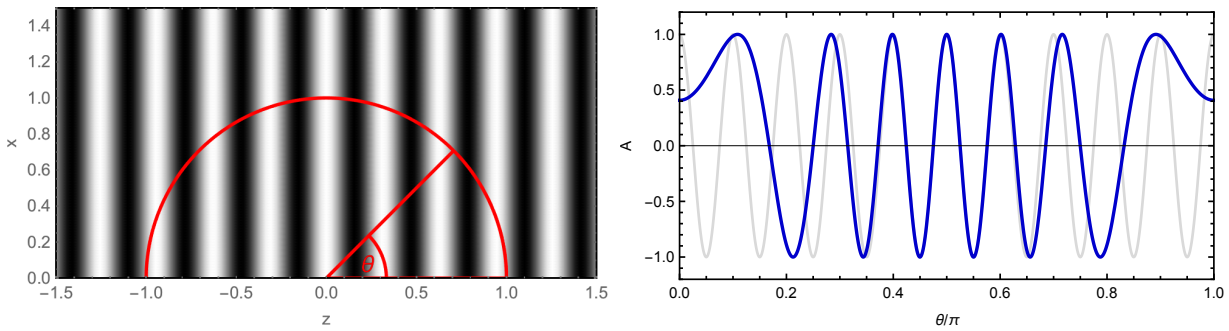

Figure 1.5.: *Left panel:* Plane wave in z-direction and intersection with a sphere. *Right panel:* Amplitude of a plane wave with $\boldsymbol{k} \parallel \hat{\boldsymbol{z}}$ on the surface of the sphere as a function of polar angle (blue line). Perpendicilar to the wavevector, the plane wave contributes to angular modes with $l \approx rk$ (gray line), whereas along the wavevector, the plane wave contributes to angular fluctuations of longer wavelength, smaller angular wavenumber $l < kr$.

1.6.3. Projection of 3D Fields

Let us now express the C_l's in terms of the 3D power spectrum. Let us consider the three dimensional quantity f on a sphere of radius χ_* surrounding the observer. You can for instance think of it as an expansion of the CMB temperature fluctuations, where r would thus be the distance from us to the last scattering surface

$$f(\hat{\boldsymbol{n}}) = \int \frac{\mathrm{d}^3k}{(2\pi)^3} f(\boldsymbol{k}) \exp\left[\mathrm{i}\hat{\boldsymbol{k}} \cdot \hat{\boldsymbol{n}} k\chi_*\right] . \tag{1.113}$$

Using the plane wave or **Rayleigh expansion**

$$\exp\left[\mathrm{i}\boldsymbol{k}\cdot\boldsymbol{r}\right] = 4\pi \sum_{lm} \mathrm{i}^l j_l(kr) Y^*_{lm}(\hat{\boldsymbol{k}}) Y_{lm}(\hat{\boldsymbol{n}}) = \sum_l (2l+1)\mathrm{i}^l j_l(kr)\mathcal{P}_l(\hat{\boldsymbol{n}}\cdot\hat{\boldsymbol{k}}) \tag{1.114}$$

we obtain

$$f_{lm} = 4\pi \int \frac{\mathrm{d}^3\boldsymbol{k}}{(2\pi)^3}\, f(\boldsymbol{k}) \sum_{l'm'} \mathrm{i}^{l'} j_{l'}(k\chi_*) Y^*_{l'm'}(\hat{\boldsymbol{k}}) \int \mathrm{d}\Omega\; Y_{l'm'}(\hat{\boldsymbol{n}}) Y^*_{lm}(\hat{\boldsymbol{n}}) \tag{1.115}$$

$$= 4\pi \int \frac{\mathrm{d}^3\boldsymbol{k}}{(2\pi)^3}\, f(\boldsymbol{k}) \mathrm{i}^l j_l(k\chi_*) Y^*_{lm}(\hat{\boldsymbol{k}}) \tag{1.116}$$

We are now well prepared to calculate the relation between the angular and the three dimensional power spectrum

$$\langle f_{lm} f^*_{l'm'} \rangle = (4\pi)^2 \int \frac{\mathrm{d}^3\boldsymbol{k}}{(2\pi)^3} \int \frac{\mathrm{d}^3\boldsymbol{k}'}{(2\pi)^3} \langle f(\boldsymbol{k}) f^*(\boldsymbol{k}')\rangle\, Y_{lm}(\hat{\boldsymbol{k}}) Y^*_{l'm'}(\hat{\boldsymbol{k}}') j_l(k\chi_*) j_{l'}(k'\chi_*) \mathrm{i}^l (-\mathrm{i})^{l'} , \tag{1.117}$$

$$= 4\pi \int \frac{\mathrm{d}k k^2}{2\pi^2} P(k) j_l(k\chi_*) j_{l'}(k\chi_*) (-\mathrm{i})^l \mathrm{i}^{l'} \int \mathrm{d}\Omega_{\boldsymbol{k}}\; Y_{lm}(\hat{\boldsymbol{k}}) Y^*_{l'm'}(\hat{\boldsymbol{k}}) , \tag{1.118}$$

$$= 4\pi \delta^{(\mathrm{K})}_{ll'} \delta^{(\mathrm{K})}_{mm'} \int \frac{\mathrm{d}k k^2}{2\pi^2} j_l^2(k\chi_*) P(k) . \tag{1.119}$$

As above, the structure of the angular power spectrum is revealed to be $C_l \delta^{(\mathrm{K})}_{ll'} \delta^{(\mathrm{K})}_{mm'}$, where

$$C_l = 4\pi \int \frac{\mathrm{d}k k^2}{2\pi^2} j_l^2(kr) P(k) = 4\pi \int \mathrm{d}\ln k\; \Delta^2(k) j_l^2(kr) . \tag{1.120}$$

In Fig. 1.5 we consider the contributions of a plane wave with wavenumber k travelling in z-direction to the spherical multipole coefficients on an intersected sphere of radius r. Transverse to the $\hat{\boldsymbol{z}}$-axis the plane wave contributes to the $l \approx k\chi_*$ spherical mode, but along the $\hat{\boldsymbol{z}}$ the plane wave has a less oscillatory contribution

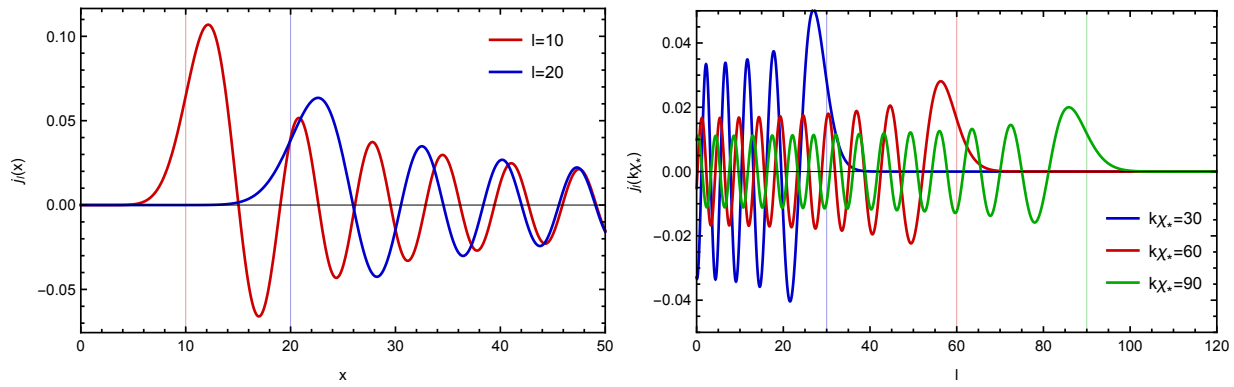

Figure 1.6.: Spherical Bessel functions $j_l(x)$ for $l = 10$ and $l = 20$. At low x the Bessel functions vanish indicating that modes with wavelength exceeding l/r do not contribute to the angular fluctuations You can see a pronounced peak at $x = l$ arising from $k \approx l/r$ transverse to the line of sight and oscillatory contributions from modes appearing as longer angular wavelenghts along the line of sight.

on the surface of the sphere, thus contributing to lower angular modes $l < k\chi_*$. Correspondingly, the spherical bessel functions in Fig. 1.6 have a pronounced positive peak at $x = k\chi_* \approx l$ and oscillatory contributions from plane waves with $k > l/\chi_*$.

The power spectrum in the above equation is the power spectrum of temperature fluctuations. This is related to the power spectrum of the primordial metric perturbation $\mathcal{R}$ through a transfer function $\Theta(\boldsymbol{k}) = \tilde{T}(k)\mathcal{R}(\boldsymbol{k})$ which can be combined with the spherical Bessel function arising from the projection $T_l(k,\chi) = \tilde{T}(k)j_l(k\chi)$

$$C_l = 4\pi \int \frac{\mathrm{d}k k^2}{2\pi^2} T_l^2(k,\chi_*) P_{\mathcal{R}}(k) = 4\pi \int \mathrm{d}\ln k\; T_l^2(k,\chi_*)\Delta^2_{\mathcal{R}}(k)\,. \tag{1.121}$$

Furthermore, we will see that the CMB photons are not necessarily being emitted from a well defined distance χ_*, but from a range of scales, such that we will actually need to integrate over a radial source function.

Large-Scale Angular Power Spectrum

Let us consider a constant dimensionless curvature power spectrum $\Delta^2_{\mathcal{R}} = A_\mathrm{s}$ and a constant transfer function $T(k) = -1/5$ on large scales

$$4\pi \int \mathrm{d}\ln k\; T^2(k) j_l^2(k\chi_*)\Delta^2_{\mathcal{R}}(k) = \frac{4\pi}{25} A_\mathrm{s} \int \mathrm{d}\ln k j_l^2(k\chi_*) = \frac{2\pi}{25}\frac{1}{l(l+1)} A_\mathrm{s} \tag{1.122}$$

Here we used that $2l(l+1)\int \mathrm{d}\ln x j_l^2(x) = 1$. We finally obtain that

$$l(l+1)C_l = \frac{2\pi}{25} A_\mathrm{s} = \text{const.} \tag{1.123}$$

1.7. CMB Estimators and Covariance

As we discussed for the 3D power spectrum $P(k)$ above in Sec. 1.5.1, we need to estimate statistics given the single realization of the cosmic fields at our disposal using ergodic theorem using an estimator. For the 3D power spectrum we averaged over directions of Fourier modes using that the power spectrum is a function of the magnitude of wavenumber only. Here the angular power spectrum can be estimated as the average over all m-modes given l

$$\hat{C}_l = \frac{1}{2l+1}\sum_m f_{lm} f^*_{lm}\,. \tag{1.124}$$

The estimator is unbiased

$$\left\langle \hat{C}_l \right\rangle = \frac{1}{2l+1} \sum_m \langle f_{lm} f^*_{lm} \rangle = \frac{1}{2l+1} \sum_m C_l = C_l \,. \tag{1.125}$$

Finally, the fact that we have only $2l+1$ modes to estimate the variance of the field leads to an uncertainty of the estimator. The covariance between the power spectrum estimators for l and l' can be estimated as

$$\begin{aligned} \mathrm{cov}(\hat{C}_l, \hat{C}_{l'}) =& \left\langle \hat{C}_l \hat{C}_{l'} \right\rangle - \left\langle \hat{C}_l \right\rangle \left\langle \hat{C}_{l'} \right\rangle \,, \\ =& \frac{1}{(2l+1)(2l'+1)} \sum_{m,m'} \langle f_{lm} f^*_{lm} f_{l'm'} f^*_{l'm'} \rangle - \langle C_l \rangle \langle C_{l'} \rangle \,, \\ =& \frac{1}{(2l+1)(2l'+1)} \sum_{m,m'} 2 C_l^2 \delta^{(\mathrm{K})}_{ll'} \delta^{(\mathrm{K})}_{mm'} = \frac{2}{2l+1} C_l^2 \delta^{(\mathrm{K})}_{ll'} \,. \end{aligned} \tag{1.126}$$

Here we used Wick theorem to express the four point function as a sum over three products of two-point functions.[6] One of the three terms cancels the product of the two C_ls. We see that for a Gaussian field the covariance matrix is diagonal, i.e., that the estimate for the power at different angular wavenumbers is independent. When performing data analysis on the CMB, one can thus work with a diagonal covariance matrix. The relative statistical error of a given angular wavenumber

$$\frac{\Delta C_l}{C_l} = \sqrt{\frac{2}{2l+1}} \tag{1.127}$$

is thus inversely proportional to the square root of the number of modes $N_{\mathrm{mode}} = 2l+1$ and thys decreases with increasing wavenumber. This explains the larger errorbars for low angular wavenumber (on the left) of the CMB power spectrum plots. The expression should be compared to the equivalent expression for the 3D power spectrum $P(k)$ in Eq. (1.74), where the relative error also scales as $N_{\mathrm{modes}}^{-1/2}$.

1.8. Angular Bispectrum

We have already discussed a simple model that would introduce a non-vanishing bispectrum in the late time Universe. Modifications to the simplest inflationary models can produce detectable levels of non-Gaussianity in the early universe, which can be detected in the CMB. Let us develop the relevant statistics for quantifying the bispectrum on S^2. The angular bispectrum is given by

$$\langle f_{lm} f_{l'm'} f_{l''m''} \rangle = B_{ll'l''} \begin{pmatrix} l & l' & l'' \\ m & m' & m'' \end{pmatrix} = b_{ll'l''} \mathcal{G}^{ll'l''}_{mm'm''} \tag{1.128}$$

where we introduced the **Wigner 3j symbols**. The second equality is based on the definition of the triple integral over spherical harmonics, the so called **Gaunt integral**

$$\begin{aligned} \mathcal{G}^{ll'l''}_{mm'm''} =& \int \mathrm{d}\Omega \; Y_{lm}(\hat{\boldsymbol{n}}) Y_{l'm'}(\hat{\boldsymbol{n}}) Y_{l''m''}(\hat{\boldsymbol{n}}) \,, \\ =& \sqrt{\frac{(2l+1)(2l'+1)(2l''+1)}{4\pi}} \begin{pmatrix} l & l' & l'' \\ 0 & 0 & 0 \end{pmatrix} \begin{pmatrix} l & l' & l'' \\ m & m' & m'' \end{pmatrix} . \end{aligned} \tag{1.129}$$

[6] As stated below Eq. (1.85) we have $f^*_{l,m} = (-1)^m f_{l,-m}$ and thus

$$\langle f_{l,m} f_{l',m'} \rangle = (-1)^{m'} \left\langle f_{l,m} f^*_{l',-m'} \right\rangle = (-1)^{m'} C_l \delta^{(\mathrm{K})}_{l,l'} \delta^{(\mathrm{K})}_{m,-m'}$$

$$\left\langle f^*_{l,m} f^*_{l',m'} \right\rangle = (-1)^m \left\langle f_{l,-m} f^*_{l',m'} \right\rangle = (-1)^m C_l \delta^{(\mathrm{K})}_{l,l'} \delta^{(\mathrm{K})}_{-m,m'}$$

These results should be familiar from angular momentum coupling in quantum mechanics. The product state of two systems $|j_1 j_2 m_1 m_2\rangle = |j_1 m_1\rangle \otimes |j_2 m_2\rangle$ can also be expressed in terms of the total angular momentum $|j_1 j_2 JM\rangle$. The two representations are related to each other using the identity operator $\mathbb{1} = \sum_x |x\rangle\langle x|$

$$|j_1 j_2 m_1 m_2\rangle = \sum_{J,M} \langle j_1 j_2 JM | j_1 j_2 m_1 m_2\rangle |j_1 j_2 JM\rangle\,, \tag{1.130}$$

$$|j_1 j_2 JM\rangle = \sum_{m_1,m_2} \langle j_1 j_2 m_1 m_2 | j_1 j_2 JM\rangle |j_1 j_2 m_1 m_2\rangle\,. \tag{1.131}$$

The real expansion coefficients are the **Clebsch-Gordan coefficients**. Rotated states can be expressed in terms of the original states using the Wigner D matrices introduced above

$$\hat{D}|j_1 j_2 JM\rangle = \sum_N D^J_{NM} |j_1 j_2 JN\rangle \tag{1.132}$$

$$\hat{D}|j_1 j_2 m_1 m_2\rangle = \sum_{m_1',m_2'} D^{j_1}_{n_1 m_1} D^{j_2}_{n_2 m_2} |j_1 j_2 m_1 m_2\rangle \tag{1.133}$$

We can now employ the fact that the rotation operator is unitary $\hat{D}^\dagger \hat{D}$

$$\begin{aligned}
\langle j_1 j_2 m_1 m_2 | j_1 j_2 JM\rangle =& \langle j_1 j_2 m_1 m_2 | \hat{D}^\dagger \hat{D} | j_1 j_2 JM\rangle \\
=& \sum_{n_1,n_2,N} D^{j_1 *}_{n_1 m_1} D^{j_2 *}_{n_2 m_2} D^J_{NM} \langle j_1 j_2 n_1 n_2 | j_1 j_2 JN\rangle \\
=& \sum_{n_1,n_2,N} D^{j_1}_{n_1 m_1} D^{j_2}_{n_2 m_2} D^{J *}_{NM} \langle j_1 j_2 n_1 n_2 | j_1 j_2 JN\rangle \\
=& \sum_{n_1,n_2,N} D^{j_1}_{n_1 m_1} D^{j_2}_{n_2 m_2} D^J_{-N-M} (-1)^{N-M} \langle j_1 j_2 n_1 n_2 | j_1 j_2 JN\rangle
\end{aligned} \tag{1.134}$$

The vector addition coefficients (Clebsch-Gordan coefficients) can be expressed in terms of the Wigner 3j symbols.

$$\sqrt{2J+1} \begin{pmatrix} j_1 & j_2 & J \\ m_1 & m_2 & M \end{pmatrix} = (-1)^{j_1 - j_2 - M} \langle j_1 j_2 m_1 m_2 | j_1 j_2 J - M\rangle \tag{1.135}$$

Using this result in Eq. (1.134), we obtain

$$(-1)^{-M} \begin{pmatrix} j_1 & j_2 & J \\ m_1 & m_2 & -M \end{pmatrix} = \sum_{n_1,n_2,N} D^{j_1}_{n_1 m_1} D^{j_2}_{n_2 m_2} D^J_{-N-M} (-1)^{N-M} (-1)^{-N} \begin{pmatrix} j_1 & j_2 & J \\ n_1 & n_2 & -N \end{pmatrix} \tag{1.136}$$

We thus have

$$\begin{pmatrix} j_1 & j_2 & J \\ m_1 & m_2 & M \end{pmatrix} = \sum_{n_1,n_2,N} D^{j_1}_{n_1 m_1} D^{j_2}_{n_2 m_2} D^J_{NM} \begin{pmatrix} j_1 & j_2 & J \\ n_1 & n_2 & N \end{pmatrix} \tag{1.137}$$

Let us express the expectation value of three angular multipole coefficients in the rotated frame in terms of the original multipole coefficients

$$\left\langle \tilde{f}_{lm} \tilde{f}_{l'm'} \tilde{f}_{l''m''} \right\rangle = \sum_{\tilde{m}\tilde{m}'\tilde{m}''} D^l_{m\tilde{m}} D^{l'}_{m'\tilde{m}'} D^{l''}_{m''\tilde{m}''} \langle f_{l\tilde{m}} f_{l'\tilde{m}'} f_{l''\tilde{m}''}\rangle \tag{1.138}$$

We can now use Eq. (1.128) in the rhs

$$\begin{aligned}
\left\langle \tilde{f}_{lm} \tilde{f}_{l'm'} \tilde{f}_{l''m''} \right\rangle =& B_{ll'l''} \sum_{\tilde{m}\tilde{m}'\tilde{m}''} D^l_{m\tilde{m}} D^{l'}_{m'\tilde{m}'} D^{l''}_{m''\tilde{m}''} \begin{pmatrix} l & l' & l'' \\ \tilde{m} & \tilde{m}' & \tilde{m}'' \end{pmatrix} \\
=& B_{ll'l''} \begin{pmatrix} l & l' & l'' \\ m & m' & m'' \end{pmatrix}
\end{aligned} \tag{1.139}$$

The bispectrum estimator is thus

$$\hat{B}_{ll'l''} = \sum_{mm'm''} \begin{pmatrix} l & l' & l'' \\ m & m' & m'' \end{pmatrix} f_{lm} f_{l'm'} f_{l''m''} = \sum_{mm'm''} h^{-1}_{ll'l''} \mathcal{G}^{ll'l''}_{mm'm''} f_{lm} f_{l'm'} f_{l''m''} \tag{1.140}$$

where

$$h_{ll'l''} = \sqrt{\frac{(2l+1)(2l'+1)(2l''+1)}{4\pi}} \begin{pmatrix} l & l' & l'' \\ 0 & 0 & 0 \end{pmatrix} \tag{1.141}$$

Using the orthogonality of the Wigner $3j$ symbols, it is easy to show that this estimator is unbiased.

In the exercises you will show by explicit projection, that the bispectrum in l-space is related to the 3D bispectrum as

$$\langle f_{lm} f_{l'm'} f_{l''m''} \rangle = \left(\frac{2}{\pi}\right)^3 \int \mathrm{d}x x^2 \prod_{i=1}^{3} \left\{ \int \mathrm{d}k_i k_i^2 \; j_l(k\chi_*) j_l(kx) \right\} B(k_1, k_2, k_3) \mathcal{G}^{ll'l''}_{mm'm''} \tag{1.142}$$

which again confirms the structure to be $\langle f_{lm} f_{l'm'} f_{l''m''} \rangle = b_{ll'l''} \mathcal{G}^{ll'l''}_{mm'm''}$.

2. Large-Scale Structure

In this chapter we will be considering the evolution of fluctuations in the Universe after recombination. The growth of perturbations leads to the breakdown of linear evolution equations and we will need to consider a perturbative approach to describe the evolution of densities, displacements and velocities. The basics of clustering statistics and perturbation theory are nicely summarized in the review [Bernardeau et al., 2002]. In the end of the chapter we will go beyond the dynamically dominating dark matter component and consider models that allow us to describe observable tracers of LSS. The so called bias models employed for this purpose were recently reviewed by [Desjacques et al., 2018].

Why would we want to go through this trouble? The analysis of CMB fluctuations has tightly constrained the six parameters of the minimal ΛCDM model and further improvements are to be expected from small scale experiments, lensing and polarization measurements. However, many of the constraints are limited by the number of available modes ($N_{\rm CMB} \approx l^2_{\rm max} \approx 10^6$) in the CMB and tighter constraints will require the exploration of additional independent modes. LSS can provide this additional information, especially if one is able to increase survey volume and the maximum wavenumber up to which one can reliably analyze the data. The number of modes then scales as $N_{\rm LSS} \approx (k_{\rm max}/k_{\rm min})^3 \approx 10^8$ up to $z = 2.5$ and $k_{\rm max} = 0.3\ h{\rm Mpc}^{-1}$. A comparison of the statistical and theoretical contributions to the power spectrum uncertainties is depicted in Fig. 2.1. Furthermore, LSS probes the epoch of the Universe where dark energy is starting to dominate the energy budget.

What we will do in this section is to express the non-linear matter and galaxy fluctuations in terms of the linear, Gaussian initial conditions $\delta^{(1)}$. We will see that non-linear terms in the equations of motion and galaxy formation lead to expansions of the form $\delta_{\rm m} = \delta^{(1)} + \delta^{(2)} + \delta^{(3)}$ and $\delta_{\rm g} = b_1(\delta^{(1)} + \delta^{(2)} + \delta^{(3)}) + b_2[\delta^{(1)}]^2$, where $\delta^{(n)} \sim \mathcal{O}([\delta^{(1)}]^n)$.

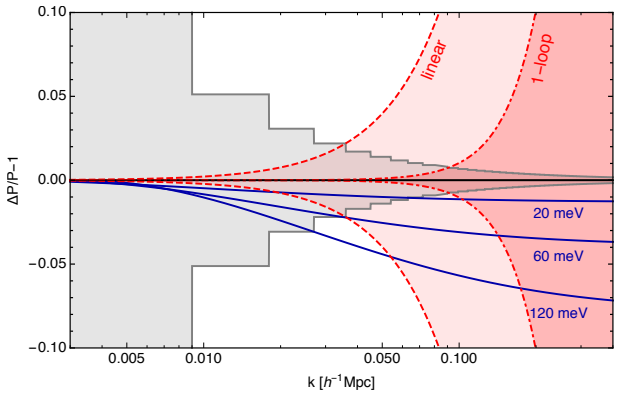

Figure 2.1.: Relative error on the power spectrum from cosmic variance (gray shaded) and uncertainty on the non-linear power spectrum (red shaded). We also overplot the effect of massive neutrinos as a physically interesting signal.

2.1. Dynamics in Newtonian Regime

2.1.1. Equations of Motion

Let us now consider the equations governing the cosmological fluid in the Newtonian limit, i.e., for small distances $r \ll H^{-1}$ and small velocities $v \ll 1$. The equation of motion for a particle at physical position $\boldsymbol{r}$ is

$$\ddot{\boldsymbol{r}} = -\boldsymbol{\nabla}_{\boldsymbol{r}}\Phi\,, \tag{2.1}$$

where the dot stands for a derivative with respect to coordinate time t.

Background

For constant comoving positions, the physical velocity is given by the Hubble law

$$\dot{\boldsymbol{r}} = H\boldsymbol{r} = \mathcal{H}\boldsymbol{x}\,. \tag{2.2}$$

The second derivative is related to the gradient of some 'background-potential' $\phi_{\rm b}$

$$\ddot{\boldsymbol{r}} = \frac{1}{a}\mathcal{H}'\boldsymbol{x} = -\frac{1}{a}\boldsymbol{\nabla}_{\boldsymbol{x}}\phi_{\rm b}\,, \tag{2.3}$$

which is related to the mean matter density in the matter dominated Universe by

$$\boldsymbol{\nabla}^2_{\boldsymbol{x}}\phi_{\rm b} = 4\pi G a^2\bar{\rho}\,. \tag{2.4}$$

Defining comoving coordinates as $\boldsymbol{r} = a\boldsymbol{x}$ we have $\boldsymbol{\nabla}_{\boldsymbol{x}} = a\boldsymbol{\nabla}_{\boldsymbol{r}}$. From now on we will use the gradient with respect to comoving coordinates and a prime to denote derivatives with respect to conformal time η defined through $a\mathrm{d}\eta = \mathrm{d}t$.[1] Let us take the derivative of the physical coordinate with respect to physical time and rewrite in terms of the comoving position

$$\dot{\boldsymbol{r}} = \mathcal{H}\boldsymbol{x} + \boldsymbol{x}'. \tag{2.5}$$

Likewise we have for the second derivative

$$\ddot{\boldsymbol{r}} = \frac{1}{a}\left(\mathcal{H}'\boldsymbol{x} + \mathcal{H}\boldsymbol{x}' + \boldsymbol{x}''\right) = -\frac{1}{a}\boldsymbol{\nabla}\Phi. \tag{2.6}$$

the term proportional to the position is peculiar, since it leads to a spatial dependence of the particle acceleration. This term arises from the comoving coordinates and accounts for the expansion of spacetime. We can thus bring it to the right hand side of the above equation and define the peculiar potential

$$\Phi = -\frac{1}{2}\mathcal{H}'x^2 + \phi. \tag{2.7}$$

Thus we have for the equations of motion

$$\boldsymbol{x}'' + \mathcal{H}\boldsymbol{x}' = -\boldsymbol{\nabla}\phi. \tag{2.8}$$

The peculiar potential is solely seeded by the energy density fluctuations in the Universe. Since we are assuming that dark energy is homogeneous, at late times these energy density fluctuations are dominated by the fluctuations in the matter density. Hence the Poisson equation for the peculiar potential can be expressed as

$$\nabla^2_{\boldsymbol{x}}\phi = \frac{3}{2}\mathcal{H}^2\Omega_{\rm m}(a)\delta = \frac{3}{2}\Omega_{\rm m,0}H_0^2\frac{\delta}{a}. \tag{2.9}$$

Defining the **canonical momentum**

$$\boldsymbol{p} = am\boldsymbol{u}, \tag{2.10}$$

[1] For an arbitrary function $f(t)$ we have $a\dot{f} = f'$ and $a^2\ddot{f} = f'' - \mathcal{H}f'$. Unless otherwise quoted we will refer to dots as derivatives with respect to coordinate time and dashes as derivatives with respect to conformal time.

where $\boldsymbol{u} = \boldsymbol{x}'$ is the comoving velocity we have for the equation of motion

$$\boldsymbol{p}' = -am\boldsymbol{\nabla}_{\boldsymbol{x}}\phi. \tag{2.11}$$

Let us finally stress again that these equations are only true in the Newtonian regime.

2.1.2. The Fluid Equations

The particle distribution in phase space is conveniently described by the distribution function $f(\boldsymbol{x}, \boldsymbol{p}, \eta)$. The number of particles in a infinitesimal phase space volume $\mathrm{d}^3x\mathrm{d}^3p$ is thus given by $\mathrm{d}N = f(\boldsymbol{x}, \boldsymbol{p}, \eta)\mathrm{d}^3x\mathrm{d}^3p$. Louiville theorem asserts the conservation of the phase space density. For collisionless dark matter, this conservation of phase space density then yields the **collisionless Boltzmann equation**, also known as **Vlasov equation**

$$\frac{\mathrm{d}f}{\mathrm{d}\eta} = \frac{\partial f}{\partial \eta} + \frac{\mathrm{d}\boldsymbol{x}}{\mathrm{d}\eta}\cdot\frac{\partial f}{\partial \boldsymbol{x}} + \frac{\mathrm{d}\boldsymbol{p}}{\mathrm{d}\eta}\frac{\partial f}{\partial \boldsymbol{p}} \tag{2.12}$$

$$= \frac{\partial f}{\partial \eta} + \frac{\boldsymbol{p}}{ma}\cdot\frac{\partial f}{\partial \boldsymbol{x}} - am\boldsymbol{\nabla}\phi\cdot\frac{\partial f}{\partial \boldsymbol{p}} = 0 \tag{2.13}$$

where we have used the equation of motion (2.11) in the last line.
We will be rarely interested in the full phase space distribution and thus there is no need to solve this non-linear seven dimensional differential equation. Instead we will be mostly concerned with fluid properties such as density, mean streaming velocity and velocity dispersion, which are readily obtained as moments of the distribution function

$$\rho(\boldsymbol{x}, \eta) = \frac{m}{a^3}\int \mathrm{d}^3p\ f(\boldsymbol{x}, \boldsymbol{p}, \eta), \tag{2.14}$$

$$v_i(\boldsymbol{x}, \eta) = \int \mathrm{d}^3p\ \frac{p_i}{am} f(\boldsymbol{x}, \boldsymbol{p}, \eta) / \int \mathrm{d}^3p\ f(\boldsymbol{x}, \boldsymbol{p}, \eta), \tag{2.15}$$

$$\sigma_{ij}(\boldsymbol{x}, \eta) = \int \mathrm{d}^3p\ \frac{p_i}{am}\frac{p_j}{am} f(\boldsymbol{x}, \boldsymbol{p}, \eta) / \int \mathrm{d}^3p\ f(\boldsymbol{x}, \boldsymbol{p}, \eta) - v_i(\boldsymbol{x})v_j(\boldsymbol{x}). \tag{2.16}$$

The velocity dispersion is sometimes also referred to as anisotropic stress and describes the deviation from a single coherent flow as is obvious in Eq (2.16).
For a collection of particles we have

$$f(\boldsymbol{x}, \boldsymbol{p}, \eta) = \sum_i \delta^{(\mathrm{D})}(\boldsymbol{x} - \boldsymbol{x}_i)\delta^{(\mathrm{D})}(\boldsymbol{p} - am\boldsymbol{u}_i)\,, \tag{2.17}$$

leading to

$$\rho(\boldsymbol{x}, \eta) = \sum_i \frac{m}{a^3}\delta^{(\mathrm{D})}(\boldsymbol{x} - \boldsymbol{x}_i)\,. \tag{2.18}$$

The equations of motion for these quantities can now be obtained by taking moments of the Vlasov equation (2.13). The zeroth moment of the Vlasov equation yields the **continuity equation**. Upon integrating over the momentum, we have to integrate the last term by parts and use that the potential is independent of the momentum

$$\delta' + \boldsymbol{\nabla}\cdot\big[(1+\delta)\boldsymbol{v}\big] = 0\,. \tag{2.19}$$

Taking the the first moment and using the continuity equation yields the **Euler equation**

$$v_i' + \mathcal{H}v_i + \boldsymbol{v}\cdot\boldsymbol{\nabla}v_i = -\nabla_i\phi - \frac{1}{\rho}\nabla_i(\rho\sigma_{ij}) \tag{2.20}$$

or conservation of momentum. In principle we could have continued to hierarchy of equations, which couples the equation of motion for n-th moment of the Vlaslov equation to the $n+1$-th moment. To close the hierarchy we will postulate that all moments beyond the velocity are vanishing, an assumption that is denoted the pressureless perfect fluid. This assumption is reasonable in the linear regime but needs to be validated numerically at late times, when structures collapse, virialize and shell crossing occurs.
The fluid velocity can be decomposed into a scalar and a vector part $\boldsymbol{v} = \boldsymbol{v}_\parallel + \boldsymbol{v}_\perp$, where $\boldsymbol{\nabla}\times\boldsymbol{v}_\parallel = 0$ and $\boldsymbol{\nabla}\cdot\boldsymbol{v}_\perp = 0$. The velocity field can thus be described by its vorticity $\boldsymbol{w} = \boldsymbol{\nabla}\times\boldsymbol{v}$ and its divergence $\theta = \nabla\cdot\boldsymbol{v}$.

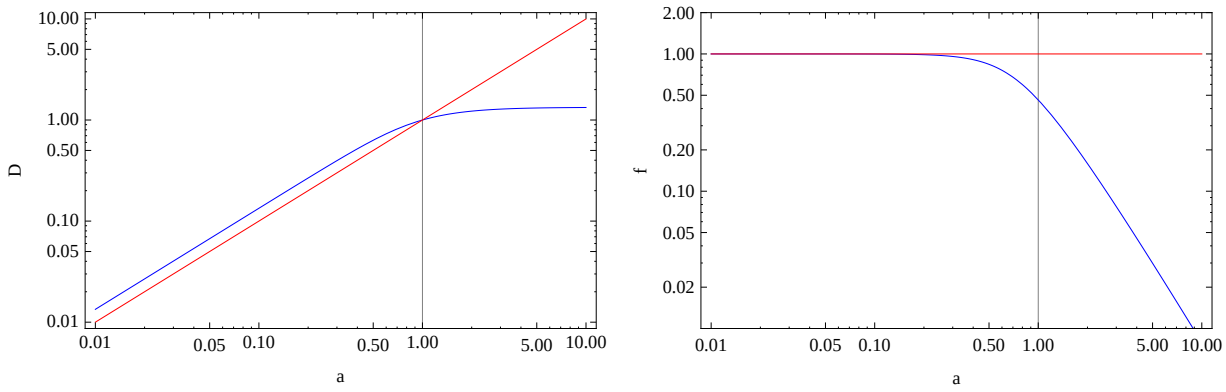

Figure 2.2.: Linear growth of structure for our fiducial ΛCDM (blue) and a matter only EdS Universe (red). *Left panel:* Linear growth factor D. *Right panel:* Logarithmic growth factor f.

2.1.3. Linearized Equations

Let us neglect all the quadratic terms in the continuity and Euler equations and assume that the velocity dispersion vanishes

$$\delta' + \theta = 0 \tag{2.21}$$
$$\boldsymbol{v}' + \mathcal{H}\boldsymbol{v} = -\boldsymbol{\nabla}\phi. \tag{2.22}$$

The system can be solved straightforwardly after rewriting the Euler equation in terms of velocity vorticity and divergence

$$\theta' + \mathcal{H}\theta = -\nabla^2\phi \tag{2.23}$$
$$\boldsymbol{w}' + \mathcal{H}\boldsymbol{w} = 0. \tag{2.24}$$

The solution of the vorticity equation is simply $\boldsymbol{w} \propto a^{-1}$, i.e., any initially present vorticity decays at linear level. To solve the scalar equation, we take the time derivative of Eq. (2.21) and replace θ' with Eq. (2.23). In the resulting equation, we can replace θ using Eq. (2.23) and $\nabla^2\phi$ using the Poisson Eq. (2.9). We obtain the **linear growth equation**

$$\delta''(\boldsymbol{x},\eta) + \mathcal{H}(\eta)\delta'(\boldsymbol{x},\eta) - \frac{3}{2}\Omega_{\rm m}(\eta)\mathcal{H}^2(\eta)\delta(\boldsymbol{x},\eta) = 0\,. \tag{2.25}$$

It is sometimes convenient to rewrite this in terms of derivatives w.r.t. scale factor a

$$-a^2\mathcal{H}^2\partial_a^2\delta + \frac{3}{2}\mathcal{H}^2\left[\Omega_{\rm m}(a) - 2\right]a\partial_a\delta + \frac{3}{2}\Omega_{\rm m}\mathcal{H}^2\delta = 0\,. \tag{2.26}$$

As can be easily confirmed the above differential equation has a growing and a decaying mode solution $\delta(\boldsymbol{k},\eta) = D_+(\eta)\delta_{+,0}(\boldsymbol{k}) + D_-(\eta)\delta_{-,0}(\boldsymbol{k})$, where $D_-(\eta) = D_{-,0}H = D_{-,0}\mathcal{H}/a$. The growing mode solution can then be obtained as

$$D_+(\eta) = D_{+,0}H(\eta)\int_0^{a(\eta)}\frac{\mathrm{d}a'}{\mathcal{H}^3(a')}, \tag{2.27}$$

where $D_{+,0}$ is a normalization factor used to achieve $D_+(a=1) = 1$. Let us first discuss the solution in a Einstein-de-Sitter (EdS) matter only Universe. Since $a \propto t^{2/3}$ we have $H = a^{-3/2}$ and thus $D_+ = a$ and $D_- = a^{-3/2}$. This special case and the solution for our fiducial ΛCDM model are shown in the left panel of Fig. 2.2. We see that the growth in the ΛCDM Universe stalls at late times when the cosmological constant starts to dominate. In what follows we will concentrate on the growing mode solutions and use $D \equiv D_+$ unless otherwise stated.

2.1.4. Velocities

In the above subsection we have seen, that the vorticity decays at linear level in the absence of anisotropic stress. At non-linear level we have

$$\boldsymbol{w}' + \mathcal{H}\boldsymbol{w} + \boldsymbol{\nabla} \times (\boldsymbol{v} \times \boldsymbol{w}) = 0. \tag{2.28}$$

This equation tells us, that even at non-linear level, if there is no initial vorticity, evolution won't generate it. Together with the knowledge that vorticity decays at early times when the fluctuations are still linear we can conclude that vorticity will be negligible throughout evolution in absence of anisotropic stress. However, there is evidence from simulations that at late times velocity dispersion and thus vorticity is generated in high density regions. In the following, we will present Standard Perturbation Theory, ignoring the possible vorticity. This assumption will restrict the validity of the solutions to large scales.
In case of vanishing curl, we have

$$\boldsymbol{v}(\boldsymbol{k}) = -\mathrm{i}\frac{\boldsymbol{k}}{k^2}\theta(\boldsymbol{k}). \tag{2.29}$$

From the linearized continuity equation in Fourier space we have

$$\theta(\boldsymbol{k}, \eta) = \mathrm{i}\boldsymbol{k} \cdot \boldsymbol{v}(\boldsymbol{k}, \eta) = -\delta'(\boldsymbol{k}, \eta) = -\mathcal{H} f \delta(\boldsymbol{k}, \eta), \tag{2.30}$$

where we defined the logarithmic growth factor

$$f = \frac{\mathrm{d}\ln D}{\mathrm{d}\ln a} \tag{2.31}$$

For the linear growing mode defined above in Eq. (2.27), we have

$$f(a) = \frac{\mathrm{d}\ln H}{\mathrm{d}\ln a} + \frac{a}{(aH)^3}\frac{1}{\int_0^a \mathrm{d}a' \left[a' H(a')\right]^3}, \tag{2.32}$$

which is unity for EdS. The right panel of Fig. 2.2 shows the logarithmic growth factor for a EdS and our fiducial ΛCDM cosmology. The late time dominance of the cosmological constant is even more apparent in this plot where f decays to $f(a = 1) \approx 0.48$ at present time.
We can now employ this result to derive simple velocity statistics, such as the linear velocity dispersion

$$\kappa_{ij} = \langle v_i v_j \rangle - \langle v_i \rangle \langle v_j \rangle = \langle v_i v_j \rangle = \mathcal{H}^2 f^2 \int \frac{\mathrm{d}^3 q}{(2\pi)^3} \frac{q_i q_j}{q^4} P_{\mathrm{lin}}(q), \tag{2.33}$$

and its trace

$$\sigma_v^2 = \frac{1}{3}\mathrm{Tr}\left(\kappa_{ij}\right) = \frac{\mathcal{H}^2 f^2}{6\pi^2} \int \mathrm{d}q \; P_{\mathrm{lin}}(q). \tag{2.34}$$

In the following we will frequently consider the displacement dispersion $\sigma_d = \sigma_v / \mathcal{H} f$, for which we obtain in our fiducial cosmology $\sigma_d \approx 6\ h^{-1}\mathrm{Mpc}$.[2] Even though this number is calculated in linear theory, it turns out to be a fairly accurate description of what is measured in N-body simulations.

2.1.5. Fluid Equations in Fourier Space

After having obtained some intuition on the solutions in the linear regime, where the quadratic terms are negligible, we will now return to the full equations. To facilitate the analysis, we will work in Fourier space,

[2] Here we have used that the displacement $\boldsymbol{\Psi}$ is given by

$$\boldsymbol{\Psi}(\boldsymbol{k}, \eta) = \int \mathrm{d}\eta \; \boldsymbol{v}(\boldsymbol{k}, \eta) = -\frac{\mathrm{i}\boldsymbol{k}}{k^2} \int \mathrm{d}\eta \; \theta(\boldsymbol{k}, \eta) = \frac{\mathrm{i}\boldsymbol{k}}{k^2} \int \mathrm{d}\eta \; \delta'(\boldsymbol{k}, \eta) = \frac{\mathrm{i}\boldsymbol{k}}{k^2}\delta(\boldsymbol{k}, \eta)\,,$$

such that $\sigma_v = \mathcal{H} f \sigma_d$.

where the Euler and continuity equations read as

$$\delta'(\boldsymbol{k}) + \theta(\boldsymbol{k}) = -\int_{\boldsymbol{q},\boldsymbol{q}'} (2\pi)^3 \delta^{(\mathrm{D})}(\boldsymbol{k}-\boldsymbol{q}-\boldsymbol{q}')\alpha(\boldsymbol{q},\boldsymbol{q}')\theta(\boldsymbol{q})\delta(\boldsymbol{q}'), \tag{2.35}$$

$$\theta'(\boldsymbol{k}) + \mathcal{H}\theta(\boldsymbol{k}) + \frac{3}{2}\Omega_{\mathrm{m}}(a)\mathcal{H}^2\delta(\boldsymbol{k}) = -\int_{\boldsymbol{q},\boldsymbol{q}'} (2\pi)^3 \delta^{(\mathrm{D})}(\boldsymbol{k}-\boldsymbol{q}-\boldsymbol{q}')\beta(\boldsymbol{q},\boldsymbol{q}')\theta(\boldsymbol{q})\theta(\boldsymbol{q}'). \tag{2.36}$$

The coupling kernels on the right hand side are defined as

$$\alpha(\boldsymbol{k}_1,\boldsymbol{k}_2) = \frac{\boldsymbol{k}_1\cdot(\boldsymbol{k}_1+\boldsymbol{k}_2)}{k_1^2} \tag{2.37}$$

$$\beta(\boldsymbol{k}_1,\boldsymbol{k}_2) = \frac{1}{2}\left(\boldsymbol{k}_1+\boldsymbol{k}_2\right)^2 \frac{\boldsymbol{k}_1\cdot\boldsymbol{k}_2}{k_1^2k_2^2} = \frac{1}{2}\frac{\boldsymbol{k}_1\cdot\boldsymbol{k}_2}{k_1k_2}\left(\frac{k_2}{k_1}+\frac{k_1}{k_2}\right) + \frac{\left(\boldsymbol{k}_1\cdot\boldsymbol{k}_2\right)^2}{k_1^2k_2^2} \tag{2.38}$$

Note that $\alpha(\boldsymbol{k}_1,\boldsymbol{k}_2)$ is not symmetric in its arguments but $\beta(\boldsymbol{k}_1,\boldsymbol{k}_2)$ is. The fluid Eqs. (2.35) and (2.36) are non-linear coupled differential equations for the density and velocity divergence. A closed form solution does in general not exist. One can however try to solve them perturbatively in the regime, where $\delta \ll 1$ and $\theta \ll 1$. We will discuss the perturbative solutions in much more detail in below.

2.2. Perturbative Solution of the Fluid Equations

The continuity and Euler equations can be rewritten as second order differential equations

$$\begin{aligned}
&\mathcal{H}^2\left\{-a^2\partial_a^2 + \frac{3}{2}\left(\Omega_{\mathrm{m}}(a)-2\right)a\partial_a + \frac{3}{2}\Omega_{\mathrm{m}}(a)\right\}\delta = \mathcal{S}_\beta - \mathcal{H}\,\partial_a\left(a\,\mathcal{S}_\alpha\right)\,,\\
&\mathcal{H}\left\{a^2\partial_a^2 + \left(4-\frac{3}{2}\Omega_{\mathrm{m}}(a)\right)a\partial_a + (2-3\Omega_m)\right\}\theta = \partial_a\left(a\,\mathcal{S}_\beta\right) - \frac{3}{2}\Omega_{\mathrm{m}}(a)\mathcal{H}\mathcal{S}_\alpha\,.
\end{aligned} \tag{2.39}$$

with source terms given by

$$\begin{aligned}
\mathcal{S}_\alpha(\boldsymbol{k},\eta) &= -\int \frac{\mathrm{d}^3q}{(2\pi)^3}\,\alpha(\boldsymbol{q},\boldsymbol{k}-\boldsymbol{q})\,\theta(\boldsymbol{q},\eta)\delta(\boldsymbol{k}-\boldsymbol{q},\eta)\,,\\
\mathcal{S}_\beta(\boldsymbol{k},\eta) &= -\int \frac{\mathrm{d}^3q}{(2\pi)^3}\,\beta(\boldsymbol{q},\boldsymbol{k}-\boldsymbol{q})\,\theta(\boldsymbol{q},\eta)\theta(\boldsymbol{k}-\boldsymbol{q},\eta)\,.
\end{aligned} \tag{2.40}$$

The corresponding Green's functions for δ and θ in ΛCDM are given by

$$\begin{aligned}
G_\delta(a,a') &= \Theta(a-a')\,\frac{2}{5}\frac{1}{\mathcal{H}_0^2\Omega_m^0}\frac{D_+(a')}{a'}\left\{\frac{D_-(a)}{D_-(a')} - \frac{D_+(a)}{D_1(a')}\right\}\,,\\
G_\theta(a,a') &= -\mathcal{H}\,f(a)\,G_\delta(a,a')\,.
\end{aligned} \tag{2.41}$$

We could solve these equations numerically order by order. We can however gain more insights into the structure of the solutions by studying a power series ansatz in a matter-only EdS Universe.

2.2.1. Series Ansatz and Coupling Kernels

Standard Perturbation Theory aims to solve the fluid equations perturbatively using a power law ansatz. This approach simplifies significantly in an EdS Universe, where $D = a$. Hence we will study this case first and discuss the generalization to ΛCDM later. We will furthermore neglect the decaying mode. The power law ansatz reads

$$\delta(\boldsymbol{k},\eta) = \sum_{i=1}^{\infty} a^i(\eta)\tilde{\delta}^{(i)}(\boldsymbol{k}) \qquad\qquad \theta(\boldsymbol{k},\eta) = -\mathcal{H}(\eta)\sum_{i=1}^{\infty} a^i(\eta)\,\tilde{\theta}^{(i)}(\boldsymbol{k}). \tag{2.42}$$

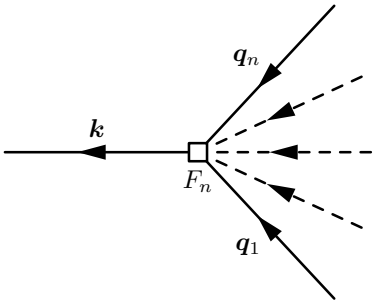

Figure 2.3.: Diagrammatic representation of the series expansion of the density field in Eq. (2.43). The points on the right side are initial density fields and the points on the left side are n-th order density fields.

Note that here we have separated the time and space dependence and that $\tilde{\delta}^{(1)}$ is normalized at present time, where $a = 1$. The expansion is in powers of the linear density field discussed above, i.e., $\delta^{(i)} = \mathcal{O}([\delta^{(1)}]^i)$. We can now write the n-th order solutions as convolutions of linear density fields

$$\tilde{\delta}^{(n)}(\boldsymbol{k}) = \prod_{m=1}^{n} \left\{ \int \frac{\mathrm{d}^3 q_m}{(2\pi)^3} \delta^{(1)}(\boldsymbol{q}_m) \right\} F_n(\boldsymbol{q}_1, \ldots, \boldsymbol{q}_n)(2\pi)^3 \delta^{(\mathrm{D})}(\boldsymbol{k} - \boldsymbol{q}|_1^n) \tag{2.43}$$

$$\tilde{\theta}^{(n)}(\boldsymbol{k}) = \prod_{m=1}^{n} \left\{ \int \frac{\mathrm{d}^3 q_m}{(2\pi)^3} \delta^{(1)}(\boldsymbol{q}_m) \right\} G_n(\boldsymbol{q}_1, \ldots, \boldsymbol{q}_n)(2\pi)^3 \delta^{(\mathrm{D})}(\boldsymbol{k} - \boldsymbol{q}|_1^n) \tag{2.44}$$

where $\boldsymbol{q}|_i^j = \sum_{m=i}^{j} \boldsymbol{q}_l$. A diagrammatic representation of this expansion is shown in Fig. 2.3. One can derive the following recursion relations for the convolution kernels (exercises)

$$\begin{aligned} F_n(\boldsymbol{q}_1, \ldots, \boldsymbol{q}_n) = \sum_{m=1}^{n-1} \frac{G_m(\boldsymbol{q}_1, \ldots, \boldsymbol{q}_m)}{(2n+3)(n-1)} \Big[& (2n+1)\alpha\left(\boldsymbol{q}|_1^m, \boldsymbol{q}|_{m+1}^n\right) F_{n-m}\left(\boldsymbol{q}_{m+1}, \ldots, \boldsymbol{q}_n\right) \\ & + 2\beta\left(\boldsymbol{q}|_1^m, \boldsymbol{q}|_{m+1}^n\right) G_{n-m}\left(\boldsymbol{q}_{m+1}, \ldots, \boldsymbol{q}_n\right) \Big] \end{aligned} \tag{2.45}$$

$$\begin{aligned} G_n(\boldsymbol{q}_1, \ldots, \boldsymbol{q}_n) = \sum_{m=1}^{n-1} \frac{G_m(\boldsymbol{q}_1, \ldots, \boldsymbol{q}_m)}{(2n+3)(n-1)} \Big[& 3\alpha\left(\boldsymbol{q}|_1^m, \boldsymbol{q}|_{m+1}^n\right) F_{n-m}\left(\boldsymbol{q}_{m+1}, \ldots, \boldsymbol{q}_n\right) \\ & + 2n\beta\left(\boldsymbol{q}|_1^m, \boldsymbol{q}|_{m+1}^n\right) G_{n-m}\left(\boldsymbol{q}_{m+1}, \ldots, \boldsymbol{q}_n\right) \Big] . \end{aligned} \tag{2.46}$$

with $F_1 = G_1 = 1$ such that $\tilde{\delta}^{(1)} = \delta^{(1)}$.

Let us see how to obtain the second order solution. For this purpose we use first order terms from the power series in the non-linear coupling terms on the right hand side and the second order terms on the left hand side

$$[\delta^{(2)}(\boldsymbol{k}, \eta)]' + \theta^{(2)}(\boldsymbol{k}, \eta) = -\int_{\boldsymbol{q}} \alpha(\boldsymbol{q}, \boldsymbol{k} - \boldsymbol{q}) \theta^{(1)}(\boldsymbol{q}, \eta) \delta^{(1)}(\boldsymbol{k} - \boldsymbol{q}, \eta) \tag{2.47}$$

$$[\theta^{(2)}(\boldsymbol{k}, \eta)]' + \mathcal{H}\theta^{(2)}(\boldsymbol{k}, \eta) + \frac{3}{2}\mathcal{H}^2 \delta^{(2)}(\boldsymbol{k}, \eta) = -\int_{\boldsymbol{q}} \beta(\boldsymbol{q}, \boldsymbol{k} - \boldsymbol{q}) \theta^{(1)}(\boldsymbol{q}, \eta) \theta^{(1)}(\boldsymbol{k} - \boldsymbol{q}, \eta) \tag{2.48}$$

Using the time dependence of the series ansatz, we obtain

$$a^2 \mathcal{H} \tilde{\delta}^{(2)}(\boldsymbol{k}) - a^2 \mathcal{H} \tilde{\theta}^{(2)}(\boldsymbol{k}, \eta) = \mathcal{H} a^2 \int_{\boldsymbol{q}} \alpha(\boldsymbol{q}, \boldsymbol{k} - \boldsymbol{q}) \tilde{\theta}^{(1)}(\boldsymbol{q}) \tilde{\delta}^{(1)}(\boldsymbol{k} - \boldsymbol{q}) \tag{2.49}$$

$$-(2a^2\mathcal{H}^2 + a^2\mathcal{H}')\tilde{\theta}^{(2)}(\boldsymbol{k}) - \mathcal{H}^2 a^2 \tilde{\theta}^{(2)}(\boldsymbol{k}) + \frac{3}{2}\mathcal{H}^2 a^2 \tilde{\delta}^{(2)}(\boldsymbol{k}) = -\mathcal{H}^2 a^2 \int_{\boldsymbol{q}} \beta(\boldsymbol{q}, \boldsymbol{k} - \boldsymbol{q}) \tilde{\theta}^{(1)}(\boldsymbol{q}) \tilde{\theta}^{(1)}(\boldsymbol{k} - \boldsymbol{q}) \tag{2.50}$$

With Eq. (A.1) we have

$$2F_2(\boldsymbol{q}_1,\boldsymbol{q}_2) - G_2(\boldsymbol{q}_1,\boldsymbol{q}_2) = \alpha(\boldsymbol{q}_1,\boldsymbol{q}_2) \tag{2.51}$$

$$\frac{3}{2}F_2(\boldsymbol{q}_1,\boldsymbol{q}_2) - \frac{5}{2}G_2(\boldsymbol{q}_1,\boldsymbol{q}_2) = -\beta(\boldsymbol{q}_1,\boldsymbol{q}_2) \tag{2.52}$$

which is a linear system that can be solved for F_2 and G_2 in terms of α and β.

The second order density kernel is thus given by

$$\begin{aligned} F_2(\boldsymbol{k}_1,\boldsymbol{k}_2) =& \frac{5}{7}\alpha(\boldsymbol{k}_1,\boldsymbol{k}_2) + \frac{2}{7}\beta(\boldsymbol{k}_1,\boldsymbol{k}_2) \\ =& \frac{5}{7} + \frac{1}{2}\frac{\boldsymbol{k}_1\cdot\boldsymbol{k}_2}{k_1k_2}\left(\frac{k_2}{k_1}+\frac{k_1}{k_2}\right) + \frac{2}{7}\frac{(\boldsymbol{k}_1\cdot\boldsymbol{k}_2)^2}{k_1^2k_2^2}\,. \end{aligned} \tag{2.53}$$

Here we defined $\boldsymbol{k}_1\cdot\boldsymbol{k}_2 = k_1k_2\mu_{12}$ and symmetrized Eq. (2.43) over the momenta. The latter can be rewritten as

$$F_2(\boldsymbol{k}_1,\boldsymbol{k}_2) = \frac{17}{21} + \frac{1}{2}\frac{\boldsymbol{k}_1\cdot\boldsymbol{k}_2}{k_1k_2}\left(\frac{k_2}{k_1}+\frac{k_1}{k_2}\right) + \frac{2}{7}\left[\frac{(\boldsymbol{k}_1\cdot\boldsymbol{k}_2)^2}{k_1^2k_2^2} - \frac{1}{3}\right]\,. \tag{2.54}$$

where the quadratic density term, the shift term and the anisotropic stress term are more obvious. At the same time, the angular structure of monopole, dipole and quadrupole is more obvious.

$$\delta^{(2)}(\boldsymbol{x}) = \underbrace{\frac{17}{21}\delta^2(\boldsymbol{x})}_{\text{growth}} \underbrace{-\boldsymbol{\Psi}(\boldsymbol{x})\cdot\boldsymbol{\nabla}\delta(\boldsymbol{x})}_{\text{advection}} \underbrace{+\frac{2}{7}s^2(\boldsymbol{x})}_{\text{tidal}}\,. \tag{2.55}$$

The growth term describes the enhanced growth factor in the presence of a long wavelength background mode, the advection term accounts for the displacement of initial perturbations due to bulk motions and the tidal term describes the coupling of long- and short-wavelength tidal fields s_{ij}.

The second order velocity kernel reads

$$\begin{aligned} G_2(\boldsymbol{k}_1,\boldsymbol{k}_2) =& \frac{3}{7}\alpha(\boldsymbol{k}_1,\boldsymbol{k}_2) + \frac{4}{7}\beta(\boldsymbol{k}_1,\boldsymbol{k}_2)\,, \\ =& \frac{3}{7} + \frac{1}{2}\frac{\boldsymbol{k}_1\cdot\boldsymbol{k}_2}{k_1k_2}\left(\frac{k_2}{k_1}+\frac{k_1}{k_2}\right) + \frac{4}{7}\frac{(\boldsymbol{k}_1\cdot\boldsymbol{k}_2)^2}{k_1^2k_2^2}\,. \end{aligned} \tag{2.56}$$

The explicit expressions for F_3 and G_3 are

$$\begin{aligned} F_3(\boldsymbol{q}_1,\boldsymbol{q}_2,\boldsymbol{q}_3) =& \frac{1}{18}\Big[7\alpha(\boldsymbol{q}_1,\boldsymbol{q}_2+\boldsymbol{q}_3)F_2(\boldsymbol{q}_2,\boldsymbol{q}_3) + 2\beta(\boldsymbol{q}_1,\boldsymbol{q}_2+\boldsymbol{q}_3)G_2(\boldsymbol{q}_2,\boldsymbol{q}_3)\Big] \\ &+\frac{G_2(\boldsymbol{q}_1,\boldsymbol{q}_2)}{18}\Big[7\alpha(\boldsymbol{q}_1+\boldsymbol{q}_2,\boldsymbol{q}_3) + 2\beta(\boldsymbol{q}_1+\boldsymbol{q}_2,\boldsymbol{q}_3)\Big] \end{aligned} \tag{2.57}$$

$$\begin{aligned} G_3(\boldsymbol{q}_1,\boldsymbol{q}_2,\boldsymbol{q}_3) =& \frac{1}{18}\Big[3\alpha(\boldsymbol{q}_1,\boldsymbol{q}_2+\boldsymbol{q}_3)F_2(\boldsymbol{q}_2,\boldsymbol{q}_3) + 6\beta(\boldsymbol{q}_1,\boldsymbol{q}_2+\boldsymbol{q}_3)G_2(\boldsymbol{q}_2,\boldsymbol{q}_3)\Big] \\ &+\frac{G_2(\boldsymbol{q}_1,\boldsymbol{q}_2)}{18}\Big[3\alpha(\boldsymbol{q}_1+\boldsymbol{q}_2,\boldsymbol{q}_3) + 6\beta(\boldsymbol{q}_1+\boldsymbol{q}_2,\boldsymbol{q}_3)\Big] \end{aligned} \tag{2.58}$$

The above formulae are not symmetrized over the arguments yet. Upon integration over three equivalent density fields $\delta(\boldsymbol{q}_1)\delta(\boldsymbol{q}_2)\delta(\boldsymbol{q}_3)$ we have to symmetrize, accounting both for the cyclic and odd permutations of the arguments in the kernels.

For the following discussion, it is important to know how the kernels scale if one of the momenta becomes very large. The kernels obey scaling laws such as

$$\lim_{q\to\infty} F_n(\boldsymbol{k}_1,\ldots,\boldsymbol{k}_{n-2},\boldsymbol{q},-\boldsymbol{q}) \;\propto\; \frac{k^2}{q^2}\,, \tag{2.59}$$

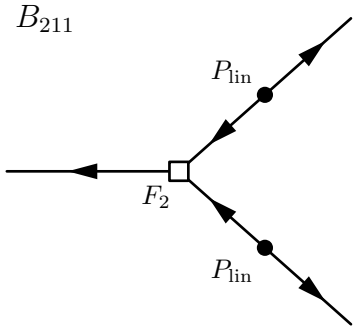

Figure 2.4.: Tree level bispectrum.

where $\boldsymbol{k} = \boldsymbol{k}_1 + \ldots \boldsymbol{k}_{n-2}$. For us it will turn out to be important that also for F_2 and F_3 a similar scaling holds when the sum of the arguments remains finite while one of the momenta goes to infinity, i.e.

$$\begin{aligned} \lim_{q\to\infty} F_2(\boldsymbol{q}, \boldsymbol{k}-\boldsymbol{q}) \propto \lim_{q\to\infty} F_2(\boldsymbol{k}_1-\boldsymbol{q}, \boldsymbol{k}_2+\boldsymbol{q}) \propto \frac{k^2}{q^2}\ , \\ \lim_{q\to\infty} F_3(\boldsymbol{q}, \boldsymbol{k}_1-\boldsymbol{q}, \boldsymbol{k}_2) \propto \frac{k^2}{q^2}\ , \end{aligned} \tag{2.60}$$

where we assumed that the momenta $k_1 \sim k_2 \sim k$ are of the same order.

For general ΛCDM the series ansatz in Eq. (2.42) can be generalized to

$$\delta(\boldsymbol{k},\eta) = \sum_{i=1}^{\infty} D^i(\eta)\tilde{\delta}^{(i)}(\boldsymbol{k}) \qquad\qquad \theta(\boldsymbol{k},\eta) = -\mathcal{H}(\eta)f(\eta)\sum_{i=1}^{\infty} D^i(\eta)\,\tilde{\theta}^{(i)}(\boldsymbol{k}). \tag{2.61}$$

The exact solution deviates from the above solution and doesn't allow for a separation of time and space dependence as in Eq. (2.61). The differences are discussed in detail in [Takahashi, 2008] (and shown in Fig. 2.7) and are generally at the sub-percent level. We will thus stick to the approximation Eq. (2.61), which is sufficiently accurate for our purpose.

2.2.2. Diagrams and Feynman Rules for the n-Spectra

We now want to evaluate the n-point functions using the above series expansion

$$\begin{aligned} \langle\delta(\boldsymbol{k},\eta)\delta(\boldsymbol{k}',\eta)\rangle &= \sum_{i,j} D^{i+j}(\eta)\left\langle\tilde{\delta}^{(i)}(\boldsymbol{k})\tilde{\delta}^{(j)}(\boldsymbol{k}')\right\rangle \\ &\sim \sum_{i,j} D^{i+j}(\eta)\int F_i F_j \left\langle\tilde{\delta}^{(1)}(\boldsymbol{q}_1)\ldots\tilde{\delta}^{(1)}(\boldsymbol{q}_i)\tilde{\delta}^{(1)}(\boldsymbol{q}_1')\tilde{\delta}^{(1)}(\boldsymbol{q}_j')\right\rangle \end{aligned} \tag{2.62}$$

We now have to use Wick's theorem to translate the correlator into products of power spectra of the linear field $(2\pi)^3\delta^{(\mathrm{D})}(\boldsymbol{k}+\boldsymbol{k}')P_{\rm lin}(k) = \left\langle\delta^{(1)}(\boldsymbol{k})\delta^{(1)}(\boldsymbol{k}')\right\rangle$. This can be achieved by pairing the field level diagrams in Fig. 2.3 to n-point functions diagrams as depicted in Figs. 2.4 and 2.5.

Even though the diagrams can be straightforwardly translated into the corresponding mathematical expressions, we write down the Feynman rules explicitly for the sake of definiteness. For the calculation of the i-th order contribution to the n-spectrum do the following

1. Draw all distinct connected diagrams with n external lines up to the desired order i in $\delta^{(1)}$. Connect the linear Gaussian density fields and draw a dot.

   i.) For each vertex V with ingoing momenta $\boldsymbol{q}_i$ and outgoing momentum $\boldsymbol{p}$ write a delta function $(2\pi)^3\delta^{(\mathrm{D})}\left(\boldsymbol{p} - \sum_i \boldsymbol{q}_i\right)$ and a coupling kernel $V(\boldsymbol{q}_1,\ldots,\boldsymbol{q}_n)$ (for instance $F_n(\boldsymbol{q}_1,\ldots,\boldsymbol{q}_n)$)

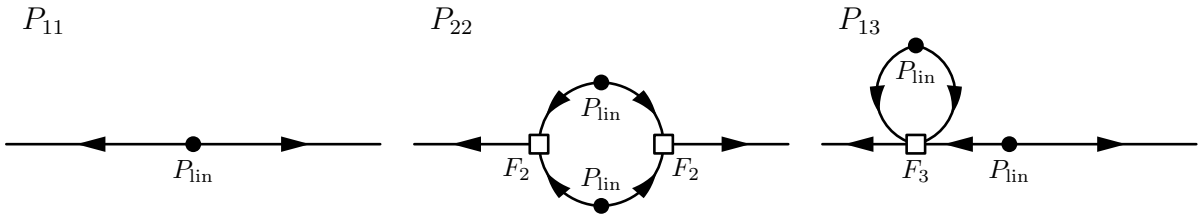

Figure 2.5.: Diagrammatic representation of the one loop matter power spectrum in Eq. (2.66) where $P_{11} = P_{\rm lin}$.

ii.) Assign a linear power spectrum $(2\pi)^3\delta^{(\rm D)}(\boldsymbol{q}+\boldsymbol{q}')P_{\rm lin}(q)$ to each of the dots with outgoing momenta $\boldsymbol{q}$ and $\boldsymbol{q}'$.

iii.) Integrate over all inner momenta $\int \mathrm{d}^3 q_i/(2\pi)^3$

iv.) Multiply with the symmetry factor

v.) Sum over all distinct labelings of the external lines

2. Add up the resulting expressions from all diagrams

2.2.3. Power Spectrum & Bispectrum

The discussion in the previous section allowed us to express non-linear density and velocity fields as a sum of products of linear density fields. If we are interested in n-spectra of the fields, we have to correlate two of these non-linear fields with each other. This will again lead to a sum of correlators. As we have seen in Sec. 1.4, only even correlators of linear density fields contribute and these correlators can be expressed as products of linear power spectra, whose form is given by the process seeding the fluctuations and the subsequent linear growth. Thus we were able to reduce the problem of calculating spectra of non-linear fields to convolutions of linear power spectra.
In Sec. 1.4 we mentioned, that Gaussian random fields have a vanishing bispectrum and that their trispectrum can be written as a product of power spectra. The gravitational evolution changes this behaviour and leads to a non-vanishing bispectrum that arises from expanding one of the fields in the correlator of three Fourier modes to second order

$$\langle \delta(\boldsymbol{k}_1, \delta(\boldsymbol{k}_2)\delta(\boldsymbol{k}_3)\rangle = \left\langle \delta^{(2)}(\boldsymbol{k}_1)\delta^{(1)}(\boldsymbol{k}_2)\delta^{(1)}(\boldsymbol{k}_3)\right\rangle + 2 \text{ cyc.} \tag{2.63}$$

We thus have

$$B(\boldsymbol{k}_1, \boldsymbol{k}_2, \boldsymbol{k}_3) = 2F_2(\boldsymbol{k}_1, \boldsymbol{k}_2)P_{\rm lin}(k_1)P_{\rm lin}(k_2) + 2 \text{ cyc.} \tag{2.64}$$

A diagrammatic depiction of this correlator is given in Fig. 2.4. Here cyc. stands for a cyclic permutation of the three k-vectors in the arguments of the power spectra and coupling kernels.
As this calculation becomes more and more tedious order by order, we usually truncate the calculation at next-to-leading order or next-to-next-to-leading order. In this context it is also useful to introduce the notion of **loops**. The leading order contribution to the power spectrum is second order in the fields and doesn't involve any momentum integrations and is thus formally a zero-loop result. The next to leading order has to be of fourth order in the fields by Wick's theorem. There are two possibilities to achieve this, by correlating two second order density fields or by correlating a linear density field with a second order density field

$$\langle \delta(\boldsymbol{k})\delta(\boldsymbol{k}')\rangle = \left\langle \delta^{(1)}(\boldsymbol{k})\delta^{(1)}(\boldsymbol{k}')\right\rangle + 2\left\langle \delta^{(1)}(\boldsymbol{k})\delta^{(3)}(\boldsymbol{k}')\right\rangle + \left\langle \delta^{(2)}(\boldsymbol{k})\delta^{(2)}(\boldsymbol{k}')\right\rangle \tag{2.65}$$

Thus

$$P_{\text{1-loop}}(k) = P_{\rm lin}(k) + 2P_{13}(k) + P_{22}(k). \tag{2.66}$$

A diagrammatic representation of the above power spectrum is given in Fig. 2.6. The coupling of two second order density fields leads to the mode coupling power spectrum P_{22}

$$P_{22}(k) = 2\int \frac{\mathrm{d}^3q}{(2\pi)^3} P_{\rm lin}(q) P_{\rm lin}(|\boldsymbol{k}-\boldsymbol{q}|)\left|F_2(\boldsymbol{q},\boldsymbol{k}-\boldsymbol{q})\right|^2 . \tag{2.67}$$

For explicit evaluations it is convenient to parametrize the momenta as $\boldsymbol{k} = (0,0,k)$ and $\boldsymbol{q} = rk(\sqrt{1-\mu^2},0,\mu)$

$$P_{22} = \frac{k^3}{2\pi^2}\int \mathrm{d}r\; r^2 \int \mathrm{d}\mu\; P_{\rm lin}(rk) P_{\rm lin}(\psi(r,\mu)k)\left|F_{2,\mathrm{d}}(q,\mu)\right|^2 , \tag{2.68}$$

where $\psi(r,\mu) = \sqrt{1+r^2-2r\mu}$ and

$$F_{2,\mathrm{d}}(r,\mu) = \frac{7\mu + \left(3-10\mu^2\right) r}{14 r\left(r^2-2\mu r+1\right)} . \tag{2.69}$$

The correlation of the linear field with a cubic field leads to the propagator P_{13}

$$P_{13}(k) = 3P_{\rm lin}(k)\int \frac{\mathrm{d}^3q}{(2\pi)^3} P_{\rm lin}(q) F_3(\boldsymbol{k},\boldsymbol{q},-\boldsymbol{q}). \tag{2.70}$$

One realises immediately that this term is a product of a linear power spectrum and a k-dependent correction. Thus, this term is usually interpreted as the gravitational modification of the initial linear power spectrum and thus denoted propagator. The integral over the angular part can be analytically calculated leading to

$$\begin{aligned} P_{13}(k) =& \frac{k^3}{252(2\pi)^2} P_{\rm lin}(k)\int \mathrm{d}r\, r^2 P_{\rm lin}(kr)\times \\ &\times\left[\frac{12}{r^4} - \frac{158}{r^2} + 100 - 42r^2 + \frac{3}{r^5}\left(7r^2+2\right)\left(r^2-1\right)^3 \log\left(\frac{r+1}{r-1}\right)\right] . \end{aligned} \tag{2.71}$$

As we will see in detail below, the next to leading order calculations involve one momentum integral and are thus one-loop terms. Up to sixth order in the fields, i.e. two loops, we have

$$\begin{aligned} \langle\delta(\boldsymbol{k})\delta(\boldsymbol{k}')\rangle =& \left\langle\delta^{(1)}(\boldsymbol{k})\delta^{(1)}(\boldsymbol{k}')\right\rangle + 2\left\langle\delta^{(1)}(\boldsymbol{k})\delta^{(3)}(\boldsymbol{k}')\right\rangle + 2\left\langle\delta^{(1)}(\boldsymbol{k})\delta^{(5)}(\boldsymbol{k}')\right\rangle \\ &+ \left\langle\delta^{(2)}(\boldsymbol{k})\delta^{(2)}(\boldsymbol{k}')\right\rangle + \left\langle\delta^{(3)}(\boldsymbol{k})\delta^{(3)}(\boldsymbol{k}')\right\rangle + 2\left\langle\delta^{(2)}(\boldsymbol{k})\delta^{(4)}(\boldsymbol{k}')\right\rangle . \end{aligned} \tag{2.72}$$

Here we separated the terms correlating non-linear density field and linear density field (propagator terms) in the first line and the mode coupling terms in the second line.

2.2.4. Properties of the one-loop power spectrum

In is interesting to understand the behaviour of the mode coupling term in the limit of very small and very large external momenta. We are first considering the high-k limit $k \gg q$

$$\begin{aligned} P_{22}(k) \xrightarrow{k\gg q}& \left[\frac{569}{735}P_{\rm lin}(k) - \frac{47}{105}k\frac{\mathrm{d}P}{\mathrm{d}k} + \frac{1}{10}k^2\frac{\mathrm{d}^2P}{\mathrm{d}k^2}\right]\int\frac{\mathrm{d}^3q}{(2\pi)^3}P_{\rm lin}(q) + \frac{1}{3}k^2P_{\rm lin}(k)\int\frac{\mathrm{d}^3q}{(2\pi)^3}\frac{P_{\rm lin}(q)}{q^2} \\ =& \left[\frac{569}{735}P_{\rm lin}(k) - \frac{47}{105}k\frac{\mathrm{d}P}{\mathrm{d}k} + \frac{1}{10}k^2\frac{\mathrm{d}^2P}{\mathrm{d}k^2}\right]\sigma^2 + k^2P_{\rm lin}(k)\sigma_d^2 \end{aligned} \tag{2.73}$$

In the last equality, we used the definition of the displacement dispersion $\sigma^2_{\rm d}$ defined below Eq. (2.34).

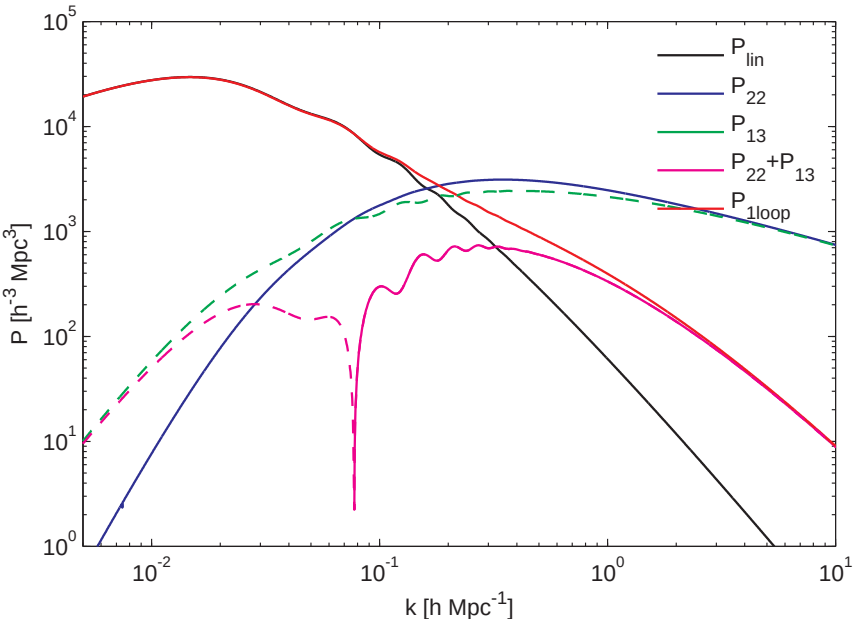

Figure 2.6.: One-loop power spectrum. As you can see there is a significant cancellation between $2P_{13}$ and P_{22} for high momenta.

	UV-divergent	IR-divergent
P_{13}	$n \geq -1$	$n \leq -1$
P_{22}	$n \geq 1/2$	$n \leq -1$
$P_{1-\mathrm{loop}}$	$n \geq -1$	$n \leq -3$

Table 2.1.: Convergence properties of the one-loop power spectrum and its components P_{22} and P_{13}.

The low-k limit yields

$$P_{22}(k) \xrightarrow{k \ll q} \frac{9}{98} k^4 \int \frac{\mathrm{d}^3 q}{(2\pi)^3} \frac{P_{\mathrm{lin}}^2(q)}{q^4}. \tag{2.74}$$

While the exact numerical prefactor needs to be calculated from taking the limit of the F_2 kernel, the k^4 scaling can be inferred from the general asymptotic properties of the F_n kernels discussed in Eq. (2.60) above.

In the high-k limit ($k \gg q$) P_{13} asymptotes to

$$P_{13}(k) \xrightarrow{k \gg q} -\frac{1}{3} k^2 P_{\mathrm{lin}}(k) \int \frac{\mathrm{d}^3 q}{(2\pi)^3} \frac{P_{\mathrm{lin}}(q)}{q^2} \left(1 - \frac{116}{105}\frac{q^2}{k^2} + \frac{188}{245}\frac{q^4}{k^4} + \dots\right) = -\frac{1}{2} k^2 P_{\mathrm{lin}}(k) \sigma_d^2(k)\,. \tag{2.75}$$

We immediately see that the σ_d^2 contribution in $2P_{13}$ exactly cancels with the corresponding positive contribution in P_{22} above in Eq. (2.73).

In the low k-limit we have instead

$$P_{13}(k) \xrightarrow{k \ll q} -\frac{1}{3} k^2 P_{\mathrm{lin}}(k) \int \frac{\mathrm{d}^3 q}{(2\pi)^3} \frac{P_{\mathrm{lin}}(q)}{q^2} \left(\frac{61}{210} - \frac{2}{35}\frac{k^2}{q^2} + \dots\right) = -\frac{61}{210} k^2 P_{\mathrm{lin}}(k) \sigma_d^2(k)\,. \tag{2.76}$$

The convergence properties of P_{13}, P_{22} and the full one-loop result are summarised in Tab. 2.1.

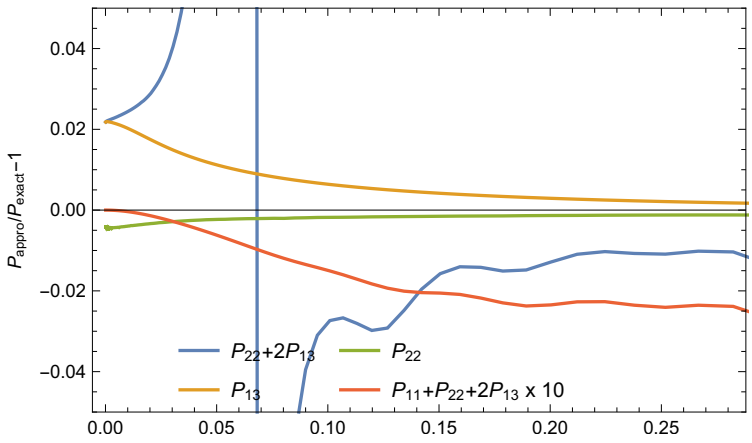

Figure 2.7.: Comparison of contributions to the one-loop matter power spectrum in the EdS approximation and the exact ΛCDM solution. Note that the fractional contribution for the full one-loop result has been multiplied by a factor of 10.

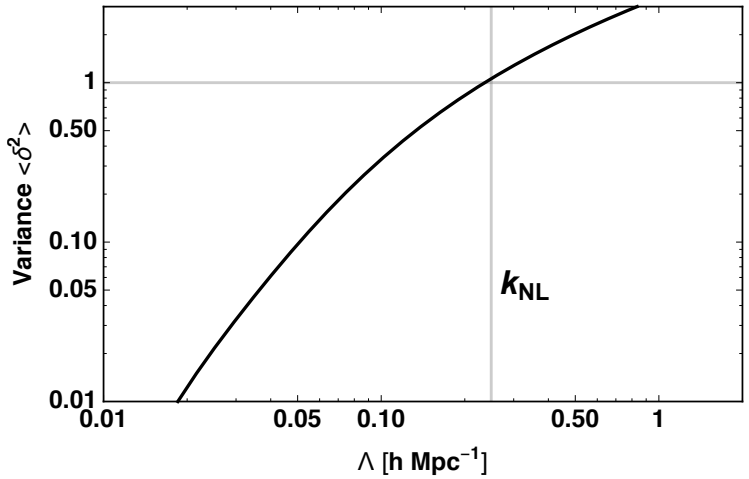

Figure 2.8.: Variance of the density field as a function of wavenumber cutoff Λ corresponding to smoothing scale $R \sim 1/\Lambda$.

2.3. Effective Field Theory Approach

Let us consider what we did so far - we wrote down a power series in density perturbations assuming that they are small. Let us calculate their typical size. The expectation value of δ itself vanishes, but we can calculate the variance. Let us be a bit more specific and consider the variance of the modes with wavenumbers below some cutoff $k < \Lambda$. This corresponds to the variance of a field smoothed on a scale $R = 1/\Lambda$

$$\sigma_\Lambda^2 = \frac{1}{2\pi^2}\int_0^\Lambda \mathrm{d}\ln q\; q^3 P_{\rm lin}(q) \approx \frac{\Lambda^3 P_{\rm lin}(\Lambda)}{2\pi^2} \approx \Delta^2(\Lambda)\,, \tag{2.77}$$

which is shown in Fig. 2.8. A power law expansion is clearly not warranted once the typical size of fluctuations exceeds unity. The variance is a growing function of Λ and the wavenumber at which it crosses unity defines the **non-linear wavenumber** $k_{\rm NL}$. For the currently favored ΛCDM model this happens at $k_{\rm NL} \approx 0.3\ h\mathrm{Mpc}^{-1}$.

Useful references for this section are [Baumann et al., 2012] and [Carrasco et al., 2012].

2.3.1. Problems of the Standard Treatment

- **no well defined expansion parameter:** On small scales the density is large, thus the power series expansion is not convergent.
- **deviations from PPF:** On small scales, shell crossing leads to multi streaming and thus deviations from the pressureless perfect fluid model.
- **divergences:** As we have seen in Tab. 2.1 for certain power law initial power spectra the loop integrals are divergent.
- **performance:** As one can see in Fig. 2.9, there is no notion of convergence towards the true answer.

2.3.2. Coarse grained equations of motion

We realized above, that the density is not a good variable to expand in as it can be large on small scales. We will thus **integrate out the small scales** by spatially smoothing the distribution function on a scale $1/\Lambda$ with $\Lambda < k_{\rm NL}$

$$f_{\rm l}(\boldsymbol{x},\boldsymbol{p},\eta) = \int \mathrm{d}^3x'\; W_\Lambda(\boldsymbol{x}-\boldsymbol{x}')f(\boldsymbol{x}',\boldsymbol{p},\eta)\,. \tag{2.78}$$

The coarse graining procedure defines the long wavelength part of fluctuations of arbitrary fields as

$$X_{\rm l} = [X]_\Lambda(\boldsymbol{x}) = \int \mathrm{d}^3x' W_\Lambda(|\boldsymbol{x}-\boldsymbol{x}'|)X(\boldsymbol{x}') \tag{2.79}$$

and we define the short wavelength part through $X_{\rm s} = X - X_{\rm l}$. While the exact functional form of the smoothing function is not extremely important, a Gaussian is very convenient.

$$W_\Lambda(\boldsymbol{x}) = \left(\frac{\Lambda}{\sqrt{2\pi}}\right)^3 \exp\left[-\frac{1}{2}\Lambda^2x^2\right], \qquad W_\Lambda(\boldsymbol{k}) = \exp\left[-\frac{1}{2}\frac{k^2}{\Lambda^2}\right].$$

The coarse grained density and momentum are then given by

$$\rho_{\rm l} = \int \mathrm{d}^3p\; f_{\rm l}(\boldsymbol{x},\boldsymbol{p},\eta)\,, \tag{2.80}$$

$$\boldsymbol{\pi}_{\rm l} = \rho_{\rm l}\boldsymbol{v}_{\rm l} = \frac{m}{a^3}\int \mathrm{d}^3p\; \frac{\boldsymbol{p}}{ma} f_{\rm l}(\boldsymbol{x},\boldsymbol{p},\eta)\,. \tag{2.81}$$

Note that the long wavelength velocity is defined through $\boldsymbol{v}_{\rm l} = \boldsymbol{\pi}_{\rm l}/\rho_{\rm l}$. The coarse grained fluid equations thus read

$$\delta_{\rm l}' + \partial_j\left[(1+\delta_{\rm l})v_{{\rm l},j}\right] = 0\,, \tag{2.82}$$

$$v_{{\rm l},i}' + \mathcal{H}v_{{\rm l},i} + \partial_i\phi_{\rm l} + v_{{\rm l},j}\partial_j v_{{\rm l},i} = -\frac{1}{\rho_{\rm l}}\partial_j\left[\tau_{ij}\right]_\Lambda\,. \tag{2.83}$$

The fact that we generated a non-vanishing stress tensor arises from the fact that coarse grained products of fluctuations lead to products of long fluctuations plus corrections, for instance the coarse grained product of short modes (see [Baumann et al., 2012] for a derivation)

$$[fg]_\Lambda = f_{\rm l}g_{\rm l} + [f_{\rm s}g_{\rm s}]_\Lambda + \frac{1}{\Lambda^2}\nabla f_{\rm l}\nabla g_{\rm l} + \cdots \tag{2.84}$$

The derivative corrections in the last term will be negligible in the end as we only consider the theory for $k \ll \Lambda$. The stress tensor then arises from the microscopic stress tensor discussed above plus corrections that arise from the coarse grained products of short fluctuations

$$\tau_{ij} = \rho\sigma_{ij} + \rho v_i^{\rm s}v_j^{\rm s} - \frac{\phi^{\rm s}_{,k}\phi^{\rm s}_{,k}\delta^{(\rm K)}_{ij} - 2\phi^{\rm s}_{,i}\phi^{\rm s}_{,j}}{8\pi G} \tag{2.85}$$

This implies that even in absence of microscopic velocity dispersion σ_{ij}, the coarse graining procedure produces an effective stress tensor or velocity dispersion.

The short scales are strongly coupled and thus can't be treated in the EFT, but we are not really interested in their behaviour. We can thus take expectation values over the short wavelength fluctuations. In QFT this procedure is known as **integrating out the UV-degrees of freedom**. The result of the expectation value will depend on the local amplitude of the long modes, for instance through tidal effects. We thus split them into an expectation value over the long modes, a response and fluctuations around the mean and response.

$$[f_{\rm s}g_{\rm s}]_\Lambda = \langle f_{\rm s}g_{\rm s}\rangle_\Lambda\big|_{\delta_{\rm l}=0} + \left.\frac{\partial\langle f_{\rm s}g_{\rm s}\rangle}{\partial\delta_\Lambda}\right|_{\delta_{\rm l}=0}\delta_{\rm l} + [f_{\rm s}g_{\rm s}]_\Lambda\big|_{\delta_{\rm l}=0} - \langle f_{\rm s}g_{\rm s}\rangle_\Lambda + \dots \tag{2.86}$$

This yields the **effective stress tensor** of an imperfect fluid, that at linear order in the fluctuations

$$\begin{aligned}[\tau_{ij}]_\Lambda =& p\delta^{(\rm K)}_{ij} + \bar\rho\tilde c^2_{\rm s}\delta^{(\rm K)}_{ij}\delta_{\rm l} - \bar\rho\frac{\tilde c^2_{\rm v,b}}{\mathcal{H}}\delta^{(\rm K)}_{ij}\partial_m v_{{\rm l},m}\\ &- \frac{3}{4}\bar\rho\frac{\tilde c^2_{v,s}}{\mathcal{H}}\left[\partial_i v_{{\rm l},j} + \partial_j v_{{\rm l},i} - \frac{2}{3}\delta^{(\rm K)}_{ij}\partial_m v_{{\rm l},m}\right] + \Delta\tau_{ij}\end{aligned} \tag{2.87}$$

Here we introduced the background pressure, the speed of sound as well as the bulk- and shear-viscosity. Finally, $\Delta\tau_{ij}$ describes the deviations between expectation values and the actual realization that does not correlate with the long modes. We will thus refer to this term as the **stochastic term**. Taking two spatial derivatives of the effective stress tensor, we obtain the source term of the Euler equation for the velocity divergence

$$\begin{aligned}\tau_\theta = \partial_i\partial_j\eta_{ij} =& \bar\rho\left[\tilde c^2_{\rm s}\partial^2\delta_{\rm l} - \frac{\tilde c^2_{\rm v,b}}{\mathcal{H}}\partial^2\theta_{\rm l} - \frac{3}{4}\frac{\tilde c^2_{v,s}}{\mathcal{H}}\partial^2\theta_{\rm l}\right] + \Delta J\\ =& \bar\rho\left[\tilde c^2_{\rm s}\partial^2\delta_{\rm l} - \frac{\tilde c^2_{v}}{\mathcal{H}}\partial^2\theta_{\rm l}\right] + \Delta J\end{aligned} \tag{2.88}$$

where $\Delta J = \partial_i\partial_j\Delta\tau_{ij}$. The effective stress tensor can in principle also be motivated from combinations of second derivatives of the gravitational potential due to equivalence principle. For instance, at first order we have[3]

$$\tau_{ij} = l_1\partial_i\partial_j\phi + l_2\delta^{(\rm K)}_{ij}\partial^2\phi \tag{2.89}$$

leading to $\partial_i\partial_j\eta_{ij} = \tilde c^2_s\partial^2\delta^{(1)}$. At second order (as relevant for the bispectrum) we would have

$$\tau_{ij} = e_1\partial_i\partial_l\phi\partial_l\partial_j\phi + e_2\delta^{(\rm K)}_{ij}\partial^2\phi\partial^2\phi + e_3\partial_i\partial_j\phi\partial^2\phi \tag{2.90}$$

Note that the second order stress tensor has these products of density fields plus explicit second order fields in the linear stress tensor.

Having calculated the stress tensor, we now need to solve the equations again in presence of this correction. For this purpose it is good to develop a notion of the size of various terms. As we will motivate in more detail below, we will consider $c^2_{\rm s} = \mathcal{O}([\delta^{(1)}]^2)$ and $\Delta J = \mathcal{O}([\delta^{(1)}]^2)$.

The inclusion of the source terms is best performed using the Greens function method for the coupled system

$$\begin{aligned}&\mathcal{H}^2\left\{-a^2\partial_a^2 + \frac{3}{2}\left(\Omega_{\rm m}(a) - 2\right)a\partial_a + \frac{3}{2}\Omega_{\rm m}(a)\right\}\delta = \mathcal{S}_\beta - \mathcal{H}\,\partial_a\left(a\,\mathcal{S}_\alpha\right)\,,\\ &\mathcal{H}\left\{a^2\partial_a^2 + \left(4 - \frac{3}{2}\Omega_{\rm m}(a)\right)a\partial_a + (2 - 3\Omega_m)\right\}\theta = \partial_a\left(a\,\mathcal{S}_\beta\right) - \frac{3}{2}\Omega_{\rm m}(a)\mathcal{H}\mathcal{S}_\alpha\,.\end{aligned} \tag{2.91}$$

$$\begin{aligned}\mathcal{S}_\alpha(\boldsymbol{k},\eta) =& -\int\frac{{\rm d}^3q}{(2\pi)^3}\,\alpha(\boldsymbol{q},\boldsymbol{k}-\boldsymbol{q})\,\theta(\boldsymbol{q},\eta)\delta(\boldsymbol{k}-\boldsymbol{q},\eta)\,,\\ \mathcal{S}_\beta(\boldsymbol{k},\eta) =& -\int\frac{{\rm d}^3q}{(2\pi)^3}\,\beta(\boldsymbol{q},\boldsymbol{k}-\boldsymbol{q})\,\theta(\boldsymbol{q},\eta)\theta(\boldsymbol{k}-\boldsymbol{q},\eta) + \eta_\theta(\boldsymbol{k},\eta)\,.\end{aligned} \tag{2.92}$$

[3] We will often consider a gravitational potential defined by $\nabla^2\phi = \delta$

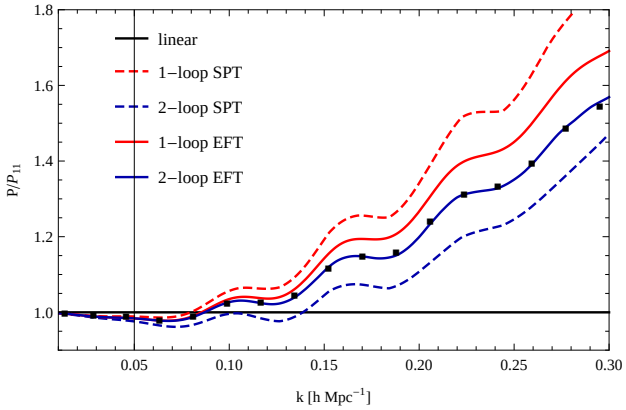

Figure 2.9.: Ratio of the non-linear and linear matter power spectrum. We show one-loop (red) and two-loop (blue) results for SPT (dashed) and EFT (solid). Clearly in SPT there is no notion of convergence as one goes to higher loops. EFT fares much better, providing a good fit to the data up to $k = 0.3\ h\mathrm{Mpc}^{-1}$.

The solution for δ can now be obtained using the Green's function

$$c_s^2 k^2 \delta^{(1)}(\boldsymbol{k}) \equiv \delta_{c_s^2} = \int \mathrm{d}a' G_\delta(a, a') k^2 \left[\tilde{c}_s^2(a') + \tilde{c}_v^2(a')\right] \delta^{(1)}(\boldsymbol{k}, a') \tag{2.93}$$

or with a power law ansatz $\tilde{c}_\mathrm{s}^2 \propto a^\gamma$ leading to recursion relations for the EFT correction terms.

At leading order we have

$$\delta(\boldsymbol{k}, \eta) = \delta^{(1)}(\boldsymbol{k}, \eta) + \delta^{(2)}(\boldsymbol{k}, \eta) + \delta^{(3)}(\boldsymbol{k}, \eta) - k^2 c_\mathrm{s}^2(\eta) \delta^{(1)}(\boldsymbol{k}, \eta) + \delta_J(\boldsymbol{k}, \eta) \tag{2.94}$$

where we have removed the tilde on c_s^2 to account for the time integration.

2.3.3. EFT and the Power Spectrum

We are now in the position to calculate the power spectrum including the counterterms

$$P(k) = P_\mathrm{lin}(k) + P_{22,\Lambda}(k) + 2P_{13,\Lambda}(k) - 2c_{\mathrm{s},\Lambda}^2 k^2 P_\mathrm{lin}(k) + P_{JJ,\Lambda}(k) \tag{2.95}$$

Here we have neglected the explicit dependence of P_{11} on the cutoff Λ as it is negligible for $k \ll \Lambda$. The above equation looks like it explicitly depends on the arbitrary cutoff scale Λ that was introduced to regularize the theory. In fact this dependence is only apparent, since the speed-of-sound and stochastic counterterms have the correct functional form to capture the cutoff dependence of P_{13} and P_{22}, respectively.

Let us first consider the effect of splitting the P_{13} integral at Λ

$$\begin{aligned} P_{13,\infty}(k) =& 3P_\mathrm{lin}(k) \int_0^\Lambda \frac{\mathrm{d}^3 q}{(2\pi)^3} F_{3,s}(\boldsymbol{k}, \boldsymbol{q}, -\boldsymbol{q}) P_\mathrm{lin}(q) + 3P_\mathrm{lin}(k) \int_\Lambda^\infty \frac{\mathrm{d}^3 q}{(2\pi)^3} F_{3,s}(\boldsymbol{k}, \boldsymbol{q}, -\boldsymbol{q}) P_\mathrm{lin}(q) \\ =& P_{13,\Lambda}(k) - k^2 P_\mathrm{lin}(k) \frac{61}{210} \frac{1}{6\pi^2} \int_\Lambda^\infty \mathrm{d}q P_\mathrm{lin}(q) \end{aligned} \tag{2.96}$$

Here we have used, that the effect of the smoothing function $W_\Lambda(k)$ is roughly equivalent to cutting off the integral at Λ and have used the low-k limit of the integral for the contributions coming from $q > \Lambda \gg k$.

The counterterms per se depend on the cutoff in a way to capture the cutoff dependence of the SPT integrals, for instance c_s^2

$$c_{s,\infty}^2 = c_{s,\Lambda}^2 - \frac{61}{210} \frac{1}{6\pi^2} \int_\Lambda^\infty \mathrm{d}q\ P_\mathrm{lin}(q) \tag{2.97}$$

We can now combine the cutoff-dependence of $P_{13,\Lambda}$ and the running of $c^2_{s,\Lambda}$ to obtain the cutoff independent result:

$$P_{13,\Lambda}(k) - c^2_{s,\Lambda} k^2 P_{\rm lin}(k) = P_{13,\infty}(k) - c^2_{s,\infty} k^2 P_{\rm lin}(k)\,. \tag{2.98}$$

The residual $c^2_{s,\infty} k^2 P_{\rm lin}(k)$ is a correction to the standard SPT result that remains even after undoing the smoothing operation. It is a free parameter of the effective theory, a so called low-energy constant, that has to be fitted to the data. There are two ways to do that. Either by fitting the one-loop power spectrum to a non-linear power spectrum or by a measurement of the effective stress tensor for a fixed smoothing scale Λ and extrapolation to $c^2_{s,\infty}$ using Eq. (2.97). As we will motivate below in Sec. 2.3.4, the EFT is an expansion in powers of $k/k_{\rm NL}$ for $k < k_{\rm NL}$. In such an expansion contributions with a shallower slope are obviously more important. This argument motivates that the P_{13} correction from c_s^2 is more relevant than the correction of P_{22} that we will discuss below.

Let us now discuss the remaining stochastic contribution. So far we haven't said anything about its behaviour, just that it arises from fluctuations in the short modes. These fluctuations can be understood as a local reshuffling of material for instance from the original linear configuration δ to a highly non-linear configuration $\tilde{\delta}$. The mere fact that the local non-linear reshuffling has to obey mass- and momentum conservation can inform us about the behaviour of the stochastic term:

$$\begin{aligned}
\delta_J(\boldsymbol{k}) =& \int_R \mathrm{d}^3x \exp\left[-\mathrm{i}\boldsymbol{k}\cdot(\boldsymbol{x}_0+\boldsymbol{x})\right]\left[\delta(\boldsymbol{x}_0+\boldsymbol{x}) - \tilde{\delta}(\boldsymbol{x}_0+\boldsymbol{x})\right] \\
=& \exp\left[-\mathrm{i}\boldsymbol{k}\cdot\boldsymbol{x}_0\right] \int_R \mathrm{d}^3x \left[1 + \mathrm{i}\boldsymbol{k}\cdot\boldsymbol{x} - \frac{1}{2}(\boldsymbol{k}\cdot\boldsymbol{x})^2\right]\left[\delta(\boldsymbol{x}_0+\boldsymbol{x}) - \tilde{\delta}(\boldsymbol{x}_0+\boldsymbol{x})\right] \\
=& \mathcal{O}(k^2)
\end{aligned} \tag{2.99}$$

Mass conservation ensures that the integral over $\delta - \tilde{\delta}$ vanishes and momentum conservation ensures that the same is true for the change of center of mass $\boldsymbol{k}\cdot\boldsymbol{x}(\delta - \tilde{\delta})$. We can thus infer that the power spectrum of the stochastic term has to scale as

$$P_{JJ}(k) \propto k^4\,. \tag{2.100}$$

This is great news, as it corresponds to the momentum dependence of P_{22} for small wavenumbers discussed in Eq. (2.74) above. In particular it alows us to set up the running or Λ-dependence of $P_{JJ}(k)$ in such a way that it cancels the corresponding cutoff dependence of P_{22}

$$P_{22,\Lambda}(k) + P_{JJ,\Lambda}(k) = P_{22,\infty}(k) + P_{JJ,\infty}(k) \tag{2.101}$$

We can thus send the cutoff to infinity, i.e., calculate the usual SPT loop integrals. In the observationally favoured ΛCDM model these integrals are formally convergent, but the fact that they are running over non-perturbative wavenumbers requires a counterterm to capture the unphysical contribitions. This counterterm is conveniently provided by the residual non-vanishing correction $c^2_{\rm s,\infty}$.

$$P(k) = P_{11}(k) + P_{22}(k) + 2P_{13}(k) - 2c_{s^2,\infty} k^2 P_{11}(k) + P_{JJ,\infty}(k) \tag{2.102}$$

Should one desire to evaluate the SPT integrals for power law initial conditions for which they would be formally divergent, the functional form of the counterterms $c^2_{s,\infty}k^2P_{\rm lin}$ and $P_{JJ,\infty}(k) \propto k^4$ are able to absorb these divergencies such that the result remains finite.

2.3.4. Importance of Terms in a Scaling Universe

The understanding of the importance of various terms and the cancellation of divergencies is somewhat difficult in the observationally favoured ΛCDM model with the somewhat complex power spectrum discussed in Sec. 1.3. To gain more insight, let us consider a matter-only EdS universe with a power law initial power spectrum. These initial conditions are also denoted scale-invariant initial conditions as there is no specific scale like the matter-radiation equality that would lead to the turnover of the linear power spectrum. There is however still the non-linear wavenumber $k_{\rm NL}$, where the variance of the linear modes crosses unity.[4] In

[4] We will consider initial power spectra $P_{\rm lin}(k) = k^n$ with $n > -3$ such that $\Delta^2(k)$ is a growing function of k.

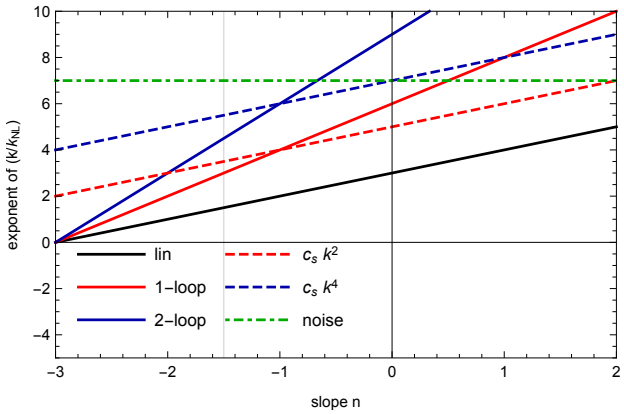

Figure 2.10.: Effective slopes of the contributions to the power spectrum in a scaling universe with initial slope n.

such a scale-invariant universe, the non-linear wavenumber is the only scale, and thus the linear power spectrum can be written as

$$\Delta^2_{\rm lin} = \left(\frac{k}{k_{\rm NL}}\right)^{3+n} \tag{2.103}$$

The finite part of the loop-integrals counts the power spectra, for instance at one-loop we have two power spectra and more generally at l-loops [Pajer and Zaldarriaga, 2013]:

$$\Delta^2_{l-\rm loop} = \left(\frac{k}{k_{\rm NL}}\right)^{(3+n)(1+l)} . \tag{2.104}$$

Finally, we have seen above that the speed of sound leads to $k^2 P_{\rm lin}$ and the stochastic term to $P_{JJ} \propto k^4$. Translating these contributions to dimensionless power spectra $\Delta^2 = k^3 P/2\pi^2$ we obtain

$$\Delta^2_{\rm stoch} = \left(\frac{k}{k_{\rm NL}}\right)^{7} , \qquad \Delta^2_{c_{\rm s}^2} = \left(\frac{k}{k_{\rm NL}}\right)^{5+n} . \tag{2.105}$$

The amplitude of the various terms is shown in Fig. 2.10 as a function of the power law slope n. Now the question arises, which slope might be relevant for our ΛCDM universe. It turns out a meaningfull approximation is to consider the effective slope of the linear power spectrum at the non-linear wavenumber $k_{\rm NL}$, which is roughly $n = -3/2$. Note that a smaller slope means a bigger contribution for $k < k_{\rm NL}$. Considering this, the ordering of importance would be: linear power > one loop SPT > one-loop counterterm c_s^2 > two loop SPT > two-loop counterterm > stochastic term. For practical purposes it is thus safe to ignore P_{JJ} in Eq. (2.102).

2.4. Lagrangian Perturbation Theory*

2.4.1. Equation of Motion

Lagrangian Perturbation Theory (LPT) starts from the initial unperturbed Lagrangian position $\boldsymbol{q}$ of the particle and follows their trajectory to their final position $\boldsymbol{x}$. The Lagrangian and Eulerian coordinates are related via the mapping $\boldsymbol{\Psi}$

$$\boldsymbol{x}(\boldsymbol{q}, \eta) = \boldsymbol{q} + \boldsymbol{\Psi}(\boldsymbol{q}, \eta). \tag{2.106}$$

The corresponding change of the density is given by the continuity relation

$$[1 + \delta(\boldsymbol{x})]\, {\rm d}^3 x = {\rm d}^3 q, \tag{2.107}$$

where the volume distortion is described by the Jacobian

$$\mathcal{J} = \left|\frac{\mathrm{d}^3 x}{\mathrm{d}^3 q}\right| = \det\left[\delta_{ij}^{(\mathrm{K})} + \frac{\partial \Psi_i}{\partial q_j}\right] = \det\left[\delta_{ij}^{(\mathrm{K})} + \Psi_{i,j}\right]. \tag{2.108}$$

Thus we have $\delta(\boldsymbol{x}) = 1/\mathcal{J} - 1$ and consequently $\delta^{(1)}(\boldsymbol{x}) = -\mathcal{J}^{(1)} = -\Psi^{(1)}_{i,i}$. Taking the divergence of the particle equation of motion Eq. (2.8) and the Poisson equation we obtain

$$\mathcal{J}\,\boldsymbol{\nabla}_{\boldsymbol{x}} \cdot \left[\frac{\mathrm{d}^2 \boldsymbol{x}}{\mathrm{d}\eta^2} + \mathcal{H}\frac{\mathrm{d}\boldsymbol{x}}{\mathrm{d}\eta}\right] = \frac{3}{2}\Omega_{\mathrm{m}}(a)\mathcal{H}^2(\mathcal{J} - 1). \tag{2.109}$$

This equation is not yet completely expressed in terms of Lagrangian variables since $\nabla_{x_i} = (\delta_{ij}^{(\mathrm{K})} + \Psi_{i,j})^{-1}\nabla_{q_j}$. The equation can be solved perturbatively with the ansatz [Bouchet et al., 1995]

$$\boldsymbol{\Psi} = \boldsymbol{\Psi}^{(1)} + \boldsymbol{\Psi}^{(2)} + \boldsymbol{\Psi}^{(3)} + \cdots \tag{2.110}$$

The determinant is equivalently expanded as

$$\mathcal{J} = 1 + \mathcal{J}^{(1)} + \mathcal{J}^{(2)} + \mathcal{J}^{(3)} + \cdots \tag{2.111}$$

expressed in terms of the displacement field as [Bouchet et al., 1995]

$$\mathcal{J}^{(1)} = \mathcal{L}^{(1)} = \sum_i \Psi^{(1)}_{i,i} \tag{2.112}$$

$$\mathcal{J}^{(2)} = \mathcal{L}^{(2)} + \mathcal{K}^{(2)} = \sum_i \Psi^{(2)}_{i,i} + \frac{1}{2}\sum_{i\neq j}\left\{\Psi^{(1)}_{i,i}\Psi^{(1)}_{j,j} - \Psi^{(1)}_{i,j}\Psi^{(1)}_{j,i}\right\} \tag{2.113}$$

$$\mathcal{J}^{(3)} = \mathcal{L}^{(3)} + \mathcal{K}^{(3)} + \mathcal{M}^{(3)} = \sum_i \Psi^{(3)}_{i,i} + \sum_{i\neq j}\left\{\Psi^{(2)}_{i,i}\Psi^{(1)}_{j,j} - \Psi^{(2)}_{i,j}\Psi^{(1)}_{j,i}\right\} + \det \Psi^{(1)}_{i,j} \tag{2.114}$$

where $\mathcal{L}$, $\mathcal{K}$ and $\mathcal{M}$ are invariant scalars of the deformation tensor. At first order we have for the equation of motion

$$\left[\frac{\mathrm{d}^2}{\mathrm{d}\eta^2} + \mathcal{H}\frac{\mathrm{d}}{\mathrm{d}\eta} - \frac{3}{2}\Omega_{\mathrm{m}}(a)\mathcal{H}^2\right]\Psi^{(1)}_{i,i} = 0. \tag{2.115}$$

This is just the linear growth equation we have seen before Eq. (2.25). At first order we thus have

$$\Psi^{(1)}(\boldsymbol{k},\eta) = \mathrm{i}\frac{\boldsymbol{k}}{k^2}\delta^{(1)}(\boldsymbol{k})D(\eta)\,. \tag{2.116}$$

Furthermore for EdS we have with $\Psi^{(n)} \propto a^n$ we have $\mathrm{d}^2\Psi^{(n)}/\mathrm{d}a^2 = n(n-1)\Psi^{(n)}/a^2$ and $\mathrm{d}\Psi^{(n)}/\mathrm{d}a = n\Psi^{(n)}/a$

$$\mathcal{J}(\delta_{ij}^{(\mathrm{K})} + \Psi_{i,j})^{-1}\left(n^2 + \frac{n}{2}\right)\mathcal{H}^2\,\Psi^{(n)}_{i,j} = \frac{3}{2}\mathcal{H}^2(\mathcal{J} - 1) \tag{2.117}$$

Up to second order one has

$$(\delta_{ij}^{(\mathrm{K})} + \Psi_{i,j})^{-1} = \delta_{ij}^{(\mathrm{K})} - \Psi_{i,j} + \Psi_{i,l}\Psi_{l,j} \tag{2.118}$$

We can now collect all the second order terms (intrinsically second order terms and products of first order terms)

$$\frac{3}{2}\mathcal{J}^{(1)}\Psi^{(1)}_{i,i} - \frac{3}{2}\Psi^{(1)}_{i,j}\Psi^{(1)}_{i,j} + 5\Psi^{(2)}_{i,i} = \frac{3}{2}\mathcal{J}^{(2)} \tag{2.119}$$

Using the expansion of the determinant we finally have

$$\frac{3}{2}\left[\Psi^{(1)}_{i,i}\Psi^{(1)}_{j,j} - \Psi^{(1)}_{i,j}\Psi^{(1)}_{i,j}\right] + 5\Psi^{(2)}_{i,i} = \frac{3}{2}\Psi^{(2)}_{i,i} + \frac{3}{4}\left[\Psi^{(1)}_{i,i}\Psi^{(1)}_{j,j} - \Psi^{(1)}_{i,j}\Psi^{(1)}_{i,j}\right]. \tag{2.120}$$

Collecting the divergence of the second order displacement field we obtain

$$\mathcal{K}^{(2)} = \Psi^{(2)}_{i,i} = -\frac{3}{14}\sum_{i,j}\left[\Psi^{(1)}_{i,i}\Psi^{(1)}_{j,j} - \Psi^{(1)}_{i,j}\Psi^{(1)}_{i,j}\right] = -\frac{3}{7}\mathcal{L}^{(2)}\,. \tag{2.121}$$

2.4.2. Perturbative solutions

Defining coupling kernels

$$\boldsymbol{\Psi}^{(n)}(\boldsymbol{k}) = \frac{\mathrm{i}}{n!}\prod_{i=1}^{n}\left\{\int \frac{\mathrm{d}^3 q_i}{(2\pi)^3}\delta^{(1)}(\boldsymbol{q}_i)\right\}\boldsymbol{L}_n(\boldsymbol{q}_1,\ldots,\boldsymbol{q}_n)(2\pi)^3\delta^{(\mathrm{D})}\left(\boldsymbol{k}-\boldsymbol{q}_1-\cdots-\boldsymbol{q}_n\right) \tag{2.122}$$

The first order kernel is obviously $L_1(\boldsymbol{k}) = \boldsymbol{k}/k^2$

$$\boldsymbol{L}_2 = \frac{3}{7}\frac{\boldsymbol{k}}{k^2}\left(1-\frac{(\boldsymbol{q}_1\cdot\boldsymbol{q}_2)^2}{q_1^2 q_2^2}\right) \tag{2.123}$$

$$\begin{aligned}\boldsymbol{L}_3 =& \frac{5}{7}\frac{\boldsymbol{k}}{k^2}\left[1-\left(\frac{\boldsymbol{q}_1\cdot\boldsymbol{q}_2}{q_1 q_2}\right)^2\right]\left[1-\left(\frac{(\boldsymbol{q}_1+\boldsymbol{q}_2)\cdot\boldsymbol{q}_3}{|\boldsymbol{q}_1+\boldsymbol{q}_2|q_3}\right)^2\right]\\ &-\frac{1}{3}\frac{\boldsymbol{k}}{k^2}\left[1-3\left(\frac{\boldsymbol{q}_1\cdot\boldsymbol{q}_2}{q_1 q_2}\right)^2+2\frac{\boldsymbol{q}_1\cdot\boldsymbol{q}_2\boldsymbol{q}_2\cdot\boldsymbol{q}_3\boldsymbol{q}_3\cdot\boldsymbol{q}_1}{q_1^2 q_2^2 q_3^2}\right]\end{aligned} \tag{2.124}$$

At third order there is also a vector component, which however only enters two point functions at sixth order, i.e., two-loops.

2.4.3. Calculation of the density field

$$\begin{aligned}\delta(\boldsymbol{k}) &= \int \mathrm{d}^3 x \exp\left[-\mathrm{i}\boldsymbol{k}\cdot\boldsymbol{x}\right]\delta(\boldsymbol{x}) = \int \mathrm{d}^3 x \exp\left[-\mathrm{i}\boldsymbol{k}\cdot\boldsymbol{x}\right]\left[1+\delta(\boldsymbol{x})\right] - \int \mathrm{d}^3 q \exp\left[-\mathrm{i}\boldsymbol{k}\cdot\boldsymbol{q}\right]\\ &= \int \mathrm{d}^3 q \exp\left[-\mathrm{i}\boldsymbol{k}\cdot\boldsymbol{q}\right]\left(\exp\left[-\mathrm{i}\boldsymbol{k}\cdot\boldsymbol{\Psi}(\boldsymbol{q})\right]-1\right)\end{aligned} \tag{2.125}$$

Where we used the continuity equation $[1+\delta(\boldsymbol{x})]\,\mathrm{d}^3 x = \mathrm{d}^3 q$. Expanding this equation in the density field one can see that order by order LPT and SPT are equivalent.

The power spectrum is given by

$$P(k) = \int \mathrm{d}^3 r \exp\left[-\mathrm{i}\boldsymbol{k}\cdot\boldsymbol{r}\right]\left\langle\exp\left[-\mathrm{i}\boldsymbol{k}\cdot\Delta\boldsymbol{\Psi}\right]-1\right\rangle \tag{2.126}$$

where $\boldsymbol{r} = \boldsymbol{q}-\boldsymbol{q}'$ and $\Delta\boldsymbol{\Psi}(\boldsymbol{r}) = \boldsymbol{\Psi}(\boldsymbol{q})-\boldsymbol{\Psi}(\boldsymbol{q}')$ and that this quantity can only depend on the distance between the points by translation invariance. One can use the cumulant expansion theorem to bring the expectation value into the exponential[5] $\left\langle\exp\left[\mathrm{i}\boldsymbol{k}\cdot\Delta\boldsymbol{\Psi}\right]\right\rangle = \exp\left[-1/2\left\langle(\boldsymbol{k}\cdot\Delta\boldsymbol{\Psi})^2\right\rangle\right]$

2.5. Biased Tracers

Apart from gravitational lensing, we have no direct way to see the dark matter distribution. What we can observe however are galaxies, which form at particular locations in the density field. In particular, galaxies tend to form in virialized blobs of dark matter that are referred to as **dark matter haloes**. We can find these dark matter haloes in simulations and study their clustering statistics, but we would like to develop some analytical understanding and extend the perturbation theory techniques developed above to the observable tracers of LSS.

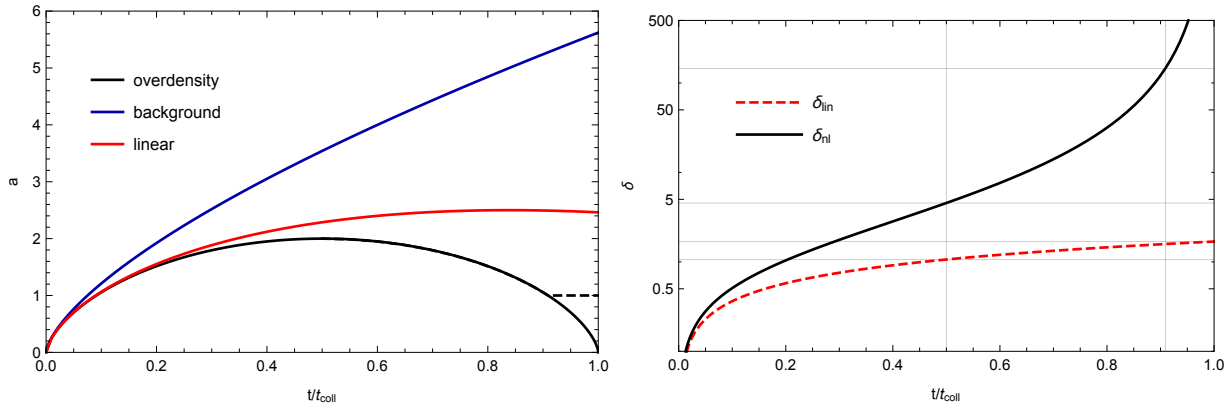

Figure 2.11.: Spherical collapse solution. *Left panel:* Evolution of the scale factor. *Right panel:* Evolution of the overdensity.

2.5.1. Spherical Collapse

The Friedmann equation for a closed Universe in a background matter-only Universe with scale factor $a_\mathrm{b} = R_\mathrm{b}/R_{\mathrm{b},0} = (3/2H_{\mathrm{b},0}t)^{2/3}$ reads as

$$H^2 = \frac{8\pi G\bar{\rho}}{3a^3} - \frac{K}{a^2} = H_0^2\left[\Omega_{\mathrm{m},0}a^{-3} + (1-\Omega_{\mathrm{m},0})\,a^{-2}\right], \tag{2.127}$$

where $K = H_0^2\,(\Omega_{\mathrm{m},0}-1) > 0$. The time evolution of the growth factor can be parametrized by the cycloid[6] solution

$$a = \frac{R}{R_0} = A\,(1-\cos\theta) \qquad\qquad t = B\,(\theta - \sin\theta) \tag{2.128}$$

where $R_0^3\bar{\rho} = R_{b,0}^3\bar{\rho}_\mathrm{b}$

$$A = \frac{4\pi G\bar{\rho}}{3K} = \frac{\Omega_{\mathrm{m},0}}{2(\Omega_{\mathrm{m},0}-1)} \qquad\qquad B = \frac{4\pi G\bar{\rho}}{3K^{3/2}} = \frac{\Omega_{\mathrm{m},0}}{2H_0(\Omega_{\mathrm{m},0}-1)^{3/2}} \tag{2.129}$$

Time runs from 0 to $t_\mathrm{coll} = 2\pi B$ One can expand to obtain

$$a = A\frac{\theta^2}{2}\left(1-\frac{\theta^2}{12}\right) \qquad\qquad t = B\frac{\theta^3}{6}\left(1-\frac{\theta^2}{20}\right) \tag{2.130}$$

The leading order solution is just $t = B\theta^3/6$ and $a = (3/2H_{\mathrm{b},0}t)^{2/3}\Omega_{\mathrm{m},0}^{1/3} \propto a_\mathrm{b}$.

$$a \approx \frac{A}{2}\left(\frac{6t}{B}\right)^{2/3}\left[1-\frac{1}{20}\left(\frac{6t}{B}\right)^{2/3}\right] \tag{2.131}$$

[5] For non-Gaussian fields we have

$$\langle\exp[X]\rangle = \exp\left[\sum_{n=1}^{\infty}\frac{1}{n!}\left\langle X^N\right\rangle_\mathrm{c}\right]$$

where the $\langle X^N\rangle_\mathrm{c}$ are the connected moments or cumulants.

[6] With the substitution $a = y^2\Omega_{\mathrm{m},0}/(\Omega_{\mathrm{m},0}-1)$ one has

$$\left(\frac{\mathrm{d}y}{\mathrm{d}\eta}\right)^2 = \frac{H_0^2(\Omega_{\mathrm{m},0}-1)}{4}\,(1-y^2)$$

which with $\theta = \sqrt{K}\eta$ yields

$$y = \sin(\theta/2)$$

and

$$a = A\left[1-\cos\theta\right].$$

With $\mathrm{d}t = a\mathrm{d}\eta$ we have

$$t = B\left[\theta - \cos\theta\right].$$

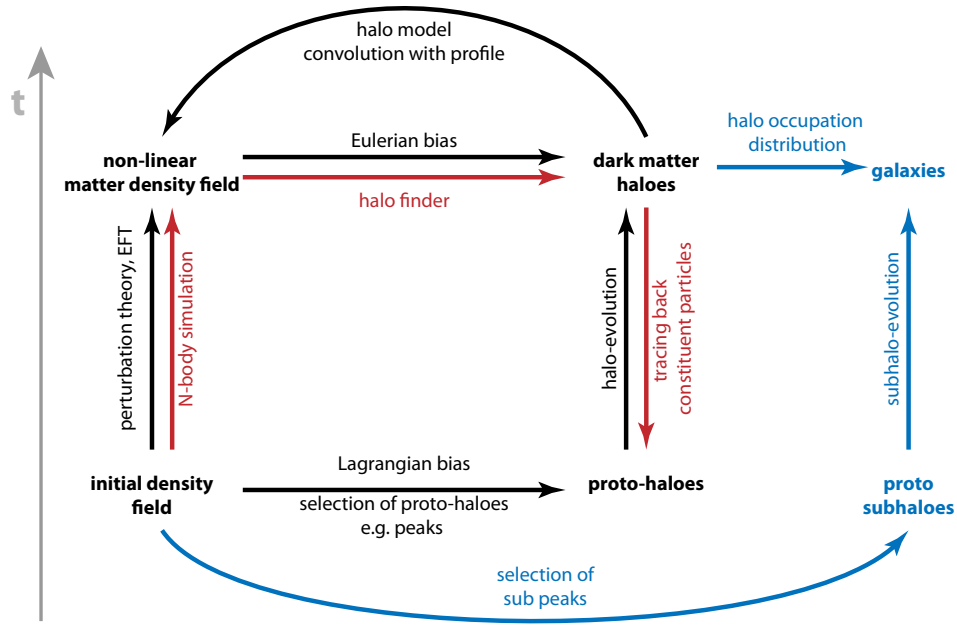

Figure 2.12.: Overview of the methods that can be employed to understand and model the distribution of matter, haloes and galaxies starting from the close to Gaussian initial conditions. As described in the main text, halo biasing can be understood as the selection of regions of the smoothed Gaussian density field that exceed a certain density threshold. Those regions then need to be propagated to Eulerian space. The Eulerian bias treatment however links the halo density to the evolved non-linear matter field. Galaxies can then be added into the framework using their halo occupation statistics.

The linear density contrast is

$$\delta_{\rm lin} = \frac{a_{\rm b}^3}{a_{\rm lin}^3} - 1 = \frac{3}{20}\left(\frac{6t}{B}\right)^{2/3} \propto a_{\rm b} \tag{2.132}$$

At collapse $\theta = 2\pi$ we have $t = 2\pi B$ and thus $\delta_{\rm lin} = \frac{3}{20}(12\pi)^{2/3} \approx 1.686$. For haloes that are collapsing today, we thus expect the present day linear overdensity to equal the critical collapse threshold $\delta_{\rm c} = 1.686$. The object will not collapse all the way, but instead virialize halfway between turnaround and collapse. The present day, non-linear overdensity of such an object is then $1 + \delta = a_{\rm b}^3(2\pi)/a^3(3\pi/2) \approx 178$.

The spherical collapse model tells us that a spherical region of size R whose present day linear overdensity is $\delta_{\rm c}$ will collapse into a virialized object of mass

$$M = \frac{4\pi}{3} R^3 \bar{\rho}. \tag{2.133}$$

Here we neglected the overdensity, since it is negligible compared to the mean density in Lagrangian space. The above one-to-one relation between mass and radius will allow use the two interchangeably in the following. Let us first estimate the probability of finding a spherical region with a given density in a Gaussian random field. For this purpose we first calculate the rms amplitude of fluctuations at the scale R or mass M, smoothing the density field with a top hat window of size R

$$\sigma^2(M) = \int \frac{{\rm d}^3 q}{(2\pi)^3} P(q) W_{\rm TH}^2(kR) \tag{2.134}$$

Then the probability of finding a region that has an overdensity of $\delta_{\rm c}$ is given by the probability density function of a Gaussian random variable

$$\mathbb{P}(\delta|M) = \frac{1}{\sqrt{2\pi\sigma^2(M)}} \exp\left[-\frac{1}{2}\frac{\delta^2}{\sigma^2(M)}\right] \tag{2.135}$$

The probability for a region to exceed the density threshold δ_c is given by

$$\mathbb{P}(>\delta_c|M) = \int_{\delta_c}^{\infty} \mathrm{d}\delta\ \mathbb{P}(\delta|M) = \int_{\nu}^{\infty} \mathrm{d}x\ \exp\left[-\frac{x^2}{2}\right], \tag{2.136}$$

where $\nu = \delta_c/\sigma$ is the **peak height** or **significance**. Since $\sigma(M)$ is a decreasing function of mass for the vanilla ΛCDM model, small scale inhomogeneities have a larger rms amplitude and are thus the first to cross the critical collapse density. Hence, structure formation happens in a **bottom up** scenario, where small scale objects collapse first and merge to form more and more massive objects as time proceeds. In Universes whose matter content is dominated by hot dark matter, structure formation follows a top down scenario, where large objects form first and subsequently disintegrate into smaller objects.
Since we are interested in the regions that form a halo of mass M, we need to account for the fact that a high overdensity of mass M might be part of a larger region containing mass $M + \mathrm{d}M$ that also exceeds the critical collapse density and could thus form a more massive halo. Thus, the fraction of regions that form haloes of mass M is given by

$$\mathbb{P}(>\delta_c|[M, M+\mathrm{d}M]) = |\mathbb{P}(>\delta_c|M+\mathrm{d}M) - \mathbb{P}(>\delta_c|M)| \approx -\frac{\mathrm{d}\mathbb{P}}{\mathrm{d}M} \tag{2.137}$$

$$= -\frac{\mathrm{d}\mathbb{P}}{\mathrm{d}\nu}\frac{\mathrm{d}\nu}{\mathrm{d}\sigma}\frac{\mathrm{d}\sigma}{\mathrm{d}M} = -\frac{1}{\sqrt{2\pi}}\frac{\delta_c}{\sigma^2}\exp\left[-\frac{\delta_c^2}{2\sigma^2}\right]\frac{\mathrm{d}\sigma}{\mathrm{d}M} \tag{2.138}$$

The above argument accounts only for half of the mass in the Universe, since underdense regions never collapse. This can be formally seen by integrating the above formula over σ or ν, yielding $1/2$. To correct for this problem, PS introduced an ad hoc factor of 2, that can be explained in the language of uncorrelated random walks.
To obtain the abundance of haloes of mass M,i.e. their **mass function**, we need to multiply this number by the maximum number of regions of mass M in a certain volume V containing mass M_{tot}, which is given by $N_{\mathrm{max}} = M_{\mathrm{tot}}/M$. Thus the maximum number density is $n_{\mathrm{max}} = M_{\mathrm{tot}}/M/V = \bar{\rho}/M$, which is independent of the norm volume.

$$n(M) = n_{\mathrm{max}}\mathbb{P}(>\delta_c|[M, M+\mathrm{d}M]) = -\sqrt{\frac{2}{\pi}}\frac{\bar{\rho}}{M}\frac{\delta_c}{\sigma^2}\exp\left[-\frac{\delta_c^2}{2\sigma^2}\right]\frac{\mathrm{d}\sigma}{\mathrm{d}M} \tag{2.139}$$

$$= \sqrt{\frac{2}{\pi}}\frac{\bar{\rho}}{M}\exp\left[-\frac{\nu^2}{2}\right]\frac{\mathrm{d}\nu}{\mathrm{d}M} \tag{2.140}$$

In the cosmology course you derived the Press-Schechter mass function by smoothing the density field on a scale $R \propto M^{1/3}$ and then looking for the biggest such region that exceeds the spherical-collapse density threshold δ_c. The resulting number density of objects can be written as

$$n(M) = -\sqrt{\frac{2}{\pi}}\frac{\bar{\rho}}{M}\frac{\nu}{\sigma}\exp\left[-\frac{\nu^2}{2}\right]\frac{\mathrm{d}\sigma}{\mathrm{d}M} = -\sqrt{\frac{2}{\pi}}\frac{\bar{\rho}}{M^2}\nu\exp\left[-\frac{\nu^2}{2}\right]\frac{\mathrm{d}\ln\sigma}{\mathrm{d}\ln M} \tag{2.141}$$

where $\nu = \delta_c/\sigma(M)$. It is important to note that the above calculation was performed in the (rescaled) Gaussian initial conditions, rather than the final Eulerian distribution of matter, where the non-linear density halo patch is roughly 180 times the background density.

2.5.2. Lagrangian Bias

Biasing can be understood in the framework of the peak-background split. Similar to what we did above for the coarse graining in the EFT, we define long wavelength fluctuations by smoothing the linear density field on a scale R. In contrast to the EFT above, where the smoothing scale was an ad-hoc regularization scale, here the scale is a physical scale related to the mass of the object. However, as a above we will be interested in the long wavelength behaviour, i.e., the large scale clustering of the haloes on scales $k < 1/R$. The scales smaller than R will determine the internal dynamics of the halo, which are somewhat irrelevant for the calculation of halo clustering statistics.

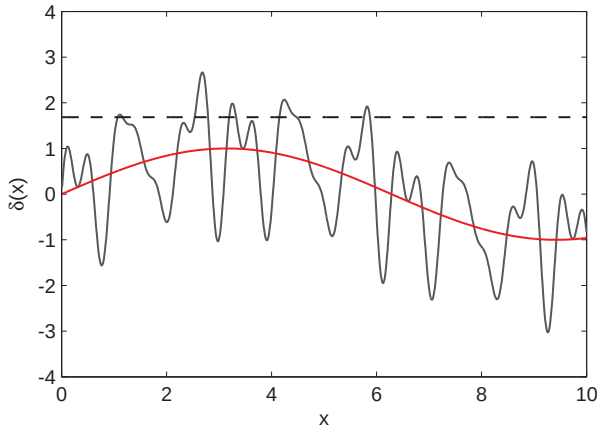

Figure 2.13.: The presence of a long wavelength mode δ_l facilitates the crossing of the collapse threshold δ_c for a short mode.

The short wavelength fluctuations with $k > 1/R$ dominate the variance, whereas the long wavelength fluctuations lead to a overall modulation of the fluctuations. In a crest of the long wavelength mode δ_l it is easier to cross the collapse threshold, the effective threshold becomes $\delta_\mathrm{c} \to \delta_\mathrm{c} - \delta_\mathrm{l}$. Thus the peak height becomes

$$\nu = \frac{\delta_\mathrm{c}}{\sigma} \to \tilde{\nu} = \frac{\delta_\mathrm{c} - \delta_\mathrm{l}}{\sigma} \,. \tag{2.142}$$

We can thus expand the mass function (local abundance of haloes) in powers of the long wavelength density fluctuation around its background value

$$n(\tilde{\nu}) = \bar{n}(\nu) + \frac{\partial n(\tilde{\nu})}{\partial \delta_\mathrm{l}} \delta_\mathrm{l} + \frac{1}{2} \frac{\partial^2 n(\tilde{\nu})}{\partial \delta_\mathrm{l}^2} \delta_\mathrm{l}^2 + \cdots \,. \tag{2.143}$$

Usually we are not interested in the number density per se, but the fluctuations around the mean number density, the **galaxy overdensity**

$$\delta_\mathrm{g}(\boldsymbol{q}) = \frac{n}{\bar{n}} - 1 = b_1^{(\mathrm{L})} \delta_\mathrm{l}(\boldsymbol{q}) + \frac{b_2^{(\mathrm{L})}}{2} \delta_\mathrm{l}^2(\boldsymbol{q}) + \frac{b_3^{(\mathrm{L})}}{3!} \delta_\mathrm{l}^3(\boldsymbol{q}) + \cdots \,, \tag{2.144}$$

where the Lagrangian bias parameters are defined as

$$b_i^{(\mathrm{L})} = \frac{1}{\bar{n}} \frac{\partial^i n}{\partial \delta_\mathrm{l}^i} \,. \tag{2.145}$$

At first order this yields

$$b_1^{(\mathrm{L})} = \frac{1}{\bar{n}} \frac{\partial n}{\partial \nu} \frac{\partial \tilde{\nu}}{\partial \delta_\mathrm{l}} = -\frac{1}{\bar{n}} \frac{\partial n}{\partial \nu} \frac{\partial \nu}{\partial \delta_\mathrm{c}} \,. \tag{2.146}$$

Here we introduced the superscript (L) to highlight the fact that this expansion is performed in Lagrangian space, i.e., before the non-linear gravitational evolution sets in. It turns out that a power series expansion has some odd effects, starting with $\langle \delta_\mathrm{g} \rangle \neq 0$, so we rather expand in Hermite polynomials

$$\delta_\mathrm{g}(\boldsymbol{q}) = \sum \frac{1}{i!} b_i^{(\mathrm{L})} H_i(\delta_\mathrm{l}(\boldsymbol{q})/\sigma) \sigma^i \tag{2.147}$$

where $H_1(x) = x$, $H_2(x) = x^2 - 1$ and $H_3(x) = x^3 - 3x$.

For the Press-Schechter mass function we have

$$b_1^{(\mathrm{L})} = \frac{\nu^2 - 1}{\delta_\mathrm{c}} \,, \qquad\qquad b_2^{(\mathrm{L})} = \frac{\nu^2 \left(\nu^2 - 3\right)}{\delta_\mathrm{c}^2} \,. \tag{2.148}$$

Before we discuss biasing in the Eulerian, i.e., observational late time setting, let us get the two point function of biased tracers in Lagrangian space directly from our considerations about n-point functions of Gaussian random fields.

2.5.3. Threshold Bias*

The Lagrangian matter density field is a Gaussian random field, whose statistical properties are fully described by its two-point function. This remains to be true after smoothing the density field at the mass scale of the halo sample under consideration. Hence, we can calculate the exact correlation function of regions above threshold following [Kaiser, 1984].
The one and two point Probability Density Functions (PDFs) of a Gaussian random field are given by

$$\mathbb{P}_{1\mathrm{pt}}(\delta) = \frac{1}{\sqrt{2\pi\sigma^2}} \exp\left[-\frac{1}{2}\frac{\delta^2}{\sigma^2}\right] \qquad \mathbb{P}_{2\mathrm{pt}}(\boldsymbol{Y}) = \frac{1}{\sqrt{(2\pi)^2 \det C}} \exp\left[-\frac{1}{2}\boldsymbol{Y} C^{-1} \boldsymbol{Y}^T\right] \tag{2.149}$$

where $\boldsymbol{Y} = (\delta(\boldsymbol{x}_1), \delta(\boldsymbol{x}_2)) = (\delta_1, \delta_2)$ and C is the covariance matrix of density fluctuations at positions $\boldsymbol{x}_1$ and $\boldsymbol{x}_2$. The covariance matrix is given by

$$C = \langle \delta(\boldsymbol{x}_1)\delta(\boldsymbol{x}_2)\rangle = \begin{pmatrix} \sigma^2 & \xi(r) \\ \xi(r) & \sigma^2 \end{pmatrix}, \tag{2.150}$$

where $r = |\boldsymbol{x}_1 - \boldsymbol{x}_2|$ and ξ is the usual correlation function of the smoothed linear density field. Here we omitted the subscript R, but the density fields, correlation functions and variance should be understood as smoothed on the scale R using a top hat filter. The inverse covariance matrix is readily written as

$$C^{-1} = \frac{1}{\sigma^4 - \xi^2(r)} \begin{pmatrix} \sigma^2 & -\xi(r) \\ -\xi(r) & \sigma^2 \end{pmatrix}. \tag{2.151}$$

Introducing $\delta = \sigma\nu$ the two point PDF can be written as

$$\mathbb{P}_{2\mathrm{pt}}(\nu_1, \nu_2) = \frac{1}{(2\pi)^3\sigma^2\sqrt{1 - \xi^2(r)/\sigma^4}} \exp\left[-\frac{1}{2}\frac{\nu_1^2 + \nu_2^2 - 2\nu_1\nu_2\xi(r)/\sigma^2}{1 - \xi^2(r)/\sigma^4}\right]. \tag{2.152}$$

Integrating the two point PDF over all peak heights, we recover the underlying two-point function. If we are interested in the distribution of protohaloes, we would rather like to consider the regions above threshold in a Gaussian field smoothed on the mass scale of the halo sample under consideration. The probability for finding the overdensity in a certain regime of peak heights can be found by integrating the above PDFs between two limiting peak heights or from a threshold peak height to infinity. The latter case will select all haloes above a certain mass threshold and be dominated by peak heights close to the threshold due to the steeply decreasing mass function.
As we have seen in Sec. 1.1.2, the correlation function is defined as the excess over random probability of finding two objects separated by a distance r

$$\mathbb{P}_{2\mathrm{pt}}(r) = \mathbb{P}_{1\mathrm{pt}}^2 \left[1 + \xi_{\mathrm{tr}}(r)\right]. \tag{2.153}$$

Thus we have for the correlation function of the thresholded regions

$$1 + \xi_{\mathrm{tr}}(r) = \frac{\int \mathrm{d}\nu_1 \int \mathrm{d}\nu_2 \mathbb{P}_{2\mathrm{pt}}(\nu_1, \nu_2)}{\int \mathrm{d}\nu_1 \mathbb{P}_{1\mathrm{pt}}(\nu_1) \int \mathrm{d}\nu_2 \mathbb{P}_{1\mathrm{pt}}(\nu_2)} \tag{2.154}$$

The one point function or abundance in the denominator reminds us of the PS results discussed above. The difference is that we are not considering the differential abundance between masses M and $M + \mathrm{d}M$. The above equation is a non-perturbative expression for the correlation of thresholded regions in a Gaussian random field. To find the relation between the correlation function of thresholded regions and the underlying matter correlation function we can expand in the large distance, small correlation limit and obtain

$$\xi_{\mathrm{tr}}(r) = \sum_{i=1}^{\infty} \frac{b_i^2}{i!} \xi^i(r). \tag{2.155}$$

We see that at leading order in this expansion, the correlation function of thresholded regions is a linearly biased version of the smoothed correlation function. The bias is given by

$$b_1 = \frac{1}{\sigma} \frac{\int \mathrm{d}\nu \nu \exp\left[-\nu^2/2\right]}{\int \mathrm{d}\nu \exp\left[-\nu^2/2\right]} \approx \frac{\nu}{\sigma} \approx \frac{\nu^2}{\delta_{\mathrm{c}}} \tag{2.156}$$

The higher order biases are given as

$$b_i = \frac{\int \mathrm{d}\nu f_i(\nu) \exp\left[-\nu^2/2\right]}{\int \mathrm{d}\nu \exp\left[-\nu^2/2\right]} \approx \frac{\nu^i}{\sigma^i} \approx b_1^i, \tag{2.157}$$

where the integral kernels can be expressed in terms of the probabilists Hermite polynomials H_n as

$$f_n = \frac{1}{n!\sigma^2} H_n(\nu) \tag{2.158}$$

2.5.4. Eulerian Bias

Traditionally people wrote down the galaxy density as a functional of the halo density and made a local approximation

$$\delta_{\mathrm{g}}^{(\mathrm{E})}(\boldsymbol{x}) = \delta_{\mathrm{g}}\left[\delta(\boldsymbol{x}')\right] = b_1^{(\mathrm{E})}\delta(\boldsymbol{x}) + \frac{1}{2}b_2^{(\mathrm{E})}\left(\delta^2(\boldsymbol{x}) - \left\langle\delta^2\right\rangle\right) + \cdots \tag{2.159}$$

It turns out that this model is too restrictive. It doesn't provide a consistent fit to various halo statistics in simulations and it turns out that it is incompatible with time evolution even if the Lagrangian initial bias turns out to be local.

Dynamical Prediction

The Eulerian bias model by itself is not predictive in the sense that the Eulerian bias parameters in Eq. (2.159) are free parameters that would have to be measured from the data. Under some simplifying assumptions we can however gain some insight on their amplitude by considering a mapping from the properties of the halo formation sites in Lagrangian space to the final evolved haloes. In Sec. 2.4.1 we saw that the mapping between the Lagrangian and Eulerian volume elements can be expressed as

$$\left[1 + \delta(\boldsymbol{x})\right] \mathrm{d}^3x = \mathrm{d}^3q. \tag{2.160}$$

Assuming that the haloes are comoving with the matter and that the number of haloes is conserved, we can write down a similar equation relating the halo overdensities in Lagrangian and Eulerian space

$$\left[1 + \delta_{\mathrm{g}}^{(\mathrm{E})}(\boldsymbol{x})\right] \mathrm{d}^3x = \left[1 + \delta_{\mathrm{g}}^{(\mathrm{L})}(\boldsymbol{q})\right] \mathrm{d}^3q. \tag{2.161}$$

Combining the two equations yields

$$\delta_{\mathrm{g}}^{(\mathrm{E})}(\boldsymbol{x}) = \delta_{\mathrm{g}}^{(\mathrm{L})}(\boldsymbol{q}) + \delta(\boldsymbol{x})\delta_{\mathrm{g}}^{(\mathrm{L})}(\boldsymbol{q}) + \delta(\boldsymbol{x}) \tag{2.162}$$

At first order we thus have

$$\delta_{\mathrm{g}}^{(\mathrm{E},1)}(\boldsymbol{x}) = \delta_{\mathrm{g}}^{(\mathrm{L},1)}(\boldsymbol{q}) + \delta^{(1)}(\boldsymbol{x}) = \left[b_1^{(\mathrm{L})} + 1\right] \delta^{(1)}(\boldsymbol{x}) \tag{2.163}$$

where we used that at first order $\delta^{(1)}(\boldsymbol{q}) = \delta^{(1)}(\boldsymbol{x})$. We thus found the well known relation $b_1^{(\mathrm{E})} = 1 + b_1^{(\mathrm{L})}$. At second order we have (for a derivation see example sheet III)

$$\delta_{\mathrm{g}}^{(\mathrm{E},2)}(\boldsymbol{x}) = \left(b_1^{(\mathrm{L})} + 1\right) \delta^{(2)}(\boldsymbol{x}) + \frac{1}{2}\left(b_2^{(\mathrm{L})} + \frac{8}{21}b_1^{(\mathrm{L})}\right)\left[\delta^{(1)}(\boldsymbol{x})\right]^2 - \frac{2}{7}b_1^{(\mathrm{L})}s^2(\boldsymbol{x}) \tag{2.164}$$

A similar calculation can be extended to cubic order bias parameters, which are relevant for the one-loop galaxy or halo power spectrum.

Symmetry based Bias Expansion

One can also argue that the galaxy or halo overdensity can be written in a basis that is constructed out of all non-degenerate terms that can be constructed from scalar combinations of second derivatives of the gravitational (here defined as $\partial^2\phi = \delta$) and velocity potential. At first order there is obviously only $\delta = \partial^2\phi$. The velocity and gravitational potential agree at this order.

$$\delta_{\rm g}^{(\rm E,1)}(\boldsymbol{x}) = b_1^{(\rm E)}\delta^{(1)}(\boldsymbol{x}) \tag{2.165}$$

At second order we can obviously consider the $(\partial^2\phi)^2 = \delta^2$ but also $\phi_{,ij}\phi_{,ij}$. Subtracting the trace, we can define the tidal field

$$s_{ij} = \phi_{,ij} - \frac{1}{3}\partial^2\phi\delta_{ij}^{(\rm K)} = \left(\frac{\partial_i\partial_j}{\partial^2} - \frac{1}{3}\delta_{ij}^{(\rm K)}\right)\delta \tag{2.166}$$

From this we define $s^2 = s_{ij}s^{ij}$. The difference between the velocity and gravitational potential is a second order quantity, but can be expressed as a linear combination of δ^2 and s^2 as

$$\partial^2\phi_{\rm v} - \partial^2\phi = \delta^{(2)} - \theta^{(2)} = -\frac{4}{21}\delta^2 + \frac{2}{7}s^2 \tag{2.167}$$

$$\delta_{\rm g}^{(\rm E,2)}(\boldsymbol{x}) = b_1^{(\rm E)}\delta^{(2)}(\boldsymbol{x}) + \frac{b_2^{(\rm E)}}{2}\delta^2(\boldsymbol{x}) + b_{s^2}^{(\rm E)}s^2(\boldsymbol{x}) \tag{2.168}$$

Note that the functional form agrees exactly with what we predicted from the dynamics in Eq. (2.164).

2.5.5. Shotnoise*

Let us consider a finite number of tracers N such as galaxies at positions $\boldsymbol{x}_i$ in a finite volume V

$$\delta_{\rm g}(\boldsymbol{x}) = \frac{1}{\bar{n}}\sum_i \delta^{(\rm D)}(\boldsymbol{x} - \boldsymbol{x}_i)\,. \tag{2.169}$$

Their Fourier space density field is then given by

$$\delta_{\rm g}(\boldsymbol{k}) = \frac{1}{\bar{n}}\sum_i \exp\left[i\boldsymbol{k}\cdot\boldsymbol{x}_i\right]\ , \tag{2.170}$$

where $\bar{n} = N/V$. The power spectrum of the discrete tracers in the finite volume can then be computed as

$$\begin{aligned} P_g(k) =& \frac{1}{V}\left\langle\delta(\boldsymbol{k})\delta(-\boldsymbol{k})\right\rangle\ , \\ =& \frac{V}{N^2}\sum_{i=j}\left\langle\exp\left[i\boldsymbol{k}(\boldsymbol{x}_i - \boldsymbol{x}_j)\right]\right\rangle + \frac{V}{N^2}\sum_{i\neq j}\left\langle\exp\left[i\boldsymbol{k}(\boldsymbol{x}_i - \boldsymbol{x}_j)\right]\right\rangle\ , \\ =& \frac{1}{\bar{n}} + P_{\rm g,cont}(k)\ . \end{aligned} \tag{2.171}$$

Here, the constant $1/\bar{n}$ is denoted the shot noise term and have identified the non-zero lag expectation value with the continuous part of the discrete tracer power spectrum $P_{\rm g,cont}(k)$. In the local bias model at linear order we have $P_{\rm g,cont}(k) = b_1^2P(k)$. This is clearly just an approximation for the continuous part of the tracer correlation function. Let us now consider the bispectrum. Following the same steps that lead to the

power spectrum above, we obtain

$$\begin{aligned} B_{\rm g} =&\frac{1}{V}\left\langle\delta(\boldsymbol{k}_1)\delta(\boldsymbol{k}_2)\delta(-\boldsymbol{k}_1-\boldsymbol{k}_2)\right\rangle\ , \\ =&\frac{V^2}{N^3}\sum_{i=j=l}\left\langle\exp\left[i\boldsymbol{k}_1(\boldsymbol{x}_i-\boldsymbol{x}_l)+i\boldsymbol{k}_2(\boldsymbol{x}_j-\boldsymbol{x}_l)\right]\right\rangle \\ +&3\frac{V^2}{N^3}\sum_{i=l\neq j}\left\langle\exp\left[i\boldsymbol{k}_1(\boldsymbol{x}_i-\boldsymbol{x}_l)+i\boldsymbol{k}_2(\boldsymbol{x}_j-\boldsymbol{x}_l)\right]\right\rangle \\ +&\frac{V^2}{N^3}\sum_{i\neq j\neq l}\left\langle\exp\left[i\boldsymbol{k}_1(\boldsymbol{x}_i-\boldsymbol{x}_l)+i\boldsymbol{k}_2(\boldsymbol{x}_j-\boldsymbol{x}_l)\right]\right\rangle\ , \\ =&\frac{1}{\bar{n}^2}+\frac{1}{\bar{n}}\left[P_{\rm g,cont}(k_1)+2\text{ perm}\right]+B_{\rm g,cont}(k_1,k_2,k_3)\ . \end{aligned} \tag{2.172}$$

Again, the non-zero lag correlators are identified with the continuous power spectrum and bispectrum of the tracer field. We see that two different stochasticity corrections arise: a $1/\bar{n}^2$ constant shot noise term and a product of the shot noise and the continuous power spectrum.

2.5.6. Summary: Bias Parameters

In summary the n-point functions of the galaxy/halo density field depend on the following bias parameters

Tree level power spectrum The galaxy/halo auto power depends on the linear bias parameter b_1 multiplying the linear power spectrum and the stochasticity ϵ_2.

Tree level bispectrum The tree level bispectrum has a linear bias parameter multiplying the matter bispectrum as well as terms arising from the explicit quadratic couplings in the galaxy/halo density field proportional to b_2, b_{s^2} in Eq. (2.168). The bispectrum shotnoise needs to be parametrized by an effective stochasticity ϵ_3.

One-loop power spectrum The linear bias b_1 multiplies the one-loop matter power spectrum in Eq. (2.102) including c_s^2. Beyond the second order bias parameters b_2, b_{s^2} only the cubic bias parameter b_{Γ_3} explicitly contributes [Assassi et al., 2014, Abidi and Baldauf, 2018]. The derivative bias $b_{\nabla^2\delta}$ has to be considered at this order and can absorb all of the speed-of-sound corrections in the matter power spectrum. Finally, the stochasticity needs to be accounted for by ϵ_2. The latter can differ from the tree-level calculation as it gets renormalized by b_2 and b_{s^2}. The final expression for the galaxy-galaxy power spectrum is

$$\begin{aligned} P_{\rm gg}(k) =&b_1^2P_{\delta,\delta}^{(\rm loop)}(k)+\frac{1}{4}b_2^2P_{\delta^2,\delta^2}(k)+b_2b_{s^2}P_{\delta^2,s^2}(k)+2b_{s^2}^2P_{s^2,s^2}(k) \\ &+2b_1\Big(b_{s^2}+\frac{2}{5}b_{\Gamma_3}\Big)\mathcal{I}_{s^2\delta^{(1)}}(k)+b_1b_2\mathcal{I}_{\delta^{(2)}\delta^2}(k)+2b_1b_{s^2}\mathcal{I}_{\delta^{(2)}s^2}(k) \\ &-2b_1b_{\nabla^2\delta}k^2P_{\delta,\delta}^{(\rm tree)}(k)+\epsilon_2\ , \end{aligned} \tag{2.173}$$

where

$$\mathcal{I}_{s^2\delta}(k) =4P_{\rm lin}(k)\int_{\boldsymbol{q}}\left(S_2(\boldsymbol{q},\boldsymbol{k}-\boldsymbol{q})F_2(\boldsymbol{k},-\boldsymbol{q})-\frac{34}{63}\right)P_{\rm lin}(q)\,, \tag{2.174}$$

$$\mathcal{I}_{\delta^{(2)}\delta^2}(k) =2\int_{\boldsymbol{q}}F_2(\boldsymbol{k}-\boldsymbol{q},\boldsymbol{q})P_{\rm lin}(q)P_{\rm lin}(|\boldsymbol{k}-\boldsymbol{q}|)\,, \tag{2.175}$$

$$\mathcal{I}_{\delta^{(2)}s^2}(k) =2\int_{\boldsymbol{q}}F_2(\boldsymbol{k}-\boldsymbol{q},\boldsymbol{q})S_2(\boldsymbol{k}-\boldsymbol{q},\boldsymbol{q})P_{\rm lin}(q)P_{\rm lin}(|\boldsymbol{k}-\boldsymbol{q}|)\,. \tag{2.176}$$

This model captures the weakly non-linear regime of the halo power spectrum [Abidi and Baldauf, 2018, Saito et al., 2014].

2.6. Redshift Space Distortions

While the angular positions of galaxies can be directly observed, the radial distance needs to be inferred from the redshift of the spectral lines. If the the galaxies were comoving with the Hubble flow, this would indeed provide an accurate distance. However, as we have seen before, inhomogeneities in the density distribution lead to velocities beyond the Hubble flow. These peculiar velocities lead to a shift between the observed and true radial position, referred to as redshift-space distortions. We will only provide a very brief description of the consequences for the observed galaxy power spectrum and refer the reader to [Hamilton, 1997] for a more in-depth discussion.
The position in redshift space $\boldsymbol{s}$ is given by the position in configuration space plus a correction proportional to the line of sight velocity

$$\boldsymbol{s} = \boldsymbol{x} + \frac{\boldsymbol{v}\cdot\hat{\boldsymbol{n}}}{\mathcal{H}}\hat{\boldsymbol{n}}\,. \tag{2.177}$$

As the objects are simply displaced rather then created, we can employ a continuity equation between configuration and redshift space

$$[1+\delta_s(\boldsymbol{s})]\,\mathrm{d}^3 s = [1+\delta(\boldsymbol{x})]\,\mathrm{d}^3 x\,. \tag{2.178}$$

In the limit of far away galaxies with a transverse spread small compared to the distance, we can work in the plane-parallel approximation and take the line of sight to agree with the z-axis. For the density field we thus have in analogy with the above transformations between Lagrangian and Eulerian space

$$\begin{aligned}\delta_s(\boldsymbol{k}) =& \int \mathrm{d}^3 s\ \exp\left[-\mathrm{i}\boldsymbol{k}\cdot\boldsymbol{s}\right]\delta_s(\boldsymbol{s})\\ =& \int \mathrm{d}^3 x\ \exp\left[-\mathrm{i}\boldsymbol{k}\cdot(\boldsymbol{x}+\hat{\boldsymbol{n}}\cdot\boldsymbol{v}\ \hat{\boldsymbol{n}}/\mathcal{H})\right]\big[1+\delta(\boldsymbol{x})\big] - \int \mathrm{d}^3 x \exp\left[-\mathrm{i}\boldsymbol{k}\cdot\boldsymbol{x}\right]\\ =& \delta(\boldsymbol{k}) + \int \mathrm{d}^3 x\ \exp\left[-\mathrm{i}\boldsymbol{k}\cdot\boldsymbol{x}\right]\big\{\exp\left[-\mathrm{i}\boldsymbol{k}\cdot\hat{\boldsymbol{n}}\ \hat{\boldsymbol{n}}\cdot\boldsymbol{v}/\mathcal{H}\right]-1\big\}\big[1+\delta(\boldsymbol{x})\big]\end{aligned} \tag{2.179}$$

At leading order, we obtain the **Kaiser formula**.

$$\delta_s(\boldsymbol{k}) = \delta(\boldsymbol{k}) - \mathrm{i}\boldsymbol{k}\cdot\hat{\boldsymbol{n}}\frac{\hat{\boldsymbol{n}}\cdot\boldsymbol{v}(\boldsymbol{k})}{\mathcal{H}} = \left(1+f\mu^2\right)\delta(\boldsymbol{k}) \tag{2.180}$$

where $\mu = k_\parallel/k$. Due to equivalence principle, on large scales biased tracers are comoving with the dark matter. Thus only the density is biased with respect to the dark matter such that we obtain for the galaxy density field in redshift space

$$\delta_s(\boldsymbol{k}) = \delta_{\mathrm{g}}(\boldsymbol{k}) - \mathrm{i}\boldsymbol{k}\cdot\hat{\boldsymbol{n}}\frac{\hat{\boldsymbol{n}}\cdot\boldsymbol{v}(\boldsymbol{k})}{\mathcal{H}} = \left(1+\beta\mu^2\right)b_1\delta(\boldsymbol{k}) \tag{2.181}$$

where $\beta = f/b_1$. The power spectrum is thus given by

$$P_{\mathrm{s}}(k,\mu) = b_1^2\left(1+\beta\mu^2\right)^2 P_{\mathrm{lin}}(k)\,. \tag{2.182}$$

It is immediately obvious that redshift space distortions break statistical isotropy and that the power spectrum now has a monopole, quadrupole and hexadecupole in terms of the direction cosine between k-mode and line of sight. As one should expect, modes transverse to the line-of-sight ($\mu = 0$) agree with the underlying matter or tracer distribution.

Up to third order we have (exercise)

$$\begin{aligned}\delta_s(\boldsymbol{k}) = \delta(\boldsymbol{k}) - \mathrm{i}\frac{k_\parallel}{\mathcal{H}}v_\parallel(\boldsymbol{k}) + \frac{\mathrm{i}^2}{2}\left(\frac{k_\parallel}{\mathcal{H}}\right)^2[v_\parallel\star v_\parallel](\boldsymbol{k}) - \frac{\mathrm{i}^3}{3!}\left(\frac{k_\parallel}{\mathcal{H}}\right)^3[v_\parallel\star v_\parallel\star v_\parallel](\boldsymbol{k})\\ -\mathrm{i}\frac{k_\parallel}{\mathcal{H}}[\delta\star v_\parallel](\boldsymbol{k}) + \frac{\mathrm{i}^2}{2!}\left(\frac{k_\parallel}{\mathcal{H}}\right)^2[\delta\star v_\parallel\star v_\parallel](\boldsymbol{k})\,.\end{aligned} \tag{2.183}$$

This expression contains products of density and velocity fields in configuration space, these so called contact operators thus contain products of long and short modes, which need to be regularized by appropriate counterterms. These corrections are discussed in detail in [Senatore and Zaldarriaga, 2014] and can be included by replacing the bare correlators by a sum of the bare correlator and the appropriate counterterms

2.7. Summary

- Gravitational instability leads to mode coupling, producing a non vanishing gravitational bispectrum.
- A peturbative expansion can be developed, where higher order corrections correspond to loops, i.e., momentum integrals over the power spectrum weighted by coupling kernels.
- A well defined perturbation theory requires a formalism to account for small scale, non-perturbative effects.
- The clustering of tracers of LSS in relation to the underlying matter distribution is described by a bias expansion.

3. Cosmic Microwave Background Anisotropies

The Cosmic Microwave Background is a sort of baby picture of the Universe, that allows us a first glimpse of the young Universe when it was only 380.000 years old.[1] Up to last scattering, the Universe was opaque due to the high density of free electrons. Once the temperature had fallen sufficiently (to about 3000 K), electrons (re)combined with the nuclei and formed neutral hydrogen (and helium). Thus, fairly suddenly the photons were able to propagate freely all the way until they reach our telescopes today. During the free-streaming the photons conserve the blackbody spectrum of $T = 2.27255$ K.

We will first derive an evolution equation for the photon temperature. It will turn out that we will mostly be interested in the monopole and dipole of the photons, i.e., we will obtain the equations of motion that resemble those of a fluid. We will then have to relate the temperature that the observer sees in direction $\hat{\boldsymbol{n}}$ to the intrinsic temperature of the CMB photons at the time of last scattering. We will see that the photon perturbations undergo acoustic oscillations as they enter the horizon and the phase of these oscillations at the time of last scattering will yield the oscillatory fluctuation spectrum. We will then go to the next-to-leading order in the tight coupling approximation to derive the damping of fluctuations on small scales. Having derived the temperature fluctuations, we will then consider the role of polarization and calculate the effect of gravitational lensing on the intrinsic CMB fluctuations.

We will be considering the following effects:

- primordial anisotropies (Sachs-Wolfe effect, Doppler effect, polarization, damping - linear)
- secondary anisotropies (integrated Sachs-Wolfe effect, SZ effect, gravitational lensing - mostly non-linear)

As a reference for this Chapter, I recommend the textbook by Dodelson [Dodelson, 2003] and for a more detailed treatment the book by Durrer [Durrer, 2008]. The review article [Challinor and Peiris, 2009] is based on the CMB chapters of Advanced Cosmology as previously taught by Prof. Challinor. Pedagogical explanations are also provided in the review article [Hu, 1996].

3.1. Boltzmann Equation

We shall use kinetic theory to describe the transition from the fluid-like, pre-recombination tightly coupled regime to the free-streaming radiation. The CMB photons can be described by the one-particle distribution function $f(x^\mu, p^\mu)$, which is a function of the spacetime position and four-momentum. The distribution function is Lorentz-invariant and, in the absence of scattering, it is conserved along the photon path in phase space.

The collision term C is a functional of the photon distribution function f and the electron distribution function f_e

$$\frac{\mathrm{d}f}{\mathrm{d}\eta} = C[f, f_e]\,. \tag{3.1}$$

We will use the metric in conformal Newtonian gauge

$$\mathrm{d}s^2 = -a^2(1+2\Psi)\mathrm{d}\eta^2 + a^2(1-2\Phi)\delta_{ij}^{(\mathrm{K})}\mathrm{d}x^i\mathrm{d}x^j\,, \tag{3.2}$$

where in the absence of anistotropic stress $\Psi = \Phi$.[2]

[1] If the Universe was one year old at the time of last scattering, it would soon be celebrating it's 35th birthday.
[2] Note that $\Phi_{\mathrm{here}} = -\Phi_{\mathrm{Dodelson}}$.

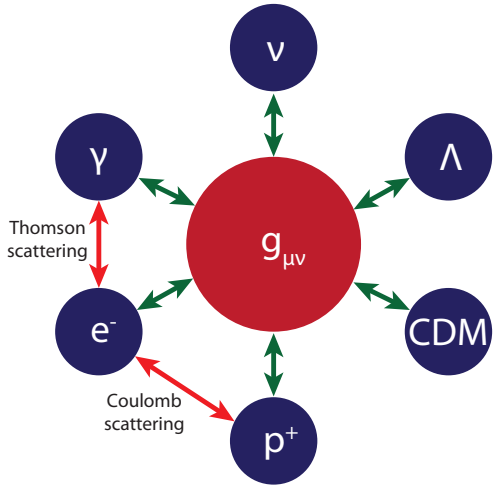

Figure 3.1.: Interaction between the perturbations in the various species in the universe. All of the species are coupled to the metric. Coulomb-scattering couples the electrons and protons, and the photons are Thomson scattering on free electrons before recombination. Adapted from [Dodelson, 2003].

Einstein Equations

The Einstein Equations in Newtonian Gauge are given by

$$-k^2\Phi - 3\mathcal{H}(\Phi' + \mathcal{H}\Phi) = 4\pi G a^2 \delta\rho_{\mathrm{N}}, \tag{3.3}$$

$$\Phi' + \mathcal{H}\Psi = 4\pi G a^2 \left(\bar{\rho} + \bar{p}\right) v_{\mathrm{N}}, \tag{3.4}$$

$$k^2(\Phi - \Psi) = 8\pi G a^2 \Sigma. \tag{3.5}$$

In the absence of anisotropic stress $\Sigma = 0$ the last equation entails $\Phi = \Psi$.

The photon momentum can be defined in a local tetrad. The photon momentum $P^\mu = \mathrm{d}x^\mu/\mathrm{d}\lambda$ is subject to the constraint $g_{\mu\nu}P^\mu P^\nu = -a^2(1+2\Psi)(P^0)^2 + p^2 = 0$, where $p^2 = g_{ij}P^iP^j = a^2(1-2\Phi)\delta^{(\mathrm{K})}_{ij}P^iP^j$ such that the temporal component can be expressed as

$$P^0 = \frac{p}{a}(1-\Psi)\,. \tag{3.6}$$

We can now factorize the spatial part of the momentum into a direction cosine satisfying $\delta^{(\mathrm{K})}_{ij}\hat{p}^i\hat{p}^j = 1$ and an amplitude $P^i = \kappa\hat{p}^i$. The constraint then yields $a^2(1-2\Phi)\delta^{(\mathrm{K})}_{ij}\kappa^2\hat{p}^i\hat{p}^j = p^2$ and thus $\kappa = \frac{p}{a}(1+\Phi)$. Finally, we obtain for the momentum four-vector in terms of the **comoving energy** $\epsilon = pa = Ea$

$$P^\mu = \frac{\epsilon}{a^2}\left[1-\Psi, (1+\Phi)\hat{p}^i\right]\,. \tag{3.7}$$

The comoving energy is conserved in the background. Let us start by considering the distribution of photons in the homogeneous and isotropic FRW background, where they are described by the massless version of the **Bose-Einstein distribution function** with vanishing chemical potential

$$\bar{f}(\epsilon) = \left\{\exp\left[\frac{E}{\bar{T}(\eta)}\right] - 1\right\}^{-1} = \left\{\exp\left[\frac{\epsilon}{a\bar{T}(\eta)}\right] - 1\right\}^{-1}\,, \tag{3.8}$$

where $\bar{T}(\eta) = T_0/a = T_0(1+z)$. We can now rewrite the total derivative in the Boltzmann equation in terms of the partial derivatives with respect to the dependencies of the distribution function

$$\frac{\mathrm{d}f}{\mathrm{d}\eta} = \frac{\partial f}{\partial\eta} + \frac{\partial f}{\partial x^i}\frac{\mathrm{d}x^i}{\mathrm{d}\eta} + \frac{\partial f}{\partial \ln\epsilon}\frac{\mathrm{d}\ln\epsilon}{\mathrm{d}\eta} + \frac{\partial f}{\partial\hat{p}^i}\frac{\mathrm{d}\hat{p}^i}{\mathrm{d}\eta} = C[f]\,. \tag{3.9}$$

The last term is second order and can thus be dropped in the first order treatment, to which we are restricting ourselves to right now.[3] The comoving time derivative of the photon position can be calculated from the momentum as

$$\frac{\mathrm{d}x^i}{\mathrm{d}\eta} = \frac{\mathrm{d}x^i}{\mathrm{d}\lambda}\frac{\mathrm{d}\lambda}{\mathrm{d}x^0} = \frac{P^i}{P^0} = (1+\Phi+\Psi)\hat{p}^i\,. \tag{3.10}$$

Since the derivative of the distribution function with respect to the photon position is already first order, we can ignore the metric perturbations in the above equation, restricting ourselves to the zeroth order. Furthermore, the comoving energy is conserved in the background, such that $\mathrm{d}\ln\epsilon/\mathrm{d}\eta$ starts at first order and $\partial f/\partial\hat{p}^i$ can thus be evaluated in the background. Finally, we obtain for the lhs of the Boltzmann equation

$$\frac{\partial f}{\partial\eta} + \hat{\boldsymbol{p}}\cdot\boldsymbol{\nabla} f + \frac{\partial\bar{f}}{\partial\ln\epsilon}\frac{\mathrm{d}\ln\epsilon}{\mathrm{d}\eta} = C\,. \tag{3.11}$$

As we will show later in §3.1.2, scattering starts at first order. Let us introduce the **temperature perturbation** $T = \bar{T}(1+\Theta)$ and expand the distribution function around the equilibrium distribution function $\bar{f}$

$$\begin{aligned} f(\eta,\boldsymbol{x},\hat{\boldsymbol{p}},\epsilon) &= \left\{\exp\left[\frac{\epsilon}{a\bar{T}(\eta)(1+\Theta)}\right]-1\right\}^{-1} \\ &\approx \left\{\exp\left[\frac{\epsilon(1-\Theta)}{a\bar{T}(\eta)}\right]-1\right\}^{-1} \approx \bar{f}(\epsilon)\left[1-\Theta(\eta,\boldsymbol{x},\hat{\boldsymbol{p}})\frac{\partial\ln\bar{f}}{\partial\ln\epsilon}\right]\,. \end{aligned} \tag{3.12}$$

We thus have for the lhs of the Boltzmann equation

$$-\frac{\partial\bar{f}}{\partial\ln\epsilon}\left[\frac{\partial\Theta}{\partial\eta} + \hat{\boldsymbol{p}}\cdot\boldsymbol{\nabla}\Theta - \frac{\mathrm{d}\ln\epsilon}{\mathrm{d}\eta}\right] = C \tag{3.13}$$

The first two terms in brackets form a total derivative

$$-\frac{\partial\bar{f}}{\partial\ln\epsilon}\left[\frac{\mathrm{d}\Theta}{\mathrm{d}\eta} - \frac{\mathrm{d}\ln\epsilon}{\mathrm{d}\eta}\right] = C \tag{3.14}$$

We are missing one ingredient in the above equation, the time dependence of the photon energy at first order $\mathrm{d}\ln\epsilon/\mathrm{d}\ln\eta$. The photons are obviously described by the **geodesic equation**

$$\frac{\mathrm{d}P^\mu}{\mathrm{d}\lambda} + \Gamma^\mu_{\alpha\beta}P^\alpha P^\beta = 0\,. \tag{3.15}$$

We can express the derivative with respect to the affine parameter as

$$\frac{\mathrm{d}P^\mu}{\mathrm{d}\lambda} = \frac{\mathrm{d}P^\mu}{\mathrm{d}\eta}\frac{\mathrm{d}\eta}{\mathrm{d}\lambda} = P^0\frac{\mathrm{d}P^\mu}{\mathrm{d}\eta}\,. \tag{3.16}$$

Using the Christoffel symbols[4] for the metric Eq. (3.2), we obtain

$$\begin{aligned} \frac{\epsilon}{a^2}(1-\Psi)\frac{\mathrm{d}}{\mathrm{d}\eta}\frac{\epsilon}{a^2}(1-\Psi) = &-(\mathcal{H}+\Psi')\frac{\epsilon^2}{a^4}(1-\Psi)^2 - 2\partial_i\Psi\hat{p}^i\frac{\epsilon^2}{a^4}(1-\Psi)(1+\Phi) \\ &- \left[\mathcal{H}+\Phi'-2\mathcal{H}(\Psi-\Phi)\right]\frac{\epsilon^2}{a^4}(1+\Phi)^2 \end{aligned} \tag{3.18}$$

Linearising and identifying $\mathrm{d}\Psi/\mathrm{d}\eta = \Psi' + \hat{p}^i\partial_i\Psi$ we get the remarkably short equation

$$\frac{\mathrm{d}\ln\epsilon}{\mathrm{d}\eta} = -\frac{\mathrm{d}\Psi}{\mathrm{d}\eta} + (\Psi'+\Phi')\,. \tag{3.19}$$

[3] We will consider the lensing of the primordial CMB later in §3.4.

[4]
$$\Gamma^0_{00} = \mathcal{H}+\Psi' \qquad \Gamma^0_{0i} = \partial_i\Psi \qquad \Gamma^0_{ij} = \left[\mathcal{H}+\Phi'-2\mathcal{H}(\Psi-\Phi)\right]\delta^{(\mathrm{K})}_{ij} \tag{3.17}$$

The photon energy thus changes due to changes of the gravitational potential along the photon trajectory (first term) and the time dependence of the gravitational potentials (last two terms). The latter is suppressed during matter domination when the potentials are constant on large scales, but contributes at early times during the matter-radiation transition and at late times when dark energy starts to dominate the Universe.

Lorentz-invariance of the phase-space density

Let us establish Lorentz-invariance of the phase space density by considering a number of massive particles occupying a phase-space volume $\mathrm{d}N = f\mathrm{d}^3x\mathrm{d}^3p$. Another observer will see the *same number* of particles in a different phase-space volume $\mathrm{d}N = f'\mathrm{d}^3x'\mathrm{d}^3p'$. We will establish that the phase-space volume is Lorentz-invariant and thus $f = f'$.

As you will be well aware from special relativity or QFT, the on-shell, Lorentz-invariant measure for momentum integrals can be written as

$$\int \mathrm{d}^4p\ \delta^{(\mathrm{D})}\left(E^2 - \boldsymbol{p}^2 - m^2\right) = \int \frac{\mathrm{d}^3p}{2E(p)}\,, \tag{3.20}$$

where we have used

$$\delta^{(\mathrm{D})}\left(E^2 - \boldsymbol{p}^2 - m^2\right) = \frac{1}{2E}\delta^{(\mathrm{D})}\left(E - \sqrt{p^2 + m^2}\right)\,. \tag{3.21}$$

Under a Lorentz transformation we have due to length contraction that $\mathrm{d}^3x' = \mathrm{d}^3x/\gamma$ and the energy scales as $E' = \gamma E$. Thus $E\mathrm{d}^3x$ is Lorentz-invariant. Multiplying the Lorentz-invariant quantities $E\mathrm{d}^3x$ and d^3p/E, we see that $\mathrm{d}^3x\mathrm{d}^3p$ has to be Lorentz-invariant. Thus

$$\mathrm{d}^3x'\mathrm{d}^3p'\ f'(x',p') = \mathrm{d}^3x\mathrm{d}^3p\ f(x,p)\,. \tag{3.22}$$

And the phase space density needs to be invariant.

The CMB Dipole

The solar system and earth within it, are moving with respect to the CMB restframe. This motion is introducing the leading CMB anisotropy, which we have to correct for. Let us consider a Lorentz boost of the observer

$$\epsilon = \gamma\epsilon'(1 + \hat{\boldsymbol{p}}'\cdot\boldsymbol{v}_\odot)\,. \tag{3.23}$$

The Bosonic distribution function can then be written as

$$\bar{f}(\epsilon) = \left\{\exp\left[\frac{\epsilon}{a\bar{T}(\eta)}\right] - 1\right\}^{-1} = \left\{\exp\left[\frac{\gamma\epsilon'(1 + \hat{\boldsymbol{p}}'\cdot\boldsymbol{v}_\odot)}{T_0}\right] - 1\right\}^{-1}\,. \tag{3.24}$$

It follows that the effective temperature of the CMB photons is related to the underlying homogeneous temperature by

$$T = \frac{T_0}{\gamma(1 + \hat{\boldsymbol{p}}'\cdot\boldsymbol{v}_\odot)} \approx T_0(1 - \hat{\boldsymbol{p}}'\cdot\boldsymbol{v}_\odot)\,. \tag{3.25}$$

It thus introduces a temperature dipole. The motion of the solar system barycenter of 3.68×10^5m/s with respect to the CMB rest frame introduces a 3 mK dipole perturbation.

3.1.1. Spectral Distortions*

The spectrum of the CMB has been observed by the FIRAS instrument on the COBE satellite in 1989/90. The measurements are shown in Fig. 3.2 together with the Planck blackbody spectral distribution function [Fixsen et al., 1996]

$$I_\nu = \frac{2h\nu^3}{c^2}\frac{1}{e^{h\nu/k_\mathrm{B}T} - 1}\,. \tag{3.26}$$

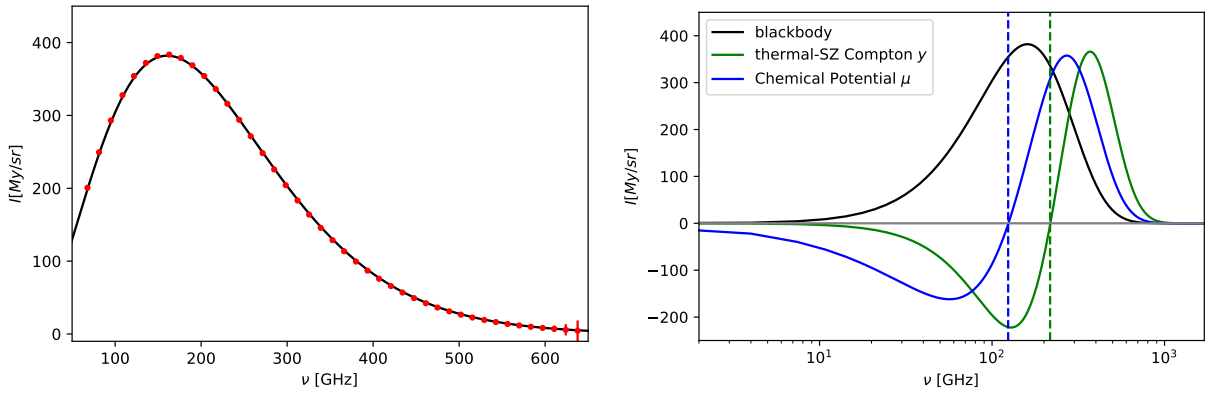

Figure 3.2.: *Left panel:* Spectral density of the CMB monopole as measured by COBE/FIRAS and the black body spectrum corresponding to $T_{\rm CMB} = 2.27255$ K. Error bars have been enhanced by a factor of 50 for clearer visibility. *Right panel:* Spectral distortions arising from energy injection in the early universe (μ-distortions) or the thermal Sunayev-Zel'dovich effect (Compton y-distortion).

While the CMB looks like an almost perfect blackbody, there can be small residual deviations that originate either from the physics of the early Universe or from the propagation of the photons between the last scattering surface to the observer. In the early Universe the blackbody is maintained by Compton scattering, double Compton scattering and bremsstrahlung. Due to the expansion of the Universe, these effects become more and more inefficient and energy injections after $z \approx 10^6$ can lead to spectra distortions. Energy injections in the very early Universe $10^5 < z < 10^6$ typically leads to μ-distortions. The thermal Sunyaev-Zel'dovich effect describes the scattering of CMB photons off hot electrons within galaxy clusters and causes spectral distortions of Compton y-type, which are characteristic for late time energy injections.

Spectral distortions are extremely tightly constrained, with limits $|\mu| < 9 \times 10^{-5}$ for the chemical potential and $|y| < 1.5 \times 10^{-9}$ for Compton y-distortions.

Furthermore, galactic foregrounds contaminate measurements of the primary CMB. Since the foregrounds and secondary effects have a spectral distribution that differs from the primary CMB blackbody, current CMB experiments observe in a number of spectral bands and combine those measurements to remove contaminations.

3.1.2. Thomson Scattering

Photons are scattering off free electrons without loosing energy with the **scattering rate** $\Gamma = a\sigma_{\rm T} n_{\rm e}$, where $\sigma_{\rm T}$ is the Thomson cross section

$$\sigma_{\rm T} = \frac{8\pi}{3}\left(\frac{q_{\rm e}}{4\pi\epsilon_0 m_{\rm e} c^2}\right)^2 = 6.65 \times 10^{-29}{\rm m}^2\,. \tag{3.27}$$

The number density of free electron $n_{\rm e}$ is given by the product of baryon density and ionization fraction $n_{\rm e} = n_{\rm b} x_{\rm e}$. Scattering is important before recombination, when the free electrons combine with the nuclei to form neutral atoms. After recombination the photons can propagate fairly uninhibitedly. We will first consider the scattering process in the electron rest frame, before moving to a general frame, where the electrons are moving.

Electron rest frame

Quantities in the electron rest frame will be indicated by a prime, which should not be confused with its meaning as a time derivative in the rest of these notes. Thomson scattering does not change the energy of

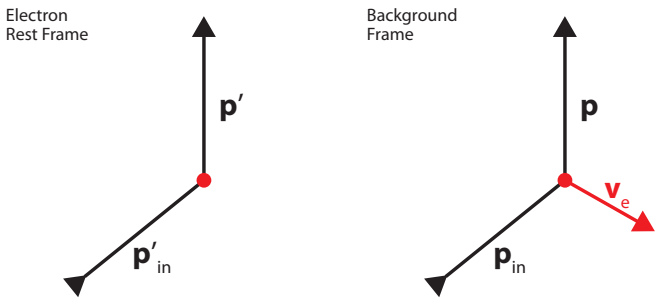

Figure 3.3.: Thomson scattering in the electron rest frame (left) and background frame (right).

the photon, such that $\epsilon'_{\rm in} = \epsilon'$ and the scattering is described by the ingoing and outgoing photon directions as

$$\boldsymbol{p}'_{\rm in} = \epsilon'_{\rm in}\hat{\boldsymbol{p}}'_{\rm in} \quad \rightarrow \quad \boldsymbol{p}' = \epsilon'_{\rm in}\hat{\boldsymbol{p}}' \,. \tag{3.28}$$

The cross section for Thomson scattering of unpolarized radiation is then given by

$$\frac{\mathrm{d}\sigma}{\mathrm{d}\Omega} = \frac{3\sigma_{\rm T}}{16\pi}\left[1 + (\hat{\boldsymbol{p}}'_{\rm in}\cdot\hat{\boldsymbol{p}}')^2\right] \approx \frac{\sigma_{\rm T}}{4\pi} \,. \tag{3.29}$$

In what follows we will mostly ignore the $\hat{\boldsymbol{p}}'_{\rm in}\cdot\hat{\boldsymbol{p}}$ term as it is not relevant unless percent level accuracy is required. We will reintroduce the polarization dependence in §3.3, when considering CMB polarization. The collision term describes the difference between photons scattered into the phase space volume and the photons scattered out of the phase space volume. We have to average over all possible directions for the in-scattering

$$\begin{aligned} C'[f'(\epsilon',\hat{\boldsymbol{p}}')] = \frac{\mathrm{d}f'}{\mathrm{d}\tau'} =& n_e \int \mathrm{d}\hat{\boldsymbol{p}}'_{\rm in}\frac{\mathrm{d}\sigma}{\mathrm{d}\Omega}\left[f'(\epsilon',\hat{\boldsymbol{p}}'_{\rm in}) - f'(\epsilon',\hat{\boldsymbol{p}}')\right] \\ =& -n_e\sigma_{\rm T} f'(\epsilon',\hat{\boldsymbol{p}}') + n_e\sigma_{\rm T}\int\frac{\mathrm{d}\hat{\boldsymbol{p}}'_{\rm in}}{4\pi} f'(\epsilon',\hat{\boldsymbol{p}}'_{\rm in}) \end{aligned} \tag{3.30}$$

This is the scattering rate with respect to proper time in the electron rest frame.

Background frame

The collision term in Eq. (3.1) describes the scattering per unit conformal time, whereas the collision term in the rest frame was computed for unit proper time. We thus have for their relation

$$C = \frac{\mathrm{d}f}{\mathrm{d}\eta} = a\frac{\mathrm{d}f}{\mathrm{d}\tau} = aC' \,. \tag{3.31}$$

We can now transform to a generic frame in which the electrons are moving with velocity $\boldsymbol{v}_e$, performing a Lorentz transform with $\boldsymbol{v}_e$

$$\boldsymbol{p}_{\rm in} = \epsilon_{\rm in}\hat{\boldsymbol{p}}_{\rm in} \quad \rightarrow \quad \boldsymbol{p} = \epsilon\hat{\boldsymbol{p}} \,. \tag{3.32}$$

with

$$\epsilon' = \gamma\epsilon(1 - \hat{\boldsymbol{p}}\cdot\boldsymbol{v}_e) \qquad\qquad \epsilon = \gamma\epsilon'(1 + \hat{\boldsymbol{p}}'\cdot\boldsymbol{v}_e) \tag{3.33}$$

we can use $\epsilon' = \epsilon'_{\rm in}$ to obtain

$$\begin{aligned} \epsilon_{\rm in} =& \gamma\epsilon'_{\rm in}\,(1 + \hat{\boldsymbol{p}}'_{\rm in}\cdot\boldsymbol{v}_e) = \gamma\epsilon'\,(1 + \hat{\boldsymbol{p}}'_{\rm in}\cdot\boldsymbol{v}_e) \\ =& \gamma^2\epsilon\,(1 + (\hat{\boldsymbol{p}}'_{\rm in} - \hat{\boldsymbol{p}})\cdot\boldsymbol{v}_e) \end{aligned} \tag{3.34}$$

We can now use the invariance of the phase space density and expand around the blackbody distribution function

$$f'(\epsilon'_{\rm in},\hat{\boldsymbol{p}}'_{\rm in}) = f(\epsilon_{\rm in},\hat{\boldsymbol{p}}_{\rm in}) = \bar{f}(\epsilon) - \frac{\mathrm{d}\bar{f}}{\mathrm{d}\ln\epsilon}(\hat{\boldsymbol{p}}-\hat{\boldsymbol{p}}'_{\rm in})\cdot\boldsymbol{v}_e - \frac{\mathrm{d}\bar{f}}{\mathrm{d}\ln\epsilon}\Theta(\hat{\boldsymbol{p}}_{\rm in}) \tag{3.35}$$

$$f'(\epsilon',\hat{\boldsymbol{p}}') = f(\epsilon,\hat{\boldsymbol{p}}) = \bar{f}(\epsilon) - \frac{\mathrm{d}\bar{f}}{\mathrm{d}\ln\epsilon}\Theta(\hat{\boldsymbol{p}}) \tag{3.36}$$

We can now use the above result to evaluate the collision term

$$\begin{aligned} C[f(\epsilon,\hat{\boldsymbol{p}})] =& -\Gamma f'(\epsilon',\hat{\boldsymbol{p}}') + \Gamma\int\frac{\mathrm{d}\hat{\boldsymbol{p}}'_{\rm in}}{4\pi}f'(\epsilon',\hat{\boldsymbol{p}}'_{\rm in}) \\ =& -\Gamma\bar{f}(\epsilon) + \Gamma\frac{\mathrm{d}\bar{f}}{\mathrm{d}\ln\epsilon}\Theta(\hat{\boldsymbol{p}}) + \Gamma\int\frac{\mathrm{d}\hat{\boldsymbol{p}}'_{\rm in}}{4\pi}\left[\bar{f}(\epsilon) - \frac{\mathrm{d}\bar{f}}{\mathrm{d}\ln\epsilon}(\hat{\boldsymbol{p}}-\hat{\boldsymbol{p}}'_{\rm in})\cdot\boldsymbol{v}_e - \frac{\mathrm{d}\bar{f}}{\mathrm{d}\ln\epsilon}\Theta(\hat{\boldsymbol{p}}_{\rm in})\right] \\ =& \frac{\mathrm{d}\bar{f}}{\mathrm{d}\ln\epsilon}\Theta(\hat{\boldsymbol{p}}) - \Gamma\frac{\mathrm{d}\bar{f}}{\mathrm{d}\ln\epsilon}\hat{\boldsymbol{p}}\cdot\boldsymbol{v}_e - \Gamma\frac{\mathrm{d}\bar{f}}{\mathrm{d}\ln\epsilon}\int\frac{\mathrm{d}\hat{\boldsymbol{p}}'_{\rm in}}{4\pi}\Theta(\hat{\boldsymbol{p}}_{\rm in})\,. \end{aligned} \tag{3.37}$$

In the last term we can replace $\mathrm{d}\hat{\boldsymbol{p}}'_{\rm in} \to \mathrm{d}\hat{\boldsymbol{p}}_{\rm in}$ at zeroth order. The angular average then yields the **monopole** Θ_0 of the temperature distribution

$$\Theta_0(\boldsymbol{x},\eta) = \int\frac{\mathrm{d}^2\hat{\boldsymbol{p}}}{4\pi}\Theta(\boldsymbol{x},\hat{\boldsymbol{p}},\eta)\,. \tag{3.38}$$

In summary we have for the collision term

$$C = \frac{\mathrm{d}\bar{f}}{\mathrm{d}\ln\epsilon}\Gamma\left[\Theta - \Theta_0 - \hat{\boldsymbol{p}}\cdot\boldsymbol{v}_{\rm e}\right]\,. \tag{3.39}$$

Had we kept the angular dependence the Thomson cross-section we would have obtained

$$C = \frac{\mathrm{d}\bar{f}}{\mathrm{d}\ln\epsilon}\Gamma\left\{\Theta - \hat{\boldsymbol{p}}\cdot\boldsymbol{v}_{\rm e} - \frac{3}{16\pi}\int\mathrm{d}\hat{\boldsymbol{p}}_{\rm in}\Theta(\hat{\boldsymbol{p}}_{\rm in})\left[1+(\hat{\boldsymbol{p}}_{\rm in}\cdot\hat{\boldsymbol{p}})^2\right]\right\}\,. \tag{3.40}$$

Combining the collision term with the left hand side of the Boltzmann equation (3.14), we get

$$\boxed{\frac{\mathrm{d}\Theta}{\mathrm{d}\eta} = \frac{\mathrm{d}\ln\epsilon}{\mathrm{d}\eta} - \Gamma\left[\Theta - \Theta_0 - \hat{\boldsymbol{p}}\cdot\boldsymbol{v}_e\right]\,.} \tag{3.41}$$

At early times, when the scattering rate is high $\Gamma \gg \mathcal{H}$, the second term needs to vanish. This means that the scattering isotropizes the radiation in the electron rest frame and leads to a distribution with a monopole and dipole in a generic frame $\Theta \to \Theta_0 + \hat{\boldsymbol{p}}\cdot\boldsymbol{v}_e$.

Combining the geodesic equation (3.19) and collision term we obtain

$$\boxed{\frac{\partial\Theta}{\partial\eta} + \hat{\boldsymbol{p}}\cdot\boldsymbol{\nabla}\Theta = \Phi' - \hat{\boldsymbol{p}}\cdot\boldsymbol{\nabla}\Psi - \Gamma\left[\Theta - \Theta_0 - \hat{\boldsymbol{p}}\cdot\boldsymbol{v}_e\right]\,.} \tag{3.42}$$

Restricting ourselves to curl-free velocities[5] $\boldsymbol{v}_e(\boldsymbol{k}) = \mathrm{i}\hat{\boldsymbol{k}}v_e(\boldsymbol{k})$ we can rewrite the above equation in Fourier space

$$\boxed{\Theta' + \mathrm{i}k\mu\Theta = \Phi' - \mathrm{i}k\mu\Psi + \Gamma\left[\Theta_0 - \Theta + \mathrm{i}\mu v_{\rm e}\right]\,,} \tag{3.43}$$

where $\mu = \hat{\boldsymbol{k}}\cdot\hat{\boldsymbol{p}}$.

The equation of motion for Θ has a dependence on $\hat{\boldsymbol{p}}$ and $\boldsymbol{k}$ through k and $\mu = \hat{\boldsymbol{p}}\cdot\hat{\boldsymbol{k}}$ only, but not $\boldsymbol{k}$ explicitly. For scalar perturbations, the fluctuations are axis-symmetric around $\hat{\boldsymbol{k}}$ and thus allow for a Legendre expansion:

[5] Note that $v_{\rm b,Dodelson} = \mathrm{i}v_{\rm b,here}$ and that $v_e = \theta/k$.

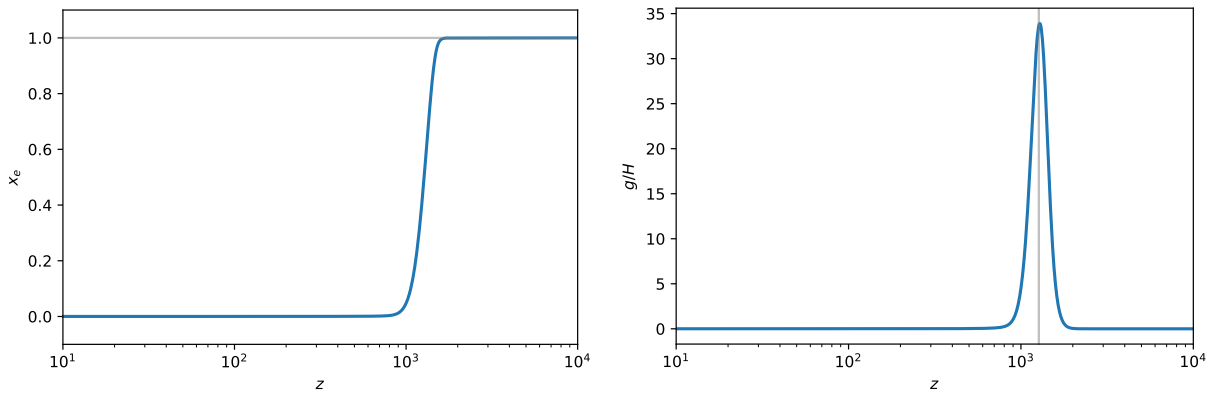

Figure 3.4.: *Left panel:* Ionization fraction x_e calculated using RECFAST. *Right panel:* visibility function g.

Multipole Expansion

$$\Theta(\eta, \boldsymbol{k}, \mu = \hat{\boldsymbol{k}} \cdot \hat{\boldsymbol{n}}) = \sum_l (-\mathrm{i})^l (2l+1) \Theta_l(\eta, \boldsymbol{k}) \mathcal{P}_l(\mu) \tag{3.44}$$

$$\Theta_l(\eta, \boldsymbol{k}) = \frac{1}{(-\mathrm{i})^l} \int \frac{\mathrm{d}\mu}{2} \mathcal{P}_l(\mu) \Theta(\eta, \boldsymbol{k}, \mu) \tag{3.45}$$

3.2. Anisotropies

3.2.1. Optical Depth and Visibility Function

The **optical depth**

$$\tau = \int_\eta^{\eta_0} \mathrm{d}\eta' \; \Gamma(\eta') \,. \tag{3.46}$$

denotes the probability for a photon not to scatter between conformal time η and today at η_0 as $e^{-\tau}$. Note that the integral bounds in the above definition are set up such that the conformal time derivative of the optical depth is given by

$$\tau' = -\Gamma = -a \sigma_\mathrm{T} x_\mathrm{e} n_\mathrm{b} \,, \tag{3.47}$$

where the number density of free electrons is expressed in terms of the free electron or ionization fraction and the baryon number density $n_\mathrm{b} = n_p + n_H$ as $n_\mathrm{e} = x_\mathrm{e} n_\mathrm{b}$. The **visibility function** encodes the probability that a photon last scattered at η

$$g = -\tau' e^{-\tau} \,. \tag{3.48}$$

By definition, the visibility function integrates to unity

$$\int \mathrm{d}\eta \; g = -e^{-\tau} \Big|_{\eta_0}^{\eta} = 1 \,. \tag{3.49}$$

Here we used that at early times $\tau \to \infty$ and at late times $\tau \to 0$. The ionization fraction $x_\mathrm{e} = n_\mathrm{e}/(n_\mathrm{e} + n_H)$ encodes the ratio of free electrons and the total number of electrons (free and bound in hydrogen) and the visibility function g are shown in Fig. 3.4. The visibility function is peaked at the time of recombination with at width of $\Delta z \approx 10$ or $\Delta\eta \approx 10\ h^{-1}\mathrm{Mpc}$.

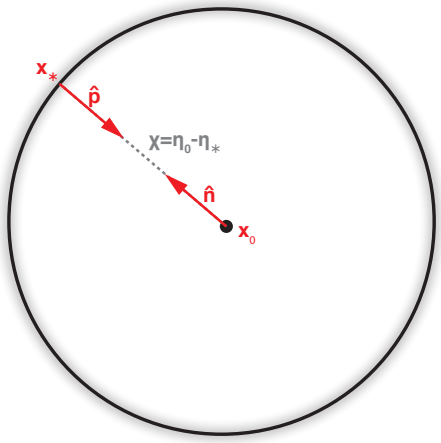

Figure 3.5.: Photons released at the last scattering surface travel to the observer fairly uninhibitedly.

3.2.2. Line of Sight Solution

While a direct solution of Eq. (3.42) is possible, the line of sight solution introduced by [Seljak and Zaldarriaga, 1996] is much more transparent and numerically efficient. Let use multiply Eq. (3.41) by $e^{-\tau}$ and rewrite

$$\begin{aligned}\frac{\mathrm{d}e^{-\tau}\Theta}{\mathrm{d}\eta} = e^{-\tau}\left[\frac{\mathrm{d}\Theta}{\mathrm{d}\eta} + \Gamma\Theta\right] &= e^{-\tau}\frac{\mathrm{d}\ln\epsilon}{\mathrm{d}\eta} + g\left[\Theta_0 - \hat{\boldsymbol{n}}\cdot\boldsymbol{v}_e\right] \\ &= e^{-\tau}(\Phi' + \Psi') - e^{-\tau}\frac{\mathrm{d}\Psi}{\mathrm{d}\eta} + g\left[\Theta_0 - \hat{\boldsymbol{n}}\cdot\boldsymbol{v}_e\right] \\ &= e^{-\tau}(\Phi' + \Psi') - \frac{\mathrm{d}e^{-\tau}\Psi}{\mathrm{d}\eta} + g\left[\Theta_0 + \Psi - \hat{\boldsymbol{n}}\cdot\boldsymbol{v}_e\right]\end{aligned} \tag{3.50}$$

We can bring the metric perturbation Ψ to the lhs

$$\frac{\mathrm{d}}{\mathrm{d}\eta}e^{-\tau}(\Theta + \Psi) = \hat{S}\,, \tag{3.51}$$

with

$$\hat{S}(\eta, \boldsymbol{x}, \hat{\boldsymbol{n}}) = e^{-\tau}\left(\Phi' + \Psi'\right) + g\left[\Theta_0 + \Psi - \hat{\boldsymbol{n}}\cdot\boldsymbol{v}_e\right]\,. \tag{3.52}$$

The photons detected in direction $\hat{\boldsymbol{n}}$ by an observer at $\boldsymbol{x}_0$ are propagating in direction $\hat{\boldsymbol{p}} = -\hat{\boldsymbol{n}}$.

We can now use the fact that at present time the visibility function is zero $\tau(\eta_0) \to 0$ and that at early times it is $\tau(0) = \infty$. Furthermore, the present day potential $\Psi(\eta_0, \boldsymbol{x}_0)$ leads to an unobservable monopole and can thus be dropped

$$\Theta(\eta_0, \boldsymbol{x}_0, \hat{\boldsymbol{n}}) = e^{-\tau}(\Theta + \Psi)\Big|_0^{\eta_0} = \int_0^{\eta_0}\mathrm{d}\eta'\;\hat{S}(\eta', \boldsymbol{x}_0 + (\eta_0 - \eta')\hat{\boldsymbol{n}}, \hat{\boldsymbol{n}})\,. \tag{3.53}$$

3.2.3. Instantaneous Recombination

The line-of-sight solution can be further simplified by assuming that recombination happened instantaneously at η_*.

With $g(\eta) = \delta^{(\mathrm{D})}(\eta - \eta_\star)$

$$\tilde{\Theta} = \underbrace{(\Theta_0 + \Psi)_\star}_{\text{SW}} - \underbrace{(\hat{\boldsymbol{n}}\cdot\boldsymbol{v}_\mathrm{e})_\star}_{\text{Doppler}} + \underbrace{\int_{\eta_\star}^{\eta_0}\mathrm{d}\eta'\;(\Psi' + \Phi')}_{\text{ISW}} \tag{3.54}$$

Sachs-Wolfe Effect: The effect of the intrinsic temperature perturbation at the surface of last scattering and the effect of the photon having to climb out of the potential well

Doppler Effect: Change in photon energy due to scattering off moving electrons.

Integrated Sachs-Wolfe Effect: During Matter domination the metric perturbations are constant, but they do evolve during the radiation-matter transition and again once dark energy starts to affect the expansion of the Universe.

Relation between potential and radiation overdensity

On large scales during matter domination we have $\Theta_0 = \delta_\gamma/4 = -2\Psi_{\rm md}/3$

$$\Theta_0 + \Psi_{\rm md} = \delta_\gamma/4 + \Psi_{\rm md} = \Psi_{\rm md}/3 = -\delta_\gamma/8 \tag{3.55}$$

Thus, overdensities in the photon distribution ($\delta_\gamma > 0$) appear as cold spots in the CMB ($\Theta_0 + \Psi_{\rm md} < 0$), because the gravitational redshift acquired from climbing out of the potential well dominates over the intrinsic temperature monopole of the photons.

3.2.4. Angular Power Spectrum

Let us express the source term in Fourier space

$$\hat{S}(\eta', \boldsymbol{x}_0 + (\eta_0 - \eta')\hat{\boldsymbol{n}}, \hat{\boldsymbol{n}}) = \int \frac{\mathrm{d}^3k}{(2\pi)^3} \exp\left[\mathrm{i}\boldsymbol{k}\cdot\boldsymbol{x}_0\right] \exp\left[\mathrm{i}k\chi\hat{\boldsymbol{k}}\cdot\hat{\boldsymbol{n}}\right] \hat{S}(\eta', \boldsymbol{k}, \hat{\boldsymbol{n}}) \tag{3.56}$$

Without loss of generality we can set $\boldsymbol{x}_0 = \boldsymbol{0}$. The source term depends on $\boldsymbol{k}$ through the initial conditions $\mathcal{R}(\boldsymbol{k})$ and on the photon propagation direction $\hat{\boldsymbol{n}}$ through $\mu = \hat{\boldsymbol{k}}\cdot\hat{\boldsymbol{n}}$. There is no further explicit dependence on the propagation direction of the photon $\hat{\boldsymbol{n}}$ and the wavevector k itself. It will be useful to factorize the angular dependence μ, which will determine the multipole expansion of the observed fluctuations, and the dependence on the initial conditions through $\mathcal{R}$.

$$\begin{aligned}\hat{S}(\eta', k, \mu = \hat{\boldsymbol{k}}\cdot\hat{\boldsymbol{n}}) =& e^{-\tau}\left(\Phi' + \Psi'\right) + g\left[\Theta_0 + \Psi - \mathrm{i}\mu v_e\right] \\ =& \left[\mu^0\tilde{T}_0(\eta', k) + \mathrm{i}\mu^1\tilde{T}_1(\eta', k)\right]\mathcal{R}(\boldsymbol{k})\end{aligned} \tag{3.57}$$

$$\begin{aligned}\hat{S}(\eta', \boldsymbol{k}, \hat{\boldsymbol{n}}) \exp\left[\mathrm{i}k\chi\hat{\boldsymbol{k}}\cdot\hat{\boldsymbol{n}}\right] =& \mathcal{R}(\boldsymbol{k})\left[\mu^0\tilde{T}_0(\eta', k) + \mathrm{i}\mu^1\tilde{T}_1(\eta', k)\right]\exp\left[\mathrm{i}k\chi\mu\right] \\ =& \mathcal{R}(\boldsymbol{k})\left[\tilde{T}_{\rm SW}(\eta', k) + \tilde{T}_{\rm ISW}(\eta', k) + \tilde{T}_{\rm D}(\eta', k)\frac{\mathrm{d}}{\mathrm{d}k\chi}\right]\exp\left[\mathrm{i}k\chi\mu\right]\end{aligned} \tag{3.58}$$

We can now use the Rayleigh expansion of the plane wave Eq. (1.114). The derivative in the above equation only acts on the spherical Bessel function

$$\begin{aligned}\hat{S}(\eta', (\eta_0 - \eta')\hat{\boldsymbol{n}}, \hat{\boldsymbol{n}}) &= \int \frac{\mathrm{d}^3k}{(2\pi)^3}\hat{S}(\eta', \boldsymbol{k}, \hat{\boldsymbol{n}}) \exp\left[\mathrm{i}k\chi\hat{\boldsymbol{k}}\cdot\hat{\boldsymbol{n}}\right] \\ &= \int \frac{\mathrm{d}^3k}{(2\pi)^3}\sum_l \mathrm{i}^l(2l+1)\mathcal{P}_l(\hat{\boldsymbol{k}}\cdot\hat{\boldsymbol{n}})\mathcal{R}(\boldsymbol{k})\left[\tilde{T}_0(\eta', k)j_l(k\chi) + \tilde{T}_1(\eta', k)j_l'(k\chi)\right] \\ &= \int \frac{\mathrm{d}^3k}{(2\pi)^3}\sum_l \mathrm{i}^l(2l+1)\mathcal{P}_l(\hat{\boldsymbol{k}}\cdot\hat{\boldsymbol{n}})\mathcal{R}(\boldsymbol{k})T_l(\eta', k)\end{aligned} \tag{3.59}$$

Here we have defined the combination of the spherical bessel functions and the transfer functions as a new l-dependent transfer function

$$T_l(\eta, k) = \tilde{T}_0(\eta, k)j_l(k\chi) + \tilde{T}_1(\eta, k)j_l'(k\chi)\,. \tag{3.60}$$

Conversion between Multipoles

Axissymmetric perturbations allow an expansion in multipoles

$$\Theta(\boldsymbol{k},\hat{\boldsymbol{n}}) = \sum_l (2l+1)\Theta_l(\boldsymbol{k})\mathrm{i}^l \mathcal{P}_l(\hat{\boldsymbol{k}}\cdot\hat{\boldsymbol{n}})\,. \tag{3.61}$$

We can also expand in spherical multipoles

$$\Theta(\boldsymbol{k},\hat{\boldsymbol{n}}) = \sum_{l,m} \Theta_{lm}(\boldsymbol{k}) Y_{lm}(\hat{\boldsymbol{n}})\,. \tag{3.62}$$

Thus we have for the spherical multipole coefficients in terms of the (Legendre) multipole coefficients

$$\Theta_{lm}(\boldsymbol{k}) = 4\pi\mathrm{i}^l \Theta_l(\boldsymbol{k}) Y^*_{lm}(\hat{\boldsymbol{k}})\,. \tag{3.63}$$

We can expand the Legendre polynomials in spherical harmonics as

$$\begin{aligned}\Theta(\eta_0,\boldsymbol{x}_0=\boldsymbol{0},\hat{\boldsymbol{n}}) =& \sum_{l'}\int_0^{\eta_0}\mathrm{d}\eta'\int\frac{\mathrm{d}^3k}{(2\pi)^3}\mathrm{i}^l(2l+1)T_{l'}(\eta',k)\mathcal{R}(\boldsymbol{k})P_l(\hat{\boldsymbol{k}}\cdot\hat{\boldsymbol{n}})\\ =&4\pi\sum_{l',m'}\int_0^{\eta_0}\mathrm{d}\eta'\int\frac{\mathrm{d}^3k}{(2\pi)^3}\mathrm{i}^l T_{l'}(\eta',k)\mathcal{R}(\boldsymbol{k})Y^*_{l'm'}(\hat{\boldsymbol{k}})Y_{l'm'}(\hat{\boldsymbol{n}})\end{aligned} \tag{3.64}$$

The spherical multipoles are thus given by

$$\Theta_{lm} = \int \mathrm{d}^2\hat{\boldsymbol{n}}\;\Theta(\hat{\boldsymbol{n}})Y^*_{lm}(\hat{\boldsymbol{n}}) = 4\pi\int_0^{\eta_0}\mathrm{d}\eta'\int_{\boldsymbol{k}}\mathcal{R}(\boldsymbol{k})\mathrm{i}^l T_l(\eta',k)Y^*_{lm}(\hat{\boldsymbol{k}}) \tag{3.65}$$

With Eq. (1.120) we thus have

$$C_l = 4\pi\int_0^{\eta_0}\mathrm{d}\eta'\int_0^{\eta_0}\mathrm{d}\eta''\int\mathrm{d}\ln k\;\Delta^2_{\mathcal{R}}(k)T_l(\eta',k)T_l(\eta'',k)\,. \tag{3.66}$$

For instantaneous recombination at η_* this simplifies to

$$C_l = 4\pi\int\mathrm{d}\ln k\;\Delta^2_{\mathcal{R}}(k)T_l^2(\eta_*,k)\,. \tag{3.67}$$

It thus remains to calculate the transfer functions relating the Sachs-Wolfe and Doppler terms in terms of the primordial curvature perturbation $\mathcal{R}$

$$\tilde{T}_{\mathrm{SW}}(\eta,k) = \frac{\Theta_0+\Psi}{\mathcal{R}(\boldsymbol{k})}\,, \qquad \tilde{T}_{\mathrm{D}}(\eta,k) = \frac{v_b(\eta,\boldsymbol{k})}{\mathcal{R}(\boldsymbol{k})}\,. \tag{3.68}$$

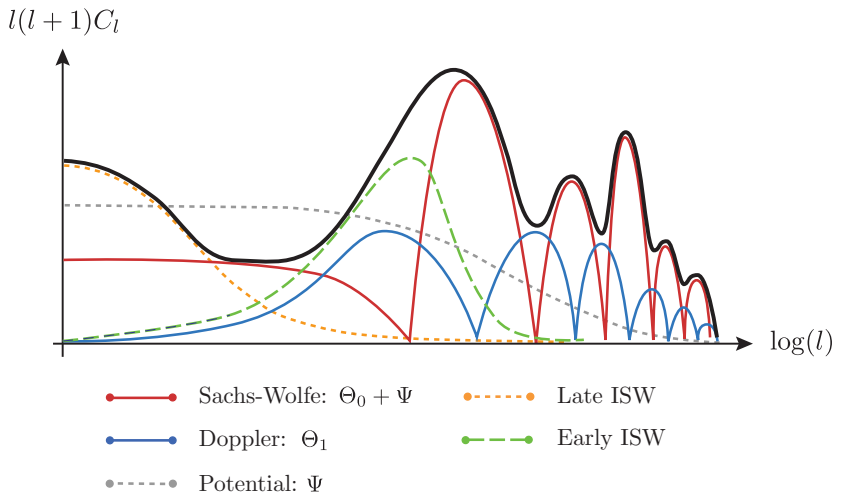

Figure 3.6.: Overview of the contributions to the angular power spectrum [Baumann, 2017].

Recap: Angular Correlation Function

$$\Theta(\hat{\boldsymbol{n}}) = \sum_l (2l+1)\mathrm{i}^l \int \frac{\mathrm{d}k k^2}{2\pi^2} T_l(\eta_*, k) \int \frac{\mathrm{d}\hat{\boldsymbol{k}}}{4\pi} \mathcal{P}_l(\hat{\boldsymbol{k}} \cdot \hat{\boldsymbol{n}}) \mathcal{R}(\boldsymbol{k}) \tag{3.69}$$

$$\begin{aligned}\langle \Theta(\hat{\boldsymbol{n}})\Theta(\hat{\boldsymbol{n}}')\rangle &= \sum_{l,l'} (2l+1)(2l'+1)\mathrm{i}^{l-l'} \int_{\boldsymbol{k},\boldsymbol{k}'} \langle \mathcal{R}(\boldsymbol{k})\mathcal{R}(\boldsymbol{k}')\rangle\, T_l(\eta_*, k) T_{l'}(\eta_*, k) \mathcal{P}_l(\hat{\boldsymbol{k}} \cdot \hat{\boldsymbol{n}}) \mathcal{P}_{l'}(\hat{\boldsymbol{k}}' \cdot \hat{\boldsymbol{n}}') \\ &= \sum_{l,l'} (2l+1)(2l'+1)\mathrm{i}^{l-l'} \int \frac{k^2 \mathrm{d}k}{2\pi^2} P_{\mathcal{R}}(k) T_l(\eta_*, k) T_{l'}(\eta_*, k) \int \frac{\mathrm{d}^2\hat{\boldsymbol{k}}}{4\pi} \mathcal{P}_l(\hat{\boldsymbol{k}} \cdot \hat{\boldsymbol{n}}) \mathcal{P}_{l'}(\hat{\boldsymbol{k}} \cdot \hat{\boldsymbol{n}}')\end{aligned} \tag{3.70}$$

Using an orthogonality of the Legendre polynomials[a] we have

$$\langle \Theta(\hat{\boldsymbol{n}})\Theta(\hat{\boldsymbol{n}}')\rangle = \sum_l \frac{(2l+1)}{4\pi} \mathcal{P}_l(\hat{\boldsymbol{n}} \cdot \hat{\boldsymbol{n}}') \underbrace{4\pi \int \frac{k^2 \mathrm{d}k}{2\pi^2} P_{\mathcal{R}}(k) T_l^2(\eta_*, k)}_{C_l} \tag{3.72}$$

Where we used Eq. (1.86).

[a]
$$\begin{aligned}\int \mathrm{d}^2\hat{\boldsymbol{k}}\ \mathcal{P}_l(\hat{\boldsymbol{k}} \cdot \hat{\boldsymbol{n}}) \mathcal{P}_{l'}(\hat{\boldsymbol{k}} \cdot \hat{\boldsymbol{n}}') &= \frac{4\pi}{2l+1} \frac{4\pi}{2l'+1} \sum_{m,m'} \int \mathrm{d}^2\hat{\boldsymbol{k}}\ Y_{lm}(\hat{\boldsymbol{k}}) Y^*_{lm}(\hat{\boldsymbol{n}}) Y^*_{l'm'}(\hat{\boldsymbol{k}}) Y_{l'm'}(\hat{\boldsymbol{n}}') \\ &= \left(\frac{4\pi}{2l+1}\right)^2 \delta^{(\mathrm{K})}_{l,l'} \sum_m Y^*_{lm}(\hat{\boldsymbol{n}}) Y_{lm}(\hat{\boldsymbol{n}}') \\ &= \frac{4\pi}{2l+1} \delta^{(\mathrm{K})}_{l,l'} \mathcal{P}_l(\hat{\boldsymbol{n}} \cdot \hat{\boldsymbol{n}}')\end{aligned} \tag{3.71}$$

3.2.5. Tight Coupling

Multiplying the evolution equation Eq. (3.43), with $\mathcal{P}_{l\geq 2}$ and integrating over the photon direction, most of the terms vanish. We finally obtain[6]

$$\Theta_l' + k\left(\frac{l+1}{2l+1}\Theta_{l+1} - \frac{l}{2l+1}\Theta_{l-1}\right) = -\Gamma\Theta_l\,. \tag{3.74}$$

We will now consider the limit of large optical depth $\tau \gg 1$ or scattering rate larger than the expansion rate $\Gamma \gg k \gtrsim \mathcal{H}$ and large scales $k\eta \approx 1$. Moments of order exceeding two $\Theta_l, l > 2$ are suppressed for $\Gamma \gg k$. To see this let us first drop the Θ_{l+1}-term (we'll justify this later) and replace the derivative in the first term by a η^{-1}

$$\Theta_l - \eta k\frac{l}{2l+1}\Theta_{l-1} + \eta\Gamma\Theta_l = 0 \tag{3.75}$$

With our approximations, we can drop Θ_l in comparison to $\eta\Gamma\Theta_l$ in the above equation. We thus have for the relation of Θ_l and Θ_{l-1}

$$\Theta_l \approx \frac{k}{\Gamma}\Theta_{l-1} \ll \Theta_{l-1} \tag{3.76}$$

where we used that $k \ll \Gamma$. The fact that $\Theta_l \ll \Theta_{l-1}$ obviously justifies dropping Θ_{l+1} above. Multiplying the evolution equations with $\mathcal{P}_0$ and $\mathcal{P}_1$ and integrating we obtain the continuity and Euler equations for photons in the tight-coupling-approximation

$$\Theta_0' = -k\Theta_1 + \Phi'\,, \tag{3.77}$$
$$3\Theta_1' = k\Theta_0 - k\Psi - \Gamma(3\Theta_1 + v_\mathrm{b})\,. \tag{3.78}$$

Moments of the stress-energy tensor

$$T^\mu_{\ \nu} = \int \mathrm{d}^3p\ f P^\mu P_\nu \tag{3.79}$$

can be associated with the fluid overdensity and momentum, yielding $\delta_\gamma = 4\Theta_0$, $v_\gamma = -3\Theta_1$ and $\sigma_\gamma = -3\Theta_2$. For dark matter we have

$$\delta_\mathrm{dm}' = -kv_\mathrm{dm} + 3\Phi'\,, \tag{3.80}$$
$$v_\mathrm{dm}' = -\mathcal{H}v_\mathrm{dm} - k\Psi\,. \tag{3.81}$$

For the baryons we have

$$\delta_\mathrm{b}' = -kv_\mathrm{b} + 3\Phi'\,, \tag{3.82}$$
$$v_\mathrm{b}' = -\mathcal{H}v_\mathrm{b} - k\Psi - \frac{\Gamma}{R}(3\Theta_1 + v_\mathrm{b})\,. \tag{3.83}$$

Here we have introduced the **baryon-to-photon ratio**

$$R = \frac{\rho_\mathrm{b}}{\rho_\gamma + p_\gamma} = \frac{3}{4}\frac{\rho_\mathrm{b}}{\rho_\gamma} \propto a\,. \tag{3.84}$$

The baryon to photon ratio is zero early on an approaches unity at recombination. The presence of baryons makes the fluid heavier, thus reducing the speed of sound as

$$c_\mathrm{s}^2 = \frac{1}{3}\frac{1}{1+R}\,. \tag{3.85}$$

[6] This can be seen using the recursion relation

$$(2l+1)\mu P_l(\mu) = (l+1)P_{l+1}(\mu) + lP_{l-1}(\mu) \tag{3.73}$$

3.2.6. Evolution/Acoustic Oscillations

Let us slightly rewrite the baryon Euler equation (3.83)

$$v_\mathrm{b} = -3\Theta_1 - \frac{R}{\Gamma}\left[v_\mathrm{b}' + \mathcal{H}v_\mathrm{b} + k\Psi\right] . \tag{3.86}$$

At leading order $v_\mathrm{b} = -3\Theta_1$. The correction term is suppressed by Γ^{-1}, but in the photon Euler equation (3.78) the baryon velocity is multiplied with Γ. We can solve the equation perturbatively by replacing $v_\mathrm{b} = -3\Theta_1$ in the correction term to obtain

$$v_\mathrm{b} = -3\Theta_1 + \frac{R}{\Gamma}\left[3\Theta_1' + 3\mathcal{H}\Theta_1 - k\Psi\right] . \tag{3.87}$$

Using this result in the photon Euler equation we obtain

$$\Theta_1' = \frac{k}{3(1+R)}\Theta_0 - \frac{\mathcal{H}R}{1+R}\Theta_1 + \frac{k}{3}\Psi . \tag{3.88}$$

Taking another time derivative of the photon continuity equation in Eq. (3.78) and using the above solution we finally have

$$\Theta_0'' + \frac{\mathcal{H}R}{1+R}\Theta_0' + c_s^2k^2\Theta_0 = -\frac{1}{3}k^2\Psi + \Phi'' + \frac{\mathcal{H}R}{1+R}\Phi' . \tag{3.89}$$

On the left hand side we have a friction term and a pressure term and on the right hand side a gravitational term and dilation terms. For constant metric perturbations we obtain

$$\Theta_0'' + c_s^2k^2\Theta_0 = -\frac{1}{3}k^2\Psi . \tag{3.90}$$

This is a forced harmonic oscillator. Defining the **sound horizon** as $r_\mathrm{s} = \int \mathrm{d}\eta'\; c_\mathrm{s}(\eta') \approx c_\mathrm{s}\eta$ we have

$$\Theta_0(\eta, \boldsymbol{k}) = \left[\Theta_0(0, \boldsymbol{k}) + (1+R)\Psi\right]\cos(kr_\mathrm{s}) + \frac{1}{kc_\mathrm{s}}\Theta_0'\sin(kr_\mathrm{s}) - (1+R)\Psi \tag{3.91}$$

For adiabatic initial conditions $\Theta_0'(0) = 0$, which means that the sine mode has to vanish. The tight coupling approximation entails that at leading order $v_e = v_b = v_\gamma = -3\Theta_1$.

$$\Theta_{0,\mathrm{SW}} = \Theta_0(\eta, \boldsymbol{k}) + \Psi = \left[\Theta_0(0, \boldsymbol{k}) + (1+R)\Psi\right]\cos(kr_{s,\star}) - R\Psi \tag{3.92}$$

$$\Theta_{0,\mathrm{D}} = -\hat{\boldsymbol{n}}\cdot\boldsymbol{v}_e = -\left[\Theta_0(\eta, \boldsymbol{k}) + (1+R)\Psi\right]\sin(kr_{s,\star}) \tag{3.93}$$

Gauge Transformations

The comoving curvature perturbation $\mathcal{R}$ is related to the Newtonian gauge metric perturbations via

$$\mathcal{R} = -\Phi - \frac{\mathcal{H}(\Phi' + \mathcal{H}\Phi)}{4\pi G a^2(\bar{\rho} + \bar{P})} = -\Phi - \frac{2}{3}\frac{\mathcal{H}^{-1}\Phi' + \Psi}{1+\omega} , \tag{3.94}$$

such that

$$\Phi = -\frac{3+3\omega}{5+3\omega}\mathcal{R}. \tag{3.95}$$

During the matter-radiation transition the curvature perturbation $\mathcal{R}$ remains constant outside the horizon. The change in the equation of state thus implies a change in the amplitude of the Newtonian potential Φ

$$\mathcal{R} = -\frac{3}{2}\Phi_\mathrm{rd} = -\frac{5}{3}\Phi_\mathrm{md} \quad \Rightarrow \quad \Phi_\mathrm{md} = \frac{9}{10}\Phi_\mathrm{rd} . \tag{3.96}$$

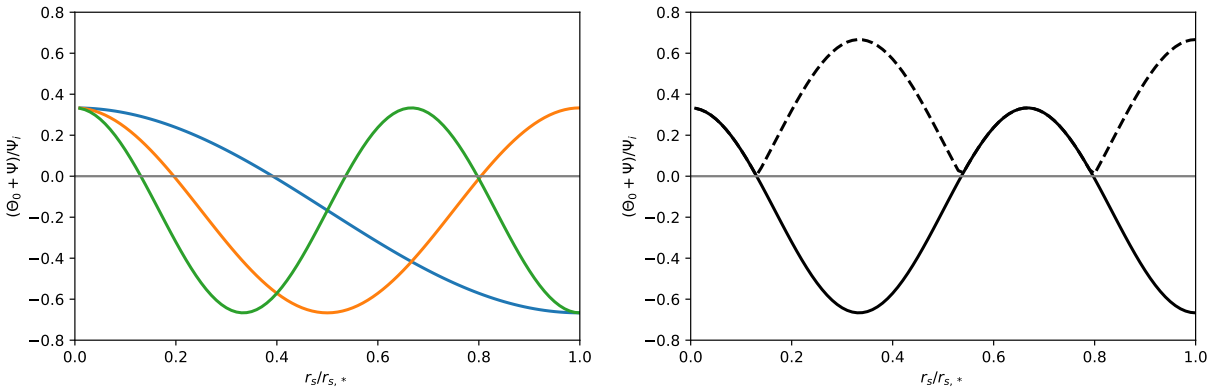

Figure 3.7.: *Left panel:* Observed temperature perturbation $\Theta_0 + \Psi$ in units of the metric perturbation Ψ for several wavenumbers k. Following Eq. (3.55), the modes start at $\Theta_0 + \Psi = \Psi/3$. *Right panel:* As you can see the baryon loading shifts the cuves downwards, leading to the magnitude of the odd peaks being larger than that of the even peaks.

Large Scale Initial Conditions

On very large scales we can ignore the terms multiplied by k in Eqs. (3.77) and (3.82)

$$\Theta_0' = \Phi' \,, \qquad \delta_{\rm m}' = 3\Phi' \,. \tag{3.97}$$

Thus $\delta_{\rm m} = 3\Theta_0 + \text{const.}$. For adiabatic initial conditions this constant needs to vanish. With $\Theta_0 = \delta_\gamma/4$ we thus have $\delta_{\rm m} = 3/4\delta_\gamma$.
On large scales, for constant potentials $\Phi' = 0$ we have from Eq. (3.3) that

$$-3\mathcal{H}^2\Phi = 4\pi G a^2 \left(\bar{\rho}_{\rm m}\delta_{\rm m} + \bar{\rho}_{\rm r}\delta_{\rm r}\right) \,. \tag{3.98}$$

Matter Domination:
Eq. (3.98) entails that $\delta_{\rm m} = -2\Phi_{\rm md}$ and thus $\delta_\gamma = -8/3\Phi_{\rm md}$ or $\Theta_0 = -2/3\Phi_{\rm md}$. This leads to $\Theta_0 + \Psi = \Psi/3$.

Radiation Domination:
Eq. (3.98) that $\Theta_0 = -\Phi_{\rm rd}/2$ and thus $\delta_\gamma = -2\Phi_{\rm rd}$ or $\delta_{\rm m} = -3/2\Phi_{\rm rd}$.

Using $\Theta_0 = 2/5\mathcal{R} = -2/3\Psi_{\rm md}$ we have for the transfer functions expressing Θ in terms of $\mathcal{R}$ in Eq. (3.68)

$$\tilde{T}_{\rm SW} = \frac{\Theta_0 + \Psi}{\mathcal{R}} = -\frac{1+3R}{5}\cos(kr_{\rm s}) - \frac{3R}{5} \,, \tag{3.99}$$

$$\tilde{T}_{\rm D} = \frac{\boldsymbol{v}_{\rm b}\cdot\hat{\boldsymbol{p}}}{\mathcal{R}} = 3c_{\rm s}\frac{1+3R}{5}\sin(kr_{\rm s}) \,. \tag{3.100}$$

We show these dependencies in Fig. 3.7.

For modes that enter during radiation domination the gravitational potential is not constant but decaying. Counterintuitively, this decaying potential can enhance the first compression. This happens by pulling the photons into overdensity then decaying and thus not being able to halt the subsequent rarefaction [Hu and Sugiyama, 1995].

3.2.7. Scales

In Fig. 3.8 we show the relevant scales for CMB physics.

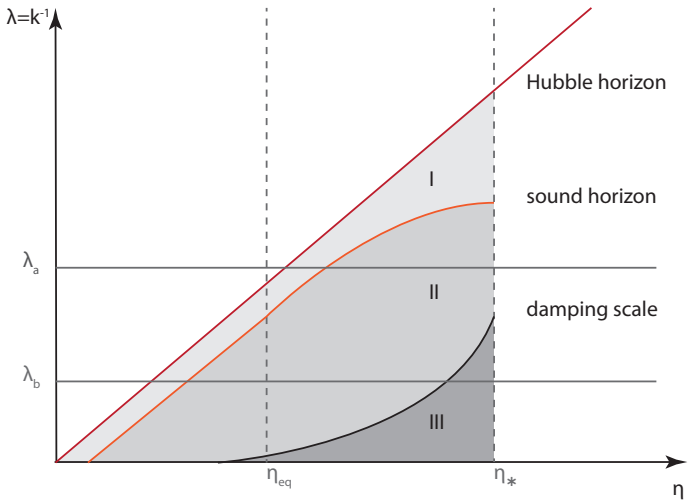

Figure 3.8.: Scales affecting the evolution of perturbations in the photon-baryon fluid. As time proceeds fluctuations are moving through the regions horizontally. Adapted from [Baumann, 2017].

Hubble radius Fluctuations outside the comoving Hubble radius $r_\mathrm{H} \approx \mathcal{H}^{-1}$ are frozen but they start to evolve once they cross into the horizon.

Sound horizon Photon perturbations remain frozen until they cross the sound horizon $r_\mathrm{s} = c_\mathrm{s}\eta$, which is when they start to oscillate. At early times $R \to 0$ and thus $c_\mathrm{s} \approx 1/\sqrt{3}$, whereas R becomes significant just before recombination, driving the speed of sound to zero. After recombination, the concept of a sound horizon is ill defined.

Damping scale On scales of order the photon mean free path fluctuations are damped by viscosity and heat conduction arising from diffusion.

3.2.8. Diffusion Damping

Damping arises from a non-vanishing quadrupole. We will thus need to consider higher orders in $1/\tau' = -1/\Gamma$. The mean free path of the photons in the plasma is given by

$$\lambda_\mathrm{MFP} = (a\sigma_\mathrm{T} n_\mathrm{b} x_\mathrm{e})^{-1}\,. \tag{3.101}$$

In a Hubble time the photon scatters $N_\mathrm{step} = \Gamma\eta_\mathcal{H} = a\sigma_\mathrm{T} n_\mathrm{b} x_\mathrm{e}/\mathcal{H}$ times and thus the root-mean-square displacement of the random walk is

$$\sigma_\mathrm{D} = \lambda_\mathrm{MFP}\sqrt{N_\mathrm{step}} = \frac{1}{\sqrt{a\sigma_\mathrm{T} n_\mathrm{b} x_\mathrm{e}\mathcal{H}}} = \frac{1}{\sqrt{\Gamma\mathcal{H}}}. \tag{3.102}$$

Perturbations on scales below this rms displacement scale will be washed out. We can also see this effect a bit more formally considering the dispersion relation of the photon waves. In the WKB approximation we can write for high frequencies

$$\Theta_l, v_\mathrm{b} \propto \exp\left[\mathrm{i}\int \mathrm{d}\eta\;\omega\right] \tag{3.103}$$

leading to $v_\mathrm{b}' = \mathrm{i}\omega v_\mathrm{b}$.

Diffusion damping is relevant on small scales, where the expansion is much slower than the small scale dynamics. It follows that we can drop the gravitational terms and get for the evolution equations

$$\begin{aligned}
\Theta_0' &= -k\Theta_1 \\
3\Theta_1' &= k\left(\Theta_0 - 2\Theta_2\right) - \Gamma(3\Theta_1 + v_\mathrm{b}) \\
5\Theta_2' &= 2k\Theta_1 - \frac{9}{2}\Gamma\Theta_2
\end{aligned} \tag{3.104}$$

Since $\Theta_2' \ll \Gamma\Theta_2$ we have

$$\Theta_2 = \frac{4}{9}\frac{k}{\Gamma}\Theta_1 \qquad\qquad \Theta_0 = \frac{\mathrm{i}k}{3\omega}\Theta_1\,. \tag{3.105}$$

It remains to relate the baryon velocity to the moments of the photon temperature

$$v_\mathrm{b}' + \left(\mathcal{H} + \frac{\Gamma}{R}\right) v_\mathrm{b} = -3\frac{\Gamma}{R}\Theta_1 \tag{3.106}$$

As $\mathcal{H} \ll \Gamma$ we have

$$\left(1 + \mathrm{i}\frac{\omega R}{\Gamma}\right) v_\mathrm{b} = -3\Theta_1 \tag{3.107}$$

Thus

$$v_\mathrm{b} = -3\Theta_1 \left(1 + \mathrm{i}\frac{\omega R}{\Gamma}\right)^{-1} \approx -3\Theta_1 \left[1 - \mathrm{i}\frac{\omega R}{\Gamma} - \left(\frac{\omega R}{\Gamma}\right)^2\right] \tag{3.108}$$

We can now use this result as well as the solutions for Θ_0 and Θ_2 in the dynamical equation for Θ_1 (the Euler equation)

$$\omega^2(1+R) - \frac{k^2}{3} - \mathrm{i}\frac{\omega}{\Gamma}\left(\frac{8}{27}k^2 + R^2\omega^2\right) = 0\,. \tag{3.109}$$

At leading order the dispersion relation is solved by

$$\omega = c_\mathrm{s}k = \frac{1}{\sqrt{3(1+R)}}k\,. \tag{3.110}$$

Using this solution in the imaginary part of the dispersion relation suppressed by Γ^{-1} and expanding $\omega \to \omega + \delta\omega$ in the leading order real part, we obtain

$$\delta\omega = \mathrm{i}\frac{k^2}{\Gamma}\frac{1}{(1+R)}\left(\frac{8}{9} + \frac{R^2}{1+R}\right) \tag{3.111}$$

The imaginary form of the dispersion relation leads to the damping $\exp\left[\mathrm{i}\int \mathrm{d}\eta\ \delta\omega\right] = \exp\left[-k^2/k_\mathrm{D}^2\right]$, where

$$\frac{1}{k_\mathrm{D}^2} = \frac{1}{6}\int \mathrm{d}\eta\ \frac{1}{\Gamma}\frac{1}{(1+R)}\left(\frac{8}{9} + \frac{R^2}{1+R}\right) \tag{3.112}$$

We see that our naïve estimate of $k_\mathrm{D}^2 \sim \sigma_\mathrm{D}^{-2} \sim \Gamma$ was correct.

When using the instantaneous recombination approximation discussed above, the finite width of the last scattering surface can be accounted for by an additional Gaussian damping [Seljak, 1994] with standard deviation $\sigma_\mathrm{LSS} \approx 0.03$.

3.3. Polarization

The CMB is polarized at the 10% level. The scalar part of the polarization arises from Thomson scattering of incident unpolarized quadrupole radiation. As we have seen before, during tight coupling, the quadrupole is suppressed with respect to the monopole and thus the generation of polarization is restricted to a brief period during recombination. It will also be much smaller in amplitude than the temperature fluctuations. We will discuss how we can describe the statistics of polarized radiation on the whole sky (hard but general) and in the small-angle limit (more intuitive but restricted). We will see that E- and B-modes are the coordinate invariant way of quantifying polarization. Scalar perturbations only generate E-modes, which can however be transformed into B-modes by CMB lensing, as we will discuss in the next section. Primordial B-modes are also generated from inflationary gravitational waves.

CMB polarization is a nontrilvial and advanced subject. If you would like to read up, I can recommend the pedagocial but not very mathematical CMB Polarization Primer [Hu and White, 1997]. Dodelson's

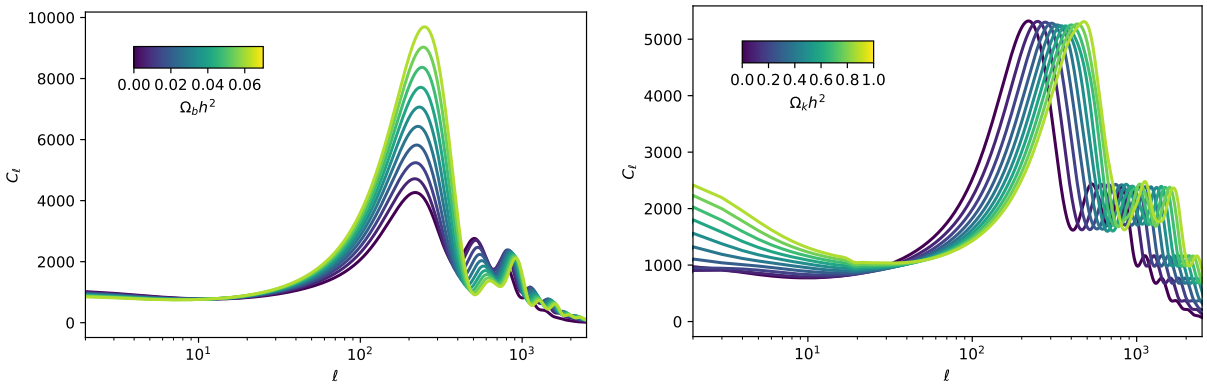

Figure 3.9.: Impact of baryon density and curvature on the angular power spectrum. C_ls calculated using CAMB.

textbook also provides a detailed discussion. More detailed explanations can be found in Durrer's textbook, [Kamionkowski and Kovetz, 2016], [Kosowsky, 1996] and [Challinor and Peiris, 2009].

Let us consider an electromagnetic wave propagating in the $\hat{\boldsymbol{z}}$-direction

$$\boldsymbol{E} = (E_x \hat{\boldsymbol{e}}_{\boldsymbol{x}} + E_y \hat{\boldsymbol{e}}_{\boldsymbol{y}}) \exp\left[\mathrm{i}(kz - \omega t)\right] . \tag{3.113}$$

The intensity-polarization tensor can be expressed in terms of the temperature T and the Q and U polarization parameters

$$I_{ij} = T\delta_{ij}^{(\mathrm{K})} + 2\mathcal{P}_{ij} = \begin{pmatrix} T+Q & U \\ U & T-Q \end{pmatrix} = \begin{pmatrix} \langle E_x E_x * \rangle & \langle E_x E_y * \rangle \\ \langle E_y E_x * \rangle & \langle E_y E_y * \rangle \end{pmatrix} . \tag{3.114}$$

Here we have omitted the circular polarization V, which is irrelevant for our discussion here. The averages are over several periods ω^{-1} of the wave. In terms of the electric field strength they can be expressed as $Q = E_x^2 - E_y^2$ and $U = 2E_x E_y$ for a wave propagating in $\hat{\boldsymbol{z}}$ direction. Under a rotation by φ in the x-y-plane (or generally around the propagation direction) Q and U transform as

$$\begin{pmatrix} Q' \\ U' \end{pmatrix} = \begin{pmatrix} \cos 2\varphi & \sin 2\varphi \\ -\sin 2\varphi & \cos 2\varphi \end{pmatrix} \begin{pmatrix} Q \\ U \end{pmatrix} , \tag{3.115}$$

where

$$\begin{pmatrix} \hat{\boldsymbol{e}}'_\theta \\ \hat{\boldsymbol{e}}'_\varphi \end{pmatrix} = \begin{pmatrix} \cos\varphi & -\sin\varphi \\ \sin\varphi & \cos\varphi \end{pmatrix} \begin{pmatrix} \hat{\boldsymbol{e}}_\theta \\ \hat{\boldsymbol{e}}_\varphi \end{pmatrix} . \tag{3.116}$$

Polarization patterns for pure Q- and pure U-polarization are shown in Fig. 3.11.

The polarization can also be expressed as a complex number

$$P = |P| e^{\pm 2\mathrm{i}\alpha} = Q \pm \mathrm{i}U , \tag{3.117}$$

where under a rotation by φ we have $Q' + \mathrm{i}U' = e^{-2\mathrm{i}\varphi}(Q + \mathrm{i}U)$. The polarization magnitude and angle are given by $|P| = \sqrt{Q^2 + U^2}$ and $\cos 2\alpha = Q/|P|$, $\sin 2\alpha = U/|P|$.

Quantities that change under rotations as $\tilde{f} = e^{-s\mathrm{i}\varphi} f$ are said to be **spin-s quantities**.

3.3.1. Polarization from incoming Unpolarized Radiation

Let us start with incoming unpolarized radiation. The differential cross-section for outgoing polarization in the ϵ_i direction is given by

$$\frac{\mathrm{d}\sigma}{\mathrm{d}\Omega} = \frac{3}{8\pi}\sigma_{\mathrm{T}} \sum_{j=1}^{2} |\hat{\boldsymbol{\epsilon}}_i(\hat{\boldsymbol{n}}) \cdot \hat{\boldsymbol{\epsilon}}'_j(\hat{\boldsymbol{n}}')|^2 \tag{3.118}$$

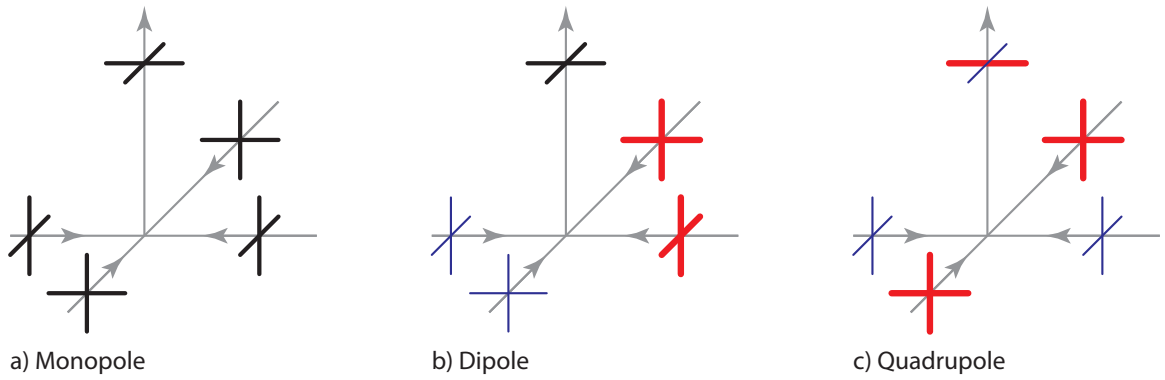

Figure 3.10.: Scattering of incoming unpolarized radiation along the x and y axis to outgoing radiation in the z-direction. *a*): If the incoming radiation is pure monopole, the components in the x-y-plane have the same amplitudes and thus the outgoing radiation is unpolarized. *b*): If the incoming radiation is pure dipole, the hotter and colder photons average to the same temperature giving unpolarized outgoing radiation. *c*): If the incoming radiation is a quadrupole, the cold radiation determines the y-polarization direction and the hot radiation dominates the x-polarization direction, leading to net polarized outgoing radiation.

If the outgoing radiation is propagating along the $\hat{\boldsymbol{z}}$-direction, the outgoing polarization basis vectors can be chosen to be $\hat{\boldsymbol{e}}_1 = \hat{\boldsymbol{x}}$ and $\hat{\boldsymbol{e}}_2 = \hat{\boldsymbol{y}}$

$$Q \propto \sum_{j=1}^{2} \left\{ |\hat{\boldsymbol{x}} \cdot \hat{\boldsymbol{\epsilon}}'_j(\hat{\boldsymbol{n}}')|^2 - |\hat{\boldsymbol{y}} \cdot \hat{\boldsymbol{\epsilon}}'_j(\hat{\boldsymbol{n}}')|^2 \right\} , \tag{3.119}$$

$$U \propto \sum_{j=1}^{2} \hat{\boldsymbol{x}} \cdot \hat{\boldsymbol{\epsilon}}'_j(\hat{\boldsymbol{n}}') \hat{\boldsymbol{y}} \cdot \hat{\boldsymbol{\epsilon}}'_j(\hat{\boldsymbol{n}}') . \tag{3.120}$$

Integrating over incoming unpolarized radiation (i.e. the amplitude depends on the direction but not the polarization vector) we have

$$Q(\hat{\boldsymbol{z}}) = A \int \mathrm{d}\hat{\boldsymbol{n}}' \; \Theta(\hat{\boldsymbol{n}}') \sum_{j=1}^{2} \left\{ |\hat{\boldsymbol{x}} \cdot \hat{\boldsymbol{\epsilon}}'_j(\hat{\boldsymbol{n}}')|^2 - |\hat{\boldsymbol{y}} \cdot \hat{\boldsymbol{\epsilon}}'_j(\hat{\boldsymbol{n}}')|^2 \right\} . \tag{3.121}$$

The polarization basis vectors for the incoming radiation from direction $\hat{\boldsymbol{n}}'$ can the chosen as the $\hat{\boldsymbol{e}}_\theta$ and $\hat{\boldsymbol{e}}_\varphi$ tangent vectors

$$\begin{aligned} \hat{\boldsymbol{e}}_\theta &= (\cos\theta \cos\varphi, \cos\theta \sin\varphi, -\sin\theta) , \\ \hat{\boldsymbol{e}}_\phi &= (-\sin\varphi, \cos\varphi, 0) . \end{aligned} \tag{3.122}$$

Evaluating Eq. (3.121) using these basis vectors, we obtain

$$\begin{aligned} Q(\hat{\boldsymbol{z}}) &= \int \mathrm{d}\hat{\boldsymbol{n}}' \; \Theta(\hat{\boldsymbol{n}}')(\cos^2\theta' - 1)(\cos^2\varphi' - \sin^2\varphi') \\ &= -\int \mathrm{d}\hat{\boldsymbol{n}}' \; \Theta(\hat{\boldsymbol{n}}') \sin^2\theta \cos(2\varphi') \\ &= -\int \mathrm{d}\hat{\boldsymbol{n}}' \; \Theta(\hat{\boldsymbol{n}}') \left[Y_{2,2}(\hat{\boldsymbol{n}}') + Y_{2,-2}(\hat{\boldsymbol{n}}') \right] \end{aligned} \tag{3.123}$$

If the incoming radiation is unpolarized, it will only generate polarization if it has a quadrupole moment.

This situation is depicted in Fig. 3.10.

$$\begin{aligned} U(\hat{\boldsymbol{z}}) =& 2\int \mathrm{d}\hat{\boldsymbol{n}}'\ \Theta(\hat{\boldsymbol{n}}')(\cos^2\theta' - 1)\cos\varphi\sin\varphi' \\ =& -\int \mathrm{d}\hat{\boldsymbol{n}}'\ \Theta(\hat{\boldsymbol{n}}')\sin^2\theta\sin(2\varphi') \\ =& -\int \mathrm{d}\hat{\boldsymbol{n}}'\ \Theta(\hat{\boldsymbol{n}}')\left[Y_{2,2}(\hat{\boldsymbol{n}}') - Y_{2,-2}(\hat{\boldsymbol{n}}')\right] \end{aligned} \tag{3.124}$$

$$(Q \pm \mathrm{i}U)(\hat{\boldsymbol{z}}) = \int \mathrm{d}\hat{\boldsymbol{n}}'\ \Theta(\hat{\boldsymbol{n}}')\sin^2\theta' e^{\pm 2\mathrm{i}\varphi'} = \int \mathrm{d}\hat{\boldsymbol{n}}'\ \Theta(\hat{\boldsymbol{n}}')Y_{2\pm 2}(\hat{\boldsymbol{n}}') \tag{3.125}$$

If we expand

$$\Theta(\hat{\boldsymbol{n}}) = \sum_{lm} \tilde{a}_{lm} Y_{lm}(\hat{\boldsymbol{n}}) \tag{3.126}$$

the above equation obviously picks out the a_{22} moment of the incident unpolarized radiation field. So far we have been concentrating on outgoing radiation along the $\hat{\boldsymbol{z}}$-axis. If we want the outgoing radiation field in another direction, we can simply express the incoming radiation in a rotated frame [Kosowsky, 1999]. According to Eq. (1.102), the coefficients

$$\tilde{a}_{22} = \sum_m D^2_{2m} a_{2m}. \tag{3.127}$$

If the incoming radiation is independent of the angle ϕ it will only have a $m = 0$ mode, in which case $D_{2m} \propto \sin^2\beta$, where β is the angle between the outgoing axis $\hat{\boldsymbol{n}}$ and the $\hat{\boldsymbol{z}}$-axis. We hus have

$$(Q \pm \mathrm{i}U)(\hat{\boldsymbol{n}}) = a_{20}Y_{22}(\hat{\boldsymbol{n}}) = a_{20}\sin^2\beta\left[\cos(2\phi) \pm \mathrm{i}\sin(2\phi)\right]. \tag{3.128}$$

We can express the incoming radiation by its Fourier modes, which in turn allow an expansion in multipoles as per Eq. (3.44)

$$\Theta(\boldsymbol{k}, \hat{\boldsymbol{n}}'\cdot\hat{\boldsymbol{k}}) = \sum_l (2l+1)(-\mathrm{i})^l \mathcal{P}_l(\hat{\boldsymbol{n}}'\cdot\hat{\boldsymbol{k}})\Theta_l(\boldsymbol{k}) = 4\pi\sum_l (-\mathrm{i})^l Y_{lm}(\hat{\boldsymbol{n}}')Y^*_{lm}(\hat{\boldsymbol{k}})\Theta_l(\boldsymbol{k}) \tag{3.129}$$

we have

$$\begin{aligned} (Q \pm \mathrm{i}U)(\boldsymbol{k}) = \Theta_2(\boldsymbol{k})Y_{2\pm 2}(\hat{\boldsymbol{k}}) =& \Theta_2(\boldsymbol{k})\sin^2\theta_{\hat{\boldsymbol{k}}}\left[\cos(2\phi_{\hat{\boldsymbol{k}}}) \pm \mathrm{i}\sin(2\phi_{\hat{\boldsymbol{k}}})\right], \\ =& \Theta_P(\boldsymbol{k}, \hat{\boldsymbol{k}}\cdot\hat{\boldsymbol{n}})\left[\cos(2\phi_{\hat{\boldsymbol{k}}}) \pm \mathrm{i}\sin(2\phi_{\hat{\boldsymbol{k}}})\right] \end{aligned} \tag{3.130}$$

If $\hat{\boldsymbol{k}}$ lies in the $x-z$-plane, $\phi_{\hat{\boldsymbol{k}}} = 0$ and we produce pure Q-polarization.

3.3.2. Boltzmann Equation for Polarization

The Boltzmann equation for polarization is given by

$$\frac{\mathrm{d}\Theta_P}{\mathrm{d}\eta} = \Theta'_P + \mathrm{i}k\mu\Theta_P = \Gamma\left[-\Theta_P + \frac{1}{2}\Big(1 - \mathcal{P}_2(\mu)\Big)\Pi\right], \tag{3.131}$$

where $\Pi = \Theta_2 + \Theta_{P2} + \Theta_{P0}$. There is no $\mathrm{d}\ln\epsilon/\mathrm{d}\eta$ term here, since there is no zero-order polarization. If $\hat{\boldsymbol{k}}$ lies in the $\hat{\boldsymbol{x}} - \hat{\boldsymbol{z}}$-plane, then $\phi_{\hat{\boldsymbol{k}}} = 0$ and $Q = \Theta_P$.

If there is no prior polarization, we furthermore have $\Pi = \Theta_2$ and thus

$$\Theta'_P = -\frac{3}{2}\tau'(1-\mu^2)\Theta_2 \quad \Rightarrow \quad \Theta_P = \frac{3\tau}{2}(1-\mu^2)\Theta_2 \tag{3.132}$$

With

$$\frac{\mathrm{d}e^{-\tau}\Theta_P}{\mathrm{d}\eta} = e^{-\tau}\left(\frac{\mathrm{d}\Theta_P}{\mathrm{d}\eta} + \Gamma\Theta_P\right) = \frac{3}{4}(1-\mu^2)g\Pi \tag{3.133}$$

The line-of-sight solution yields

$$\Theta_P(\eta,\boldsymbol{k}) = \int \mathrm{d}\eta'\ S_P \exp\left[\mathrm{i}k\chi'\hat{\boldsymbol{n}}\cdot\hat{\boldsymbol{k}}\right] = \frac{3}{4}(1-\mu^2)\int \mathrm{d}\eta'\ g\Pi \exp\left[\mathrm{i}k\chi'\hat{\boldsymbol{n}}\cdot\hat{\boldsymbol{k}}\right] \tag{3.134}$$

For instantaneous recombination we thus have

$$\begin{aligned}\Theta_P(\eta,\boldsymbol{k}) =& \frac{3}{4}\left[1+\left(\frac{\partial}{\partial k\chi_*}\right)^2\right]\Pi(\eta_*,\boldsymbol{k})\exp\left[\mathrm{i}k\chi_*\hat{\boldsymbol{n}}\cdot\hat{\boldsymbol{k}}\right]\\ =& \frac{3}{4}g\Pi(\eta_*,\boldsymbol{k})\sum_l (2l+1)\mathrm{i}^l\left[j_l(k\chi_*)+j_l''(k\chi_*)\right]\end{aligned} \tag{3.135}$$

Using a recursion relation for the spherical Bessel functions[7] and selecting the dominant terms we have

$$\Theta_P(\boldsymbol{k},\hat{\boldsymbol{n}}) \approx \sum_l \frac{15}{8} l^2 \frac{j_l(k\chi_*)}{(k\chi_*)^2}\Theta_2(\eta_*,\boldsymbol{k})\,. \tag{3.136}$$

With Eq. (3.105), we have $\Theta_2 \approx k/\Gamma\ \Theta_1$

$$\Theta_P(\boldsymbol{k},\hat{\boldsymbol{n}}) \approx \sum_l \frac{5}{6}\frac{k}{\Gamma} l^2 \frac{j_l(k\chi_*)}{(k\chi_*)^2}\Theta_1(\eta_*,\boldsymbol{k})\,. \tag{3.137}$$

The polarization fluctuations are thus in phase with the Doppler dipole and out of phase with the temperature monopole fluctuations. They are furthermore suppressed by k/Γ.

The polarization fluctuations have sharper peaks because only one phase is present rather than a superposition of the Sachs-Wolfe monopole and the Doppler dipole which are out of phase. Only Q is generated in the frame with $\hat{\boldsymbol{k}} \parallel \hat{\boldsymbol{z}}$ because of azimuthal symmetry.

3.3.3. Flat Sky

If we are interested in polarization fluctuations over a small patch of the sky, we can employ the flat sky approximation and perform a two-dimensional Fourier transform in the angles

$$Q(\hat{\boldsymbol{n}}) = \int \frac{\mathrm{d}^2 l}{(2\pi)^2} e^{\mathrm{i}\hat{\boldsymbol{n}}\cdot\boldsymbol{l}} Q(\boldsymbol{l})\,, \qquad\qquad Q(\boldsymbol{l}) = \int \mathrm{d}^2\hat{\boldsymbol{n}}\ e^{-\mathrm{i}\hat{\boldsymbol{n}}\cdot\boldsymbol{l}} Q(\hat{\boldsymbol{n}})\,, \tag{3.138}$$

and likewise for U and Θ_P. The angular power spectrum is then defined as

$$\langle f(\boldsymbol{l}) f(\boldsymbol{l}')\rangle = (2\pi)^2\delta^{(\mathrm{D})}(\boldsymbol{l}+\boldsymbol{l}')C_l\,. \tag{3.139}$$

We noted above that Q and U change under rotations around $\hat{\boldsymbol{n}}$. We can define linear combinations of Q and U that are independent of this choice of coordinate system

$$\begin{pmatrix} E(\boldsymbol{l}) \\ B(\boldsymbol{l}) \end{pmatrix} = \begin{pmatrix} \cos 2\phi_l & \sin 2\phi_l \\ -\sin 2\phi_l & \cos 2\phi_l \end{pmatrix} \begin{pmatrix} Q(\boldsymbol{l}) \\ U(\boldsymbol{l}) \end{pmatrix}\,, \tag{3.140}$$

and vice versa

$$\begin{pmatrix} Q(\boldsymbol{l}) \\ U(\boldsymbol{l}) \end{pmatrix} = \begin{pmatrix} \cos 2\phi_l & -\sin 2\phi_l \\ \sin 2\phi_l & \cos 2\phi_l \end{pmatrix} \begin{pmatrix} E(\boldsymbol{l}) \\ B(\boldsymbol{l}) \end{pmatrix}\,. \tag{3.141}$$

Alternatively

$$E \pm \mathrm{i}B = e^{\mp 2\mathrm{i}\phi_l}(Q \pm \mathrm{i}U) \tag{3.142}$$

[7]

$$j_l(x) + j_l''(x) = -\frac{2}{x}j_{l-1}(x) + \frac{2(l+1)}{x^2}j_l(x) + \frac{l(l+1)}{x^2}j_{l-1}(x)$$

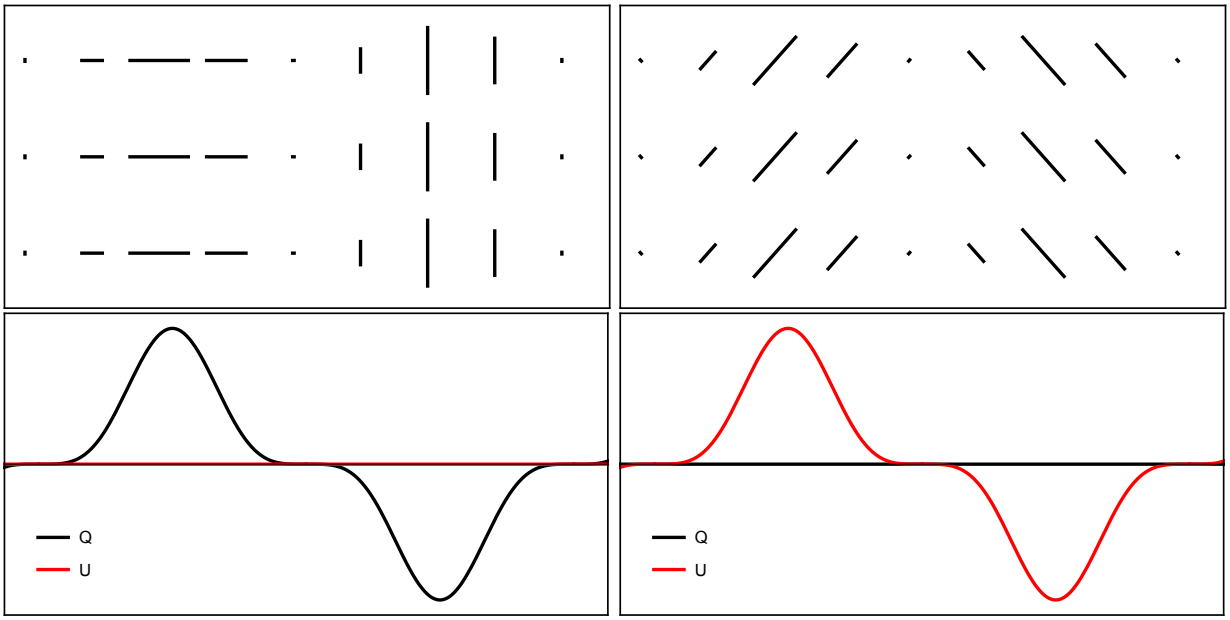

Figure 3.11.: Q (left) und U (right) patterns for $l = l\hat{\boldsymbol{x}}$. The distinctive pattern of U polarization is that the polarization vector is parallel and orthogonal to the wavevector whereas U-polarization is characterized by a polarization vector at 45° to the wavevector.

Under a rotation of the coordinate system by φ, the angle of the Fourier wavevector changes as $\phi_{\boldsymbol{l}} \to \phi_{\boldsymbol{l}} - \varphi$. Thus E and B are invariant under rotations.

The polarization at $\boldsymbol{x} = 0$ can be written as

$$(Q + \mathrm{i}U)(\chi\hat{\boldsymbol{n}}, \hat{\boldsymbol{n}}) = \int_{\boldsymbol{k}} \Theta_P(\boldsymbol{k}) \left[\cos(2\phi_{\hat{\boldsymbol{k}}}) \pm \mathrm{i}\sin(2\phi_{\hat{\boldsymbol{k}}})\right] \exp\left[\mathrm{i}k\chi\hat{\boldsymbol{n}} \cdot \hat{\boldsymbol{k}}\right] \tag{3.143}$$

With

$$\cos(2\phi_k) = \frac{k_x^2 - k_y^2}{k_x^2 + k_y^2} \qquad \sin(2\phi_k) = \frac{k_x k_y}{k_x^2 + k_y^2} \tag{3.144}$$

we have

$$\begin{aligned}(Q \pm \mathrm{i}U)(\chi\hat{\boldsymbol{n}}, \hat{\boldsymbol{n}}) &= \int_{\boldsymbol{k}} \Theta_P(\boldsymbol{k}) \left[\frac{k_x^2 - k_y^2}{k_x^2 + k_y^2} \pm \mathrm{i}\frac{k_x k_y}{k_x^2 + k_y^2}\right] \exp\left[\mathrm{i}k\chi\hat{\boldsymbol{n}} \cdot \hat{\boldsymbol{k}}\right] \\ &= \left(\frac{\partial^2_{\hat{\boldsymbol{n}}_x} - \partial^2_{\hat{\boldsymbol{n}}_y}}{\partial^2_{\hat{\boldsymbol{n}}_x} + \partial^2_{\hat{\boldsymbol{n}}_y}} \pm \mathrm{i}\frac{\partial_{\hat{\boldsymbol{n}}_x}\partial_{\hat{\boldsymbol{n}}_y}}{\partial^2_{\hat{\boldsymbol{n}}_x} + \partial^2_{\hat{\boldsymbol{n}}_y}}\right) \Theta_P(\chi\hat{\boldsymbol{n}}, \hat{\boldsymbol{n}})\end{aligned} \tag{3.145}$$

With Eq. (3.138) we have

$$(Q \pm \mathrm{i}U)(\boldsymbol{l}) = \Theta_P(\boldsymbol{l}) \left[\cos(2\phi_{\boldsymbol{l}}) \pm \mathrm{i}\sin(2\phi_{\boldsymbol{l}})\right] . \tag{3.146}$$

With Eq. (3.140) we have that for scalar perturbations $E(\boldsymbol{l}) = \Theta_P(\boldsymbol{l})$ and $B(\boldsymbol{l}) = 0$. In summary: scalar density fluctuations can generate quadrupolar brightness fluctuations and thus polarization in the form of E-modes. T and E remain unchanged under a parity transformation, while B changes sign. Assuming parity conserving physics, we thus expect $C_l^{TB} = C_l^{EB} = 0$. The non-vanishing spectra are thus C_l^{TT}, C_l^{TE}, C_l^{EE} and C_l^{BB}

$$\begin{aligned}\langle\Theta(\boldsymbol{l})\Theta(\boldsymbol{l}')\rangle &= (2\pi)^2\delta^{(\mathrm{D})}(\boldsymbol{l} + \boldsymbol{l}')C_l^{TT} \\ \langle E(\boldsymbol{l})E(\boldsymbol{l}')\rangle &= (2\pi)^2\delta^{(\mathrm{D})}(\boldsymbol{l} + \boldsymbol{l}')C_l^{EE} \\ \langle\Theta(\boldsymbol{l})E(\boldsymbol{l}')\rangle &= (2\pi)^2\delta^{(\mathrm{D})}(\boldsymbol{l} + \boldsymbol{l}')C_l^{TE} \\ \langle B(\boldsymbol{l})B(\boldsymbol{l}')\rangle &= (2\pi)^2\delta^{(\mathrm{D})}(\boldsymbol{l} + \boldsymbol{l}')C_l^{BB}\end{aligned} \tag{3.147}$$

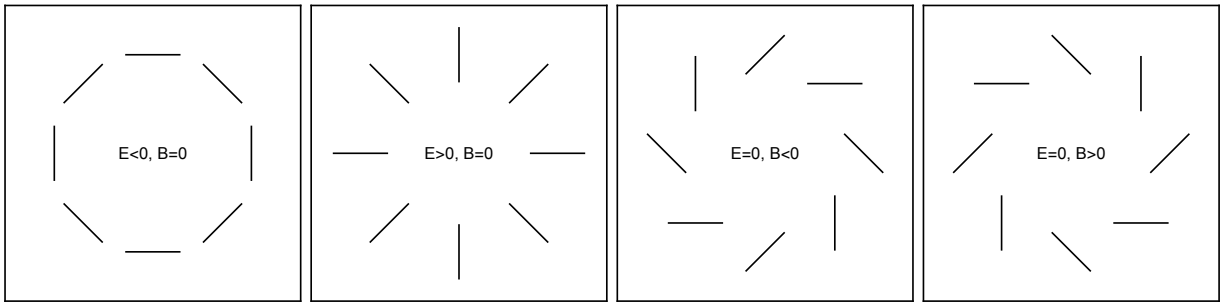

Figure 3.12.: Polarization pattern as a function of φ_l.

3.3.4. Full Sky: Spin-weighted spherical harmonics*

The **spin-weighted spherical harmonics** are forming a basis for spin weighted functions on S_2. We can define the spin raising and spin lowering operators $\eth$ and $\tilde{\eth}$

$$\begin{aligned} \eth_s Y_{lm} =& \sqrt{(l-s)(l+s+1)}\ {}_{s+1}Y_{lm} \\ \tilde{\eth}_s Y_{lm} =& -\sqrt{(l+s)(l-s+1)}\ {}_{s-1}Y_{lm} \end{aligned} \tag{3.148}$$

Using ${}_0Y_{lm} = Y_{lm}$ the spin weighted spherical harmonics can thus be computed from the standard spherical harmonics

$${}_sY_{lm} = \begin{cases} \sqrt{\frac{(l-s)!}{(l+s)!}}\eth^s Y_{lm} & \text{for } s > 0\,, \\ (-1)^s\sqrt{\frac{(l-|s|)!}{(l+|s|)!}}\tilde{\eth}^s Y_{lm} & \text{for } s < 0\,. \end{cases} \tag{3.149}$$

It follows

$$\begin{aligned} \tilde{\eth}^2\,{}_2Y_{lm} &= \sqrt{\frac{(l+2)!}{(l-2)!}}\ Y_{lm} \\ \eth^2\,{}_{-2}Y_{lm} &= \sqrt{\frac{(l+2)!}{(l-2)!}}\ Y_{lm} \end{aligned} \tag{3.150}$$

The spin-weighted spherical harmonics satisfy the familiar orthogonality relation

$$\int \mathrm{d}^2\hat{\boldsymbol{n}}\ {}_sY_{lm}(\hat{\boldsymbol{n}})\,{}_sY^*_{l'm'}(\hat{\boldsymbol{n}}) = \delta^{(\mathrm{K})}_{ll'}\delta^{(\mathrm{K})}_{mm'}\,, \tag{3.151}$$

and the completeness relation

$$\sum_{lm} {}_sY_{lm}(\hat{\boldsymbol{n}})\,{}_sY^*_{lm}(\hat{\boldsymbol{n}}) = \delta^{(\mathrm{D})}(\varphi-\varphi')\delta^{(\mathrm{D})}(\mu-\mu')\,. \tag{3.152}$$

The spin-2 quantity $Q \pm \mathrm{i}U$ can thus be expanded in the spin-weighted spherical harmonics

$$(Q \pm \mathrm{i}U)(\hat{\boldsymbol{n}}) = \sum_{lm} {}_{\pm2}a_{lm}\ {}_{\pm2}Y_{lm}(\hat{\boldsymbol{n}}) = \sum_{lm}(E_{lm} \pm \mathrm{i}B_{lm})\,{}_{\pm2}Y_{lm}(\hat{\boldsymbol{n}})\,, \tag{3.153}$$

with expansion coefficients given by

$${}_{\pm2}a_{lm} = \int \mathrm{d}^2\hat{\boldsymbol{n}}\ {}_{\pm2}Y^*_{lm}(\hat{\boldsymbol{n}})(Q \pm \mathrm{i}U)(\hat{\boldsymbol{n}})\,. \tag{3.154}$$

Simple algebra reveals that the E and B modes are related to the ${}_{\pm2}a_{lm}$ by

$$\begin{aligned} E_{lm} =& \frac{1}{2}({}_{+2}a_{lm} + {}_{-2}a_{lm}) \\ B_{lm} =& -\mathrm{i}\frac{1}{2}({}_{+2}a_{lm} - {}_{-2}a_{lm}) \end{aligned} \tag{3.155}$$

$$\begin{aligned} {}_{+2}a_{lm} =& (E_{lm} + \mathrm{i}B_{lm}) \\ {}_{-2}a_{lm} =& (E_{lm} - \mathrm{i}B_{lm}) \end{aligned} \tag{3.156}$$

Applying the spin-lowering operator $\tilde{\eth}$ twice to $Q + \mathrm{i}U$ gives a spin-0 quantity, as does applying the spin-raising operator $\eth$ twice to $Q - \mathrm{i}U$. The spin-0 quantities $\tilde{\eth}^2(Q + \mathrm{i}U)(\hat{\boldsymbol{n}})$ and $\eth^2(Q - \mathrm{i}U)(\hat{\boldsymbol{n}})$ can thus be expanded in the ordinary spherical harmonics

$$\begin{aligned} \tilde{\eth}^2(Q + \mathrm{i}U)(\hat{\boldsymbol{n}}) =& \sum_{lm} {}_{+2}a_{lm} \sqrt{\frac{(l+2)!}{(l-2)!}} Y_{lm}(\hat{\boldsymbol{n}}) = \sum_{lm} (E_{lm} + \mathrm{i}B_{lm}) \sqrt{\frac{(l+2)!}{(l-2)!}} Y_{lm}(\hat{\boldsymbol{n}}) \,, \\ \eth^2(Q - \mathrm{i}U)(\hat{\boldsymbol{n}}) =& \sum_{lm} {}_{-2}a_{lm} \sqrt{\frac{(l+2)!}{(l-2)!}} Y_{lm}(\hat{\boldsymbol{n}}) = \sum_{lm} (E_{lm} - \mathrm{i}B_{lm}) \sqrt{\frac{(l+2)!}{(l-2)!}} Y_{lm}(\hat{\boldsymbol{n}}) \,. \end{aligned} \tag{3.157}$$

For scalar perturbations $\tilde{\eth}^2(Q + \mathrm{i}U) = \eth^2(Q + \mathrm{i}U)$ and ${}_{+2}a_{lm} = {}_{-2}a_{lm}$ - scalar modes only generate E and B vanishes.

We can also define the scalar potentials P_E and P_B

$$\mathcal{P}_{ab} = \nabla_{\langle a} \nabla_{b\rangle} P_E + \epsilon^c{}_{(a} \nabla_{b)} \nabla_c P_B \,. \tag{3.158}$$

$$\nabla_{\langle a} \nabla_{b\rangle} = \nabla_{(a} \nabla_{b)} - \frac{1}{2} g_{ab} \nabla^2 \tag{3.159}$$

They are spin-0, and can thus be expanded in the usual spherical harmonics

$$P_E = \sum_{lm} E_{lm} \sqrt{\frac{(l-2)!}{(l+2)!}} Y_{lm} \,, \qquad\qquad P_B = \sum_{lm} B_{lm} \sqrt{\frac{(l-2)!}{(l+2)!}} Y_{lm} \,. \tag{3.160}$$

For axissymmetric P_E and P_B we have

$$Q = (1 - \mu^2) \frac{\mathrm{d}^2 P_E}{\mathrm{d}\mu^2} \qquad U = (1 - \mu^2) \frac{\mathrm{d}^2 P_B}{\mathrm{d}\mu^2} \tag{3.161}$$

$$\begin{aligned} Q + \mathrm{i}U =& \eth^2 (P_E + \mathrm{i}P_B) \\ Q - \mathrm{i}U =& \tilde{\eth}^2 (P_E - \mathrm{i}P_B) \end{aligned} \tag{3.162}$$

3.3.5. Gravitational Waves from Inflation*

Gravitational waves induce a polarization pattern on the surface of last scattering. A gravitational wave passing through a plane causes certain directions to expand more than others. This uneven redshifting causes a quadrupolar temperature variation. Gravitational waves have two independent degrees of freedom, often referred to as the + and × polarization. This additional degree of freedom allows the generation of polarization at angles differing from 90 degrees, thus leading to B modes.

Gravitational Waves in Cosmology

The spacetime metric in presence of a gravitational wave and absence of scalar perturbations is given by

$$\mathrm{d}s^2 = -a^2(\eta)\left[\mathrm{d}\eta^2 + (\delta^{(\mathrm{K})}_{ij} + h_{ij})\mathrm{d}x^i\mathrm{d}x^j\right] \tag{3.163}$$

where h_{ij} is a transverse $\partial_i h^i{}_j = 0$, traceless tensor $h^i{}_i = 0$. The tensor mode has two independent degrees of freedom that are encoded by the + and × polarization

$$h_{ij} = \begin{pmatrix} h_+ & h_\times & 0 \\ h_\times & -h_+ & 0 \\ 0 & 0 & 0 \end{pmatrix} = h_+\epsilon^+_{ij} + h_\times\epsilon^\times_{ij} = \sum_{I=+,\times} h_I\epsilon^I_{ij}\,. \tag{3.164}$$

$$S^{(2)} = \frac{1}{8}\int \mathrm{d}\eta\mathrm{d}^3x\; a^2\left[(h'_{ij})^2 - (\nabla h_{ij})^2\right] \tag{3.165}$$

Each of the polarizations is an independent harmonic oscillator with power spectrum

$$\Delta^2_{\mathrm{t}} = \frac{8}{M^2_{\mathrm{Pl}}}\left(\frac{H}{2\pi}\right)^2 = A_{\mathrm{t}}\left(\frac{k}{k_*}\right)^{n_{\mathrm{t}}} \tag{3.166}$$

$$n_{\mathrm{t}} = \frac{\mathrm{d}\ln\Delta^2_{\mathrm{t}}}{\mathrm{d}\ln k} = -2\epsilon \tag{3.167}$$

The **scalar-to-tensor ratio**

$$r = \frac{A_{\mathrm{t}}}{A_{\mathrm{s}}} = 16\epsilon = -8n_{\mathrm{t}} = 0.1\left[\frac{V}{(2\times 10^{16}\mathrm{GeV})^4}\right] \tag{3.168}$$

As we can see there is a consistency condition between the scalar-to-tensor ratio and Evolution of tensor perturbations

$$h''_{ij} + 2\mathcal{H}h'_{ij} - \nabla^2 h_{ij} = \Pi_{ij} \tag{3.169}$$

$$h''_I + 2\mathcal{H}h'_I + k^2 h_I \xrightarrow{k\to 0} h''_I + 2\mathcal{H}h'_I = 0 \tag{3.170}$$

This has a constant and a decaying solution. Outside the horizon the graviational waves are conserved but decay as $1/a$ inside.

The geodesic equation for tensor modes reads as

$$\frac{\mathrm{d}\ln\epsilon}{\mathrm{d}\eta} = -\frac{1}{2}h'_{ij}\hat{p}^i\hat{p}^j\,. \tag{3.171}$$

Thus the Boltzmann equation for temperature perturbations reads

$$\frac{\mathrm{d}\Theta}{\mathrm{d}\eta} + \frac{1}{2}\epsilon h'_{ij}\hat{p}^i\hat{p}^j = -\Gamma\Theta + \frac{3}{16\pi}\Gamma\int \mathrm{d}^2\hat{\boldsymbol{n}}\;\Theta(\hat{\boldsymbol{n}})\left[1 + (\hat{\boldsymbol{p}}\cdot\hat{\boldsymbol{n}})^2\right] \tag{3.172}$$

Gravitational waves generate temperature perturbations and polarization. For the polarization power spectra we finally have [Seljak and Zaldarriaga, 1997]

$$\begin{aligned} C_{E,l} &= (4\pi)^2\int \mathrm{d}k k^2 P_h(k)\left|\int \mathrm{d}\eta\; g(\eta)\Psi(k)\left[j_l(x) + j''_l(x) + \frac{2j_l(x)}{x^2} + \frac{4j'_l(x)}{x^2}\right]\right|^2, \\ C_{B,l} &= (4\pi)^2\int \mathrm{d}k k^2 P_h(k)\left|\int \mathrm{d}\eta\; g(\eta)\Psi(k)\left[2j'_l(x) + \frac{4j_l(x)}{x}\right]\right|^2, \end{aligned} \tag{3.173}$$

where the source term in terms of the temperature and polarization fluctuations is defined as

$$\Psi = \frac{1}{10}\Theta^T_0 + \frac{1}{7}\Theta^T_2 + \frac{3}{70}\Theta^T_4 - \frac{3}{5}\Theta^P_0 + \frac{6}{7}\Theta^P_2 - \frac{3}{70}\Theta^P_4\,. \tag{3.174}$$

3.4. CMB Lensing

So far we have assumed that the photons released at recombination travel to us unimpededly. Obviously, the photons travel through the LSS fluctuations and their associated gravitational potentials, resulting in lensing deflections.

As both the temperature fluctuations and the potential along the line of sight are first order perturbations, CMB lensing is a second order effect, that would have been accounted for by keeping the $\mathrm{d}\hat{\boldsymbol{p}}/\mathrm{d}\eta\partial f/\partial\hat{\boldsymbol{p}}$ term in Eq. (3.9).

CMB lensing affects both the temperature fluctuations as well as the CMB polarization. It changes the spectra of Θ and E by smoothing the peaks and can produce non-primordial B-modes from E-modes. Lensing allows us to reconstruct the lensing potential encountered by the photons and to measure the spectrum of the projected gravitational potential. This is one of the most direct ways to observe the dark matter distribution.

There are a number of very pedagogical reviews on CMB lensing, for instance [Hanson et al., 2010] and [Lewis and Challinor, 2006].

3.4.1. Lensing of temperature fluctuations

The observed CMB photons have been deflected by inhomogeneities along the way. Thus, the observed direction $\hat{\boldsymbol{n}}$ differs from the original direction by a deflection angle $\boldsymbol{\alpha}$

$$\tilde{\Theta}(\hat{\boldsymbol{n}}) = \Theta(\hat{\boldsymbol{n}}+\boldsymbol{\alpha}) \approx \Theta(\hat{\boldsymbol{n}}) + \boldsymbol{\alpha}\cdot\boldsymbol{\nabla}_{\hat{\boldsymbol{n}}}\Theta(\hat{\boldsymbol{n}}) = \Theta(\hat{\boldsymbol{n}}) + \delta\Theta(\hat{\boldsymbol{n}}) \tag{3.175}$$

The deflection angle is the perpendicular gradient of the deflection potential $\boldsymbol{\alpha} = \boldsymbol{\nabla}\Phi$.

$$\phi(\hat{\boldsymbol{n}}) = \int \mathrm{d}\chi\ \frac{\chi_* - \chi}{\chi\chi_*}\phi(\chi\hat{\boldsymbol{n}}) \tag{3.176}$$

In l-space this leads to a multiplication with the angular wavenumber

$$\boldsymbol{\alpha} = \mathrm{i}\int \frac{\mathrm{d}^2\boldsymbol{l}}{(2\pi)^2}\phi(\boldsymbol{l})\boldsymbol{l}e^{\mathrm{i}\boldsymbol{l}\cdot\hat{\boldsymbol{n}}}\,. \tag{3.177}$$

$$\boldsymbol{\nabla}_{\hat{\boldsymbol{n}}}\Theta = \mathrm{i}\int \frac{\mathrm{d}^2\boldsymbol{l}}{(2\pi)^2}T(\boldsymbol{l})\boldsymbol{l}e^{\mathrm{i}\boldsymbol{l}\cdot\hat{\boldsymbol{n}}} \tag{3.178}$$

The $\delta\Theta$ term is a product in angular space, leading to a convolution in l-space

$$\delta\Theta(\boldsymbol{l}) = [\boldsymbol{\nabla}\phi\star\boldsymbol{\nabla}\Theta](\boldsymbol{l}) = -\int \frac{\mathrm{d}^2\boldsymbol{l}'}{(2\pi)^2}\boldsymbol{l}'\cdot(\boldsymbol{l}-\boldsymbol{l}')\Theta(\boldsymbol{l}')\phi(\boldsymbol{l}-\boldsymbol{l}')\,. \tag{3.179}$$

We can now calculate the power spectrum of the lensed

$$C_l^{\tilde{\Theta}\tilde{\Theta}} = C_l^{TT} + \int \frac{\mathrm{d}^2\boldsymbol{l}'}{(2\pi)^2}\left[\boldsymbol{l}'\cdot(\boldsymbol{l}-\boldsymbol{l}')\right]^2 C_{l'}^{TT}C_{|\boldsymbol{l}-\boldsymbol{l}'|}^{\phi\phi} \tag{3.180}$$

A comparison between the lensed and unlensed temperature power spectrum is shown in Fig. 3.13.

The power spectrum of the lensing potential is given by

$$C_l^{\phi\phi} = 16\pi\int \mathrm{d}\ln k\Delta_{\mathcal{R}}^2(k)\left[\int_0^{\chi_*}\mathrm{d}\chi\ T_\phi(\chi)j_l(k\chi)\frac{\chi_*-\chi}{\chi\chi_*}\right]^2\,. \tag{3.181}$$

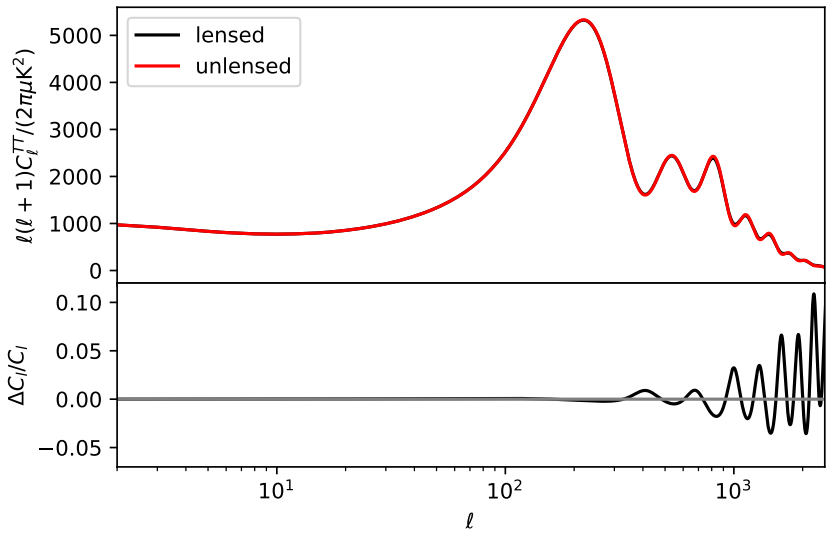

Figure 3.13.: Effect of lensing on the temperature power spectrum. The lensed power spectrum (black) has slightly smoother peaks than the unlensed, primordial power spectrum (red). The differences are sizeable, at the 10%-level on small scales (high l).

3.4.2. Lensing Reconstruction

The gravitational lensing of the CMB can be used to infer the projected gravitational potential or deflection potential between us and the surface of last scattering. Let us consider the quadratic estimator

$$\hat{\phi}(\boldsymbol{l}) = A \int \frac{\mathrm{d}^2\boldsymbol{l}'}{(2\pi)^2} \tilde{\Theta}(\boldsymbol{l}')\tilde{\Theta}(\boldsymbol{l}-\boldsymbol{l}')g(\boldsymbol{l}',\boldsymbol{l})\,. \tag{3.182}$$

We can now calculate the expectation value over short temperature fluctuations

$$\begin{aligned}
\left\langle \hat{\phi}(\boldsymbol{l}) \right\rangle =& A \int \frac{\mathrm{d}^2\boldsymbol{l}'}{(2\pi)^2} \left\langle \delta\Theta(\boldsymbol{l}')\Theta(\boldsymbol{l}-\boldsymbol{l}') + \Theta(\boldsymbol{l}')\delta\Theta(\boldsymbol{l}-\boldsymbol{l}') \right\rangle g(\boldsymbol{l}',\boldsymbol{l}-\boldsymbol{l}') \\
=& A \int \frac{\mathrm{d}^2\boldsymbol{l}'}{(2\pi)^2} \int \frac{\mathrm{d}^2\boldsymbol{l}''}{(2\pi)^2} \boldsymbol{l}''\cdot(\boldsymbol{l}'-\boldsymbol{l}'') \left\langle \Theta(\boldsymbol{l}'')\phi(\boldsymbol{l}'-\boldsymbol{l}'')\Theta(\boldsymbol{l}-\boldsymbol{l}') \right\rangle g(\boldsymbol{l}',\boldsymbol{l}) \\
&+ A \int \frac{\mathrm{d}^2\boldsymbol{l}'}{(2\pi)^2} \int \frac{\mathrm{d}^2\boldsymbol{l}''}{(2\pi)^2} \boldsymbol{l}''\cdot(\boldsymbol{l}-\boldsymbol{l}'-\boldsymbol{l}'') \left\langle \Theta(\boldsymbol{l}')\phi(\boldsymbol{l}-\boldsymbol{l}'-\boldsymbol{l}'')\Theta(\boldsymbol{l}'') \right\rangle g(\boldsymbol{l}',\boldsymbol{l}) \\
=& A\phi(\boldsymbol{l}) \int \frac{\mathrm{d}^2\boldsymbol{l}'}{(2\pi)^2} \Big\{ (\boldsymbol{l}'-\boldsymbol{l})\cdot\boldsymbol{l} C_{|\boldsymbol{l}-\boldsymbol{l}'|} + \boldsymbol{l}'\cdot\boldsymbol{l} C_{l'} \Big\} g(\boldsymbol{l}',\boldsymbol{l})
\end{aligned} \tag{3.183}$$

Requiring the estimator to be unbiased $\left\langle \hat{\phi}(\boldsymbol{l}) \right\rangle = \phi(\boldsymbol{l})$ yields

$$A^{-1} = \int \frac{\mathrm{d}^2\boldsymbol{l}'}{(2\pi)^2} \Big\{ (\boldsymbol{l}'-\boldsymbol{l})\cdot\boldsymbol{l} C_{|\boldsymbol{l}-\boldsymbol{l}'|} + \boldsymbol{l}'\cdot\boldsymbol{l} C_{l'} \Big\} g(\boldsymbol{l}',\boldsymbol{l})\,. \tag{3.184}$$

The weight function g can be chosen by requiring the estimator to be minimum variance

$$\left\langle \hat{\phi}(\boldsymbol{l})\hat{\phi}(\boldsymbol{l}') \right\rangle = (2\pi)^2\delta^{(\mathrm{D})}(\boldsymbol{l}+\boldsymbol{l}')\; 2A^2 \int \frac{\mathrm{d}^2 l'}{(2\pi)^2} C_{l'}^{TT} C_{|\boldsymbol{l}-\boldsymbol{l}'|}^{TT} g^2(\boldsymbol{l}',\boldsymbol{l}-\boldsymbol{l}') \tag{3.185}$$

leading to

$$g(\boldsymbol{l}',\boldsymbol{l}) = \frac{(\boldsymbol{l}'-\boldsymbol{l})\cdot\boldsymbol{l} C_{|\boldsymbol{l}-\boldsymbol{l}'|} + \boldsymbol{l}'\cdot\boldsymbol{l} C_{l'}}{2 C_{l'}^{TT} C_{|\boldsymbol{l}-\boldsymbol{l}'|}^{TT}}\,. \tag{3.186}$$

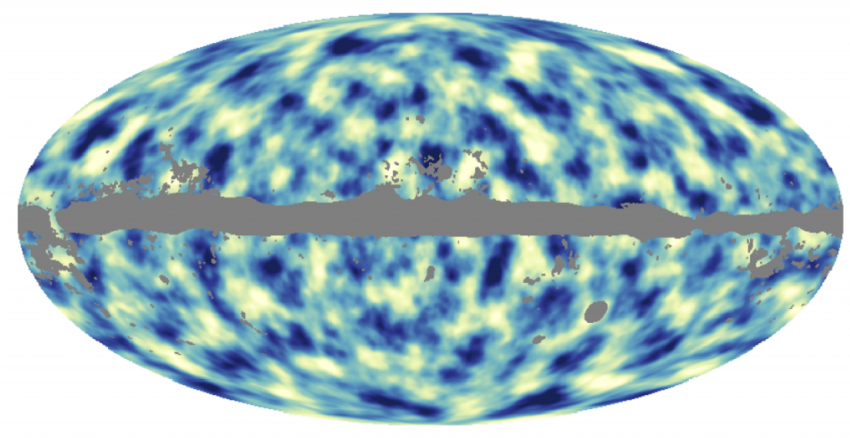

Figure 3.14.: Reconstructed lensing potential from Planck [Aghanim et al., 2018].

A map of the reconstructed lensing potential from Planck is shown in Fig. 3.14. As shown in the bottom panel of Fig. 3.15, this prediction is in very good agreement with the lensing potential power spectrum extracted from the map.

3.4.3. Lensing B-Modes

Let us now see how B-modes can be generated from primordial E-modes through gravitational lensing. We will discuss the case in which there are no primordial B-modes. Introducing the composite vector of temperature and polarizaion $\boldsymbol{W} = (T, Q, U)$ we can generalize Eq. (3.175) to

$$\tilde{\boldsymbol{W}}(\hat{\boldsymbol{n}}) = \boldsymbol{W}(\boldsymbol{n} + \boldsymbol{\alpha}) \approx \boldsymbol{W}(\hat{\boldsymbol{n}}) + \boldsymbol{\alpha} \cdot \boldsymbol{\nabla} \boldsymbol{W}(\hat{\boldsymbol{n}}) \,. \tag{3.187}$$

In the absence of primordial B modes we have from Eq. (3.141) that $Q = 2E(\boldsymbol{l}) \cos(2\varphi_{\boldsymbol{l}})$ and $U = -2E(\boldsymbol{l}) \sin(2\varphi_{\boldsymbol{l}})$. We can express the gradients of Q and U in Fourier space

$$\begin{aligned} \boldsymbol{\nabla}_{\hat{\boldsymbol{n}}} Q =& 2\mathrm{i} \int \frac{\mathrm{d}^2 \boldsymbol{l}}{(2\pi)^2} E(\boldsymbol{l}) \cos(2\varphi_{\boldsymbol{l}}) \boldsymbol{l} e^{\mathrm{i}\boldsymbol{l}\cdot\hat{\boldsymbol{n}}} \\ \boldsymbol{\nabla}_{\hat{\boldsymbol{n}}} U =& -2\mathrm{i} \int \frac{\mathrm{d}^2 \boldsymbol{l}}{(2\pi)^2} E(\boldsymbol{l}) \sin(2\varphi_{\boldsymbol{l}}) \boldsymbol{l} e^{\mathrm{i}\boldsymbol{l}\cdot\hat{\boldsymbol{n}}} \end{aligned} \tag{3.188}$$

In analogy with Eq. (3.178) the deflected Q- and U-polarization is then given as a convolution of the deflection angle and the gradient of the bare polarization

$$\begin{aligned} \delta Q(\boldsymbol{l}) = [\boldsymbol{\nabla}\phi \star \boldsymbol{\nabla} Q](\boldsymbol{l}) =& -2 \int \frac{\mathrm{d}^2 \boldsymbol{l}'}{(2\pi)^2} \boldsymbol{l}' \cdot (\boldsymbol{l} - \boldsymbol{l}') E(\boldsymbol{l}') \phi(\boldsymbol{l} - \boldsymbol{l}') \cos(2\varphi_{\boldsymbol{l}'}) \,, \\ \delta U(\boldsymbol{l}) = [\boldsymbol{\nabla}\phi \star \boldsymbol{\nabla} U](\boldsymbol{l}) =& 2 \int \frac{\mathrm{d}^2 \boldsymbol{l}'}{(2\pi)^2} \boldsymbol{l}' \cdot (\boldsymbol{l} - \boldsymbol{l}') E(\boldsymbol{l}') \phi(\boldsymbol{l} - \boldsymbol{l}') \sin(2\varphi_{\boldsymbol{l}'}) \,. \end{aligned} \tag{3.189}$$

We can now use Eq. (3.140) to calculate the resulting B-mode

$$B(\boldsymbol{l}) = \frac{1}{2} \left[-\sin(2\phi_{\boldsymbol{l}}) \delta Q(\boldsymbol{l}) + \cos(2\phi_{\boldsymbol{l}}) \delta U(\boldsymbol{l}) \right] = \int \frac{\mathrm{d}^2 \boldsymbol{l}'}{(2\pi)^2} \boldsymbol{l}' \cdot (\boldsymbol{l} - \boldsymbol{l}') \boldsymbol{E}(\boldsymbol{l}') \phi(\boldsymbol{l} - \boldsymbol{l}') \sin\left[2(\varphi_{\boldsymbol{l}'} - \varphi_{\boldsymbol{l}})\right] \,. \tag{3.190}$$

The angular power spectrum of the lensing induced B-modes is then given by

$$C_l^{BB} = \int \frac{\mathrm{d}^2 \boldsymbol{l}'}{(2\pi)^2} \left[\boldsymbol{l}' \cdot (\boldsymbol{l} - \boldsymbol{l}')\right]^2 C_{l'}^{EE} C_{|\boldsymbol{l} - \boldsymbol{l}'|}^{\phi\phi} \sin^2\left[2(\varphi_{\boldsymbol{l}'} - \varphi_{\boldsymbol{l}})\right] \,. \tag{3.191}$$

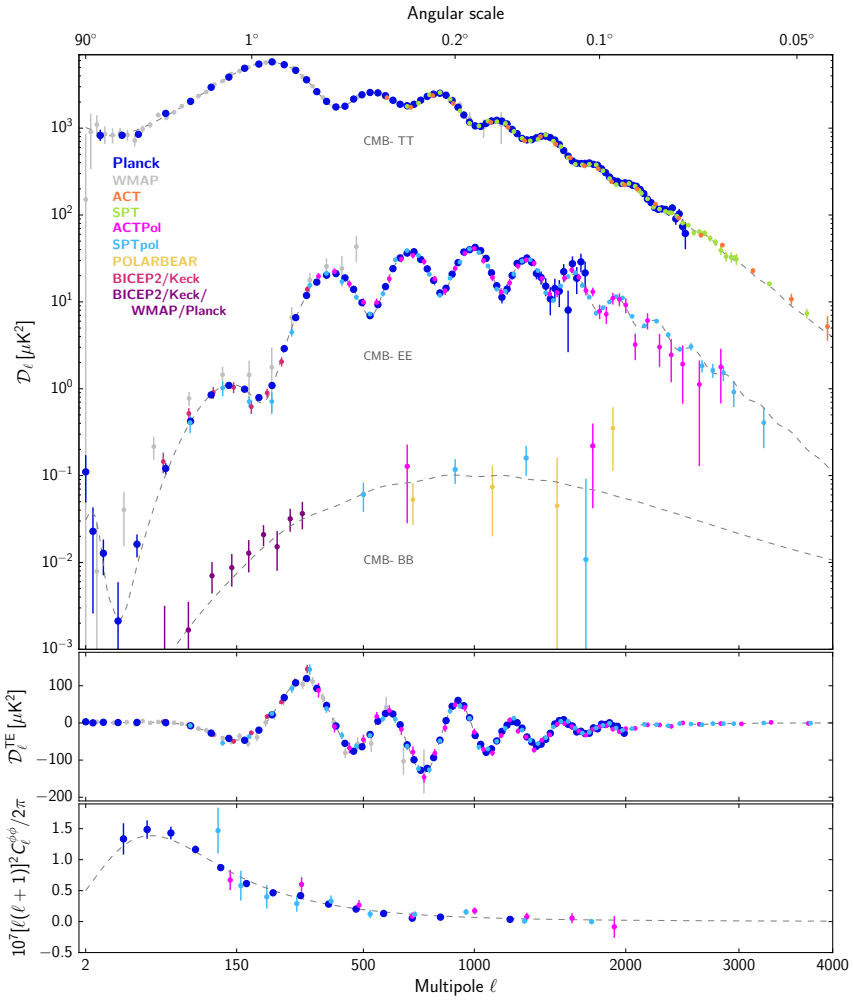

Figure 3.15.: Measured angular power spectra of the CMB radiation $C_l^{TT}, C_l^{EE}, C_l^{BB}$ (upper panel), C_l^{TE} (center panel) and the lensing potential $C_l^{\phi\phi}$ (bottom panel). Note that the B-modes detected here are compatible with lensing B modes only and that there is no evidence yet for primordial B-modes.

The lensing B-modes can be removed in a procedure called **delensing**

$$B_{\rm del} = B_{\rm obs} - \hat{B}\,. \tag{3.192}$$

3.5. Summary

- Before recombination baryons and photons are tightly coupled. The calculation of CMB perturbations requires us to calculate the temperature monopole and the electron velocity, which is related to the temperature dipole.
- Polarization can be decomposed into two components with opposite parity E and B.
- Magnetic or B-modes do not correlate with temperature or electric modes and are not directly produced from scalar fluctuations, but can be generated by lensing.
- Polarization from scalar fluctuations is only produced from a incident quadrupole, which is suppressed during tight-coupling.

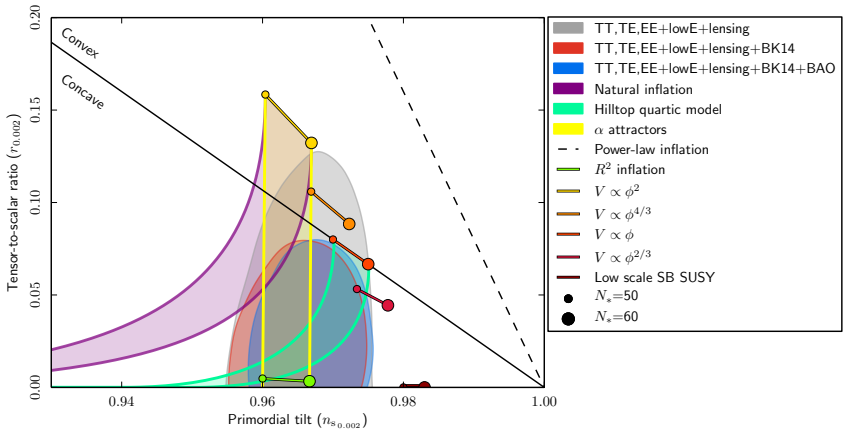

Figure 3.16.: CMB-constraints on the $n_s - r$-plane from Planck/BICEP and predictions of inflationary models. The measurements are starting to rule out the simplest inflationary models, such as ϕ^2-inflation.

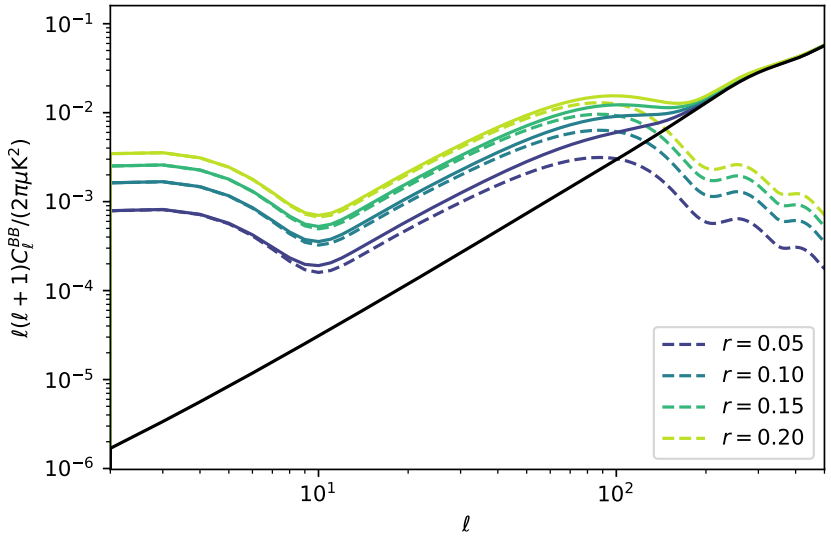

Figure 3.17.: Angular power spectrum of B-modes for various scalar-to-tensor ratios r with and without the lensing induced B-modes. For high multipoles the B-modes generated by lensed E-modes (black solid) are dominant, leaving a small window at $l < 200$ where the primoridal B-modes could be seen in isolation.

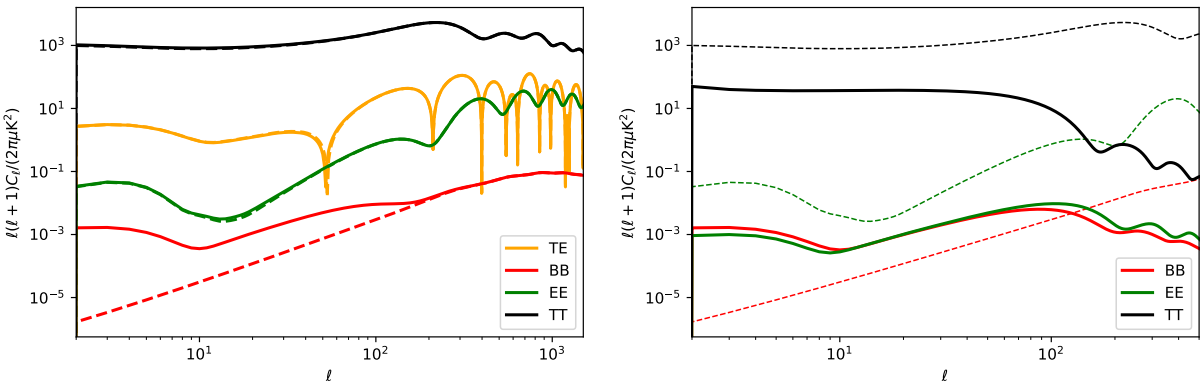

Figure 3.18.: *Left panel:* Angular power spectra of T, E and B modes calculated using CAMB. *Right panel:* Tensor (thick solid) and scalar (dashed) contributions to the T, E and B power spectra.

4. Primordial non-Gaussianity

This part of the course was taught by Dr. E. Pajer in Lent 2021, and his notes contain the relevant material for the exam. This Chapter is provided for the sake of completeness of these notes and as a reference for the interested reader.

So far you have been mostly focusing on Gaussian fluctuations generated in vanilla single-field slow-roll inflation and their linear evolution. In this part of the course we will go beyond the simplest inflationary models and understand to what extend primordial non-Gaussianity can teach us about the physics of inflation. Even in absence of primordial non-Gaussianities, there is a multitude of effects that can generate non-Gaussian features in the CMB and in Large-Scale Structure (LSS). For instance, the gravitational lensing effect of the CMB leads to a substantial non-Gaussian signal that exceeds the current constraints on local non-Gaussianity. At very late times, gravitational evolution becomes non-linear and the relation between the matter density and observables can introduce additional non-Gaussianities. The latter two topics will be subject of the last part of this course.

Useful resources for this chapter are the review *Primordial Non-Gaussianities from Inflation Models* by Xingang Chen [Chen, 2010] and the seminal paper *Non-Gaussian features of primordial fluctuations in single field inflationary models* by Juan Maldacena [Maldacena, 2003]. Additional pedagogical material on primordial non-Gaussianity can be found in Eugene Lim's lecture notes on Advanced Cosmology[1] as well as Daniel Baumann's lecture notes on the Physics of Inflation.[2]

4.1. Local non-Gaussianity and the Shape Function

4.1.1. Local Ansatz

As we discussed before in Sec. 1.4.4, a simple way to introduce non-Gaussianity, i.e., a non-vanishing bispectrum, is to consider powers of a Gaussian field. Based on the Gaussian curvature perturbation $\mathcal{R}_{\rm G}$, a phenomenological ansatz for non-Gaussianity, the **local template**, was introduced by Komatsu & Spergel [Komatsu and Spergel, 2001]

$$\mathcal{R}(\boldsymbol{x}) = \mathcal{R}_{\rm G}(\boldsymbol{x}) + \frac{3}{5} f_{\rm NL,loc} \left[\mathcal{R}^2_{\rm G}(\boldsymbol{x}) - \left\langle \mathcal{R}^2_{\rm G} \right\rangle\right] . \tag{4.1}$$

The factor of 3/5 has historical reasons, as this model was first written down in terms of the Newtonian gauge metric perturbation for which in matter dominance $\Phi = -\frac{3}{5}\mathcal{R}$. The subtraction of the variance $\langle \mathcal{R}^2 \rangle$ ensures a mean zero field. In Fourier space the square of the fields leads to a convolution

$$\mathcal{R}(\boldsymbol{k}) = \mathcal{R}_{\rm G}(\boldsymbol{k}) + \frac{3}{5} f_{\rm NL,loc} \int \frac{{\rm d}^3 q}{(2\pi)^3} \mathcal{R}_{\rm G}(\boldsymbol{q}) \mathcal{R}_{\rm G}(\boldsymbol{k}-\boldsymbol{q}) . \tag{4.2}$$

The correlator of three Fourier modes is thus given by

$$\langle \mathcal{R}(\boldsymbol{k}_1)\mathcal{R}(\boldsymbol{k}_2)\mathcal{R}(\boldsymbol{k}_3)\rangle = (2\pi)^3 \delta^{(\rm D)}(\boldsymbol{k}_1+\boldsymbol{k}_2+\boldsymbol{k}_3)\, \frac{6}{5} f_{\rm NL,loc} \left[P_{\mathcal{R}}(k_1)P_{\mathcal{R}}(k_2) + P_{\mathcal{R}}(k_2)P_{\mathcal{R}}(k_3) + P_{\mathcal{R}}(k_3)P_{\mathcal{R}}(k_1)\right] , \tag{4.3}$$

where we used

$$\langle \mathcal{R}_{\rm G}(\boldsymbol{k}) \mathcal{R}_{\rm G}(\boldsymbol{k}')\rangle = (2\pi)^3 \delta^{(\rm D)}(\boldsymbol{k}+\boldsymbol{k}') P_{\mathcal{R}}(\boldsymbol{k}) . \tag{4.4}$$

[1] `http://www.damtp.cam.ac.uk/user/eal40/AdvCos/lecture2.pdf`
[2] Chapter 5 of `http://www.damtp.cam.ac.uk/user/db275/TEACHING/INFLATION/Lectures.pdf`

This allows us to identify

$$B_{\mathcal{R}}(k_1,k_2,k_3) = \frac{6}{5} f_{\rm NL,loc}\left[P_{\mathcal{R}}(k_1)P_{\mathcal{R}}(k_2) + P_{\mathcal{R}}(k_2)P_{\mathcal{R}}(k_3) + P_{\mathcal{R}}(k_3)P_{\mathcal{R}}(k_1)\right]. \tag{4.5}$$

One often factors out the dimensionless power spectrum $\Delta^2_{\mathcal{R}} = k^3 P_{\mathcal{R}}/(2\pi^2) \propto k^0$ to obtain

$$B = \frac{6}{5} f_{\rm NL,loc} \frac{(2\pi^2\Delta^2_{\mathcal{R}})^2}{(k_1k_2k_3)^2}\left(\frac{k_3^2}{k_1k_2} + \frac{k_1^2}{k_2k_3} + \frac{k_2^2}{k_3k_1}\right). \tag{4.6}$$

4.1.2. Shape Functions

The **shape function** can be defined as

$$S(k_1,k_2,k_3) = \frac{(k_1k_2k_3)^2}{(2\pi^2\Delta^2_{\mathcal{R}})^2} B(k_1,k_2,k_3) \tag{4.7}$$

The amplitude of non-Gaussianities is defined in the equilateral configuration ($k_1 = k_2 = k_3 = k$)

$$f_{\rm NL} := \frac{5}{18} S(k,k,k). \tag{4.8}$$

Other definitions of the shape function don't include the amplitude and rather normalize as $\tilde{S}(k,k,k) = 1$. The **shape** is now characterised as the behaviour of S under changes of $x_2 = k_2/k_1$ and $x_3 = k_3/k_1$ at fixed $K = k_1 + k_2 + k_3$. To avoid degeneracies we can set $0 < x_3 < x_2 < 1$. Then the triangle inequality furthermore restricts x_3 to $1-x_2 < x_3 < x_2$ and x_2 to $x_2 > 0.5$. We show some of the most relevant shapes in Fig. 4.1. Bispectra and their corresponding shape functions can be calculated from theoretical models of the early Universe (such as inflation), as we will do later on in this Chapter. On the other hand, the amplitude of a given shape can be constrained from the data, for instance in the CMB or in LSS. For obtaining constraints, it is often useful to approximate theoretical shapes by simpler, separable templates and to constrain the amplitude of these templates. Working with templates has the additional advantage that instead of constraining the infinite space of models one can put constraints on some important templates. Theorists can subsequently assess the viability of their models by projecting the full model bispectrum on the template. The **running** describes how the bispectrum changes under changes of the total momentum K at fixed shape, i.e., x_2=const. and x_3=const.

The shape function for local non-Gaussianity is given by

$$S_{\rm loc}(k_1,k_2,k_3) = \frac{6}{5} f_{\rm NL,loc}\left(\frac{k_3^2}{k_1k_2} + \frac{k_1^2}{k_2k_3} + \frac{k_2^2}{k_3k_1}\right) \tag{4.9}$$

and indeed

$$S_{\rm loc}(k,k,k) = \frac{18}{5} f_{\rm NL,loc} \tag{4.10}$$

A configuration of particular importance when considering local non-Gaussianities is the **squeezed limit**, where one wavenumber is much smaller than the other two ($k_1 \ll k_2 \sim k_3$), i.e., two of the wavevectors are almost perfectly counteraligned

$$\lim_{k_1\ll k_2\sim k_3} S_{\rm loc} = \frac{12}{5}\frac{k_{2,3}}{k_1} f_{\rm NL,loc}. \tag{4.11}$$

Non-Gaussianity with a strong **squeezed limit** cannot arise in single field inflation, independent of the details of the inflationary action.[3] This shape is generally produced outside the horizon. As we will discuss in much more detail later, single field inflation generates local non-Gaussianity of amplitude $f_{\rm NL} \approx \epsilon$. Planck constrained the amplitude of local non-Gaussianity from the CMB to be[4] $f_{\rm NL,loc} = 0.8 \pm 5.0$.

[3] Creminelli & Zaldarriaga 2004 `https://arxiv.org/abs/astro-ph/0407059` [Creminelli and Zaldarriaga, 2004]
[4] Planck 2015: Constraints on primordial non-Gaussianity `https://arxiv.org/abs/1502.01592` [Ade et al., 2016]

One can define a **scalar product of shapes** with a weight function $w(k_1, k_2, k_3)$ as

$$S_1 \cdot S_2 = \int \mathrm{d}k_1 \int \mathrm{d}k_2 \int \mathrm{d}k_3 \; S_1(k_1, k_2, k_3) S_2(k_1, k_2, k_3) w(k_1, k_2, k_3) \,, \tag{4.12}$$

where the integration is restricted to valid triangular configurations and a **shape correlation** as

$$C(S_1, S_2) = \frac{S_1 \cdot S_2}{\sqrt{S_1 \cdot S_1 \; S_2 \cdot S_2}}. \tag{4.13}$$

The weight can be chosen appropriately for various applications, usually one would choose the inverse variance of bispectrum measurements $w^{-1} \propto \Delta B^2 \propto P^3$. The shape correlator tells us how similar two shapes are. If they are very correlated, looking for one in the data will also picking up signal on the other. On the other hand, if we have two uncorrelated shapes, looking for one type of non-Gaussianity will not pick up any non-Gaussian signal proportional to the other shape.

4.1.3. Bispectrum Estimation

The primordial bispectrum signal is way too weak to be measurable at a mode-by-mode basis. We thus need to come up with an estimator that combines the available information from all possible bispectrum configurations in an optimal way. The way to achieve this goal is to devise an optimal (minimum variance, unbiased) estimator for the amplitude f_{NL} of a particular bispectrum shape $B_{\mathrm{theo}} = f_{\mathrm{NL}} B_{\mathrm{theo}}^{f_{\mathrm{NL}}=1}$ given the data. Under the assumption of Gaussian distributed bispectrum amplitudes, maximizing the likelihood is equivalent to minimizing the χ^2

$$\chi^2 = \sum_k \frac{\left(\hat{B} - f_{\mathrm{NL}} B_{\mathrm{theo}}^{f_{\mathrm{NL}}=1}\right)^2}{\Delta \hat{B}^2} \,, \tag{4.14}$$

where $\Delta \hat{B}^2$ is the variance of the bispectrum measurement. Here the sum runs over all valid bispectrum configurations, i.e., configurations that satisfy the triangle inequality $|k_1 - k_2| < k_2 < k_1 + k_2$. Maximizing the likelihood leads to the estimator

$$\hat{f}_{\mathrm{NL}} = \sum_k \frac{\hat{B} B_{\mathrm{theo}}^{f_{\mathrm{NL}}=1}}{\Delta \hat{B}^2} \left(\sum_k \frac{\left(B_{\mathrm{theo}}^{f_{\mathrm{NL}}=1}\right)^2}{\Delta \hat{B}^2} \right)^{-1} = \frac{\hat{B} \cdot B_{\mathrm{theo}}^{f_{\mathrm{NL}}=1}}{B_{\mathrm{theo}}^{f_{\mathrm{NL}}=1} \cdot B_{\mathrm{theo}}^{f_{\mathrm{NL}}=1}} \tag{4.15}$$

We can see that this is a projection of the measured bispectrum on the theoretical template. We can write down a equivalent Gaussian likelihood for the CMB bispectrum using relations from Sec. 1.8. We can make the expression explicit by writing the variance of the bispectrum estimator as $\left\langle \mathcal{G}^2 b^2 \right\rangle \sim \left\langle a^6 \right\rangle \sim C_l^3$.

$$\chi^2 = \sum_{l,m} \frac{\left(a_{l_1 m_1} a_{l_2 m_2} a_{l_3 m_3} - f_{\mathrm{NL}} \mathcal{G}_{l_1 l_2 l_3}^{m_1 m_2 m_3} b_{l_1 l_2 l_3}^{f_{\mathrm{NL}}=1}\right)^2}{C_{l_1} C_{l_2} C_{l_3}} \tag{4.16}$$

We finally obtain the cubic estimator for CMB non-Gaussianities

$$\hat{f}_{\mathrm{NL}} = \left(\sum_{l,m} \frac{\left(\mathcal{G}_{l_1 l_2 l_3}^{m_1 m_2 m_3} b_{l_1 l_2 l_3}^{f_{\mathrm{NL}}=1}\right)^2}{C_{l_1} C_{l_2} C_{l_3}} \right)^{-1} \sum_{l,m} \frac{\mathcal{G}_{l_1 l_2 l_3}^{m_1 m_2 m_3} b_{l_1 l_2 l_3}^{f_{\mathrm{NL}}=1}}{C_{l_1} C_{l_2} C_{l_3}} a_{l_1 m_1} a_{l_2 m_2} a_{l_3 m_3} \,. \tag{4.17}$$

The assumption of bispectrum amplitudes being Gaussian distributed might seem a bit suspicious to the critical reader. More appropriately, one should have started by using the Edgeworth expansion of the Gaussian PDF for the spherical multipole coefficients

$$\begin{aligned} \mathbb{P}(a_{lm}|f_{\mathrm{NL}}) = & \left\{ 1 + f_{NL} \sum_{l,m} \mathcal{G}_{l_1 l_2 l_3}^{m_1 m_2 m_3} b_{l_1 l_2 l_3}^{f_{\mathrm{NL}}=1} \left[\frac{a_{l_1 m_1}}{C_{l_1}} \frac{a_{l_2 m_2}}{C_{l_2}} \frac{a_{l_3 m_3}}{C_{l_3}} - \left(\frac{a_{l_1 m_1} \delta_{l_2 l_3}^{(\mathrm{K})}}{C_{l_1} C_{l_2}} + 2 \text{ perm.} \right) \right] \right\} \\ & \times \frac{1}{\sqrt{(2\pi)^N C}} \exp\left[-\frac{1}{2} \frac{a_{lm} a_{lm}^*}{C_l} \right]. \end{aligned} \tag{4.18}$$

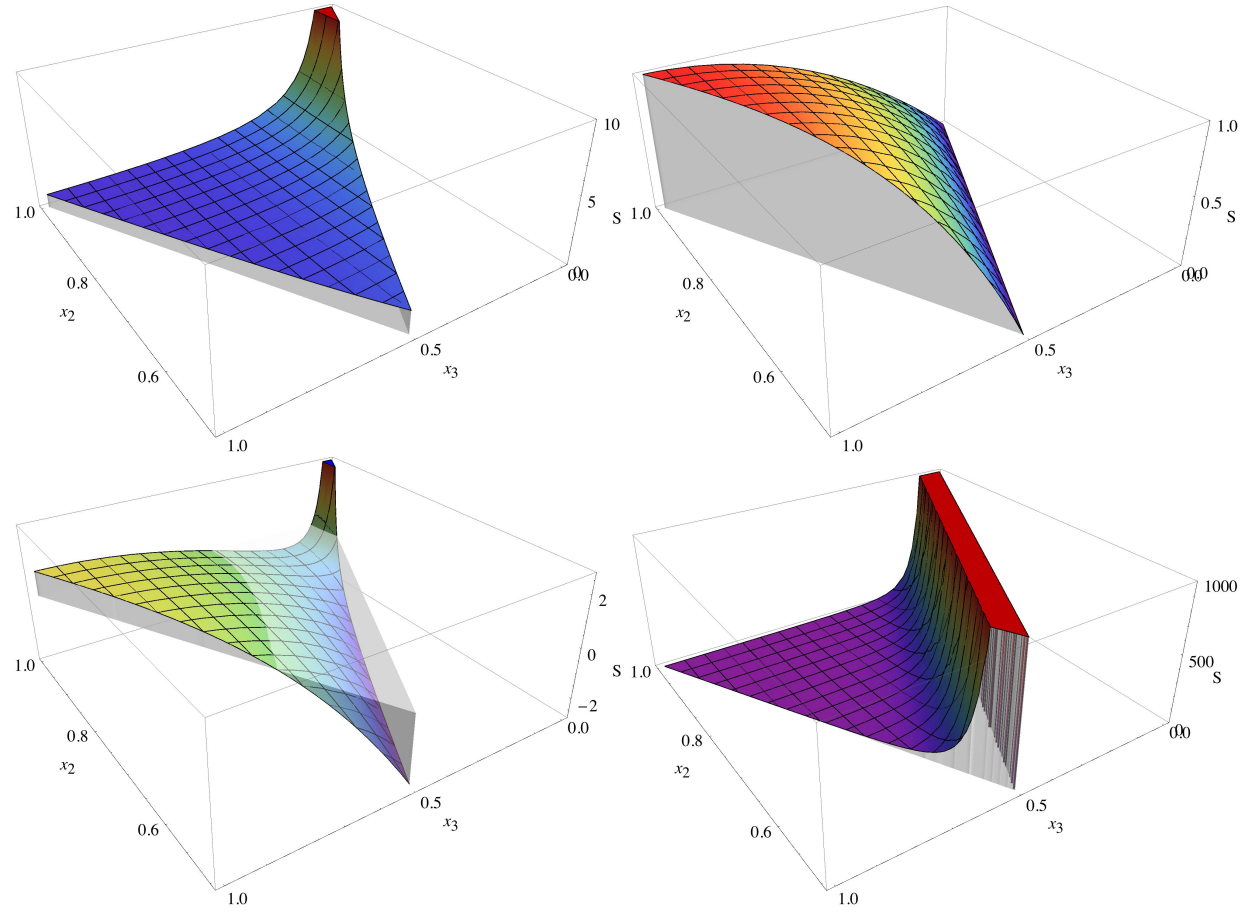

Figure 4.1.: Shape functions of the primordial bispectra. *Top left:* Local *Top right:* Equilateral *Bottom left:* Orthogonal *Bottom right:* Folded

In case of rotational invariance, the Gaunt integral reduces the linear term to the (vanishing) monopole and maximizing the likelihood reproduces Eq. (4.17).[5]

4.1.4. Other shapes

Another form of non-Gaussianity, described by the **equilateral template**

$$\tilde{S}_{\text{equi}}(k_1, k_2, k_3) = \left(\frac{k_1}{k_2} + 5 \text{ perms.}\right) - \left(\frac{k_1^2}{k_2 k_3} + 2 \text{ cyc.}\right) - 2 \tag{4.19}$$

peaks when all sides are equal. This shape is generated when all modes are equal and inside the horizon, for instance from non-standard kinetic terms like higher derivative interactions. The best constraint from Planck is $f_{\text{NL,equi}} = -4 \pm 43$.

The **orthogonal template** [Senatore et al., 2010] is defined to be roughly orthogonal to both the local and

[5] For more details see M. Liguori et al. *Primordial non-Gaussianity and Bispectrum Measurements in the Cosmic Microwave Background and Large-Scale Structure* `https://arxiv.org/abs/1001.4707` [Liguori et al., 2010]

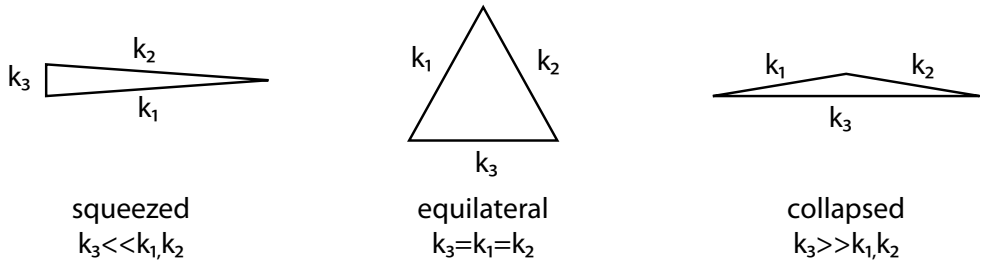

Figure 4.2.: Dominant triangle configurations of the local (squeezed), equilateral and folded non-Gaussianities.

equilateral template[6]

$$\tilde{S}_{\rm orth}(k_1,k_2,k_3) = 3\left(\frac{k_1}{k_2} + 5 \text{ perm.}\right) - 3\left(\frac{k_1^2}{k_2 k_3} + 2 \text{ cyc.}\right) - 8\,, \tag{4.21}$$

where orthogonality is defined using the shape correlator defined in Eq. (4.12). Planck constrained its amplitude to be $f_{\rm NL,orth} = -26 \pm 21$. Yet another shape is the folded shape

$$\tilde{S}_{\rm fold}(k_1,k_2,k_3) = \frac{1}{3}\left(\frac{1}{(k_1+k_2-k_3)^3} + 2 \text{ cyc.}\right)\,, \tag{4.22}$$

which peaks for $k_1 + k_2 \sim k_3$ and can arise from modifications of the inflationary Bunch-Davies vacuum state.

Other shapes can be defined for models with steps or resonant features in the potential but they are in general not scale invariant. We will not be able to cover these shapes and their underlying inflationary models but refer the interested reader to [Chen, 2010].

4.2. In-In Formalism

Having introduced the statistical tools that describe the shape and amplitude of non-Gaussianities and allow to quantify their strength in the data let us now consider how non-Gaussianities can be generated from first principles in the context of inflation. We will first need to introduce some calculational tools that allow us to go beyond the two-point function discussed in the cosmology course last term. Once we have this machinery in place we will first show that the amount of non-Gaussianity produced by canonical single-field, slow-roll inflation is vanishingly small. Having established this fact, we will then consider modifications of the assumptions of canonical inflation and consider the consequences on the three point function.

Primordial non-Gaussianities can be generated from:

- quantum mechanical effects during inflation at or before horizon exit
- classical non-linear evolution or interactions can generate non-Gaussianities after horizon exit

We will focus on the quantum non-Gaussianities first. The program for the next few lectures will be as follows:

1. How do we evaluate inflationary correlators in presence of interactions? - in-in-formalism
2. Calculation of the interaction Hamiltonian - cubic action

[6] This is the form that you will find in the Planck papers [Ade et al., 2016] and that was introduced in [Senatore et al., 2010]. A truly orthogonal template is defined in [Chen, 2010]

$$\tilde{S}_{\rm orth}(k_1,k_2,k_3) = -3.84\left(\frac{k_1^2}{k_2 k_3} + 2 \text{ cyc.}\right) + 3.94\left(\frac{k_1}{k_2} + 5 \text{ perm.}\right) - 11.1\,. \tag{4.20}$$

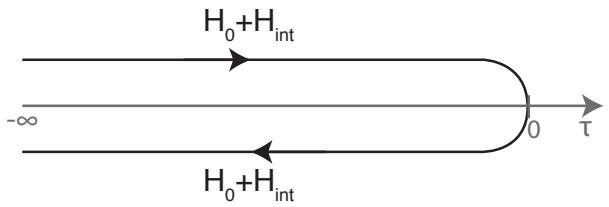

Figure 4.3.: The integration contour of the in-in formalism goes from $\tau = -\infty(1 + \mathrm{i}\varepsilon)$ to the end of inflation at $\tau = 0$ and then back to $\tau = -\infty(1 - \mathrm{i}\varepsilon)$.

3. Non-Gaussianities in slow roll, single field - combination of 1. and 2.
4. Non-Gaussianities in alternative models - extensions of 2., then again 1.

In particle physics applications of QFT we commonly calculate the transition probability or S-matrix between asymptotically free $|\mathrm{in}\rangle$ states in the far past and asymptotically free $|\mathrm{out}\rangle$ states in the far future

$$\langle \mathrm{out}|S|\mathrm{in}\rangle \,. \tag{4.23}$$

It makes sense to impose asymptotic conditions at very early and very late times, when the interacting particles are far away from the interaction zone. These asymptotic states are vacuum eigenstates of the non-interacting theory and the free Hamiltonian H_0. The interactions H_{int} are restricted to the interaction region.

In cosmology, our boundary conditions are given by the Bunch-Davies vacuum, the free vacuum in Minkowski space which is defined at asymptotically early times when the wavelength of fluctuations is much smaller than the horizon. The goal is to calculate expectation values of products of operators at a fixed time. More specifically, we want to calculate n-point functions of cosmological fields such as $\mathcal{R}, h^{\times}$ or h^{+}. We will collectively refer to them as ϕ and write $Q = \delta\phi_{\boldsymbol{k}_1}\delta\phi_{\boldsymbol{k}_2}\ldots\phi_{\boldsymbol{k}_n}$. As our know vacuum states are defined at asymptotically early times, we will need to calculate expectation values of operators at time t with $|\mathrm{in}\rangle$ vacuum states

$$\langle Q\rangle = \langle \mathrm{in}|Q(t)|\mathrm{in}\rangle \,. \tag{4.24}$$

The $|\mathrm{in}\rangle$ state is the vacuum of the interacting theory at an asymptotocally early time and t is the time at which we evaluate the correlator, for instance the end of inflation or horizon crossing. As shown in Fig. 4.3, evaluating this correlator will require us to evolve the operator Q from the beginning to the end of inflation (and back) in the interacting theory. As in QFT, we will consider the full time evolution under the free Hamiltonian and consider the corrections arising from the interacting part of the Hamiltonian perturbatively.

The Hamiltonian has three parts, the background part H_{b} describing the "classical" evolution of the inflaton, the quadratic part H_0 describing the linear equations of motion of the fluctuations and finally a cubic part H_{int} that describes the interactions

$$H = H_{\mathrm{b}} + \tilde{H} = H_{\mathrm{b}} + H_0 + H_{\mathrm{int}} \,. \tag{4.25}$$

The formalism we will describe now was laid out by Steven Weinberg.[7]

The field ϕ and its conjugate momentum $\pi = \partial L/\partial\dot{\phi}$ are perturbed around the background

$$\phi(\boldsymbol{x}, t) = \bar{\phi}(t) + \delta\phi(\boldsymbol{x}, t) \tag{4.26}$$
$$\pi(\boldsymbol{x}, t) = \bar{\pi}(t) + \delta\pi(\boldsymbol{x}, t) \tag{4.27}$$

and satisfy the **canonical commutation relation**

$$[\delta\phi(\boldsymbol{x}, t), \delta\pi(\boldsymbol{y}, t)] = \mathrm{i}\delta(\boldsymbol{x} - \boldsymbol{y}) \,. \tag{4.28}$$

[7] S. Weinberg *Quantum Contributions to Cosmological Correlations* https://arxiv.org/abs/hep-th/0506236 [Weinberg, 2005]

The background fields are evolved under the background Hamiltonian H_b

$$\dot{\bar{\phi}}(t) = \frac{\partial \mathcal{H}_\mathrm{b}}{\partial \bar{\pi}} \qquad\qquad \dot{\bar{\pi}}(t) = -\frac{\partial \mathcal{H}_\mathrm{b}}{\partial \bar{\phi}}\,, \tag{4.29}$$

where $H = \int \mathrm{d}^3x\ \mathcal{H}$. H_0 is the quadratic Hamiltonian leading to linear equations of motion and H_int containts the interactions. It starts at third order and leads to quadratic and higher order equations of motion.

We can expand the Hamiltonian as

$$H = H_\mathrm{b} + \frac{\delta H}{\delta \bar{\phi}}\delta\phi + \frac{\delta H}{\delta \bar{\pi}}\delta\pi + \tilde{H}, \tag{4.30}$$

where we have included all terms that are second order and higher into $\tilde{H}$

$$\begin{aligned}
\dot{\bar{\phi}} + \dot{\delta\phi} =& \mathrm{i}\left[\bar{H} + \frac{\delta H}{\delta \bar{\phi}}\delta\phi + \frac{\delta H}{\delta \bar{\pi}}\delta\pi + \tilde{H}, \bar{\phi} + \delta\phi\right] \\
=& \mathrm{i}\left[\frac{\delta H}{\delta \bar{\phi}}\delta\phi + \frac{\delta H}{\delta \bar{\pi}}\delta\pi + \tilde{H}, \delta\phi\right] \\
=& \mathrm{i}\left[\frac{\delta H}{\delta \bar{\pi}}\delta\pi + \tilde{H}, \delta\phi\right] \\
=& \dot{\bar{\phi}} + \mathrm{i}\left[\tilde{H}, \delta\phi\right]
\end{aligned} \tag{4.31}$$

Thus, the Heisenberg equations of motion for the perturbations are

$$\dot{\delta\phi}(\boldsymbol{x}, t) = \mathrm{i}\left[\tilde{H}[\delta\phi, \delta\pi; t], \delta\phi\right] \tag{4.32}$$

$$\dot{\delta\pi}(\boldsymbol{x}, t) = \mathrm{i}\left[\tilde{H}[\delta\phi, \delta\pi; t], \delta\pi\right] \tag{4.33}$$

The Heisenberg equations of motion can be solved using the unitary **time evolution operator** $U(t, t_\mathrm{i})$ obeying $U^\dagger(t, t_\mathrm{i})U(t, t_\mathrm{i}) = 1$

$$\delta\phi(\boldsymbol{x}, t) = U^{-1}(t, t_\mathrm{i})\delta\phi(\boldsymbol{x}, t_\mathrm{i})U(t, t_\mathrm{i})\,, \tag{4.34}$$

$$\delta\pi(\boldsymbol{x}, t) = U^{-1}(t, t_\mathrm{i})\delta\pi(\boldsymbol{x}, t_\mathrm{i})U(t, t_\mathrm{i})\,, \tag{4.35}$$

which satisfies the initial condition $U(t_\mathrm{i}, t_\mathrm{i}) = 1$. The time evolution operator satisfies

$$\frac{\mathrm{d}U(t, t_\mathrm{i})}{\mathrm{d}t} = -\mathrm{i}\tilde{H}[\delta\phi, \delta\pi; t]U(t, t_\mathrm{i}) \tag{4.36}$$

As you know from QFT this equation can be solved by

$$U(t, t_\mathrm{i}) = \mathrm{T}\exp\left[-\mathrm{i}\int_{t_\mathrm{i}}^{t} \mathrm{d}t'\ \tilde{H}(t')\right] \tag{4.37}$$

where T is the time ordering operator. This solution is not very practical due to the presence of interactions in $\tilde{H}$.

To overcome the presence of the interaction Hamiltonian in the time evolution, we are now introducing the **interaction picture** in which the time evolution of the fields $\delta\phi$ is determined by the free Hamiltonian and the action of the interaction Hamiltonian can be treated perturbatively through a power series. For that purpose, let us now split the Hamiltonian as

$$\tilde{H} = H_0 + H_\mathrm{int}\,, \tag{4.38}$$

where H_0 contains quadratic interactions leading to linear equations of motion and H_int starts at cubic order. We will now introduce interaction picture fields $\delta\phi^\mathrm{I}$ and $\delta\pi^\mathrm{I}$, which agree with the full theory fields at some initial time t_i. At this point we assume the fields to be in the Bunch-Davies vacuum state

$$\delta\phi^\mathrm{I}(\boldsymbol{x}, t_\mathrm{i}) = \delta\phi(\boldsymbol{x}, t_\mathrm{i})\,, \qquad\qquad \delta\pi^\mathrm{I}(\boldsymbol{x}, t_\mathrm{i}) = \delta\pi(\boldsymbol{x}, t_\mathrm{i})\,. \tag{4.39}$$

The interaction picture fields obey the Heisenberg equations of motion

$$\dot{\delta\phi^{\rm I}}(\boldsymbol{x},t) = {\rm i}\left[H_0[\delta\phi^{\rm I},\delta\pi^{\rm I};t],\delta\phi^{\rm I}\right] \tag{4.40}$$

$$\dot{\delta\pi^{\rm I}}(\boldsymbol{x},t) = {\rm i}\left[H_0[\delta\phi^{\rm I},\delta\pi^{\rm I};t],\delta\pi^{\rm I}\right] \tag{4.41}$$

As H_0 is evaluated in the interaction picture and commutes with itself, we can choose to evaluate it at $t_{\rm i}$. The time evolution can now be encoded by the unitary operator U_0

$$\delta\phi^{\rm I}(\boldsymbol{x},t) = U_0^{-1}(t,t_{\rm i})\delta\phi(\boldsymbol{x},t_{\rm i})U_0(t,t_{\rm i})\,, \tag{4.42}$$

$$\delta\pi^{\rm I}(\boldsymbol{x},t) = U_0^{-1}(t,t_{\rm i})\delta\pi(\boldsymbol{x},t_{\rm i})U_0(t,t_{\rm i})\,, \tag{4.43}$$

which in turn obeys

$$\frac{{\rm d}U_0(t,t_{\rm i})}{{\rm d}t} = -{\rm i}H_0[\delta\phi(\boldsymbol{x},t_{\rm i}),\delta\pi(\boldsymbol{x},t_{\rm i});t]U_0(t,t_{\rm i})\,. \tag{4.44}$$

The interaction picture fields evolved by the free-field Hamiltonian H_0 are the linear solutions of the Mukhanov-Sasaki equation.

Let us now evaluate an inflationary correlator and express it in terms of interaction picture fields

$$\begin{aligned}\langle 0|Q[\delta\phi(\boldsymbol{x},t),\delta\pi(\boldsymbol{x},t)]|0\rangle &= \left\langle 0|U^{-1}(t,t_{\rm i})Q[\delta\phi(\boldsymbol{x},t_{\rm i}),\delta\pi(\boldsymbol{x},t_{\rm i})]U(t,t_{\rm i})|0\right\rangle\\ &= \left\langle 0|F^{-1}(t,t_{\rm i})U_0^{-1}(t,t_{\rm i})Q[\delta\phi(\boldsymbol{x},t_{\rm i}),\delta\pi(\boldsymbol{x},t_{\rm i})]U_0(t,t_{\rm i})F(t,t_{\rm i})|0\right\rangle\\ &= \left\langle 0|F^{-1}(t,t_{\rm i})Q[\delta\phi^{\rm I}(\boldsymbol{x},t),\delta\pi^{\rm I}(\boldsymbol{x},t)]F(t,t_{\rm i})|0\right\rangle\\ &= \left\langle 0|F^{-1}(t,t_{\rm i})Q^{\rm I}F(t,t_{\rm i})|0\right\rangle\,,\end{aligned} \tag{4.45}$$

where we have defined

$$F(t,t_{\rm i}) = U_0^{-1}(t,t_{\rm i})U(t,t_{\rm i})\,. \tag{4.46}$$

Let us calculate the equation of motion for $F(t,t_{\rm i})$

$$\begin{aligned}\frac{{\rm d}F(t,t_{\rm i})}{{\rm d}t} =& \frac{{\rm d}U_0^{-1}(t,t_{\rm i})}{{\rm d}t}U(t,t_{\rm i}) + U_0^{-1}(t,t_{\rm i})\frac{{\rm d}U(t,t_{\rm i})}{{\rm d}t}\\ =& {\rm i}U_0^{-1}(t,t_{\rm i})H_0[\delta\phi(\boldsymbol{x},t_{\rm i}),\delta\pi(\boldsymbol{x},t_{\rm i});t]U(t,t_{\rm i}) - {\rm i}U_0^{-1}(t,t_{\rm i})\tilde{H}[\delta\phi(\boldsymbol{x},t_{\rm i}),\delta\pi(\boldsymbol{x},t_{\rm i});t]U(t,t_{\rm i})\\ =& -{\rm i}U_0^{-1}(t,t_{\rm i})H_{\rm int}[\delta\phi(\boldsymbol{x},t_{\rm i}),\delta\pi(\boldsymbol{x},t_{\rm i});t]U_0(t,t_{\rm i})U_0^{-1}(t,t_{\rm i})U(t,t_{\rm i})\\ =& -{\rm i}H_{\rm int}^{\rm I}[\delta\phi^{\rm I}(t),\delta\pi^{\rm I}(t);t]F(t,t_{\rm i})\end{aligned} \tag{4.47}$$

$F(t,t_{\rm i})$ is the time evolution operator associated with the interaction Hamiltonian $H_{\rm int}$. The solution is given by

$$F(t,t_{\rm i}) = T\exp\left[-{\rm i}\int_{t_{\rm i}}^{t}{\rm d}t\ H_{\rm int}^{\rm I}(t)\right]. \tag{4.48}$$

We now only need to project the initial state on the free vacuum using $\tau_{\rm i}\to-\infty(1+{\rm i}\varepsilon)$

$$\langle Q(\tau)\rangle = \left\langle \bar{T}\exp\left[{\rm i}\int_{-\infty(1-{\rm i}\varepsilon)}^{\tau}a(\tau'){\rm d}\tau' H_{\rm int}^{\rm I}(\tau')\right]\ Q^{\rm I}(\tau)\ \ T\exp\left[-{\rm i}\int_{-\infty(1+{\rm i}\varepsilon)}^{\tau}a(\tau'){\rm d}\tau'\ H_{\rm int}^{\rm I}(\tau')\right]\right\rangle\,, \tag{4.49}$$

where $\bar{T}$ is the anti-time ordering operator. Note that the conjugation acts on the integration limit and thus the integration contour goes from $-\infty(1-{\rm i}\epsilon)$ to t and then back to $-\infty(1+{\rm i}\epsilon)$, i.e., the contour doesn't close (see Fig. 4.3).

For cubic interactions relevant to our considerations here $Q\sim\delta\phi^3\sim\mathcal{R}^3$ the term at zeroth order in the interaction Hamiltonian $\left\langle Q^{\rm I}\right\rangle$ in the above equation vanishes. Expanding the above equation to leading order in the interaction Hamiltonian, we obtain

$$\langle Q(\tau)\rangle = {\rm i}\int_{-\infty(1+{\rm i}\varepsilon)}^{\tau}a(\tau'){\rm d}\tau'\ \left\langle\left[H_{\rm int}^{\rm I}(\tau'),Q^{\rm I}(\tau)\right]\right\rangle\,. \tag{4.50}$$

which for a cubic Hamiltonian is of sixth order in the fields and thus has non-vanishing contributions. We can further simplify using hermiticity

$$\langle Q(\tau)\rangle = \Re\langle 0| - 2\mathrm{i}Q^{\mathrm{I}}(\tau)\int_{-\infty(1+\mathrm{i}\varepsilon)}^{\tau} a(\tau')\mathrm{d}\tau' H^{\mathrm{I}}_{\mathrm{int}}(\tau')|0\rangle\,. \tag{4.51}$$

4.3. Derivation of the Cubic Hamiltonian

In this Section we will derive the bispectra generated by single field inflation and its extensions.

4.3.1. Review: Slow-roll inflation and gauges

As you have discussed in the Cosmology course in Michaelmas term, canonical single field inflation is driven by a homogeneous and isotropic scalar field ϕ evolving in a potential V. As we require inflation to last sufficiently long, we impose constraints on the speed of the inflaton $\dot\phi$ and it's acceleration. These constraints can be encoded by the slow-roll parameters

$$\epsilon = -\frac{\dot H}{H^2} = \frac{1}{2}\frac{\dot\phi^2}{H^2}, \qquad \eta = \frac{\dot\epsilon}{H\epsilon}, \qquad \xi = \frac{\dot\eta}{H\eta}\,. \tag{4.52}$$

Successful inflation is thus equivalent to $\epsilon, \eta, \xi \ll 1$. Note that in the above equations we have set $1/M_{\mathrm{Pl}}^2 = 8\pi G = 1$. The equation of motion for the homogeneous inflaton is given by

$$\ddot\phi + 3H\dot\phi + V' = 0\,. \tag{4.53}$$

The Friedmann equations can be evaluated as

$$H^2 = \frac{1}{3}\left(V + \frac{\dot\phi^2}{2}\right), \qquad \dot H = -\frac{\dot\phi^2}{2}\,. \tag{4.54}$$

The slow-roll conditions are equivalent to $H \approx$ const. The inflationary background is thus in near de Sitter space. At leading order we can assume dS space to calculate the expansion history and obtain for the conformal time $a\mathrm{d}\tau = \mathrm{d}t$ we have $\tau = -1/(aH)$.

When considering fluctuations in the homogeneneous inflaton field, we need to consider relativistic perturbation theory. As you have seen before the matter is slightly complicated by the coordinate invariance of GR and the resulting gauge transformations. The four scalar metric perturbations plus one scalar field perturbation are reduced by the two degrees of freedom of the gauge transformation and the two constraint equations. We are left with one scalar degree of freedom. This allows us to either work in a frame where the metric perturbation absorbs the perturbation in the inflaton (comoving or uniform inflaton gauge) or in a gauge, where the curvature fluctuations in the metric are completely represented by the scalar field perturbations (spatially flat gauge). The two are related by the the space dependent time shift $\tilde t = t + \delta t$

$$\mathcal{R} = -H\delta t = -H\frac{\delta\phi}{\dot\phi}\,. \tag{4.55}$$

4.3.2. ADM Formalism: Introduction

Let us consider the gravitational action with a matter term (for now we will remain generic)

$$S = \frac{1}{2}\int \mathrm{d}^4x\sqrt{-g}R + \int \mathrm{d}^4x\sqrt{-g}\mathcal{L}_{\mathrm{m}}\,. \tag{4.56}$$

Solving the constraint equations for the metric perturbations beyond leading order is a tedious task, which can be simplified in the elegant Hamiltonian formulation of general relativity introduced by Arnowitt, Deser

and Misner (ADM).[8] The idea is to split spacetime into constant time hypersurfaces Σ_t and to encode spacetime metric into the internal curvature of the hypersurface as well as the relation between subsequent hypersurfaces. The metric is given by

$$\mathrm{d}s^2 = -N^2\mathrm{d}t^2 + h_{ij}(\mathrm{d}x^i + N^i\mathrm{d}t)(\mathrm{d}x^j + N^j\mathrm{d}t)\,, \tag{4.57}$$

where the **lapse function** N and **shift function** N_i are non-dynamical Lagrange multipliers. They quantify the proper time between two slices Σ_t and $\Sigma_{t+\mathrm{d}t}$ as $N\mathrm{d}t$ and the change in spatial coordinates along a normal trajectory as $x^i \to x^i + N^i\mathrm{d}t$. We can define a normal vector on these hypersurfaces

$$n_\mu = (-N, 0, 0, 0) \tag{4.58}$$

which for all tangent vectors $\boldsymbol{e}_\alpha$ satisfies $n_\mu e^\mu_\alpha = 0$. In matrix notation the metric and inverse metric are given by

$$g_{\mu\nu} = \begin{pmatrix} -N^2 + N_iN^i & N_i \\ N_i & h_{ij} \end{pmatrix}, \quad g^{\mu\nu} = \begin{pmatrix} -1/N^2 & N^i/N^2 \\ N^i/N^2 & h^{ij} - N^iN^j/N^2 \end{pmatrix}. \tag{4.59}$$

The determinant of the metric can be expressed in terms of 3-quantities as $\sqrt{-g} = \sqrt{h}N$. Note that in the ADM formalism, indices of 3-quantities are lowered and raised using the spatial metric h_{ij} and its inverse. Four dimensional quantities can be projected on Σ using the projector

$$P_{\mu\nu} = g_{\mu\nu} + n_\mu n_\nu\,. \tag{4.60}$$

The **extrinsic curvature** measures how the normal vector n_μ changes on Σ

$$\begin{aligned} K_{ij} =& n_{i;j} = n_{i,j} - \Gamma^\lambda_{ij}n_\lambda = N\Gamma^0_{ij} = \frac{1}{2}Ng^{0\mu}\left(g_{\mu j,i} + g_{i\mu,j} - g_{ij,\mu}\right) \\ =& -\frac{1}{2N}\left(g_{0j,i} + g_{i0,j} - g_{ij,0}\right) + \frac{1}{2N}N_lh^{lm}\left(h_{mj,i} + h_{im,j} - h_{ij,m}\right) \\ =& \frac{1}{2N}\left(\dot{h}_{ij} - N_{i,j} - N_{j,i}\right) + \frac{1}{N}{}^{(3)}\Gamma^l_{i,j}N_l = \frac{1}{2N}\left(\dot{h}_{ij} - N_{i|j} - N_{j|i}\right) \end{aligned} \tag{4.61}$$

in the last line we have introduced the 3-connection ${}^{(3)}\Gamma$ and the 3-covariant derivative $f_{i|j} = \partial_i f - {}^{(3)}\Gamma^l_{i,j}f_l$. Sometimes the lapse factor is factored out, yielding

$$E_{ij} = NK_{ij} = \frac{1}{2}\left(\dot{h}_{ij} - N_{j|i} - N_{i|j}\right) \tag{4.62}$$

We will be employing the latter definition in what follows as it makes the separation of lapse and shift terms more explicit in the action and constraints.

The **Gauss-Codazzi equations** relate the three dimensional to the four dimensional Ricci scalar

$$R = {}^{(3)}R + \frac{1}{N^2}\left(E_{ij}E^{ij} - E^2\right)\,. \tag{4.63}$$

Plugging these results back into the action we get

$$S = \frac{1}{2}\int \mathrm{d}^4x\sqrt{h}N\left[{}^{(3)}R + \frac{1}{N^2}(E_{ij}E^{ij} - E^2)\right] + \int \mathrm{d}^4x\mathcal{L}_\mathrm{m}\,. \tag{4.64}$$

The constraint equations follow from variation of the action with respect to N and N^i

$$\begin{aligned} {}^{(3)}R - \frac{1}{N^2}(E_{ij}E^{ij} - E^2) =& 2\rho\,, \\ \nabla_i[N^{-1}(E^i{}_j - \delta^i{}_jE)] =& \mathcal{J}_j\,. \end{aligned} \tag{4.65}$$

[8] R. Arnowitt, S. Deser, C. W. Misner *The Dynamics of General Relativity* `https://arxiv.org/abs/gr-qc/0405109` [Arnowitt et al., 2008]

Here we used that

$$T^{\mu\nu} = -\frac{2}{\sqrt{-g}}\frac{\delta\mathcal{L}}{\delta g_{\mu\nu}}\,, \tag{4.66}$$

yielding density $\rho = n_\mu n_\nu T^{\mu\nu} = N^2 T^{00}$ and momentum density $\mathcal{J}_i = -n_\mu P^{\mu\nu}_{i\nu} = NT^0_{\ i}$ and shear $S_{ij} = P^\mu_{\ i} P^\nu_{\ j} T_{\mu\nu} = T_{ij}$. The trace of the shear is $S = h^{ij}S_{ij}$.

The dynamical equations can be obtained from variation w.r.t. h_{ij}. The traceless part for instance is given by

$$\dot{K} + N^i K_{,i} - N^{|i}_{\ |i} + N\left({}^{(3)}R + K^2\right) = (S - 3\rho)/2\,. \tag{4.67}$$

4.3.3. ADM Formalism: Minimally coupled Scalar Field

Let us now consider the action for a scalar field (now with inhomogeneities) minimally coupled to gravity. The action now reads

$$S = \int \mathrm{d}^4x\sqrt{-g}\left[\frac{1}{2}R + X - V(\phi)\right]\,, \tag{4.68}$$

where $X = -1/2 g^{\mu\nu}\partial_\mu\phi\partial_\nu\phi$. Rewriting the above action in terms of 3-quantities we obtain

$$S = \frac{1}{2}\int \mathrm{d}^4x\sqrt{h}N\left[{}^{(3)}R + \frac{1}{N^2}(E_{ij}E^{ij} - E^2) + \frac{1}{N^2}(\dot{\phi} - N^i\partial_i\phi)^2 - h^{ij}\partial_i\phi\partial_j\phi - 2V\right] \tag{4.69}$$

and for the energy-momentum tensor we have

$$T^{\mu\nu} = \partial^\mu\phi\partial^\nu\phi - g^{\mu\nu}\left[\frac{1}{2}\partial_\lambda\phi\partial^\lambda\phi - V(\phi)\right]\,. \tag{4.70}$$

Note the fact that N and N^i don't have any time derivatives acting on them, highlighting their role as non-dynamical Lagrange multipliers. The hamiltonian and momentum constraints now read as

$$\begin{aligned} {}^{(3)}R - \frac{1}{N^2}(E_{ij}E^{ij} - E^2) =& \frac{1}{N^2}\left(\dot{\phi} - N^i\partial_i\phi\right)^2 + 2V + h^{ij}\partial_i\phi\partial_j\phi \\ \nabla_i[N^{-1}(E^i_j - \delta^i_j E)] =& -\frac{1}{N}\left(\dot{\phi} - N^i\partial_i\phi\right)\partial_j\phi \end{aligned} \tag{4.71}$$

Here we used that pressure and momentum density for a scalar field are given by

$$\rho = \frac{1}{2}\Pi^2 + \frac{1}{2}h^{ij}\partial_i\phi\partial_j\phi + V\,, \tag{4.72}$$

$$\mathcal{J}_i = -\Pi\partial_i\phi\,, \tag{4.73}$$

and scalar field momentum

$$\Pi = \frac{1}{N}\left(\dot{\phi} - N^i\partial_i\phi\right)\,. \tag{4.74}$$

From now on, we will be working in **comoving gauge** $\delta T^i_{\ 0} = \delta\phi = 0$ and parametrize the spatial metric[9] as

$$h_{ij} = a^2 e^{2\mathcal{R}}\delta_{ij}\,. \tag{4.75}$$

Expanding the action at leading order in derivatives, but keeping all orders in $\mathcal{R}$, it can be shown that this quantity is conserved to all orders outside horizon [Maldacena, 2003]. In comoving gauge all of the

[9] In the cosmology course you discussed gauge transformations $\tilde{x}^\mu = x_\mu + \xi^\mu$ with $\xi^0 = T$ and $\xi^i = \partial^i L$ for a metric

$$\mathrm{d}s^2 = -(1+2A)\mathrm{d}t^2 + 2aB_{,i}\mathrm{d}x^i\mathrm{d}t + a^2\left[(1+2C)\delta_{ij} + (\partial_i\partial_j - \delta_{ij}\partial^2)E\right]\mathrm{d}x^i\mathrm{d}x^j$$

The gauge transformation changes the metric perturbations as $\tilde{A} = A - \dot{T}$, $\tilde{B} = B + T - L'$, $\tilde{C} = C - HT - \partial^2 L/3$, $\tilde{E} = E - L$ and the scalar field perturbation as $\widetilde{\delta\phi} = \delta\phi - \dot{\phi}T$. At linear order we have $A = \delta N$, $aB_{,i} = N_i$, $C = \mathcal{R}$ and $E = 0$. The alternative spatially flat gauge has $\widetilde{\delta\phi} = -\dot{\phi}T$ and $\tilde{C} = \mathcal{R} - HT$, leading to the relation between the curvature perturbation in comoving gauge and the scalar field perturbation in spatially flat gauge $\mathcal{R} = -H\widetilde{\delta\phi}/\dot{\phi}$.

perturbations in the scalar field are moved into the metric and spatial derivatives of the background scalar field obviously vanish. The action thus simplifies to

$$S = \frac{1}{2}\int \mathrm{d}^4x\sqrt{h}N\left[{}^{(3)}R + \frac{1}{N^2}(E_{ij}E^{ij} - E^2) + \frac{1}{N^2}\dot{\bar{\phi}}^2 - 2V\right]. \tag{4.76}$$

Using tha Gauss-Codazzi Equation (4.63), the 3-Ricci scalar is given by

$${}^{(3)}R = -2a^{-2}e^{-2\mathcal{R}}\left[2\partial^2\mathcal{R} + (\partial\mathcal{R})^2\right] \tag{4.77}$$

This warrants denoting $\mathcal{R}$ as the **curvature perturbation** - the spatial curvature at linear order equals to $-4\partial^2\mathcal{R}$. We can now expand the lapse as $N = 1 + \delta N$ and focusing on scalar fluctuations, the shift can be written as $N_i = \partial_i\psi$. The extrinsic curvature can now be calculated as

$$E_{ij} = (H + \dot{\mathcal{R}})e^{2\mathcal{R}}a^2\delta_{ij} - \partial_i\partial_j\psi + (2\partial_{(i}\mathcal{R}\partial_{j)}\psi - \delta_{ij}\partial_i\mathcal{R}\partial_i\psi) \tag{4.78}$$

$$E = h^{ij}E_{ij} = 3(H + \dot{\mathcal{R}}) - \frac{e^{-2\mathcal{R}}}{a^2}(\partial_i\mathcal{R}\partial_i\psi + \partial^2\psi) \tag{4.79}$$

The linear constraint equations can be solved by

$$\delta N = \frac{\dot{\mathcal{R}}}{H}, \quad \psi = -\frac{\mathcal{R}}{H} + a^2\frac{\dot{\phi}^2}{2H^2}\partial^{-2}\dot{\mathcal{R}} \tag{4.80}$$

We will not need to solve them to higher order for our purposes. In the perturbative expansion of the action, the second order solutions multiply the vanishing first order constraint equation and likewise the third order solutions multiply the zeroth order constraints.

4.3.4. The Quadratic Action

Plugging the expressions into the action we obtain

$$\begin{aligned} S_2 = \frac{1}{2}\int \mathrm{d}^4x\Big\{&9a^3\mathcal{R}^2\left(\frac{1}{2}\dot{\phi}^2 - V - 3H^2\right) - 4\frac{a}{H}\partial^2\mathcal{R}\dot{\mathcal{R}} - 3\frac{a^3}{H}\mathcal{R}\dot{\mathcal{R}}\left(\dot{\phi}^2 + 2V + 6H^2\right) \\ &+ \frac{a^3\dot{\phi}^2}{H^2}\dot{\mathcal{R}}^2 - 2(\partial\mathcal{R})^2 + 4aH\partial_i\mathcal{R}\partial_i\psi - 4a\mathcal{R}\partial^2\mathcal{R} + 4aH\mathcal{R}\partial^2\psi \\ &+ \frac{1}{a}\left(\partial^2\psi\partial^2\psi - \partial_i\partial_j\psi\partial_i\partial_j\psi\right)\Big\} \end{aligned} \tag{4.81}$$

Doing lots of integrations by part and using the definition of ψ in Eq. (4.80) as well as the background equations of motion, we finally arrive at

$$S_2 = \int \mathrm{d}^4x\ a^3\epsilon\left[\dot{\mathcal{R}}^2 - \frac{1}{a^2}(\partial_i\mathcal{R})^2\right]. \tag{4.82}$$

We immediately see that the quadratic action is of order of the slow roll parameter ϵ, but this result is true to all orders in slow roll.

Using the transformation $v = z\mathcal{R} = a\sqrt{2\epsilon}\mathcal{R}$ and switching to conformal time $\mathrm{d}t = a\mathrm{d}\tau$ we get

$$S_2 = \int \mathrm{d}\tau\mathrm{d}^3x\left(v'^2 - (\partial v)^2 + \frac{z''}{z}v^2\right) \tag{4.83}$$

The Euler-Lagrange equation thus reads

$$v'' - \partial^2 v - \frac{z''}{z}v = 0 \quad \Rightarrow \quad v'' + \left(k^2 - \frac{z''}{z}\right)v = 0 \tag{4.84}$$

The effective mass term can be written in terms of the slow roll parameters defined above in Eq. (4.52)

$$\frac{z''}{z} = a^2H^2\left(2-\epsilon+\frac{3}{2}\eta-\frac{1}{2}\eta\epsilon+\frac{1}{2}\eta\xi+\frac{1}{4}\eta^2\right) \tag{4.85}$$

In de-Sitter space dominated by a cosmological constant ($H = \text{const.}$) we thus have with $\tau \approx -1/aH$

$$v'' + \left(k^2 - \frac{2}{\tau^2}\right)v = 0 \tag{4.86}$$

The general solution of this equation is

$$v = \frac{-\mathrm{i}}{\tau\sqrt{2k^3}}\left(1+\mathrm{i}k\tau\right)e^{-\mathrm{i}k\tau} \tag{4.87}$$

The conformal time $a\mathrm{d}\tau = \mathrm{d}t$ in inflation is given by $\tau \approx -1/aH$. The interaction picture fields used here are just the solutions of the Mukhanov-Sasaki equation.

$$\mathcal{R}^{\mathrm{I}}(\boldsymbol{x}) = \int \frac{\mathrm{d}^3k}{(2\pi)^3}\left[a^{\mathrm{I}}_{\boldsymbol{k}}u_k(t)e^{-\mathrm{i}\boldsymbol{k}\cdot\boldsymbol{x}} + a^{\mathrm{I}\dagger}_{\boldsymbol{k}}u^*_k(t)e^{\mathrm{i}\boldsymbol{k}\cdot\boldsymbol{x}}\right] = \mathcal{R}^{\mathrm{I}}_+(\boldsymbol{x},t) + \mathcal{R}^{\mathrm{I}}_-(\boldsymbol{x},t) \tag{4.88}$$

or

$$\mathcal{R}^{\mathrm{I}}_{\boldsymbol{k}}(t) = a^{\mathrm{I}}_{\boldsymbol{k}}u_k(t) + a^{\mathrm{I}\dagger}_{-\boldsymbol{k}}u^*_k(t) \tag{4.89}$$

where the mode functions satisfy

$$u_k = \frac{H}{\sqrt{4\epsilon k^3}}(1+\mathrm{i}k\tau)e^{-\mathrm{i}k\tau} \tag{4.90}$$

and the time derivative

$$u'_k = \frac{H}{\sqrt{4\epsilon k^3}}k^2\tau e^{-\mathrm{i}k\tau} \tag{4.91}$$

The creation and destruction operators obey the canonical commutation relations

$$\left[a_{\boldsymbol{k}}, a^\dagger_{\boldsymbol{k}'}\right] = (2\pi)^3\delta^{(\mathrm{D})}(\boldsymbol{k}-\boldsymbol{k}') \qquad \left[a_{\boldsymbol{k}}, a_{\boldsymbol{k}'}\right] = \left[a^\dagger_{\boldsymbol{k}}, a^\dagger_{\boldsymbol{k}'}\right] = 0 \tag{4.92}$$

Calculating expectation values of products of annihilation and creation operators involves moving the annihilation operators to the right and the creation operators to the left using the commutation relations. The power spectrum is thus with $a_{\boldsymbol{k}}a^\dagger_{\boldsymbol{k}'} = a^\dagger_{\boldsymbol{k}'}a_{\boldsymbol{k}} + (2\pi)^3\delta^{(\mathrm{D})}(\boldsymbol{k}+\boldsymbol{k}')$

$$\langle 0|\mathcal{R}(\boldsymbol{k})\mathcal{R}(\boldsymbol{k}')|0\rangle = (2\pi)^3u_ku^*_k\delta^{(\mathrm{D})}(\boldsymbol{k}+\boldsymbol{k}') \tag{4.93}$$

Thus we have for the power spectrum and dimensionless power spectrum

$$P_{\mathcal{R}}(k) = |u_k|^2 = \frac{H^2}{4\epsilon k^3}\,, \qquad \Delta^2_{\mathcal{R}} = \frac{k^3}{2\pi^2}P_{\mathcal{R}} = \frac{H^2}{8\pi^2\epsilon}\,. \tag{4.94}$$

The slope of the power spectrum can be calculated as

$$n_{\mathrm{s}} - 1 = \frac{\mathrm{d}\ln\Delta^2_{\mathcal{R}}}{\mathrm{d}\ln k}\Big|_{k=aH} = -2\epsilon - \eta\,. \tag{4.95}$$

4.3.5. The Cubic Action

Expanding the action to third order

$$\begin{aligned} S_3 = \int \mathrm{d}^4x\Big\{ & a^3\epsilon^2\mathcal{R}\dot{\mathcal{R}}^2 + a\epsilon^2\mathcal{R}(\partial_i\mathcal{R})^2 - 2a\epsilon^2\dot{\mathcal{R}}(\partial_i\mathcal{R})(\partial_i\psi) \\ & + \frac{a}{2}\epsilon\dot{\eta}\mathcal{R}^2\dot{\mathcal{R}} + \frac{1}{2}\frac{\epsilon}{a}\partial_i\mathcal{R}\partial_i\psi\partial^2\psi + \frac{\epsilon}{4a}\partial^2\mathcal{R}(\partial\psi)^2 + 2f(\mathcal{R})\frac{\delta\mathcal{L}_2}{\delta\mathcal{R}}\Big\} \end{aligned} \tag{4.96}$$

where

$$f(\mathcal{R}) = \frac{\eta}{4}\mathcal{R}^2 + \dots \tag{4.97}$$

Maldacena[10] found that the terms proportional to $\delta\mathcal{L}_2/\delta\mathcal{R}$ can be removed by a field redefinition

$$\mathcal{R}_\mathrm{n} = \mathcal{R} - f(\mathcal{R}) \tag{4.98}$$

This field redifinition obviously changes the three point function through it's quadratic term and contributes a local type term to the bispectrum

$$\langle \mathcal{R}\mathcal{R}\mathcal{R}\rangle = \langle \mathcal{R}_\mathrm{n}\mathcal{R}_\mathrm{n}\mathcal{R}_\mathrm{n}\rangle + \frac{\eta}{4}\langle \mathcal{R}_\mathrm{n}\mathcal{R}_\mathrm{n}\rangle\langle \mathcal{R}_\mathrm{n}\mathcal{R}_\mathrm{n}\rangle \tag{4.99}$$

At leading order in the slow roll parameters $\mathcal{O}(\epsilon^2)$ one finally obtains

$$\begin{aligned} S_3 = \int \mathrm{d}^4x \Big(& a^3\epsilon^2\mathcal{R}\dot{\mathcal{R}}^2 - 2a^3\epsilon^2\dot{\mathcal{R}}\partial_i\mathcal{R}\partial_i(\partial^{-2}\dot{\mathcal{R}}) + a\epsilon^2\mathcal{R}(\partial\mathcal{R})^2 \\ & + \frac{1}{2}a^3\epsilon\dot{\eta}\mathcal{R}^2\dot{\mathcal{R}} + \frac{1}{2}a^3\epsilon^3\dot{\mathcal{R}}\partial_i\mathcal{R}\partial_i(\partial^{-2}\dot{\mathcal{R}}) + \frac{1}{4}\epsilon^3\partial^2\mathcal{R}\partial_i(\partial^{-2}\dot{\mathcal{R}})\partial_i(\partial^{-2}\dot{\mathcal{R}})\Big) . \end{aligned} \tag{4.100}$$

Note that the terms in the second row are higher order in slow roll.

We can now calculate the interaction Hamiltonian from $H_\mathrm{int} = \int \mathrm{d}^3x\mathcal{H}_\mathrm{int} = -\int \mathrm{d}^3x\mathcal{L}_\mathrm{int}$. Note that this relation for the Hamiltonian and Lagrange density is only valid as long as we can solve $\pi = \partial\mathcal{L}/\partial\dot{\mathcal{R}}$ perturbatively for $\dot{\mathcal{R}}$. Also, it doesn't hold for the quadratic Hamiltonian $\mathcal{H}_0 \neq -\mathcal{L}_0$.

Let us for example consider the action

$$\mathcal{L} = \mathcal{L}_0 + \mathcal{L}_\mathrm{int} = \underbrace{\frac{1}{2}\dot{\mathcal{R}}^2 - F(\mathcal{R},\partial\mathcal{R})}_{\mathcal{L}_0}\underbrace{+\alpha\dot{\mathcal{R}}^3}_{\mathcal{L}_\mathrm{int}} \tag{4.101}$$

The canonical momentum is given by

$$\pi = \dot{\mathcal{R}} + 3\alpha\dot{\mathcal{R}}^2 \quad \Rightarrow \quad \dot{\mathcal{R}} = \pi - 3\alpha\dot{\mathcal{R}}^2 \tag{4.102}$$

Thus we have for the Legendre transformation

$$\begin{aligned} \tilde{\mathcal{H}} =& \pi\dot{\mathcal{R}} - \mathcal{L} = \pi^2 - 3\alpha\pi^3 - \frac{1}{2}\left(\pi^2 - 6\alpha\pi^3 + 9\alpha^2\pi^4\right) - \alpha\pi^3 + F(\mathcal{R},\partial\mathcal{R}) + \mathcal{O}(\pi^4) \\ =& \underbrace{\frac{1}{2}\pi^2 + F_0(\mathcal{R},\partial\mathcal{R})}_{\mathcal{H}_0}\underbrace{-\alpha\pi^3}_{\mathcal{H}_\mathrm{int}} + \mathcal{O}(\pi^4) \end{aligned} \tag{4.103}$$

Which proves that indeed $\mathcal{H}_\mathrm{int} = -\mathcal{L}_\mathrm{int}$.

[10] J. Maldacena *Non-Gaussian features of primordial fluctuations in single field inflationary models* `https://arxiv.org/abs/astro-ph/0210603`

4.4. The three point function in slow-roll single-field inflation

4.4.1. Explicit Calculation with In-In

Let us consider the term $a^3\epsilon^2\mathcal{R}\dot{\mathcal{R}}^2$ in the cubic action Eq. (4.100). First we Fourier transform the three curvature perturbation fields in the Hamiltonian and rewrite in terms of conformal time

$$\begin{aligned}\Big\langle\mathcal{R}(\boldsymbol{k}_1,0)\mathcal{R}(\boldsymbol{k}_2,0)\mathcal{R}(\boldsymbol{k}_3,0)\Big\rangle =& \Re\Big\langle -2\mathrm{i}\mathcal{R}(\boldsymbol{k}_1,0)\mathcal{R}(\boldsymbol{k}_2,0)\mathcal{R}(\boldsymbol{k}_3,0)\int \mathrm{d}^3x\int \mathrm{d}\tau a^2\epsilon^2\\ &\times\prod_{i=1}^{3}\left\{\int\frac{\mathrm{d}^3q_i}{(2\pi)^3}\exp\left[-\mathrm{i}\boldsymbol{q}_i\cdot\boldsymbol{x}\right]\right\}\mathcal{R}(\boldsymbol{q}_1,\tau)\mathcal{R}'(\boldsymbol{q}_2,\tau)\mathcal{R}'(\boldsymbol{q}_3,\tau)\Big\rangle\\ =&\prod_{i=1}^{3}\left\{\int\frac{\mathrm{d}^3q_i}{(2\pi)^3}\right\}\ (2\pi)^{12}\delta^{(\mathrm{D})}\left(\sum_{i=1}^{3}\boldsymbol{q}_i\right)\Big[\delta^{(\mathrm{D})}(\boldsymbol{k}_1+\boldsymbol{q}_1)\delta^{(\mathrm{D})}(\boldsymbol{k}_2+\boldsymbol{q}_2)\delta^{(\mathrm{D})}(\boldsymbol{k}_3+\boldsymbol{q}_3)+2\text{ cyc.}\Big]\\ &\times\Re\left\{-2\mathrm{i}\int\mathrm{d}\tau\frac{\epsilon^2}{(H\tau)^2}u_{k_1}(0)u_{k_2}(0)u_{k_3}(0)u^*_{q_1}(\tau)u'^*_{q_2}(\tau)u'^*_{q_3}(\tau)\right\}\end{aligned} \tag{4.104}$$

In the second step we have moved all the annihilation operators of $\boldsymbol{k}_1,\boldsymbol{k}_2$ and $\boldsymbol{k}_3$ to the right using the commutation relations in Eq. (4.92). We have furthermore used the definition of the Dirac delta in terms of the integral over plane waves. We can now plug in the mode functions $u_k(\tau)$ and perform the time integral to obtain

$$\begin{aligned}B^{\mathcal{R}\dot{\mathcal{R}}^2}_{\mathcal{R}}(k_1,k_2,k_3) =& -\frac{H^4}{32\epsilon(k_1k_2k_3)^3}\Re\left[\mathrm{i}k_2^2k_3^2\int_{-\infty(1+\mathrm{i}\varepsilon)}^{0}\mathrm{d}\tau(1+\mathrm{i}k_1\tau)e^{-\mathrm{i}K\tau}+2\text{ cyc.}\right]\\ =&\frac{H^4}{32\epsilon}\frac{1}{(k_1k_2k_3)^3}\left[\frac{k_2^2k_3^2}{K}+\frac{k_1k_2^2k_3^2}{K^2}+2\text{ cyc.}\right]\\ =&\frac{1}{2}\frac{(2\pi^2\Delta^2_{\mathcal{R}})^2}{(k_1k_2k_3)^2}\epsilon\left[\frac{k_2k_3}{Kk_1}+\frac{k_2k_3}{K^2}+2\text{ cyc.}\right]\end{aligned} \tag{4.105}$$

Combining all terms from the $\mathcal{R}\dot{\mathcal{R}}^2$, $\mathcal{R}\partial\mathcal{R}^2$ and $\dot{\mathcal{R}}\partial_i\mathcal{R}\partial_i(\partial^{-2}\dot{\mathcal{R}})$ operators in Eq. (4.100), the slow-roll bispectrum is given by

$$B_{\mathcal{R}}(k_1,k_2,k_3)=\frac{H^4}{(k_1k_2k_3)^3}\frac{1}{4\epsilon^2}\left[\frac{\eta}{8}\sum k_i^3+\frac{\epsilon}{8}\left(-\sum k_i^3+\sum_{i\neq j}k_ik_j^2+\frac{8}{K}\sum_{i>j}k_i^2k_j^2\right)\right] \tag{4.106}$$

The first term proportional to η arises from the field redefinition Eq. (4.98). Factoring out the power spectra, we get for the shape function

$$S=\left[\frac{(\eta-\epsilon)}{8}\left(\frac{k_1^2}{k_2k_3}+2\text{ cyc.}\right)+\frac{\epsilon}{8}\left(\frac{k_1}{k_2}+5\text{ perm}\right)+\frac{\epsilon}{K}\left(\frac{k_1k_2}{k_3}+2\text{ cyc.}\right)\right] \tag{4.107}$$

This isn't exactly of the squeezed form, but typically correlated (using the shape correlator) with the local shape at the 95% level.

The squeezed limit yields

$$\lim_{k_1\ll k_2\sim k_3}S=(\eta+2\epsilon)\frac{k_2}{k_1} \tag{4.108}$$

Comparing to Eq. (4.11), we see that $f_{\mathrm{NL,loc}}\propto\eta+2\epsilon$, $\eta+2\epsilon=1-n_{\mathrm{s}}\ll 1$.

4.4.2. Consistency Condition

In the previous section we have shown through an explicit perturbative calculation, which non-Gaussian shapes can be produced in single-field, slow-roll inflation and that their amplitude is slow-roll suppressed.

We will now consider a much more powerful and general argument that proves non-Gaussianities to be small in any single field inflationary model, irrespective of the form of the kinetic term, the explicit form of the initial conditions or the potential.

A fixed superhorizon long mode $\mathcal{R}_\mathrm{l}$ corresponds to a rescaling of the length scales as $x \to (1+\mathcal{R}_\mathrm{l})x$. This can be immediately deduced from the spatial part of the metric $a^2 e^{2\mathcal{R}_\mathrm{l}}$. For the correlation function this implies a rescaling of the argument $\xi(r) \to \xi[(1+\mathcal{R}_\mathrm{l})r]$. Thus, the power spectrum in presence of a long mode can be expressed as

$$\begin{aligned} P(k)\Big|_{\mathcal{R}_\mathrm{l}} =& \int \mathrm{d}^3 r\; e^{-\mathrm{i}\boldsymbol{k}_\mathrm{s}\cdot\boldsymbol{r}} \xi[(1+\mathcal{R}_\mathrm{l})r] = (1-\mathcal{R}_\mathrm{l})^3 P[k(1-\mathcal{R}_\mathrm{l})] \\ =& P(k)\left[1 - 3\mathcal{R}_\mathrm{l} - \mathcal{R}_\mathrm{l} k \frac{P'(k)}{P(k)}\right] = P(k)\left[1 - \mathcal{R}_\mathrm{l}\frac{\mathrm{d}\ln k^3 P}{\mathrm{d}\ln k}\right] \\ =& P(k)\left[1 + (1-n_\mathrm{s})\mathcal{R}_\mathrm{l}\right] \end{aligned} \tag{4.109}$$

where $P(k)$ is the usual short power spectrum in absence of the long mode. Here we used the deviation of the spectal index from unity $1-n_\mathrm{s}$, which we know is related to the slow-roll parameters and thus small. We can now correlate with another long mode and get for the bispectrum

$$\langle \mathcal{R}_\mathrm{l}(\boldsymbol{k}_\mathrm{l}) \mathcal{R}_\mathrm{s}(\boldsymbol{k}_2) \mathcal{R}_\mathrm{s}(\boldsymbol{k}_3)\rangle \sim P(k_l) P(k_2)(1-n_\mathrm{s})\,. \tag{4.110}$$

While this brief motivation describes the key steps in the derivation, it doesn't address the issue of overall momentum conservation.

Let us repeat this derivation in a bit more detail, explicitly accounting for momentum conservation. With $\boldsymbol{x}_+ = (\boldsymbol{x}_2 + \boldsymbol{x}_3)/2$ and $\boldsymbol{x}_- = \boldsymbol{x}_2 - \boldsymbol{x}_3$ we can write the correlation function as

$$\langle \mathcal{R}_s(\boldsymbol{x}_2)\mathcal{R}_s(\boldsymbol{x}_3)\rangle \Big|_{\mathcal{R}_\mathrm{l}} = \xi_\mathrm{s}\big((1+\mathcal{R}_\mathrm{l})x_-\big) = \xi_s(x_-) + \mathcal{R}_l \boldsymbol{x}_- \cdot \boldsymbol{\nabla}\xi_s(x_-)\,, \tag{4.111}$$

where

$$\xi(r) = \int \frac{\mathrm{d}^3 k}{(2\pi)^3} \exp\left[\mathrm{i}\boldsymbol{k}\cdot\boldsymbol{r}\right] P(k) \tag{4.112}$$

Given this rescaling of the correlation function[11]

$$\begin{aligned} \langle \mathcal{R}_\mathrm{l}(\boldsymbol{x}_1)\mathcal{R}(\boldsymbol{x}_2)\mathcal{R}(\boldsymbol{x}_3)\rangle =& \langle \mathcal{R}_\mathrm{l}(\boldsymbol{x}_1)\mathcal{R}_\mathrm{l}(\boldsymbol{x}_+)\rangle\, \boldsymbol{x}_- \nabla\xi_\mathrm{s}(x_-) \\ =& \int \frac{\mathrm{d}^3 k_l}{(2\pi)^3} \int \frac{\mathrm{d}^3 k_s}{(2\pi)^3} e^{\mathrm{i}\boldsymbol{k}_l\cdot(\boldsymbol{x}_1 - \boldsymbol{x}_+)} P(k_l) P(k_s) \boldsymbol{k}_s \cdot \nabla_{\boldsymbol{k}_s} e^{\mathrm{i}\boldsymbol{k}_s\cdot\boldsymbol{x}_-} \end{aligned} \tag{4.113}$$

We can now perform a partial integration in k_s and $\nabla_{\boldsymbol{k}_s}\cdot[\boldsymbol{k}_s P_s(k_s)] = P(k_s)\mathrm{d}\ln k_\mathrm{s}^3 P(k_\mathrm{s})/\mathrm{d}\ln k_\mathrm{s}$ and introduce a new integration variable as well as a Dirac delta

$$\begin{aligned} \langle \mathcal{R}(\boldsymbol{x}_1)\mathcal{R}(\boldsymbol{x}_2)\mathcal{R}(\boldsymbol{x}_3)\rangle =& \int \frac{\mathrm{d}^3 k_1}{(2\pi)^3} \int \frac{\mathrm{d}^3 k_l}{(2\pi)^3} \int \frac{\mathrm{d}^3 k_s}{(2\pi)^3} e^{-\mathrm{i}\boldsymbol{k}_1\cdot\boldsymbol{x}_1 - \mathrm{i}\boldsymbol{k}_l\cdot\boldsymbol{x}_+ + \mathrm{i}\boldsymbol{k}_s\cdot\boldsymbol{x}_-} \\ & \times (2\pi)^3 \delta^{(\mathrm{D})}(\boldsymbol{k}_l + \boldsymbol{k}_1) P(k_l) P(k_s) \frac{\mathrm{d}\ln k^3 P}{\mathrm{d}\ln k} \end{aligned} \tag{4.114}$$

Relabeling $\boldsymbol{k}_\mathrm{l} = \boldsymbol{k}_2 + \boldsymbol{k}_3$ and $\boldsymbol{k}_\mathrm{s} = (\boldsymbol{k}_3 - \boldsymbol{k}_2)/2$, we finally get

$$-\boldsymbol{k}_\mathrm{l}\boldsymbol{x}_+ + \boldsymbol{k}_s\boldsymbol{x}_- = -\boldsymbol{k}_3\boldsymbol{x}_3 - \boldsymbol{k}_2\boldsymbol{x}_2 \tag{4.115}$$

[11] Here we are swapping the derivative using

$$\begin{aligned} \boldsymbol{x}_-\cdot\boldsymbol{\nabla}_{\boldsymbol{x}_-}\xi(x_-) =& \int \frac{\mathrm{d}^3 k}{(2\pi)^3} P(k) \boldsymbol{x}_-\cdot\boldsymbol{\nabla}_{\boldsymbol{x}_-} \exp\left[-\mathrm{i}\boldsymbol{k}\cdot\boldsymbol{x}_-\right] = \int \frac{\mathrm{d}^3 k}{(2\pi)^3} P(k)(-\mathrm{i})\boldsymbol{x}_-\cdot\boldsymbol{k}\exp\left[-\mathrm{i}\boldsymbol{k}\cdot\boldsymbol{x}_-\right] \\ =& \int \frac{\mathrm{d}^3 k}{(2\pi)^3} P(k)\boldsymbol{k}\cdot\nabla_{\boldsymbol{k}}\exp\left[-\mathrm{i}\boldsymbol{k}\cdot\boldsymbol{x}_-\right]. \end{aligned}$$

As $k_1 \ll k_2, k_3$ we have $|\boldsymbol{k}_2 - \boldsymbol{k}_3|/2 \approx k_2 \approx k_3$. The integrand is now just the three point function in Fourier space

$$\lim_{k_1 \to 0} \langle \mathcal{R}(\boldsymbol{k}_1)\mathcal{R}(\boldsymbol{k}_2)\mathcal{R}(\boldsymbol{k}_3)\rangle = -(2\pi)^3 \delta^{(\mathrm{D})}(\boldsymbol{k}_1 + \boldsymbol{k}_2 + \boldsymbol{k}_3) P_{\mathcal{R}}(k_1) P_{\mathcal{R}}(k_3) \frac{\mathrm{d}k_3^3 P_{\mathcal{R}}(k_3)}{\mathrm{d}\ln k_3} \,. \tag{4.116}$$

We thus have that for all single-field models the following **consistency condition** between the squeezed limit bispectrum and the power spectrum needs to hold

$$\lim_{k_1 \to 0} \langle \mathcal{R}(\boldsymbol{k}_1)\mathcal{R}(\boldsymbol{k}_2)\mathcal{R}(\boldsymbol{k}_3)\rangle = (2\pi)^3 \delta^{(\mathrm{D})}(\boldsymbol{k}_1 + \boldsymbol{k}_2 + \boldsymbol{k}_3) P_{\mathcal{R}}(k_1) P_{\mathcal{R}}(k_3)(1 - n_{\mathrm{s}}) \tag{4.117}$$

This is an extremely powerful result as it states that single field inflation can't produce non-Gaussianities with a large squeezed limit irrespective of the dynamics. It means that in single field models the squeezed limit is suppressed by $1 - n_{\mathrm{s}} \ll 1$ and vanishes for scale invariant perturbations.

4.5. Non-standard kinetic terms – $P(x)$ theories

Having established that standard slow-roll, single-field inflation produces vanishingly small (and probably undetectable) levels of primordial non-Gaussianity, let us now consider the consequences of a generalization of the simplest inflationary model. In particular, we will consider modifications to the kinetic term.

$$S = \int \mathrm{d}^4x\sqrt{-g}\left[\frac{1}{2}R + P(X,\phi)\right] \,, \tag{4.118}$$

where $X = -1/2\partial_\mu\phi\partial^\mu\phi$ and the canonical scalar field action discussed above can be restored by setting $P(X,\phi) = X - V(\phi)$. Let us first derive the homogeneous background dynamics with $\phi(\boldsymbol{x},t) = \bar{\phi}(t)$ and $g_{\mu\nu} = \mathrm{diag}(-1, a^2, a^2, a^2)$. The Friedmann equations are given by

$$3H^2 = \rho = 2XP_{,\bar{X}} - P \,, \qquad \dot{H} = \frac{\ddot{a}}{a} - H^2 = -\frac{1}{2}(\rho + p) = -XP_{,\bar{X}} \,, \tag{4.119}$$

where we used[12]

$$\rho = 2XP_{,\bar{X}} - P \,, \qquad p = P \,. \tag{4.120}$$

From the above equations we can immediately infer that

$$\epsilon = \frac{3XP_{,\bar{X}}}{2XP_{,\bar{X}} - P} = \frac{XP_{,\bar{X}}}{H^2}. \tag{4.121}$$

We could proceed as we did previously and solve the constraint equations, plug the results back into the action and calculate the cubic action. This procedure would be tedious. We will rather make use of the fact that large, i.e. interesting, non-Gaussianities can only be produced by self-couplings of the inflaton. We will thus ignore the coupling between perturbations and the metric and work with a flat background metric $g_{\mu\nu} = \mathrm{diag}(-1, a^2, a^2, a^2)$. For later use it will be beneficial to define a **speed of sound**

$$c_{\mathrm{s}}^2 = \frac{\mathrm{d}p}{\mathrm{d}\rho} = \frac{\mathrm{d}P}{\mathrm{d}X}\left(\frac{\mathrm{d}\rho}{\mathrm{d}X}\right)^{-1} = \frac{P_{,\bar{X}}}{P_{,\bar{X}} + 2XP_{,\bar{X}\bar{X}}} \,. \tag{4.122}$$

[12] This can be seen from

$$T_{\mu\nu} = -\frac{2}{\sqrt{-g}}\frac{\delta\mathcal{L}_{\mathrm{m}}}{\delta g^{\mu\nu}} = g_{\mu\nu}P + \partial_\mu\phi\partial_\nu\phi P_{,\bar{X}}$$

Thus we have for the homogeneous background $\partial_i\phi = 0$ with $g_{\mu\nu} = \mathrm{diag}(-1, a^2, a^2, a^2)$ and $X = \dot{\bar{\phi}}^2/2$

$$T_{00} = \rho = 2XP_{,\bar{X}} - P \,, \qquad T_{ii} = g_{ii}p = g_{ii}P \quad \Rightarrow p = P(X) \,.$$

We can now expand X around the background as

$$X = \bar{X} + \delta X = -\frac{1}{2} g^{\mu\nu} \partial_\mu \phi \partial_\nu \phi = \frac{1}{2} \dot{\bar{\phi}} + \dot{\bar{\phi}} \dot{\delta\phi} + \frac{1}{2} \dot{\delta\phi}^2 - \frac{1}{2a^2} (\partial \delta\phi)^2 \,. \tag{4.123}$$

From the gauge transformation, you can see that $\delta\phi = -\dot{\bar{\phi}} \mathcal{R}/H$

$$\delta X = \frac{\bar{X}}{H^2} \left[-2H\dot{\mathcal{R}} + \dot{\mathcal{R}}^2 - \frac{1}{a^2} (\partial \mathcal{R})^2 + \dots \right] , \tag{4.124}$$

where the ellipses stand for operators that arise from the slow-roll suppressed derivatives of H and $\dot{\bar{\phi}}$. The function $P(X)$ can now be expanded up to cubic order

$$P(X) = P(\bar{X}) + P_{,\bar{X}} \delta X + \frac{1}{2!} P_{,\bar{X}\bar{X}} \delta X^2 + \frac{1}{3!} P_{,\bar{X}\bar{X}\bar{X}} \delta X^3 \,. \tag{4.125}$$

The action is now given by

$$\begin{aligned} S &= \int \mathrm{d}^4x \; a^3 \left[P_{,X} \delta X + \frac{1}{2} P_{,\bar{X}\bar{X}} \delta X^2 + \frac{1}{6} P_{,XXX} \delta X^3 \right] \\ &= \int \mathrm{d}^4x \; a^3 \left[\frac{X P_{,X}}{H^2} \left(\dot{\mathcal{R}}^2 - \frac{1}{a^2} (\partial \mathcal{R})^2 \right) + \frac{X^2 P_{,\bar{X}\bar{X}}}{2H^4} \left(4H^2 \dot{\mathcal{R}}^2 - 4H \dot{\mathcal{R}}^3 + \frac{4H}{a^2} \dot{\mathcal{R}} (\partial \mathcal{R})^2 \right) - \frac{4X^3 P_{,\bar{X}\bar{X}\bar{X}}}{3H^3} \dot{\mathcal{R}}^3 \right] \end{aligned} \tag{4.126}$$

Note that in the effective field theory of single field inflation[13] this is written as

$$S = \int \mathrm{d}^4x \; a^3 \left[-\dot{H} \left(\dot{\pi}^2 - \frac{1}{a^2} (\partial_i \pi)^2 \right) + 2M_2^4 \left(\dot{\pi}^2 + \dot{\pi}^3 - \frac{1}{a^2} \dot{\pi} (\partial_i \pi)^2 \right) + \frac{4}{3} M_3^4 \dot{\pi}^3 \right] \tag{4.127}$$

where $\mathcal{R} = -H\pi$. In this approach $M_2^4 = X^2 P_{,\bar{X}\bar{X}}$, $M_3^4 = X^3 P_{,\bar{X}\bar{X}\bar{X}}$ and $c_\mathrm{s}^{-2} = 1 - 2M_2^4/\dot{H}$.

The quadratic action is now given by

$$S_2 = \int \mathrm{d}^4x \frac{a^3 \epsilon}{c_\mathrm{s}^2} \left[\dot{\mathcal{R}}^2 - \frac{c_\mathrm{s}^2}{a^2} (\partial \mathcal{R})^2 \right] = \int \mathrm{d}^3x \mathrm{d}\tau \left[v'^2 - c_\mathrm{s}^2 (\partial v)^2 - \frac{z''}{z} v^2 \right] \tag{4.128}$$

The Bunch-Davies mode functions thus pick up an explicit dependence on the sound speed

$$u(k) = \frac{H}{\sqrt{4\epsilon c_\mathrm{s} k^3}} \left(1 + \mathrm{i} k c_\mathrm{s} \tau \right) e^{-\mathrm{i} k c_\mathrm{s} \tau} \,, \tag{4.129}$$

which is inherited by the power spectrum

$$P_\mathcal{R} = \frac{H^2}{4\epsilon c_\mathrm{s} k^3} \,. \tag{4.130}$$

Let us now get to the interesting part, the interactions

$$S_3 = \int \mathrm{d}^4x \; \left[\frac{2X^2 P_{,\bar{X}\bar{X}}}{H^3 a^2} \dot{\mathcal{R}} (\partial \mathcal{R})^2 - \frac{2}{H^3} \left(X^2 P_{,\bar{X}\bar{X}} + \frac{2}{3} X^3 P_{,\bar{X}\bar{X}\bar{X}} \right) \dot{\mathcal{R}}^3 \right] . \tag{4.131}$$

Parametrizing the amplitude of $\dot{\mathcal{R}}^3$ as

$$\mathcal{A} = -1 - \frac{2}{3} X \frac{P_{,\bar{X}\bar{X}\bar{X}}}{P_{,\bar{X}\bar{X}}} = -1 - \frac{2}{3} \frac{\tilde{c}_3}{c_s^2} \,. \tag{4.132}$$

and using the definition of the speed of sound, we finally obtain

$$S_3 = \int \mathrm{d}^4x \; \frac{a^3 \epsilon}{c_\mathrm{s}^2} \frac{1 - c_s^2}{H} \left[\frac{1}{a^2} \dot{\mathcal{R}} (\partial \mathcal{R})^2 + \mathcal{A} \dot{\mathcal{R}}^3 \right] . \tag{4.133}$$

[13] Cheung, Creminelli, Fitzpatrick, Kaplan, Senatore *The Effective Field Theory of Inflation* `https://arxiv.org/abs/0709.0293` [Cheung et al., 2008]

The shape functions are given by

$$\begin{aligned} S_{\dot{\mathcal{R}}(\partial\mathcal{R})^2} =& \frac{1}{k_1k_2k_3}\left(-\frac{1}{K}\sum_{i<j}k_i^2k_j^2+\frac{1}{2K^2}\sum_{i\neq j}k_i^2k_j^3+\frac{1}{8}\sum_i k_i^3\right) \\ S_{\dot{\mathcal{R}}^3} =& \frac{k_1k_2k_3}{K^3} \end{aligned} \tag{4.134}$$

The non-Gaussian amplitudes are

$$f_{\rm NL}^{\dot{\mathcal{R}}(\partial\mathcal{R})^2} = \frac{85}{324}\left(1-\frac{1}{c_s^2}\right) \qquad f_{\rm NL}^{\dot{\mathcal{R}}^3} = \frac{10}{243}\left(1-\frac{1}{c_s^2}\right)\left(\tilde{c}_3+\frac{3}{2}c_s^2\right) = -\frac{15}{243}\mathcal{A}(c_s^2-1) \tag{4.135}$$

For $c_{\rm s}^2 \to 0$ these shapes can be enhanced. The shapes are peaked in the equilateral configuration $k_1 \approx k_2 \approx k_3$ and highly correlated with the equilateral shape. The difference between the two shapes motivated the definition of the orthogonal shape in Eq. (4.21).

One example of $P(X)$ theories is **DBI inflation**, where a 3+1 dimensional brane moves in a warped external spacetime. The DBI action can be mapped on our above consideration by defining

$$P(X,\phi) = \frac{1}{f(\phi)}\left[1-\sqrt{1-2Xf(\phi)}\right]+V(\phi) \tag{4.136}$$

where $f(\phi)$ is a warp factor (inverse brane tension). Typically in DBI inflation $2Xf(\phi) \to 1$ and thus $c_{\rm s}^2 = \gamma^{-2} = 1-2Xf \to 0$. Furthermore we have $\tilde{c}_3 = \frac{3}{2}(1-c_s^2)$ or $\mathcal{A} = -c_{\rm s}^{-2}$.

You will be able to identify the above form of the EFT action in the Planck paper on non-Gaussianity.[14] For instance, Planck constrained the sound speed to $c_{\rm s} > 0.024$.

4.6. Classical non-Gaussianities: δN Formalism*

So far we have been focusing on non-Gaussianities generated inside the horizon, let us now focus on non-Gaussianities arising from non-linearity after horizon crossing. Remember that the number of e-folds is given by

$$\Delta N(\boldsymbol{x}) = \int \mathrm{d}\ln a = \int_{t_1}^{t_2}\mathrm{d}t\ H(\boldsymbol{x},t) = \int_{t_1}^{t_2}\mathrm{d}t\bar{H}+\delta N_{12}(\boldsymbol{x}) \tag{4.137}$$

In particular, a metric perturbation $\mathcal{R}$ can be seen as a local perturbation to the scale factor $a(\boldsymbol{x},t) = \bar{a}e^{\mathcal{R}}$. Thus the perturbation between a spatially flat slice at t_1 and a uniform density slice at t_2 can be expressed as $\delta N = \mathcal{R}$. Consider a field configuration scalars ϕ_i, one of which is the inflaton and the other ones are isocurvatons. We will consider the number of e-folds between a spatially flat slice ($\delta\phi_i \neq 0$) at $t = 0$ and a uniform density slice at t $\delta\phi_i = 0$.

$$\begin{aligned} \text{classical evolution of unperturbed initial fields fields to unperturbed final slice} \quad &\Rightarrow \bar{N}(\bar{\phi}_i) \\ \text{classical evolution of perturbed initial fields } \bar{\phi}_i+\delta\phi_i \text{ to perturbed final slice} \quad &\Rightarrow N(\bar{\phi}_i+\delta\phi_i) \\ \delta N = N(\bar{\phi}_i+\delta\phi_i) &- \bar{N}(\bar{\phi}_i) \end{aligned}$$

We can thus Taylor expand $\mathcal{R}$ in terms of the scalar field fluctuations on the initial time slice

$$\mathcal{R} = N_i\delta\phi_i+\frac{1}{2}N_{ij}\delta\phi_i\delta\phi_j \tag{4.138}$$

where $N_{ij} = \partial^2 N/\partial\phi_i\partial\phi_j$. Let us assume that the scalar fields themselves are Gaussian and have a power spectrum

$$\langle\delta\phi_i(\boldsymbol{k})\delta\phi_j(\boldsymbol{k}')\rangle = \frac{H^2}{2k^3}(2\pi)^2\delta^{(\rm D)}(\boldsymbol{k}+\boldsymbol{k}')\delta_{ij}^{(\rm K)} \tag{4.139}$$

[14] Planck 2015: Constraints on primordial non-Gaussianity `https://arxiv.org/abs/1502.01592`

The power spectrum and bispectrum of $\mathcal{R}$ are then given by

$$\langle \mathcal{R}(\boldsymbol{k})\mathcal{R}(\boldsymbol{k}')\rangle = N_i N_j \langle \delta\phi_i(\boldsymbol{k})\delta\phi_j(\boldsymbol{k}')\rangle = \frac{H^2}{2k^3}(2\pi)^2\delta^{(\mathrm{D})}(\boldsymbol{k}+\boldsymbol{k}')N_i^2 \tag{4.140}$$

$$B(k_1,k_2,k_3) = \frac{N_{ij}N_iN_j}{(N_l^2)^2}\left[P_{\mathcal{R}}(k_1)P_{\mathcal{R}}(k_2) + 2 \text{ cyc.}\right] \tag{4.141}$$

We thus find a local shape (see Eq. 4.5 for comparison), as the non-linearities are local in configuration space. The amplitude is given by

$$f_{\mathrm{NL,loc}} = \frac{5}{6}\frac{N_{ij}N_iN_j}{(N_l^2)^2}\,. \tag{4.142}$$

4.7. Summary

We can summarize the above considerations on the amount of non-Gaussianity generated in various inflationary scenarios as

single field slow roll equilateral bispectrum with amplitude $\mathcal{O}(\epsilon,\eta)$

single field consistency condition ensures squeezed can not be enhanced

non-standard kinetic terms equilateral non-Gaussianity which can be enhanced for $c_{\mathrm{s}}^2 \to 0$

non-standard vacuum folded shape

multifield inflation local type non-Gaussianity

This means that there will be no observable non-Gaussianity if the following conditions are met

- Single-field inflation
- Canonical kinetic terms
- No violation of slow-roll
- Bunch-Davies vacuum
- Einstein gravity

Bibliography

[Abidi and Baldauf, 2018] Abidi, M. M. and Baldauf, T. (2018). Cubic Halo Bias in Eulerian and Lagrangian Space. *JCAP*, 1807(07):029, [arXiv:1802.07622].

[Ade et al., 2016] Ade, P. A. R. et al. (2016). Planck 2015 results. XVII. Constraints on primordial non-Gaussianity. *Astron. Astrophys.*, 594:A17, [arXiv:1502.01592].

[Aghanim et al., 2018] Aghanim, N. et al. (2018). Planck 2018 results. VIII. Gravitational lensing. [arXiv:1807.06210].

[Arnowitt et al., 2008] Arnowitt, R. L., Deser, S., and Misner, C. W. (2008). The Dynamics of general relativity. *Gen. Rel. Grav.*, 40:1997–2027, [arXiv:gr-qc/0405109].

[Assassi et al., 2014] Assassi, V., Baumann, D., Green, D., and Zaldarriaga, M. (2014). Renormalized Halo Bias. *JCAP*, 1408:056, [arXiv:1402.5916].

[Baumann, 2017] Baumann, D. (2017). Advanced cosmology.

[Baumann et al., 2012] Baumann, D., Nicolis, A., Senatore, L., and Zaldarriaga, M. (2012). Cosmological Non-Linearities as an Effective Fluid. *JCAP*, 1207:051, [arXiv:1004.2488].

[Bernardeau et al., 2002] Bernardeau, F., Colombi, S., Gaztanaga, E., and Scoccimarro, R. (2002). Large scale structure of the universe and cosmological perturbation theory. *Phys. Rept.*, 367:1–248, [arXiv:astro-ph/0112551].

[Bouchet et al., 1995] Bouchet, F. R., Colombi, S., Hivon, E., and Juszkiewicz, R. (1995). Perturbative Lagrangian approach to gravitational instability. *Astron. Astrophys.*, 296:575, [arXiv:astro-ph/9406013].

[Brink and Satchler, 1993] Brink, D. and Satchler, G. (1993). *Angular Momentum*. Oxford science publications. Clarendon Press.

[Carrasco et al., 2012] Carrasco, J. J. M., Hertzberg, M. P., and Senatore, L. (2012). The Effective Field Theory of Cosmological Large Scale Structures. *JHEP*, 09:082, [arXiv:1206.2926].

[Challinor and Peiris, 2009] Challinor, A. and Peiris, H. (2009). Lecture notes on the physics of cosmic microwave background anisotropies. In Novello, M. and Perez, S., editors, *American Institute of Physics Conference Series*, volume 1132 of *American Institute of Physics Conference Series*, pages 86–140. [arXiv:0903.5158].

[Chen, 2010] Chen, X. (2010). Primordial Non-Gaussianities from Inflation Models. *Adv. Astron.*, 2010:638979, [arXiv:1002.1416].

[Cheung et al., 2008] Cheung, C., Creminelli, P., Fitzpatrick, A. L., Kaplan, J., and Senatore, L. (2008). The Effective Field Theory of Inflation. *JHEP*, 03:014, [arXiv:0709.0293].

[Creminelli and Zaldarriaga, 2004] Creminelli, P. and Zaldarriaga, M. (2004). Single field consistency relation for the 3-point function. *JCAP*, 0410:006, [arXiv:astro-ph/0407059].

[Desjacques et al., 2018] Desjacques, V., Jeong, D., and Schmidt, F. (2018). Large-Scale Galaxy Bias. *Phys. Rept.*, 733:1–193, [arXiv:1611.09787].

[Dodelson, 2003] Dodelson, S. (2003). *Modern cosmology*. Academic Press, San Diego, CA.

[Durrer, 2008] Durrer, R. (2008). *The Cosmic Microwave Background*. Cambridge Univ. Press, Cambridge.

[Fixsen et al., 1996] Fixsen, D. J., Cheng, E. S., Gales, J. M., Mather, J. C., Shafer, R. A., and Wright, E. L. (1996). The Cosmic Microwave Background spectrum from the full COBE FIRAS data set. *Astrophys.*

J., 473:576, [arXiv:astro-ph/9605054].

[Hamilton, 1997] Hamilton, A. J. S. (1997). Linear redshift distortions: A Review. In *Ringberg Workshop on Large Scale Structure Ringberg, Germany, September 23-28, 1996*. [arXiv:astro-ph/9708102].

[Hanson et al., 2010] Hanson, D., Challinor, A., and Lewis, A. (2010). Weak lensing of the CMB. *General Relativity and Gravitation*, 42(9):2197–2218, [arXiv:0911.0612].

[Hu, 1996] Hu, W. (1996). Concepts in CMB anisotropy formation. *Lect. Notes Phys.*, 470:207, [arXiv:astro-ph/9511130].

[Hu and Sugiyama, 1995] Hu, W. and Sugiyama, N. (1995). Anisotropies in the cosmic microwave background: An Analytic approach. *Astrophys. J.*, 444:489–506, [arXiv:astro-ph/9407093].

[Hu and White, 1997] Hu, W. and White, M. J. (1997). A CMB polarization primer. *New Astron.*, 2:323, [arXiv:astro-ph/9706147].

[Kaiser, 1984] Kaiser, N. (1984). On the spatial correlations of Abell clusters. *Astrophys. J. Let.* , 284:L9–L12.

[Kamionkowski and Kovetz, 2016] Kamionkowski, M. and Kovetz, E. D. (2016). The quest for b modes from inflationary gravitational waves. *Annual Review of Astronomy and Astrophysics*, 54(1):227–269, [arXiv:https://doi.org/10.1146/annurev-astro-081915-023433].

[Komatsu and Spergel, 2001] Komatsu, E. and Spergel, D. N. (2001). Acoustic signatures in the primary microwave background bispectrum. *Phys. Rev.*, D63:063002, [arXiv:astro-ph/0005036].

[Kosowsky, 1996] Kosowsky, A. (1996). Cosmic microwave background polarization. *Annals of Physics*, 246(1):49–85, [arXiv:astro-ph/9501045].

[Kosowsky, 1999] Kosowsky, A. (1999). Introduction to microwave background polarization. *New Astron.Rev.*, 43(2-4):157–168, [arXiv:astro-ph/9904102].

[Lewis and Challinor, 2006] Lewis, A. and Challinor, A. (2006). Weak gravitational lensing of the CMB. *Phys. Rept.*, 429:1–65, [arXiv:astro-ph/0601594].

[Liguori et al., 2010] Liguori, M., Sefusatti, E., Fergusson, J. R., and Shellard, E. P. S. (2010). Primordial Non-Gaussianity and Bispectrum Measurements in the Cosmic Microwave Background and Large-Scale Structure. *Advances in Astronomy*, 2010:980523, [arXiv:1001.4707].

[Maldacena, 2003] Maldacena, J. M. (2003). Non-Gaussian features of primordial fluctuations in single field inflationary models. *JHEP*, 05:013, [arXiv:astro-ph/0210603].

[Pajer and Zaldarriaga, 2013] Pajer, E. and Zaldarriaga, M. (2013). On the Renormalization of the Effective Field Theory of Large Scale Structures. *JCAP*, 1308:037, [arXiv:1301.7182].

[Peebles, 1980] Peebles, P. J. E. (1980). *The large-scale structure of the universe*.

[Saito et al., 2014] Saito, S., Baldauf, T., Vlah, Z., Seljak, U., Okumura, T., and McDonald, P. (2014). Understanding higher-order nonlocal halo bias at large scales by combining the power spectrum with the bispectrum. *Phys. Rev.*, D90(12):123522, [arXiv:1405.1447].

[Seljak, 1994] Seljak, U. (1994). A Two fluid approximation for calculating the cosmic microwave background anisotropies. *Astrophys. J.*, 435:L87–L90, [arXiv:astro-ph/9406050].

[Seljak and Zaldarriaga, 1996] Seljak, U. and Zaldarriaga, M. (1996). A Line of sight integration approach to cosmic microwave background anisotropies. *Astrophys. J.*, 469:437–444, [arXiv:astro-ph/9603033].

[Seljak and Zaldarriaga, 1997] Seljak, U. and Zaldarriaga, M. (1997). Signature of gravity waves in polarization of the microwave background. *Phys. Rev. Lett.*, 78:2054–2057, [arXiv:astro-ph/9609169].

[Senatore et al., 2010] Senatore, L., Smith, K. M., and Zaldarriaga, M. (2010). Non-Gaussianities in Single Field Inflation and their Optimal Limits from the WMAP 5-year Data. *JCAP*, 1001:028, [arXiv:0905.3746].

[Senatore and Zaldarriaga, 2014] Senatore, L. and Zaldarriaga, M. (2014). Redshift Space Distortions in

the Effective Field Theory of Large Scale Structures. [arXiv:1409.1225].

[Takahashi, 2008] Takahashi, R. (2008). Third Order Density Perturbation and One-loop Power Spectrum in a Dark Energy Dominated Universe. *Prog. Theor. Phys.*, 120:549–559, [arXiv:0806.1437].

[Weinberg, 2005] Weinberg, S. (2005). Quantum contributions to cosmological correlations. *Phys. Rev.*, D72:043514, [arXiv:hep-th/0506236].

A. Formulae

A.1. Expansion

$$\mathcal{H}' = a^2\left(H^2 + \dot{H}\right) = \left(\Omega_\Lambda(a) - \frac{1}{2}\Omega_\mathrm{m}(a)\right)\mathcal{H}^2 = \left(1 - \frac{3}{2}\Omega_\mathrm{m}(a)\right)\mathcal{H}^2 \tag{A.1}$$

For the time dependence of the density parameters we have

$$\Omega_\mathrm{m}(a) = \frac{8\pi G\bar{\rho}a^2}{3\mathcal{H}^2} = \frac{\Omega_{\mathrm{m},0}}{a^3}\frac{H_0^2}{H^2} \qquad\qquad \Omega_\Lambda(a) = \Omega_{\Lambda,0}\frac{H_0^2}{H^2} \tag{A.2}$$

Matter domination

$$\mathcal{H}^2 \propto a^{-1} \Rightarrow \mathcal{H} \propto \eta^{-1}, a \propto \eta^2 \tag{A.3}$$

Matter domination

$$\mathcal{H}^2 \propto a^{-2} \Rightarrow \mathcal{H} \propto \eta^{-2}, a \propto \eta^1 \tag{A.4}$$

A.2. Orthogonal Polynomials

Rayleigh expansion

$$\exp\left[\mathrm{i}\boldsymbol{k}\cdot\boldsymbol{r}\right] = 4\pi\sum_{lm}\mathrm{i}^l j_l(kr)Y^*_{lm}(\hat{\boldsymbol{k}})Y_{lm}(\hat{\boldsymbol{n}}) = \sum_l(2l+1)\mathrm{i}^l j_l(kr)\mathcal{P}_l(\hat{\boldsymbol{n}}\cdot\hat{\boldsymbol{k}}) \tag{A.5}$$

$$Y_{lm}(\hat{\boldsymbol{z}}) = \sqrt{\frac{2l+1}{4\pi}}\delta^{(\mathrm{K})}_{m0} \tag{A.6}$$

Orthogonality of spherical harmonics functions

$$\int \mathrm{d}^2\Omega\; Y_{lm}(\hat{\boldsymbol{n}})Y^*_{l'm'}(\hat{\boldsymbol{n}}) = \delta^{(\mathrm{K})}_{ll'}\delta^{(\mathrm{K})}_{mm'}\,, \tag{A.7}$$

Expansion of Legendre polynomials in spherical harmonics

$$\mathcal{P}_l(\hat{\boldsymbol{n}}\cdot\hat{\boldsymbol{n}}') = \frac{4\pi}{2l+1}\sum_m Y_{lm}(\hat{\boldsymbol{n}})Y^*_{lm}(\hat{\boldsymbol{n}}') \tag{A.8}$$

Orthogonality of Legendre polynomials

$$\int \mathrm{d}\mu\; \mathcal{P}_l(\mu)\mathcal{P}_{l'}(\mu) = \frac{2}{2l+1}\delta^{(\mathrm{K})}_{l,l'} \tag{A.9}$$

$$(2l+1)\mu P_l(\mu) = (l+1)P_{l+1}(\mu) + lP_{l-1}(\mu) \tag{A.10}$$